Universitat Autònoma de Barcelona

INVESTIGATING EL ARGAR through forensic facial approximation

Joana Catarina Araújo Bruno

INVESTIGATING EL ARGAR

through forensic facial approximation

JOANA CATARINA ARAÚJO BRUNO

UAB Universitat Autònoma de Barcelona

FCT Fundação para a Ciência e a Tecnologia

Universitat Autònoma de Barcelona

Departament de Prehistòria
Facultat de Lletres

INVESTIGATING EL ARGAR

through forensic facial approximation

Doctoral dissertation
Joana Catarina Araújo Bruno

Supervisors
Dr Vicente Lull Santiago Dr Cristina Rihuete Herrada

Barcelona, March 2021

This doctoral dissertation was made possible by the Doctoral Degree Grant
no. SFRH/BD/99775/2014 attributed by the Fundação para a Ciência e a Tecnologia (Portugal).

Aos meus pais,
irmão e avós.
Ao Adrian.

Ia e vinha
E a cada coisa perguntava
Que nome tinha.

Sophia de Mello Breyner Andresen, *Coral*

ABSTRACT

The research in this dissertation is a multidisciplinary approach to the study of El Argar, a Bronze Age society established in southeastern Iberia (ca. 2200-1550 cal BCE). This dissertation gathers 40 faces represented from the skulls of individuals buried at the Argaric sites of La Bastida (Totana, Murcia) and La Almoloya (Pliego/Mula, Murcia), using the same methods employed by forensic practitioners. It is the most extensive corpus of facial representations from a single prehistoric settlement published to date. This effort aims to evaluate the potential of facial representation as an independent method to assess genetic information and formalize hypotheses in the archaeology of kinship. Our research question is founded on two premises: (1) that it is possible to depict facial morphology using cranial shape as a reference and achieve a significant level of accuracy by selecting validated guidelines; and (2) that our faces carry a percentage of our genetic imprint, as demonstrated by observable physiological similarities between close relatives and, most importantly, numerous studies on genome association (GWAS) and heritability patterns.

To address this question, a blind study was performed on the hypothetical manifestation of genetic relatedness in the variation of facial shapes in an Argaric sample. The statistical analyses of facial shape were processed with the three-dimensional geometric morphometrics (3DGM) toolset, using a sparse landmark configuration that overlaps areas under strong genetic control. The results led us to formulate hypotheses for two possible close genetic relationships between individuals from La Almoloya. The first hypothesis proposes a kinship relation between the men from tombs AY42 and AY80; the second links the man from tomb AY38 to the eldest child from AY30. The aDNA results are to be published soon and will disclose whether they shared a connection and, if it exists, to what level. Should these relationships be externally validated, then this research will help cement facial approximation as a valuable method to formulate hypotheses of relatedness, especially in those cases where it is not possible to retrieve genetic information from skeletal remains.

KEYWORDS: facial approximation; facial representation; El Argar; La Bastida (Totana); La Almoloya (Pliego/Mula); prehistoric archaeology; bioarcheology; three-dimensional geometric morphometrics (3DGM).

RESUMEN

La investigación desarrollada en esta tesis es una aproximación multidisciplinar al estudio de El Argar, una sociedad de la Edad del Bronce que se estableció en el sureste de la península ibérica (ca. 2200-1550 cal ANE). Esta tesis presenta la representación de 40 rostros que toman como referencia los cráneos de individuos de los yacimientos argáricos de La Bastida (Totana, Murcia) y La Almoloya (Pliego/Mula, Murcia) recurriendo a los mismos métodos empleados en casos forenses. Es el *corpus* más amplio de representaciones faciales para un único asentamiento prehistórico realizado hasta la fecha. La tesis tiene como objetivo evaluar el potencial de la representación facial como un método independiente para acceder a la información genética y formalizar hipótesis en la investigación arqueológica del parentesco. Nuestro punto de partida se basa en dos premisas: (1) que es posible representar la morfología facial utilizando el cráneo como referencia y lograr un nivel significativo de exactitud a través de una selección de pautas validadas; y (2), que nuestros rostros manifiestan parte de nuestra huella genética, como demuestran las similitudes fisiológicas observables entre familiares cercanos y numerosos estudios sobre asociación genómica (GWAS) y los patrones de herencia.

Para ello, se realizó un estudio ciego con el fin de evaluar la manifestación hipotética de la relación genética en la variación de las formas faciales en una muestra argárica. Los análisis estadísticos de la forma facial se procesaron con el conjunto de herramientas de morfometría geométrica tridimensional (3DGM), utilizando una configuración de puntos de referencia sobre áreas del rostro que están bajo un fuerte control genético. Los resultados nos permitieron formular hipótesis acerca de dos posibles relaciones genéticas cercanas entre individuos de La Almoloya. La primera hipótesis propone una relación de parentesco entre los hombres de las tumbas AY42 y AY80; la segunda vincula el hombre de la tumba AY38 al infantil de AY30. Los resultados de ADN antiguo de estos individuos se publicarán en un futuro próximo y revelarán si los mismos tienen lazos de parentesco y en qué grado. En el caso en que estas relaciones se vean validadas por datos externos, la presente investigación ayudará a cimentar la aproximación facial como un método ventajoso para formular hipótesis de parentesco, sobre todo en aquellos casos en los que no es posible recuperar información genética de restos óseos.

PALABRAS-CLAVE: aproximación facial; representación facial; El Argar; La Bastida (Totana); La Almoloya (Pliego/Mula); arqueología prehistórica; bioarqueología; morfometría geométrica tridimensional (3DGM).

RESUM

La recerca plantejada en aquesta tesi és una aproximació multidisciplinar a l'estudi de El Argar: una societat de l'edat del bronze del sud-est d'Ibèria. Aquesta tesi aplega 40 cares representades a partir dels cranis de persones enterrades als jaciments argàrics de La Bastida (Totana, Murcia) i La Almoloya (Pliego/Mula, Murcia) mitjançant els mètodes emprats per la pràctica forense. És el corpus més gran de representacions facials d'un únic jaciment prehistòric publicat fins el moment. Aquest esforç aspira a avaluar el potencial de la representació facial com a mètode independent per estimar la informació genètica i formalitzar hipòtesis dins l'àmbit de l'arqueologia del parentiu. Aquesta recerca es fonamenta en dues premisses: (1) que és possible retratar la morfologia facial emprant la morfologia craniana com a punt de referència i aconseguir un nivell d'exactitud significatiu seleccionant directrius validades; i (2) que a les nostres cares hi ha un percentatge de petjada genètica, com així ho demostren les semblances fisiològiques observables entre parents propers i, sobre tot, nombrosos estudis sobre associació genòmica (GWAS) i patrons d'herència.

Per assolir el nostre objectiu hem elaborat un estudi cec sobre la hipotètica manifestació de parentiu genètic en la variació de la morfologia facial en una mostra argàrica. Les anàlisis estadístiques de morfologia facial han estat realitzades mitjançant les eines del programari de morfometria geomètrica tridimensional (3DGM) i emprant una configuració de punts de referència anatòmics superposats damunt d'aquelles àrees que s'hi troben sota un marcat control genètic. Els resultats ens han permès hipotetitzar dues possibles relacions genètiques molt properes entre individus de La Almoloya. La primera estableix una relació de parentiu entre els homes de les tombes AY42 y AY80; la segona vincula l'home de la tomba AY38 amb l'individu infantil més gran de l'AY30. Els resultats d'ADN antic es publicaran properament i determinaran si aquestes relacions van existir i, en cas positiu, quin grau de parentiu expressen. Si les relacions que proposem són validades, llavors aquesta recerca contribuirà a cimentar l'aproximació facial com a mètode valuós per formular hipòtesi d'afinitat biològica, especialment en aquell casos on no és possible extreure informació genètica de les restes esquelètiques.

PARAULES CLAU: aproximació facial; representació facial; El Argar; La Bastida (Totana); La Almoloya (Pliego/Mula); arqueologia prehistòrica; bioarqueologia; morfometria geomètrica tridimensional (3DGM).

ACKNOWLEDGEMENTS

~

I write these words from a mixture of strangeness and satisfaction. Strangeness because it seems that I am closing a chapter that still feels unfinished. There is still so much left to do. And satisfaction because I finally got here and, at last, I can thank all those who helped me "dock this ship". In the end, my name is on the cover, so I guess that makes me the author. But this work is the result of the efforts of several people, along with many fortunate encounters and a little dash of luck.

My first appreciation goes to my supervisors, Vicente Lull and Cristina Rihuete. Thank you so much for letting me take the lead and for putting me back on track when I needed. Thank you for your patience, for your generosity, for understanding my silences and for believing in my work.

I thank the Fundação para a Ciência e Tecnologia of the Portuguese Ministry of Education, for providing the financial support which allowed me to come to Barcelona and develop this research.

To Miquel Molist, coordinator of the PhD in Prehistoric Archaeology at the Universitat Autònoma de Barcelona. I thank him for being supportive at all times and for attending to all the administrative knots with the calmest demeanor.

To Roberto Risch and Rafael Micó, for the generous advice and instruction.

To my friends and colleagues at the ASOME, whose kindness is unmatched. To Eva Celdrán, for her support and incentive since day 1, many years before the idea of this thesis came to fruition. In many ways, I owe her the possibility of pursuing this project and for that I will always be thankful. To Camila Oliart, for keeping and making "my skulls" whole and for doing it with a smile. To Maria Inès Fregeiro, who excels

at mimicking whichever burial position I need to understand. To Claudia Molero, for being the best laser-scanning companion. To Lourdes Andúgar, Carlos Velasco, Selina Delgado and Mireia Ache. I could not have found a more professional, gentler, and more passionate group of people. I did not know what to expect when I first embarked on this journey, and I am grateful to all of them for believing in me more than myself at times.

To Josep Potau from the Department of Anatomy of the Universitat de Barcelona. His guidance was invaluable to gain a better awareness of how the tissues entwine below the skin. To José Maria Garcia, Director of the Radiology Service at the Morales Meseguer Hospital in Murcia, for the exciting projects yet to be accomplished.

To my sculpture teachers, Robert Bodem, Silvia Juez and Grzegorz Gwiazda, who taught me how to see. To Christian Bull, who taught where to look for the story in anatomy.

To Miguel Valério, reader of my ramblings. I thank him for all the comments and suggestions, but most of all, for being a friend. To Cláudia, the sister I never had. To Pedro and Marina. I thank them for the invaluable support throughout the years. To my friends here and there, I cannot wait to embrace you all.

To my parents, my brother and my grandparents, who always helped me reach higher. To Adrian, for running by my side, holding my hand and pushing me closer to the finish line.

To all those who left a little bit of themselves with me, I promise I will keep it and treasure it forever.

TABLE OF CONTENTS

LIST OF FIGURES

LIST OF TABLES

"O autor destas páginas também desenha e não sabe expressar por palavras a extraordinária impressão que recebe sempre que copia o perfil de qualquer pessoa. A natureza chega tão complexa às feições de cada um, que somos forçados a não poder aceitar cada qual resumido ao lugar em que a sociedade o põe. Através dos séculos, uma linha única e incessantemente seguida acabou por tornar inimitável o perfil de cada um. Essa linha passa agora desde o alto da testa até por baixo do queixo, e às vezes lembra a de outros, mas é intransmissível."[1]

José de Almada Negreiros, *Nome de Guerra* (1925)

[1] "The author of these pages also draws and does not know how to put in words the extraordinary impression he receives whenever he copies someone's profile. Nature arrives so complex to each one's features that we are forced not to accept each one to be summarized to the place in which society puts him or her. Over the centuries, a single and unceasing line made each person's profile inimitable. This line now runs from the top of the forehead to under the chin, and sometimes it reminds us of others, but it is non-transferable."

INTRODUCTION

~

OVERVIEW AND OBJECTIVES

This dissertation is at the crossroads of different disciplines. It dwells on archaeology, anatomy, art and statistics. The point of departure is "El Argar" (2200–1550 cal. BCE), an archaeological group/society established in southeastern Iberia during the Bronze Age. The El Argar society, named after the eponymous settlement in Antas (Almería), began to unveil its secrets at the end of the 19th century at the hands of the Siret brothers. Decades of archaeological excavations would then reveal evidence of a state society organized in classes and which followed an elaborate intramural funerary ritual with grave goods differentiated by age, sex and social status (Lull et al., 2011a). The buildings, objects and burial places of El Argar have been uncovered at settlements such as El Oficio (Cuevas de Almanzora, Almería), Castellón Alto (Galera, Granada), Gatas (Turre, Almería), La Bastida (Totana, Murcia) and La Almoloya (Pliego/Mula, Murcia). Their faces or, to be more precise, the faces we can infer from their skulls, were unknown until now.

This thesis presents 40 Argaric faces from La Bastida (Totana) and La Almoloya (Pliego/Mula) and comprises the most extensive corpus of facial representations from a single prehistoric settlement. In general terms, this dissertation draws an effort to explore the potential of facial approximation as a tool to formalize archaeological hypotheses in kinship research. More specifically, it aims to address the Argaric facial phenotype and investigate whether facial representations from the skull can be used as independent evidence for inferring genetic relatedness. The hypotheses contained in this study will be tested with genetic information to be published in the near future (Villalba-Mouco et al., in prep).

RESEARCH QUESTIONS AND METHODS

The research questions developed throughout this work are founded on two premises. The first is the notion that it is possible to depict a face using the skull as a reference and achieve a significant level of accuracy by applying validated methods. Despite the material, methodological, practical and perceptional limitations (discussed in depth in Chapter 2), there are quantitative assessments of accuracy which establish that approximately 70% of the face can be predicted with less than ± 2.5 mm deviation.

The second premise stems from the fact that our faces carry a percentage of our genetic imprint. While this is by no means a recent realization, the past decade has seen a growth of studies that combine the capacity to process genome-wide data and access to high-resolution imagery. Research on heritability is unveiling the phenotypes we are most likely to inherit or share with our kin, and genome-wide association studies (GWAS) are uncovering more and more genetic variants that control specific facial traits. If face similarity between relatives is an indicator of their genetic relatedness, can a facial representation generated from a skull retain that same genetic signal? Is it possible to use such representations to formulate hypotheses of genetic relatedness?

The present research is designed towards answering these questions. For that purpose, I gathered the methods used to estimate the features from the skull, and critically reviewed them to establish which would provide the lowest margins of error. Then, I laser-scanned, processed and measured the crania and mandibles of all individuals selected for my sample. In addition to providing the base references for my study, this process allowed the team of ASOME-UAB to curate a digital osteological collection that is now available for other research endeavors. This work established the scientific and practical framework to develop facial representations from 40 skulls of individuals buried at the Argaric settlements of La Bastida and La Almoloya.

Following extensive rounds of revisions, the facial representations were analyzed using the three-dimensional geometric morphometrics (3DGM) toolset to quantify the shape similarity between them. For that purpose, I defined a sparse landmark protocol of 27 anatomically homologous points and, after applying them on the faces, I produced three types of exploratory graphs to investigate the shape variation within the sample. First, I addressed the different components of facial shape variation by hierarchizing

them in a Principal Components Analysis. Second, I generated a similarity matrix that compares the total configuration of shape in all individuals against each other. And third, I produced a phenetic tree to begin a preliminary exploration of the clustering pattern of all individuals. These three analyses will require external validation from the studies of the ancient DNA of the same individuals to be published in the near future.

STRUCTURE

The thesis opens with an analogy for the (forensic) practitioner's work and places facial depictions from the skull in the broader context of scientific imagery. The paths of science set the pace for constant change, and thus I acknowledge the mutable nature of scientific images as inescapable. Images reflect certain ideas behind them, and those ideas reflect available evidence and current interpretations in relation to specific scientific subjects. An image about the past is, inexorably, an image rooted in the present.

A few notes on terminology are in order. Expressions such as "reconstruction" and "approximation" remain the most widely used both in academic and public circles, but do they adequately reflect the scope of action and limitations inherent to the field? Both terms present themselves as contradictory to our main (and perhaps unattainable) objective, which is a non-biased glance at past realities. While "reconstruction" enforces our purposes and notions on the intentions of those who actually constructed the past, "approximation" implies that certain concepts may be bent, depending on the story we are bound to tell. So, "reconstruction" and "approximation" lodge in logical and spatial impracticalities. We cannot assume that our intentions were also the intentions of others, and we cannot let convenience permeate the discourse. Therefore, "representation" steps forward as a preferable term. If we follow Lull's (1988) broader definition of *representación* (in the context of archaeological theory), a facial representation generated from the skull would be understood as the result of an applied method supported by an empirical premise—in this case, the premise that bone anatomy determines the shapes on the (sur)face.

Retrieving a likeness from a particular skull stands out as a century-old process that has seen many developments, associations, and trends. Chapter 1 dedicates one section to briefly reviewing the work of those who tailored the field and the first faces to emerge from bones. Our review leaves aside most of the work done for forensic cases, which engage closely with the prospect of producing a positive identification.

The chapter closes with a reflection on the challenge of interpreting fragmentary evidence and produce from it a discourse made up of shapes and images rather than words and sentences. Ultimately, to present an image of a past countenance is also to revest it with historical meaning. Faces resonate with us because they are at the very core of our interactions as social beings and are synonyms for identity and personality. How can an anonymous face have a place in archaeological discourse? Is there more to it than the mere curiosity of "gazing upon the faces of our ancestors"?

Chapter 2 approaches the pursuit of accuracy in facial approximation and discusses how certain practical limitations can affect the outcome of a craniofacial depiction. Addressing the taphonomical issues that may affect bones is the first step. More often than not, our primordial reference (the skull) has been affected by the passage of time and exposure to the natural elements. Fragmentation, distortion, and missing pieces, they all interfere with our access to the original shape of organic materials. Often, "removing" those layers of distortion leads to creating a whole new object that drifts farther away from the original shapes that were underneath our subject's face. If a facial representation is an endeavor that cannot be detached from a particular skull, then the state of preservation of the remains must be weighed into the reliability of the outcome.

So, how accurate can a facial representation from the skull be? The following section in Chapter 2 approaches the disparity in recognition rates between a facial representation from the skull and the real face. Landmark-based assessments, heat-maps and face pool comparisons are among the different ways to measure quantitative and qualitative estimates of method accuracy. Finally, this chapter addresses the necessary standardization of practices and methods against the untamable reality of human variation. These limitations have been the main driving force behind the criticism towards the implementation of facial approximation routines.

Chapter 3 reviews the methods used to estimate the facial features and overall shape of the face from skulls. This is an elaborate task that relies, at first, on anthropological reports of skulls and their

skeleton. Osteobiographical data such as sex, age at death and population affiliation inform the selection of the standards to estimate the features. These methods have their own historiographical record, and many have become associated with the researchers that proposed them. In recent years, many anatomical standards have been derived from datasets of medical imagery and rely on extensive sample sizes. Despite the inherent limitations discussed in Chapter 2, this effort has contributed positively to increasing the precision of facial approximation techniques.

Chapter 4 sets the proper archaeological context and gathers the more technical aspects of this work. It opens with an introduction to the archaeological sites of La Bastida and La Almoloya, two of the most important settlements of the El Argar society and, indeed, of the Bronze Age in southeastern Iberia. Subsequent sections address the methodological aspects of this work. First, the research questions and the theoretical background that allowed us to define a work hypothesis. Second, the criteria to select a sample that would be representative of the population. Third, the need to find a way to evaluate method accuracy in a situation where the original faces cannot be accessed anymore. The latter will materialize in a collaborative endeavor with the Morales Meseguer Hospital in Murcia, which will supply a series of computerized tomographies to establish a control group. External factors prevented us from pursuing this collaboration until now. Nevertheless, evaluating the precision of the methodology applied to the Argaric faces remains of paramount importance and it is our hope and purpose to resume this task in the near future. Finally, the chapter ends with a comparison of the traditional against the digital approach in the production of facial depictions from the skull, and a presentation of the equipment used to gather the three-dimensional models, paired with a detailed description of the laser-scanning process.

Chapter 5 defines the selected methods according to the review of the literature in Chapter 3 and addresses the process of creating the facial representations on a case-by-case basis. It is an inventory-like exposition that should be consulted in tandem with the images gathered in Appendices A and B.

Chapter 6, the last of this dissertation, brings together the methods and discusses the results of the geometric morphometric analyses performed on the Argaric dataset. The results of the enquiries into the facial morphometry of the sample of Argaric faces led to the proposal of two genetic relationships, each involving a pair of individuals.

Chapter 1

1 Setting the first stones

~

1.1 'The Dürer's Ganda': a brief reflection on scientific imagery

I decided to first approach facial approximation by telling a story that, apparently, has little to do with facial approximation.

It is the 20th of May of 1515. The location is somewhere near the Tower of Saint Vincent (also known as the Belém Tower), which is being built on the coastline of the Tagus river. In the 16th-century, Lisbon has become a gateway for all sorts of exotic things, and the latest novelty is a beast that had not been seen in Europe since ancient Roman times. The *ganda*, as was called in Sanskrit the creature we now know as rhinoceros, disembarks after a 120-day voyage from Goa, India. News of this unusual passenger quickly spread all over Europe. The Indian rhinoceros was a diplomatic gift from Muzafar II of Gujarat to Afonso de Albuquerque, governor of Portuguese India, and was shipped to Dom Manuel I, king of Portugal. After being paraded in an arranged fight with an elephant, the rhinoceros became a part of a political strategy to obtain the goodwill of Pope Leo X and, later that same year, the *ganda* leaves on a boat to Rome. Before reaching its final destination though, the vessel sinks during a storm near Porto Venere, and the rhinoceros goes down with the ship (Clarke, 1986). It is, indeed, a very tragic ending to such a long journey.

However, the story of the *ganda*'s does not end here. One way or another, the news traveled and reached Albrecht Dürer, an influential German painter and printmaker, who then took on the task of portraying the rhinoceros without ever having seen a real one in his life. It is not clear how or where Dürer

got his references from, but it has been argued that he owned a written description and a sketch made by someone who saw the animal at the Portuguese court. The whereabouts of that initial sketch are unknown, and therefore we cannot assess how much of Dürer's drawing is actually his own. Looking at his image (Figure 1.1), it is not difficult to immediately recognize a rhinoceros. Still, the creature does present some incorrect anatomical elements, such as the armor-like plates covering the body and a twisted horn on the back. The design may represent a real suit of armor, forged to equip the animal to fight the elephant back at the Portuguese court (Ridley, 2005), or it may be a representation of the heavy folds of thick skin that the Indian rhinoceros does possess. Either way, these inaccuracies might have already been present in the earlier sketch, and the German printmaker may have ended up copying them, or perhaps they derived from Dürer's creative interpretation of his references (Clarke, 1986). Even so, Dürer's *ganda* went on to become one of the most popular and persistent images in History. The drawing was copied and reproduced multiple times and was still being used in school books at the beginning of the 20th century as a valid representation of a rhinoceros (Winkler, 1938), *apud* (Clarke, 1986).

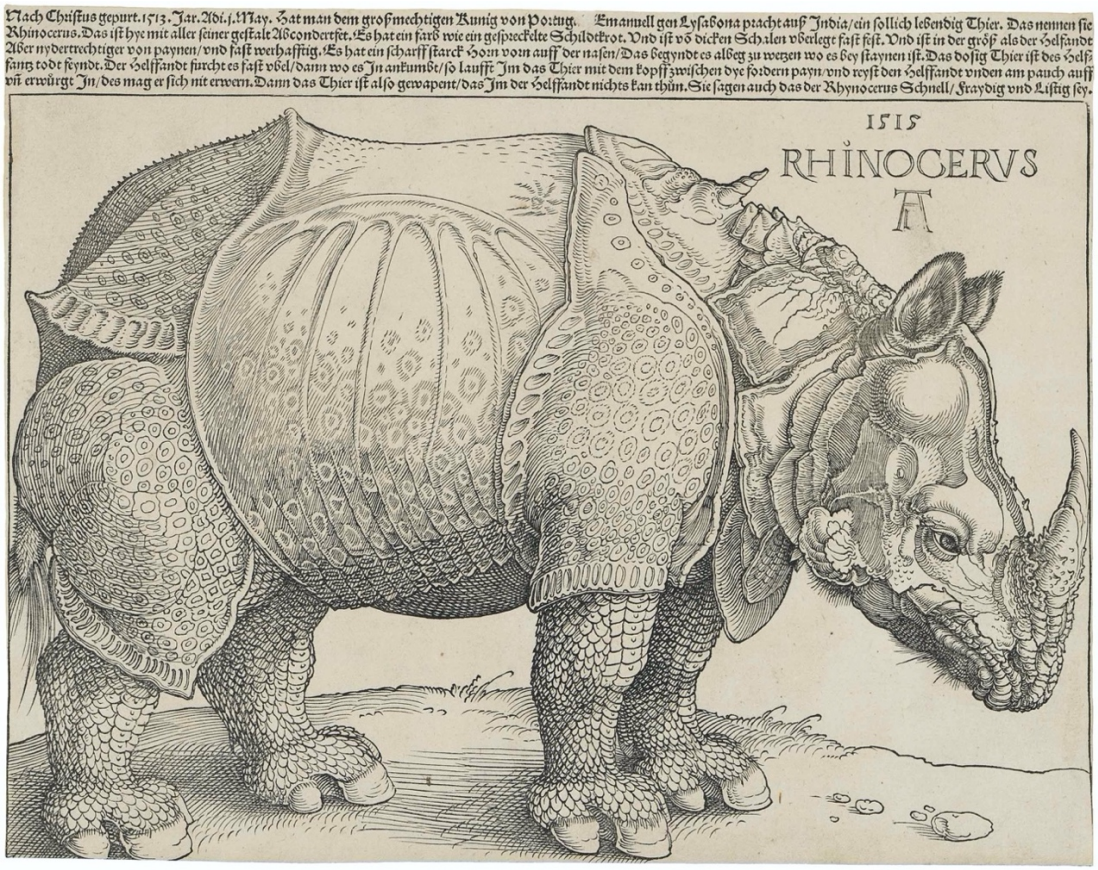

Figure 1.1 - *Dürer's Rhinoceros*, woodcut by Albrecht Dürer (1515). © Public Domain.

So, what does a 16th-century woodcut of a rhinoceros have in common with a facial approximation made five hundred years later? Visually speaking, absolutely nothing. However, there is a common undertone to both endeavors. In the same way Dürer did to create his engraving of a rhinoceros, a forensic practitioner must produce a visual record based on an interpretation of indirect sources. They have access to material evidence—the skull—or an eyewitness who provides a description, but the real face is unknown to the drafter, painter, or sculptor. Thus, like Dürer's famous depiction of a rhinoceros, a facial approximation is expected to contain a number of inaccuracies.

From another perspective, the story of the *ganda* is just another unfortunate declaration of human cruelty over other living beings. Yet Dürer's drawing of a rhinoceros is a testimonial of the nature of scientific imagery: these visual accounts usually come with an undisclosed expiry date. They are indispensable to educate the public but are as valid as the reliability of the scientific background that informs them. Sometimes, the image outruns knowledge and prevails much longer, contradicting its original intent and contributing to misinform instead of educating the audience. But when science finally picks up the pace and demands a visual update, some images, like Dürer's, give way to more precise renditions while still entering the annals of the History of Art. For that reason, in addition to being clear about the sources, procedures and decision-making behind the creation of these visual records, it is essential to acknowledge the historical context the images belong to. As with any artistic creation, grasping the timeframe and understanding the author's mindset are vital assets to analyze images produced against a naturalistic, scientific and even forensic backdrop.

Hence, it is essential to emphasize that the images included in this dissertation are facial approximations of people that lived almost four thousand years ago, but they are testimonies of their own time. They were produced upon the skulls excavated at the Spanish sites of La Bastida and La Almoloya, using the available data, methods and equipment, and to the best of my current scientific, technical and artistic skills. Hopefully, the following pages will provide a clear insight into my process and objectives. That said, one should not be too surprised if in some years' time a revision of these faces becomes necessary. While it is a privilege to witness the fast pace of discoveries being made, producing images for such an evolving scientific field has to come with the compromise that these images will likely demand new adjustments at some point. For how long will these images stand the test of time? That, we do not know.

Perhaps these faces will reveal themselves to be as accurate as a facial approximation can be, and the veil between them and us will be less thick. Or, maybe, the faces will end up assuming the role of (not less honorable) artistic interpretations and remain intriguing but, nevertheless, very far from reality. Maybe time will tell, maybe time will keep their secrets.

1.2 A few notes on terminology

Retrieving someone's likeness from its skull is a practice commonly included within the controversial field of forensic arts. The suitability of the terminology used to describe this process and its results has been a matter of an ongoing semantic discussion.

As defined by Taylor (2001), "forensic art is any art that aids in the identification, apprehension, or conviction of criminal offenders, or that aids in the location of victims or identification of unknown deceased persons". A standard definition of "forensic" relates it to the application of scientific methods and techniques to the investigation of a crime, thereby excluding the use of artistic approaches as forensic evidence (Wilkinson, 2015). With *art* being understood as the visual or material expression of human creativity, imagination or ideas over a particular concept, and *forensics* as the scientific methods used in the investigation of a crime, it might be difficult for some to conceive such a match. How can an activity rooted in creative interpretation be used within the precincts of regulations and legal protocols? Despite this seeming paradox, artists have been called upon to produce composite drawings of suspects by interpreting the memories of witnesses, to illustrate the aged face of someone that went missing years before, and to build faces on top of skulls.

This project focuses on retrieving the appearance of prehistoric individuals using the same methods employed within forensic casework. Yet, in this case, there are no criminals waiting for a trial or victims waiting for justice. The goal of producing a successful identification is not present, as there are no living relatives capable of recognizing them, and we have no depictions of the individuals involved created when they were alive or shortly after they passed. Thus, the faces included here should be understood within the

framework of science imagery or scientific art, as described in the previous section. All images rely on a visual and anthropological interpretation of each skull. As much as possible, the resulting faces follow validated guidelines and the most recent standards published to date.

The visual byproducts that originate from memory or the interpretation of bone have been referred to as scientific art before (Wilkinson, 2004b), a term which was unreasonably criticized and deemed as "bizarre" (Stephan, 2015b). Listing the extensive documentation on how art has been in the service of science for centuries would be a task well beyond our research scope, but one does not need to look too far to find numerous examples. Leonardo DaVinci's integrative approach to anatomy, relying on sharp analytical thinking and artistic skills to illustrate his experiments, is still regarded as a groundbreaking moment in a field that had seen very little progress in thirteen centuries (Pevsner, 2019). Another example is paleontology, a science that shares with archaeology the conundrum of having to produce interpretations from fragmented remains of past times. The science that studies fossils is also quick to recognize and accept the contribution of scientific imagery or, using the field's jargon, "paleoart".[2] Scientific artwork has been the foundation of public outreach for paleontology, and a tool that enables the formulation of new hypotheses concerning the anatomy, behavior and biology of extinct creatures (Witton et al., 2014). Resorting to a visual language, in the form of photographs, diagrams, tables, charts, drawings, digital images or three-dimensional models, allows scientists to interact with complex phenomena (Richards, 2003) and might convey important evidence not observable in other ways (Evagorou et al., 2015). Since rigor and aesthetics do not have to be mutually exclusive, I believe science and art should not be either.

Besides the debated integration of these techniques within a broader field of knowledge, the use of specific terminology such as "facial reconstruction", "reproduction", "recreation", "restoration", or "approximation" has also generated different reactions among experts. Too often, the confusion arises from the fact that most of these terms are borrowed from other fields of expertise such as dentistry or

[2] While the term "paleoart" seems to be more suited to art produced in prehistoric times, it has been long popularized and used within the field of paleontology to describe "any original artistic manifestation that attempts to reconstruct or depict prehistoric life according to the current knowledge and scientific evidence at the moment of creating the artwork" (Ansón et al., 2015).

plastic surgery. Of all the above, "reproduction" and "recreation" are possibly the less acceptable terms. While "reproduction" might imply achieving a perfect copy or replica of something, which is obviously impossible when our object of study is partial remains from the past, "recreation" seems to point towards something completely new, possibly created outside the boundaries of the method. The expression "facial restoration" seems to refer to embalming practices (Smith, 2018) or repairs on damaged but still intact remains (George, 1987), both of which refer to different ventures.

At first glance, "facial reconstruction" (along with "facial restoration") can be confused with reconstructive or cosmetic surgery. Undoubtedly, the contributions of maxillofacial and craniofacial surgical studies to forensic research are unquestionable. However, performing reconstructive surgery on a living person and reconstructing a face from a dry skull have different aims, methodological approaches and applications (Smith, 2018). "Facial reconstruction" remains the most widely used expression to define the task of building a face from a skull while also being the most recurrent in public media channels. However, there are claims that such definition results in a misleading perception of the process and incorrectly implies the absolute accuracy of the method (Stephan, 2003a).

With this in mind, Robert M. George (1987) proposed "facial approximation" as a definition for the procedures that allow modeling a face from the available bone evidence. Since then, some authors have endorsed the term as the most accurate designation (Haglund & Reay, 1991; Stephan & Henneberg, 2001). Stephan (2015b) goes further and analyzes the development of the methodology under a "Kuhnian perspective"[3] to justify the need for a paradigm change and the complete dismissal of the term "reconstruction" in favor of "approximation". According to Stephan's interpretation of Kuhn's philosophy, "facial reconstruction" and "facial approximation" are two distinct approaches with enough disparities between them to be considered two different "schools". The author believes that the most significant of these differences relates to how each approach processes methodical anomalies (Table 1.1).

[3] After Thomas Kuhn (1922–1997), an American philosopher of science who postulated that scientific progress does not happen in a continuum, but in periodic revolutions that motivate paradigm shifts (Kuhn, 1996).

Table 1.1 - Distinctions between facial reconstruction and facial approximation, according to Stephan (2015b).

	Facial Reconstruction	*Facial Approximation*
Philosophy	Current methods work, they need only to be refined by peripheral adjustments.	Significant degrees of error permeate current methods. Ongoing review and improvement of methods is crucial.
Aims	Correct recognition of the predicted face via facial recognition.	Recognition of the skeletal remains via any mechanism associated with the facial approximation including, but not limited to, correct facial recognition.
Ideal outcome	Same as the operational objective.	Correct recognition of the predicted face via facial recognition.
Method foundations	Methods have been built upon founding Russian and American methods, the former exclusively relying on muscle construction, the latter on average facial soft tissue depths.	Methods can be traced to European origins. All methods (including founding methods) fall on a continuum, utilizing central tendencies and individualistic face anatomy as reference points.
Methods	Preference rests with traditional methods, including artistic formulations.	Preference given to metric, quantitatively verified, methods.
Soft tissue depths	Universal use of means, often with individuals subjectively classified by normal, fat and thin categories. Little attention awarded to shape characteristics of data distributions and data uncertainty.	Shape of data is key to driving their description, which is not limited to means. All individuals are subject to measurement to elucidate dispersion without subjective exclusion of any data points.
Treatment of anomalies	Method error dismissed in favor of practitioner mistakes.	Method error considered ahead of practitioner mistakes.

While it is true that the lack of experience of practitioners has been considered the cause for low resemblance ratings in the past (Wilkinson, 2004b), faces predicted from the skull do not intend to create an accurate portrait of the deceased person. First, because the endeavor of portraiture goes way beyond a mere representation of someone's appearance, as it aims to bring together in one image the emotions, mood and personality of the sitter, and none of these traits can be inferred from our bones. Secondly, because portraits may follow idealized artistic conventions or styles intended to reaffirm religious or political influences (let us recall, for instance, the idiosyncratic representations of the Egyptian pharaoh Akhenaten),

or may even "soften" certain features of the individual making it more pleasant for the viewer. A portrait is a staged event, a manufactured narrative that expresses a belief or a wish. While it is true that a facial approximation can (and has been) revested with additional considerations like the ones I just mentioned, that is not the initial goal. That said, I would like to evoke what Betty Pat Gatliff, well-known pioneer and promoter of forensic art, wrote in 1984: "Facial sculpture is used as a last-ditch effort when other identifying techniques (…) have been unsuccessful. The outcome is uncertain in every case, but if the sculpture is done correctly and as accurately as possible within the limitations of the technique, it is usually worth a try." (Gatliff, 1984). Like Gatliff, most experts working nowadays acknowledge the existence of method restrictions and do not pretend to offer more than an approximation of what that person would have looked like.

And yet, even if the practitioners' experience cannot be at the center of the equation to obtain successful identifications, it is also fair to admit that the nature of this task does include variables that should not be overlooked. (Forensic) facial approximation develops at the crossroads of many fields – physical anthropology, anatomy, pathology, plastic surgery – and relies on a vast array of technical and artistic resources such as drawing, sculpture or the control of specialized computer hardware and software. Experts can be trained in an academic context but also a forensic one. Each setting has different paces, different availability of resources, different bureaucracies, ethical considerations, and protocols. Therefore, it is not surprising that the "artistic" quality and precision of facial depictions sometimes echoes these variables (Smith, 2018).

More than the existence of two "schools" of practice, perhaps there is a critical difference in that the term "approximation" describes the expected outcome, whereas "reconstruction" relates more to the process of reaching that same outcome. In essence, both terms aspire to describe a procedure that (1) starts from the same materials (the skulls of deceased people), (2) moves on to apply a subset of selected techniques informed by the anthropological analysis of each individual, and (3) aims at achieving the same ideal outcome, which is a successful identification, despite the layer of inaccuracy that might permeate the final result. The different approaches and, consequently, the differences we have observed stem from several related factors. Perhaps the most important one is the historical context and the current state of the art, which dictates access to more or less robust databases and tested methods to predict facial features.

Despite being a practice over a hundred years old, facial approximation has only seen a true *renaissance* about two decades ago. A study by Stephan (2002a) paved the way for a much needed revolution in the field by identifying a methodological error that consistently underpredicted the projection of the cornea and its relation with the anterior margins of the orbit. Since then and relying on the momentum gained by the ability to gather and process bigger datasets, many independent researchers developed studies that scrutinized long-established guidelines and proposed new methods (Davy-Jow et al., 2012; Guyomarc'h et al., 2012; Guyomarc'h & Stephan, 2012; Rynn & Wilkinson, 2006; Rynn et al., 2010, to name just a few). The ongoing research and the multitude of studies that have emerged, especially in the past decade, are the soundest statement that the field is actively looking for ways to reduce the existent methodological error and is not that resistant to change (or at least, not anymore).

At this point, I would like to recover two additional terms that might serve as a less partial definition for our purpose, "depiction" and "representation". The former is proposed by Kathryn Smith (2018) as an alternate nomenclature that comprises the full range of facial images produced in two- and three-dimensions, which are the result of an interpretation of human remains or eyewitness memory. As per the previous author, "depiction" is a relatively neutral and "inclusive" word that conceals no assumptions regarding the methods and their accuracies (or lack of them) or the possible results and their limitations.

The other term, *representación* or "representation", as defined by Lull (1988), is perhaps the one that offers the best shelter for our intentions. Lull (1988) argues that "reconstruction" and "approximation" dwell respectively in logical and spatial impracticalities. A "reconstruction" not only denies the primacy of those who participated in the original events, but also, and like "approximation", assumes that our methods to access those events are correct at the same time we (in a somewhat contradictory manner) acknowledge the impossibility of being accurate. Moreover, "approximation" suggests that certain concepts can be nuanced, depending on the convenience of the narrative. Thus, "representation" is brought forward as a preferable definition. As per Lull, a "representation" is not a random act of creating symbols. It expresses a systematic model that relies on preexisting theories that can either emerge from empirical provisions or from non-contradictory work hypotheses (Lull, 1988). It does not portray our intentions as the intentions of others, nor does it pretend interpretations to stem from the "past", when in reality they are *from* the "present". Under this prism, the facial representations included in this work can be understood as the result

of an applied method supported on an empirical premise that postulates that bone anatomy determines the shapes on the (sur)face. One may argue that they still involve the creation of a "new face" due to the practical unfeasibility of having the original one as a reference, and, from that perspective, they can then be understood as "reconstructions" or "approximations". While it is true that this endeavor prevents any escape from layering an actual interpretation on a partial reference, assuming our work to be a "reconstruction" or a "new face" would also contradict our initial intent, which is the representation of a specific face.

Thus, my preference goes to using "facial representation", which I find to be the expression that better encapsulates the theoretical framework that structures my proposal. I shall also recur to the term "facial approximation", in a compromise with the current tendency in the published literature in the field, along with "facial depiction", which I find worthy for its neutral character. This by no means implies an assumption that my attempts are entirely accurate. Despite its inherent inadequacy, the word "reconstruction" has almost acquired a meaning of its own when used within the multidisciplinary field of virtual anthropology. For its frequency in the specialized literature, it may also appear on occasion to refer to the act of returning biological specimens to their supposed original state. For the skull representations included here, I present a possible solution to a problem that usually has many. For that reason, neither do I assume (and could not assume) that mine is the only possible one.

1.3 A brief overview of craniofacial depiction

Taylor's monograph on forensic art (2001) dedicates a whole chapter to exploring many examples of how drawings have been used by law enforcement over a timespan of more than one hundred years. From the earliest examples of police sketches used to document the murders of "Jack the Ripper" to the 21st-century DNA phenotyping and profiling techniques, forensic art has evolved to include many different assets like composite drawings, age progression/regression, and facial approximation. Despite its instant association with forensic casework, which gained more mediatic prominence in the 1970s, the origins of craniofacial

representations as a science-based effort can be retraced to the late 19th century and were not related to criminal investigations.

Considering the general theme of this project, in this short overview of craniofacial approximation, I will focus on archaeological and paleoanthropological cases. My objective is not to compile an exhaustive report of all the facial approximations made to date but rather illustrate progress in the field throughout the years and highlight some of the significant turning points and events. Although the lines of reality and imagination get blurred sometimes, facial approximation as we know it today results from a cumulative and collective effort that found its most fertile ground on the collaboration between scholars and artists.

"Our unlimited fascination with human faces", as Wilkinson (2004b) put it, can be found in the depths of the archaeological past. Indeed, the face is a recurrent theme throughout time and space. The earliest known representation of a face with realistic traits comes in a small figurine carved in mammoth ivory, retrieved from the Grotte du Pape in southwest France in the late 1800s. It dates back to the Upper Paleolithic period, about 25 000 years ago, and goes by the definition of *La Dame à la capuche*, or the Hooded lady (Figure 1.2). It has been interpreted as a woman with a triangular face, with the forehead, nose and brows carved in relief. The hair or headdress is represented with deep vertical lines crossed by horizontal incisions (White, 2006). Engravings outlining human face profiles with realistic individualized features can also be found in other caves from the Magdalenian period in France (Fuentes, 2013).

Figure 1.2 - Venus of Brassempouy. © RMN-GP. Jean-Gilles Berizzi.

There is no doubt about humanity's early interest in faces, but what about its association with the underlying bone? Evidence of what may be considered the first attempt of creating a plastic representation of human features upon a skull can be traced back to the Pre-pottery Neolithic B (ca. 7500–5500 BCE) levels of Jericho. In 1953, under the Jordanian sun, a team of excavators led by Kathleen Kenyon at Tell es-Sultan discovered the first of many human skulls as they were about to finish that year's expedition. Not like anything seen before, these skulls had faces built upon them, with marine shells set into the orbits to simulate the eyes and brown paint mimicking hair or some form of headdress. Recently, one of Jericho's skulls found by Kanyon's team in 1953 (Figure 1.3) also gained a facial approximation that was on display at the British Museum between December 2016 and March 2017. The CT-Scans revealed that underneath the plaster, there was a man in his forties who had his nose broken and healed before he died (British Museum & Shore, 2017).

Figure 1.3 - On the left, Jericho skull from the 7th millennium BCE. On the right, the facial approximation of the man underneath the plaster (photograph by RN-DS partnership). Both images © The Trustees of the British Museum.

Since the first discoveries at Tell es-Sultan, other plastered skulls have been found in Levantine sites such as Ain Ghazal, Baysamun, Tell Ramad and Tell Aswad (Figure 1.4) (Stordeur & Khawam, 2007; Strouhal, 1973). The Nahal Hemar Cave, an early Neolithic settlement carbon-dated to 8310–8110 BCE and located on a cliff near the southern end of the Dead Sea, has also yielded some remarkable finds. These include crania adorned with a lattice-work of asphalt strips in a criss-cross design and two painted limestone masks that were probably used to cover the facial portion of the skulls (Hershkovitz & Yakar, 1988; Prag & Neave, 1997).

Figure 1.4 - Plastered skulls from Tell Aswad, in Syria (Stordeur & Khawam, 2007). © L. Dugué.

On a slightly different latitude, in Neolithic Çatalhöyük (7100–6000 cal BCE), plastered skulls were also found. One striking example is a skull with modeled facial features and covered in red ochre located between the arms of a 50-year-old female primary burial (Boz & Hager, 2013). Albeit the apparent intention of recreating something lost, it has been argued that these plastered skulls should not be considered

representations with individualized characteristics as there was no purpose of achieving a specific likeness (Kenyon, 1957). The practice of collecting skulls has been widely reported throughout several sites from the Neolithic of the Near East (Benz, 2010; Bienert, 1991; Bocquentin et al., 2016) and has been variously interpreted. The most cited interpretation sees these skulls as a form of an ancestor cult, possibly associated with the emerging sedentism and the control of resources (Bienert, 1991; Kenyon, 1956). Further interpretations link these objects to collective ritual practices that encouraged the creation of a shared social memory (Kujit, 2000, 2001, 2008), while other authors suggest that they might have had an apotropaic function (Schmandt-Besserat, 2013).

Other early examples that highlight the bone permanence against the fading of the flesh include the Chinchorro mummies from Chile, dating as far back as 7020 BCE. These bodies underwent an artificial mummification process that changed over the years but often included modeling a clay mask on top of the head as a part of the preparation rituals (Arriaza, 1994). Also, if we cross the Pacific South into Oceania, we find the practice of applying materials on top of skulls to achieve a symbolic representation of a face (Figure 1.5). These objects, known as "overmodeled skulls", result from a well-spread practice across the globe, from Egypt to Colombia (Aufderheide, 2009).

Figure 1.5 - Elongated skull for memorial head, with face modeled in clay. S. W. Malekula, New Hebrides.

Masks are also manifestations of our ancestors' interest in the face and have been associated with sacred, ritual practices, pragmatic uses (e.g., hunting) and performances. There is something primordial about the idea that our face can be veiled, hidden behind a different identity, or transformed into another human or creature. A mask can conceal or change one's social role within a group, or even act as a reaffirmation of one's identity, lineage or power (Figure 1.6).

Figure 1.6 - On the left, the death mask of Mayan King Pakal the Great (603–683 CE). © Wolfgang Saube. On the right, the golden mask of Tutankhamun (c. 1342 – 1325 BCE) © Roland Unger. Both images licensed under CC BY-SA 3.0.

In a way, masks can assume a role similar to that of facial approximations, which is the purpose of restoring or preserving a lost identity, making it last through the ages. After someone passes away, making a cast of their face is a practice known at least since ancient Egyptian times. Quibell (1909) reported a death mask made of rough plaster found in the north-west corner of the temple in Saqqara and theorized that it belonged to a high-rank personality or King Teti himself (Figure 1.7).

Figure 1.7 - On the left, death mask found at Saqqara, possibly of King Teti, first ruler of the 6th Dinasty. The center and right images are two views of a cast made from the original mould. Adapted from Quibell (1909, pl. LV).

The realistic appearance of some ancient Roman busts has been sometimes linked to the existence of wax masks taken directly from their subjects. These masks were worn by actors during Roman funerals and are mentioned in Classical texts as *imagines*, but were created in wax while the individual was alive, usually when a man attained an important political achievement between the ages of 35 and 40 (Rose & Lovink, 2014). Preserving one's face through the creation of a mask was a legitimization for the afterlife and the acquisition of a place among the venerable ancestors, and a symbolic milestone of one's accomplishments and status in Roman society (Flower, 1996).

The casting of body parts became commonplace in Europe from the 12th century onwards (Schnalke, 1995). The artists of Renaissance Italy were the first to introduce wax models to medical practitioners, and these became indispensable as dissection practices started to inform anatomical studies. Back then, the borders between anatomy and art seemed more flexible than today. Artists like Andrea del Verrocchio (ca. 1435–1488) and Michelangelo (1475–1564) used wax models for their sculpture projects (Wilkinson, 2004b), at the same time Flemish physician Vesalius (1514–1564) created intricate drawings from human dissections that later illustrated his monumental treatise in Anatomy *De Humani Corporis Fabrica.*

Wilkinson (2004b) attributes the accidental discovery of the process for generating a countenance from the skull to Gaetano Giulio Zumbo (1656–1701), a wax sculptor from Syracuse. Zumbo got his reputation from a series of macabre theater-like tableaus that depict scenes of plague, death, and disease. In Florence, the La Specola Museum displays a realistic anatomical wax model of a head (Figure 1.8) in which Zumbo modeled the muscles, glands, and face on top of a real skull. The use of wax as a medium for sculpture in the 1700s proved to be a groundbreaking moment for anatomical research, allowing for the creation of extremely accurate and detailed anatomy models as the solution to counter the ephemeral nature of the bodies used in dissections (San Juan, 2018). Zumbo's work paved the way for sculptors like Abraham Chovet (1704–1790) and Ercole Lelli (1702–1766), who used the skeleton as a base to build muscles upon. They laid the basis for the first attempts in the realm of facial approximation, even if their main concern was not to depict a specific likeness (Wilkinson, 2004b).

Figure 1.8 - Anatomical head wax by Gaetano Zumbo, on display at the La Specola Museum in Florence.

"As poles to tents and walls to houses, so are bones to living creatures, for other features naturally take form from them and change with them (…)". This sentence attributed to Galen (129–200) embodies the theoretical framework under which the earliest notions of facial approximation were developed. The hypothetical existence of a correlation between the surface morphology of the face and the underlying bone became an increasing academic interest in the 19th century, and anatomists started to compare portraits, sculptures and death masks of historical figures to validate the identity of their remains.

Hermann Welcker (1822–1897), a German anthropologist and anatomist, is responsible for the first well-documented study on facial tissue depth to support the techniques used in facial approximation. Welcker gathered tissue depth values taken from the facial muscles of a sample of 13 men and used them to compare the outline of Immanuel Kant's skull with the outline of the philosopher's death mask (Figure 1.9) (Welcker, 1883). Welcker also compared the hypothetical skull of Raphael with a self-portrait of the painter and concluded that the relationships between them seemed to correspond (Verzé, 2009; Welcker, 1883; Wilkinson, 2004b).

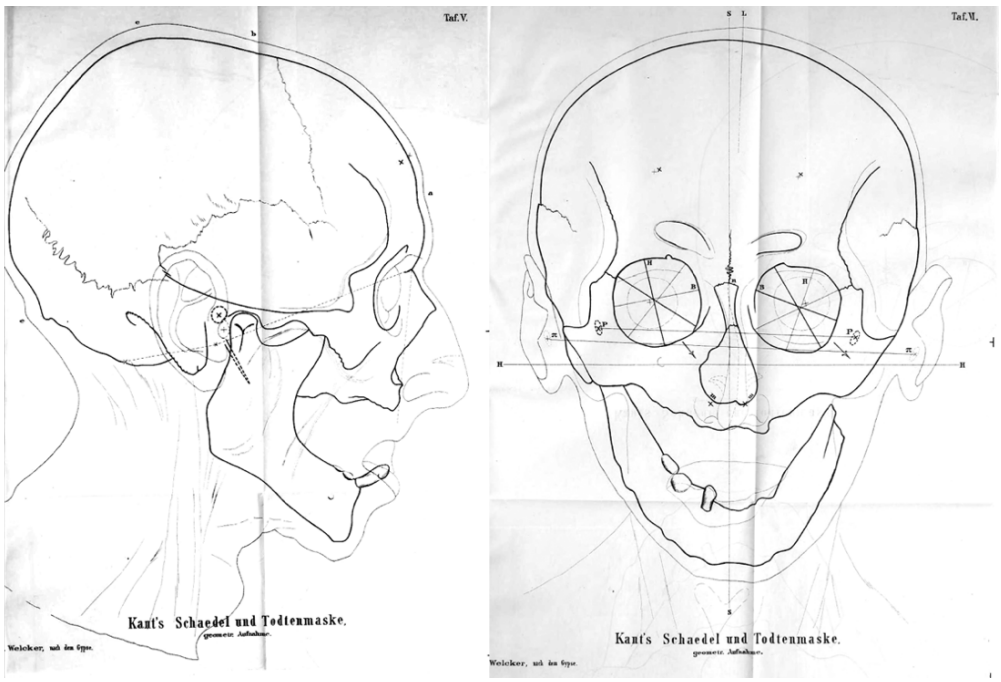

Figure 1.9 - Welcker's drawing of Kant's face superimposed on the skull (Welcker, 1883).

The facial approximation of composer and organist Johann Sebastian Bach (1685–1750) is frequently considered the first scientific attempt to identify someone through building layers of soft tissues into the skull (Prag & Neave, 1997; Verzé, 2009; Wilkinson, 2004b). Although Hermann Schaaffhausen (1816–1893) reportedly attempted a facial approximation of the head of a woman one year before Wilhem His and Carl Seffner's works, he relied on arbitrary soft tissue thicknesses (Vanezis, 2008). The facial approximation of Bach (His, 1895) was the result of the partnership between the Swiss anatomist Wilhelm His (1831–1904) and the German sculptor Carl Ludwig Seffner (1861–1932). Despite some previous unsuccessful attempts to identify Bach's grave, its precise location was still unclear at the end of the 19th century. Thus, following the efforts of Welcker a few years before, the main goal of the facial approximation led by His was to help determine if the skeleton exhumed one year earlier, in 1894, was that of Bach's (Zegers et al., 2009). The facial approximation (Figure 1.10), together with the clues provided by the local oral tradition and the estimated age of the skeleton found (a man, aged about 65 years old), led His to conclude that the remains were likely to belong to the German composer (Zegers et al., 2009). However, it should be noted that Bach's antemortem portraits were used to help the investigators produce the facial approximation (Stephan, 2015b). While objects such as death masks, antemortem portraits and photographs may qualify as useful references to compare with faces obtained through facial approximation methods, their integration in the process may also bias the results. Concerning the particular case of Bach, Zegers et al. (2009) suggest that there is not enough evidence to support or discard the positive identification proposed by His and Seffner in 1895.

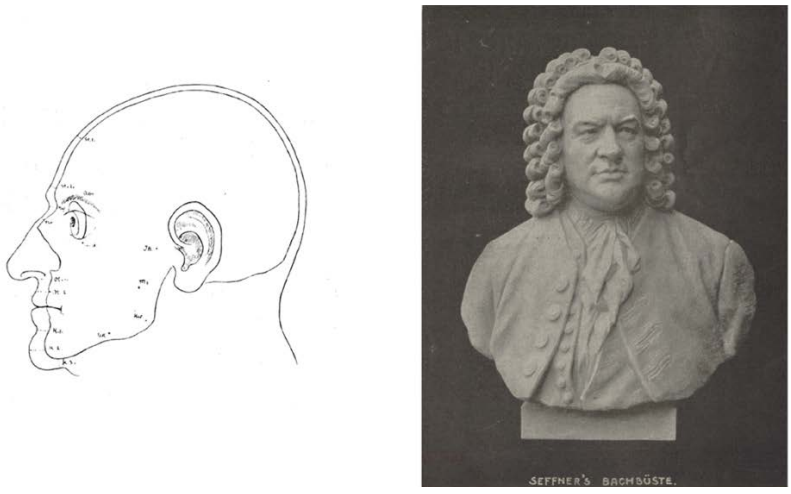

Figure 1.10 - On the left, Wilhelm His drawing of Bach's face upon the skull (His, 1895). On the right, the bust of Johann Sebastian Bach by Carl Seffner © gallica.bnf.fr / Bibliothèque nationale de France.

As mentioned before, these early attempts tried mainly to determine if the skeletal remains attributed to a famous or historical person belonged to them indeed. Besides the classical composer Bach, who gained a new facial approximation in 2008 (Hansen, 2008), the faces of Schiller (Welcker, 1883) and anonymous individuals from archaeological contexts (Figure 1.11) (Kollman & Bückly, 1898) were also built upon their skulls. These pioneers averaged the soft tissue data to four types of body type (thin, very thin, well-nourished and very well-nourished) and began to compare, compile and recommend specific guidelines for representing a face from a skull (Vanezis, 2008).

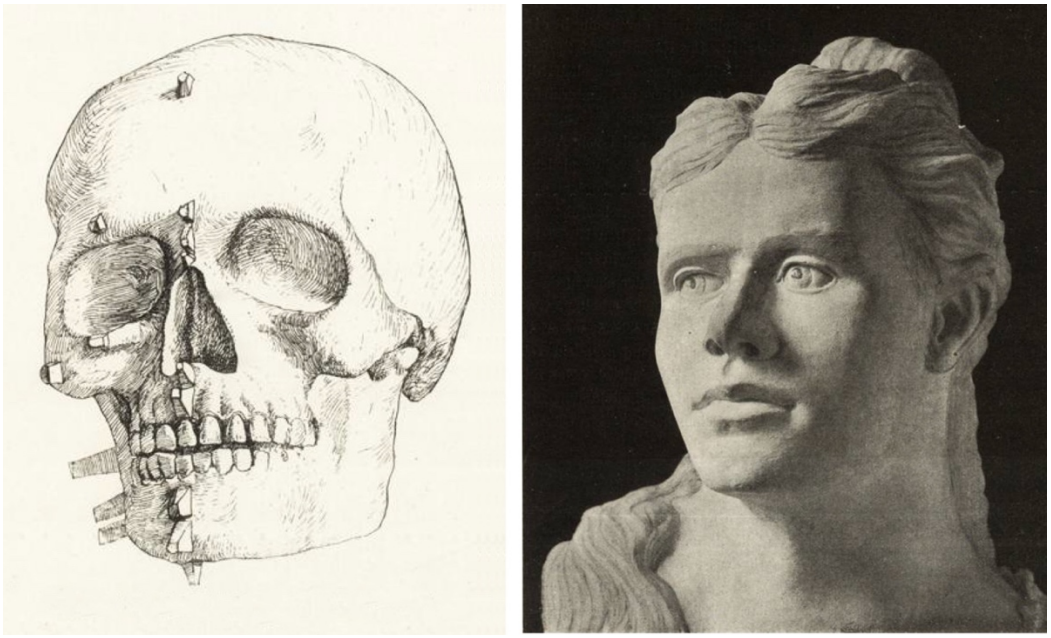

Figure 1.11 - On the left, drawing with soft tissue markers and, on the right, facial approximation of an Early Neolithic female from Auvenier (Kollman & Bückly, 1898).

From the 1850s onwards, the world witnessed the recognition of Neanderthal remains as being distinct from modern humans (1856) at the same time that evolutionary theories started to emerge after the publication of Darwin's "On the Origin of Species" in 1859. Early views on evolution began to replace the idea that humans or, according to the contemporary mindset, men were the major achievement of a divine maker. Thus, the existence of an extinct human species, with their seemingly more "primitive" features and

appearance, was discovered just in time to fill in the archetype of the "savage" from whence modern humans had evolved into a superior being (Schlager & Wittwer-Backofen, 2013). And so, along with the faces of prehistoric men and women, the skulls of Neandertals and other hominid species also started to lend themselves to experimentation with the newfound craniofacial techniques. In 1876, Schaafhausen produced the first representation of the face of a Neanderthal using the Feldhofer Grotto specimen, the first cranium to be found (Figure 1.12). The skull of the individual known as Feldhofer 1 or *Neanderthal* 1 is missing the facial portion. Despite that, Schaafhausen updated the drawing in 1888 to portray a more brutish and simian-looking individual (Schlager & Wittwer-Backofen, 2013).

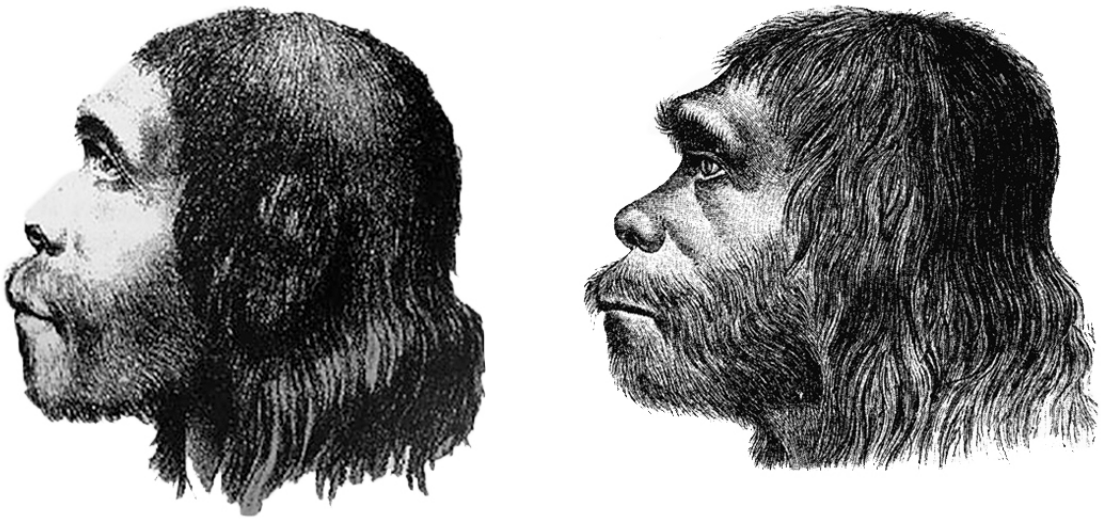

Figure 1.12 - On the left, first representation of a Neanderthal face. On the right, 1888 update.

By Hermann Schaafhausen. © Public Domain.

Finding support in the misleading interpretations of evolutionary theories, the representation of the faces and general appearance of extinct *Homo* species began to enable other narratives to fulfil notions of eugenics and nationalistic agendas. To some people's minds, looking at the faces of our ancestors with their "barbaric" appearances, "rude" features and "primitive" ways provided enough arguments for justifying their own racial superiority (Beatty, 2015). Around this time, face approximations, which had

already started to be built after scientific and anatomically informed guidelines, were used to reinforce a generalized view in which race was entangled with biology and evolution.

One of the most cited examples is that of the McGregor busts. In 1915, McGregor (1926) conducted a series of face approximations for an exhibition at the National History Museum in New York (Figure 1.13). As much as he tried to, according to his own words, "be conservative, to follow only the guidance of anatomical fact (…) and avoiding any inclination to make the result either bestial or brutal" (McGregor, 1926), American paleontologist Henry Fairfield Osborn commissioned his work. The scientist, who was the President of the American Museum of Natural History and a declared eugenicist, directed much of his energy and funds to popularize the visual displays and dioramas that are still one of the hallmarks of the institution (C. A. Clark, 2001). However, Osborn was more concerned with spreading his moralities and ideas of racial hierarchy than with science itself and not only manipulated diagrams and hominid family trees but also intentionally imbued the museum displays with his own beliefs (Haraway, 1989).

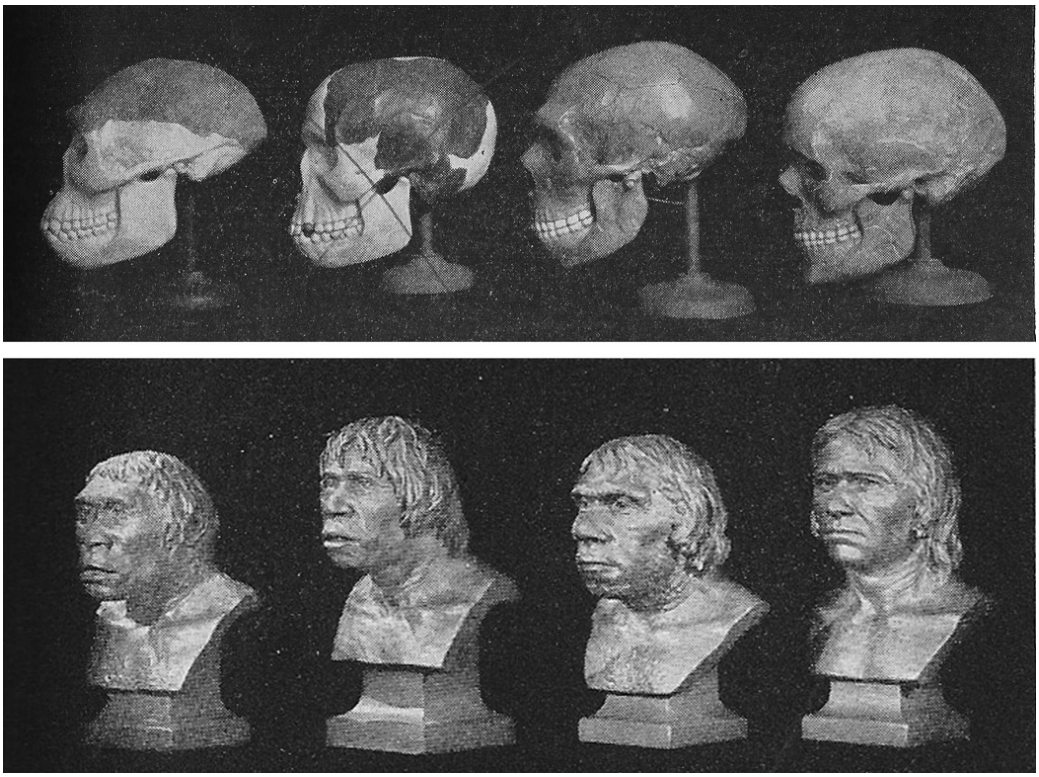

Figure 1.13 - Skulls of Java man, Piltdown man, Neanderthal man and Cro-Magnon man and McGregor busts below. © American Museum of Natural History.

The literature on the historiography of facial approximation often refers to the existence of two leading schools throughout the middle of the 20th century: the anatomical or "Russian method", whose most prominent figure was Mikhail Gerasimov (1907–1970), and the American school, pioneered by anthropologist Wilton Krogman (Prag & Neave, 1997). These two approaches have been set apart by highlighting two different courses of action. While the Russian school has been generally defined as having a process that relies on modeling each of the facial muscles on the skull, the American method uses tissue depth averages to determine the surface of the skin (Prag & Neave, 1997; Taylor, 2001; Wilkinson, 2004b). However, as we shall see in a moment, this dichotomy is not entirely correct.

Mikhail Gerasimov was perhaps one of the most prolific practitioners, having produced more than 200 reconstructions of faces from dry skulls (Gerasimov, 1971). We may find faces of hominids, Neanderthals, historical figures like the Timurids and Ivan the Terrible, and forensic cases among his work.

Ullrich and Stephan (2016) recently provided a synthesis of Gerasimov's method as he explained it in *Vosstanovlenie lica po cerepu* (1955), alleging that the published literature perpetuated some misinterpretations by referencing *The Face Finder* (Gerasimov, 1971), which is an abridged English translation from the Russian original. Gerasimov started by examining the skull to make notes regarding ancestry, age, and sex and then articulated the mandible in anatomical occlusion. At first, only one side of the face was modeled, leaving half of the skull visible for reference. After this initial assessment, Gerasimov removed the first application of clay to model the face again as a whole. Contrary to common assumptions, the Russian anthropologist did not sculpt each muscle upon the skull. Instead, he modeled only the muscles of mastication (temporalis and masseter). Gerasimov considered the muscles of facial expression ambiguous because their bony insertion points are not evident (Ullrich & Stephan, 2016). The next page (Figure 1.14) provides an insight into Gerasimov's process, extracted from *Vosstanovlenie lica po cerepu* (1955).

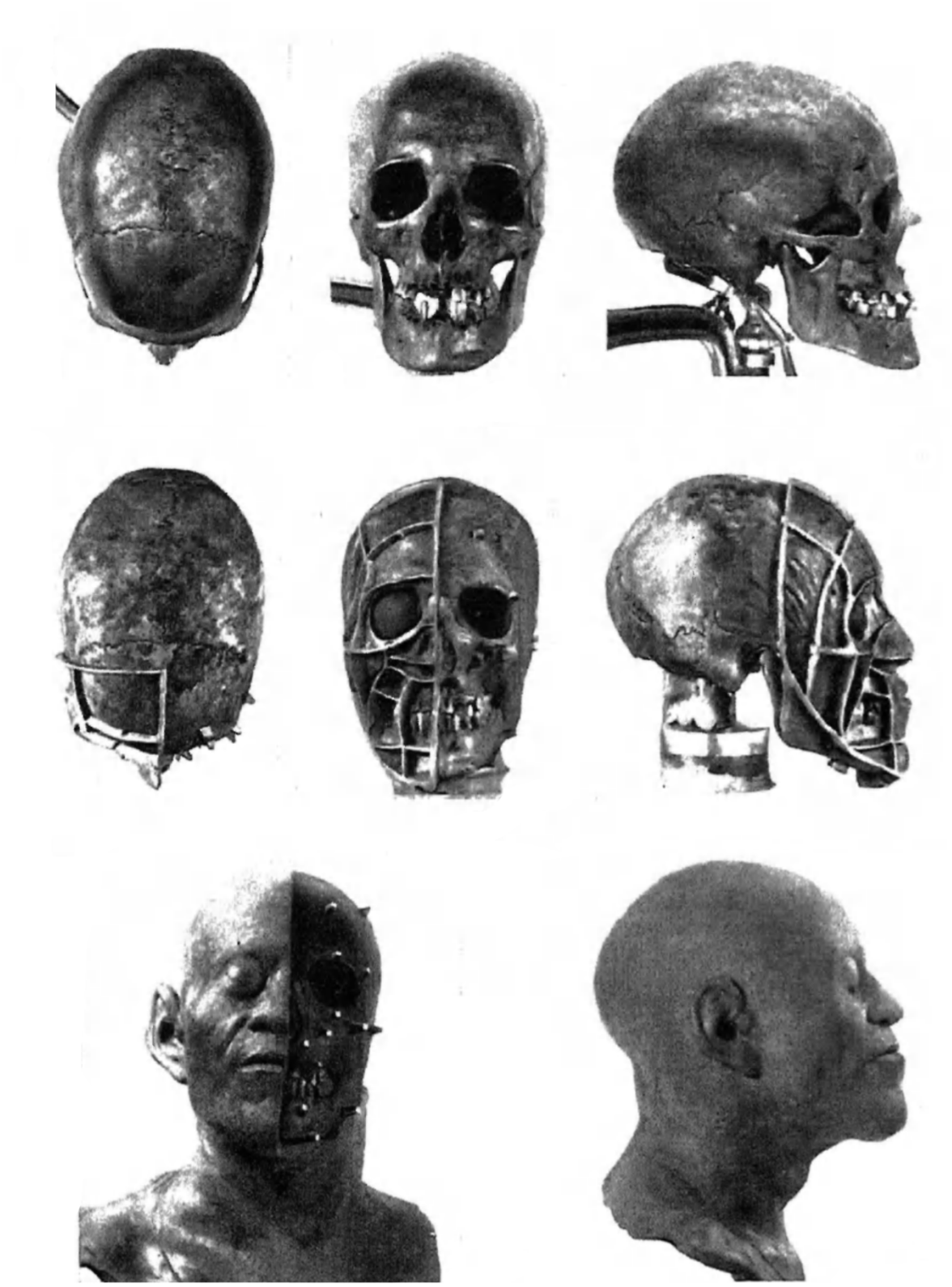

Figure 1.14 - Gerasimov's process of facial approximation. Top row: skull in three views; middle row: addition of depth stripes to inform the soft tissue outline; bottom row: final stages. From Gerasimov (1955).

As shown in the previous figure, the generalized idea that Gerasimov did not use soft tissue averages is also incorrect. In fact, Gerasimov gathered and published soft tissue depth means (Table 1.2), and his methods were inspired by those of the German anatomists, who were among the first known to use soft tissue thicknesses to define the face contour (His, 1895; Kollman & Bückly, 1898; Merkel, 1900; Welcker, 1883). Gerasimov built the tissue depth markers directly upon the skull using his formulation of modeling mastic (Ullrich & Stephan, 2016). Then, he proceeded to connect the points by creating narrow profiles and a mesh to guide the placement of the remaining tissues. A few of Gerasimov's guidelines still perform better than more recent published alternatives. His approach to estimate the anteroposterior eyeball position provides better accuracy ratings than American standards (Stephan, 2002a), and the method to predict the projection of the nose still relies on the two-tangent guideline described by the Russian author.

Table 1.2 - Soft tissue thicknesses (in mm) of 71 individuals used by Gerasimov.

Adapted from Gerasimov (1955) and Ullrich and Stephan (2016).

Landmark	Male	Female
Points in the Median Plane		
Metopion	6	5
Glabella	8	6
Nasion	6	6
Rhinion	3	2
To the side of the anterior nasal spine	11	10
Upper lip	12	10
Lower lip	8	9
Mentolabial sulcus	9	8
Pogonion	9	8
Points in the Frankfurt Horizontal Plane		
Near the edge of the aperture piriformis	3	2
Middle of the frontal process of the maxilla	4	2

Just under the orbit	4	3
The most prominent point at the frontal part of the zygomatic arch	7	5
At the zygomatic suture	7	3
The most prominent lateral point on the zygomatic arch	6	3
Above the temporomandibular joint	5	4
In the area of the ear, behind the zygomatic arch	4	3
At the lambdoidal suture	6	4
At the most prominent point on occipital bone	8	5
Additional Points		
Over the anterior lacrimal crest	3	2
Alongside the aperture piriformis at the height of the crista conchalis	3	2
Adjacent to the corner of the apertura piriformis where the inferior rim turns into lateral rim	3	3
Lateral rim of the orbit near the malar tubercle	3	3
Gonion	6	4

Gerasimov's work granted him worldwide recognition even outside of the scientific world. He inspired the character of Professor Andreev, a genius anthropologist from the University of Moscow who specializes in sculpting faces from past individuals in Martin Cruz Smith's crime novel Gorky Park (1981). On a curious side note, the process featured in the film adaptation of Smith's story in 1983 shows the combined use of muscle anatomy and soft tissue depth markers. This event has been reported as a technical error under the assumption that the Russian school did not rely on tissue depths (Taylor, 2001), but in fact is not that far from Gerasimov's true approach to sculpting these faces. Nowadays, Mikhail Gerasimov's legacy is very much alive in Russia and investigators such as Galina Lebedinskaya, Tatiana Balueva, and Elizaveta Veselovskaya (Balueva & Lebedinskaya, 1991; Balueva et al., 2009; Balueva et al., 1988, to cite a few) continue to contribute to research in facial anatomy and anthropology.

On the other side of the Atlantic, the "American school", also known as the tissue depth method, is known for applying average skin-thickness measurements at specific landmarks on the skull, which are then connected with uniform stripes of clay to guide the placement of the soft-tissues (Taylor, 2001). After looking at Gerasimov's process (Figure 1.14) it is hard not to notice the methodological resemblances. Perhaps this misunderstanding is a consequence of the poor communication and tense relations between the United States and the Soviet Union throughout most of the 20th century, together with the fact that most of Gerasimov's written ideas are either in Russian or in abridged German or English translations. In any case, the contributions from American practitioners cannot be overlooked or underestimated.

The attempts of Wilder (1912) are the first known facial approximations produced in the United States. The anatomist applied the methods and data of European predecessors to sculpt the faces of New England indigenous populations (Figure 1.15).

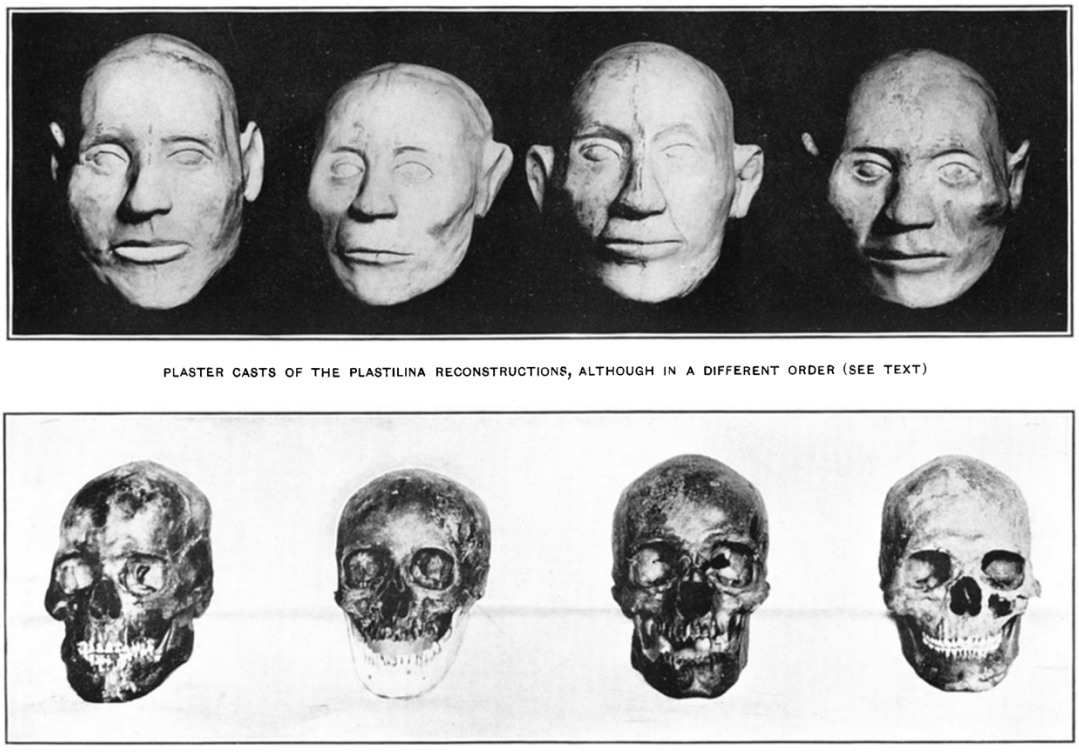

PLASTER CASTS OF THE PLASTILINA RECONSTRUCTIONS, ALTHOUGH IN A DIFFERENT ORDER (SEE TEXT)

Figure 1.15 - Wilder face approximations with the respective skulls below (Wilder, 1912).

But it was not until a few years later, around the same time that Gerasimov was developing his methods in the Soviet Union, that the "American school" started to gain a real interest in these techniques. In 1946, the anthropologist Wilton Marion Krogman (1903–1987) began collaborating with sculptors McCue and Frost, aiming to assess the accuracy of facial representations. Krogman started by selecting a corpse and, after taking photographs of the face, he would dissect it. Then, the sculptors would use the skull to perform a facial approximation based on the individual's anthropological profile and soft-tissue datasets (Wilkinson, 2004b).

Working together with anthropologist Clyde Snow, Betty Pat Gatliff (1930–2020) is maybe the most recognizable name in the field. She became known for sculpting the face of Pharaoh Tutankhamun (Figure 1.16) and working on highly mediatic forensic cases such as those of the victims of serial killer John Wayne Gacy.

Figure 1.16 - Betty Pat Gatliff with facial approximation of King Tutankhamun with headdress in 1984.

By 1980, Gatliff had already taken on almost 50 forensic cases where about 70 per cent had led to positive identifications (Cassill, 1980; Gatliff & Snow, 1979). Gatliff, a prolific lecturer, imparted numerous workshops in the United States which were attended by other well-known forensic artists such as Karen Taylor (1952–).

Drawing on the experience of German, Russian and American practitioners, Richard Neave (1936–) became involved with the Manchester Mummy Team at the University of Manchester and began working on the faces of two brothers from the 12th Dynasty of Egypt (Prag & Neave, 1997; Wilkinson, 2004b). The relationship between Nekht-Ankh and Khnum-Nakht is known from the inscriptions on their coffins and was recently confirmed by aDNA sequencing, but the morphology of their skulls and postcranium shows remarkable differences and had argued against a shared family-line (Drosou et al., 2018). Neave's approach incorporated guidelines published by Gatliff (1984), Krogman and İşcan (1986) and George (1987) and coined what has been known since as the combination or the Manchester method. Wilkinson (2004b) reports that Neave and his team worked on around 20 faces for forensic investigations, which had a success rate of 75 per cent, along with many archaeological cases such as the face approximation of Philip II of Macedon and the bog body known as "the Yde Girl".

Caroline Wilkinson (1965–), a graduate of Manchester herself, has been championing forensic techniques for the past two decades and, together with her research group at Liverpool John Moores University, bridging the gap between traditional and computerized methods (Figure 1.17). Her research team focuses not only on the production of facial representations, many times using haptic technology, but also investigates the methods, guidelines, and accuracy of facial approximation.

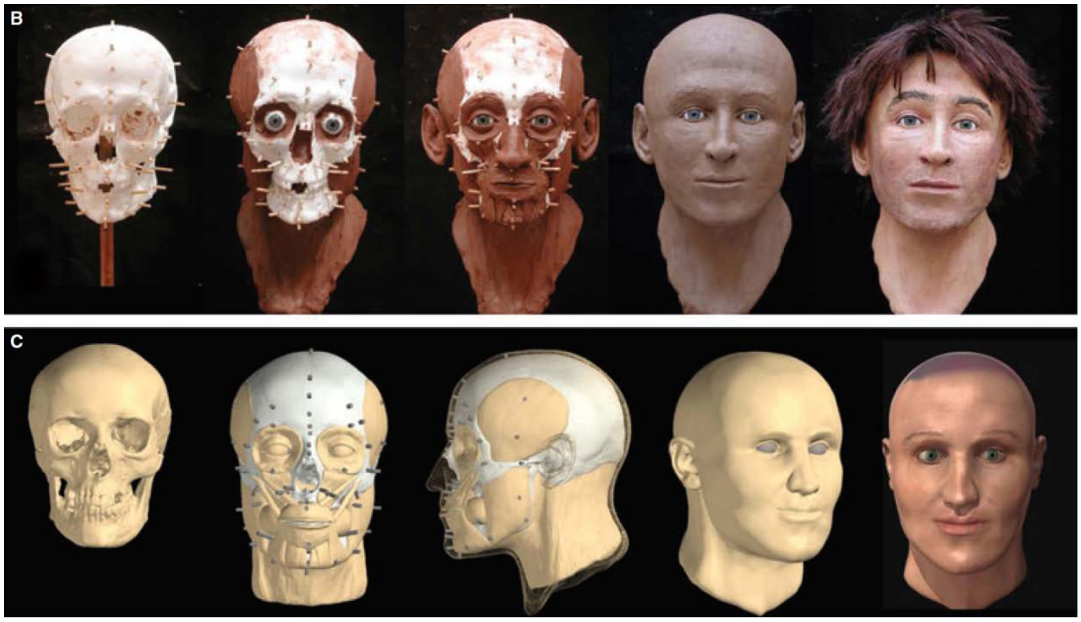

Figure 1.17 - Two approaches to three-dimensional face approximation. On top, traditional techniques. Below, computerized approach. Both by Caroline Wilkinson, adapted from Wilkinson (2010).

I believe that it does not make too much sense to talk about Russian or American "schools" of facial approximation, especially now that it has been established that both methods draw on very similar principles and practices. Doing so seems to be a perpetuation of an idea more fitting to the geopolitical context of the mid-20th century. The guidelines to sculpt or draw faces from skulls have been applied, tested, discarded and reformulated over the years. Still, the tendency to rely on soft tissues goes back to the late 1800's, to the very first attempts produced by the German anatomists. The Manchester method also stems from this same continuum, and so do most of the practices of researchers working in craniofacial approximation today. Perhaps the visual appearance of how the technique is used by different practitioners, with some using small triangles, narrow stripes, or thin cylinders to represent the tissue depths, has induced historians to think that there are other underlying principles. There is no doubt that the practice changed when it comes to is the amount of available data, how the information is processed, and which criteria define its application. However, the general method is not so different across the globe and the centuries.

After more than one hundred years of practice, facial approximation has come a long way and still has a long way to go. Hopefully, in the coming years, we will continue to see more varied and more stable datasets and the ongoing improvement of current guidelines and their applications to different populations. However, I will dare to say that the field's most promising research line for the future decades lies in the possibilities of genetic phenotyping techniques and how far these can be integrated into current methodologies. Recent DNA studies have provided insight into which genetic markers associate with facial width, eyebrow width, the distance between eyes, columella inclination, nose bridge width, nostril width and mouth shape (a non-exhaustive list of references includes Cole et al., 2017; M. K. Lee et al., 2017; Liu et al., 2012; Liu et al., 2015; Marano & Fridman, 2019).

DNA research has also been investigating which genetic markers predict externally visible characteristics (EVC), such as the color of the iris, hair color and structure, skin color and facial shape. There are already some tools available, such as the HIrisPlex system[4] (Chaitanya et al., 2018; Walsh et al., 2017; Walsh et al., 2014), which can be used to incorporate genetic data into facial approximations. A well-known example is that of the facial approximation of Richard III made by Wilkinson, whose eye and hair color was initially darker. However, the phenotype predictions published afterwards showed that the skeleton identified as Richard III had a 96 per cent of probability of having blue eyes and 77 per cent of probability of having blond hair (King et al., 2014). The release of the new evidence promptly motivated a revision of the facial features of the face of Richard III to keep up to date with the most recent information.

1.4 A place for the face in Archaeology

Many questions surround the pertinence of facial approximation in an archaeological context. Why do we need these faces, and for what? Are they not visual byproducts of assumptions we make from fragmented realities? Do they not yield countenances that have an unspecified degree of inaccuracy? And do they not

[4] The IrisPlex System is a tool that can accurately predict blue and brown eye color based on a DNA input.

result in educated guesses that often, if not most times, cannot even be compared to the real faces and hence used to produce testable scientific hypotheses? I mentioned earlier that forensic practitioners are the first to acknowledge the limits that permeate the field. I believe to attempt formulating an answer to the significance of the face in archaeological research requires first a reflection on how and why we illustrate the past.

Archaeology, and especially prehistoric archaeology, dwells in *unknown unknowns* and *unknown knowns*. While the former encompasses all things whose existence we are not aware of, the latter refers to those things we know once existed, but the true extent of their nature is mostly obscure to us. Let us take an example by Raimund Karl (2015): a posthole, at some point in time, contained a post. That we know. Suppose the posthole is all we have as evidence. In that case, we do not know exactly how high the post was (even if we can estimate its maximum height based on its maximum possible width), whether it was round or square above the ground, or whether it was plain or decorated or a mix of both. This fact is relatively simple to explain and understand when we put it in words. There was a post in the posthole, but we do not have it anymore and do not know exactly how it looked. But if we want to materialize that idea in one archaeological illustration which depicts that post, there is only one possibility: the post cannot be simultaneously plain and decorated; it has to be depicted in one or the other way. A decision has to be made, and often there is no particularly good reason to choose one option over the other. It comes down to a judgment made by the artist and the archaeologist if they are not the same person.

Usually, a more cautious stance is advised not to make unfounded assumptions and avoid speculation as much as possible. Archaeologists are more often inclined to follow Occam's Razor (much to the artists' occasional despair) and go against making more assumptions than those strictly necessary to finish the image. Therefore, and according to parsimony guidelines, a drawing of the post would show its location very precisely, but the post itself would be plain and round like a tree trunk because the easiest solution would be just to cut a tree and place it in the hole (Karl, 2015). This way, we achieve our goal of visually presenting an archaeological interpretation (the existence of a post) from hard evidence (the posthole) without making a compromise that would have taken us, for instance, to generate further assumptions and speculate on how certain decorative elements would have looked.

Alas, following this process instils a false sense of accuracy in our visual representations of the past. Because we rendered the *knowns* precisely and minimized the amount of speculation filling the gaps, we say that we made the "drawing to the best of our knowledge", often without having a clear distinction between what we know and what we do not. On a second level, this circumstance can also make our rendering of the *unknowns* look like a deliberated preference for minimalistic choices from those past societies. By not making assumptions, we are making one and reinforcing a rather dull image of prehistoric people. Ultimately, that dull view becomes a repetitive pattern in our illustrations and leaves an imprint on our perceptions of life in Prehistory and how we convey them to others (Karl, 2015).

In this light, Occam's Razor becomes a double-edged sword. Adopting parsimony as a theoretical framework for archaeological illustrations will result in visualizations that look similar in their minimalistic appearance. How would an illustrator represent the architecture of the Han Dynasty of China (206 BCE–220 CE) if there were no pottery models of their buildings (Figure 1.18) or other contemporary references? It is a rhetoric question that aims to show that we should not deny these societies the possibility of being ingeniously creative, even if we cannot see it objectively anymore and probably never will. On the other hand, disregarding parsimony principles altogether will likely lead us into a swamp of inaccurate speculation that lacks scientific support from archaeological evidence. And this is not ideal either because our final aim as researchers is to know *how things were* and not *how we think things were*.

Figure 1.18 - Central Watchtower. Eastern Han Dynasty (25–220).

Collection of The Metropolitan Museum, New York.

It seems that I just painted a very hopeless scenario that echoes not only the thoughts of Lull (1988) but also the words of Edmonds (1999) when he said, "the past is dead and, we cannot reconstruct it as it was". Still, formulating archaeological interpretations is essential. So, how do we fill the gaps?

Conway et al. (2012) did an interesting exercise that ultimately originated what has been known as the *All Yesterdays* movement in the field of paleontological illustration. *All Yesterdays* revolves around the concept that there is a lot about extinct animals that is unknown and unknowable, but that does not imply that artists should always settle for the safety net that parsimony can be. Extinct creatures were undoubtedly as diverse as extant animals, engaged in curious behaviors and put themselves in ludicrous situations. Thus, Conway and colleagues advocate the need to break away from the recurring stereotypes perpetuated by "traditional paleoart" and that artists should take an active stance in proposing new behavioral interactions, color schemes and postures. As long as the depicted species follow rigorous musculoskeletal reconstructions[5] and the illustration is grounded on educated guesses, new ways of looking at the past are more welcome than perpetuating among the public images already seen before. That does not mean that a particular scene happened precisely how we may portray it in our drawings, but it means that it is conceivable and contemplating it contributes to a richer overview of these prehistoric times.

I believe that any visual representation, be it paleontological, biological or archaeological, would benefit from the same mindset and approach. Reconstructing biological organisms obeys to certain constraints that cannot be fully extrapolated to human-made constructions or artefacts[6]. However, the idea of being able to display a wide range of possibilities is an incentive to open up new discussions and avoids

---

[5] Reasonably enough, the authors also attribute the existence of repeating patterns in the way we see extinct animals because many artists work under near-impossible deadlines and are very poorly paid. Moreover, often artists work with very little support from scientific advisors and experts. Working under this context is not the best setting to develop new and engaging concepts and compositions. Having worked as a freelancer illustrator myself for both paleontology- and archaeology-related projects, I can confirm this is usually (and unfortunately) the rule and not the exception.

[6] Biological organisms are natural objects that come into being without the need of human intervention, while artifacts are objects are produced by humans (Lull, 1988, 2017).

conditioning our perception of the past towards a specific result. Karl (2015) touches on this subject when he proposes two solutions to tackle this challenge. We can create reliable reconstructions that clearly show the difference between the hard evidence and the uncertain elements, or we establish a confidence interval by illustrating the range of possible choices instead of selecting just one. A recent example, the face reconstruction of the Egyptian mummy Ta-Kush (Smith et al., 2020), follows this philosophy and presents four different iterations of what her appearance might have been. The authors explain this build-up as a part of a humanization strategy that focuses not only on providing the visitors with a more emotional and interactive experience but also on bringing dignity and respect to the curation and display of human remains. Paired with an accessible 3D print of her face, which delivers a tactile object that enhances the museum experience, Ta-Kush is first depicted with what would have been her natural appearance, which is potentially more relatable and familiar to the contemporary visitors. Then, with the progressive addition of make-up, jewelry and wig (Figure 1.19), Ta-Kush slowly regains what could have been her more "public" or social aspect.

Figure 1.19 - Face approximation of Ta-Kush showing four different possibilities: unadorned, then with make-up, jewelry, and wig. From Smith et al. (2020).

In the end, both archaeologists and illustrators are bound by conventions and the hard evidence excavated from the field. Yet, thinking, researching, writing, and illustrating the past are ultimately all creative endeavors that only seem different because they use different media and languages.

Hopefully, I laid out my arguments as to why illustrating the past is an important exercise, even if it is impossible to retrieve all the variables. So, let us come back to the questions at hand: why knowing (or attempting to know) someone's face can be of any relevance in archaeological research? And how can a face that has never been seen and cannot be recognized have an impact or even change a particular archaeological narrative?

Expressions that include the word *face* permeate our daily communication, and I would dare to say that most languages have idioms using the equivalent of this English word. An expression like *face-to-face* denotes a sense of proximity between two people. *Written all over someone's face* is said of an emotion or thought evident by one's facial expressions. Having a *red face* shows embarrassment; a *blue face* shows exhaustion; a *long face* shows sadness; a *faceless* person is either anonymous or lacks character. Sanders (2009) mentioned that the "grammar of the face is complex". It is indeed, and even though we can *wear* our emotions in our faces, they are not always easy to read and understand, as being *two-faced* is sometimes also a part of our human condition. Thus, faces are not only a vessel for our own emotions but are at the very core of our interactions as social beings, a synonym for identity and personality.

Eventually, what we do when we try to recreate a face from an archaeological burial is to invest a face with historical meaning (Sanders, 2009). Both news media and academic press are prolific in such assertions: "the face of a medieval man", "Stone Age man's face", "putting a face in Prehistory", even this very project when the research team informally designates it as the "Faces of El Argar". By doing so, we are adding yet another layer to a face by allowing it to become a symbol. History has a record of relying on images of past countenances to shape or even create the necessary socio-cultural background to propagate theories about past humans (Moser, 1992). In the previous section, we saw how dangerous symbols could become when they are subverted to spread nefarious ideologies. Maybe that is why many are so skeptical concerning the contribution of such visualizations to the scientific dialogue. The layers of uncertainty, the inherent difficulty in assessing the complex relationships between hard evidence and the more ephemeral aspects of life raise justifiable suspicions every time we are allowed to "gaze upon the face of our ancestors".

So, our faces lay in a limbus. They are what they are, they what we see in the mirror, and they are what others make of them. But beyond the fascinating reflections concerning the philosophical, social and

symbolic value of the face, this thesis has a more specific (but no less ambitious) task. It aims to assess whether the study of the face through facial approximation can contribute to the study of kinship in excavated human remains. Our approach is inspired by that of Musgrave et al. (1995) (discussed in section 4.2, Chapter 4) but goes one step further. Instead of drawing only on visual analysis, it relies on the geometric morphometrics' toolset to examine face morphology and generate a quantitative estimation of facial similarity. Future analyses, contrasting the morphological data with the aDNA results will help determine if their faces echo their genetic history.

Chapter 2

2 A grain of salt: criticism and limitations

~

The discussion regarding the use and pertinence of facial representations made from skulls is not without justification. As we saw in the previous chapter, criticism arose early on and transpired from multiple aspects. The first relates to how decomposition affects the morphology of organic materials and how these processes can affect the outcome of a craniofacial depiction. As decay interferes directly with the bony substrate upon which facial approximations are built, it can also permeate the subsequent layers with error. Secondly, the so-called disparity in recognition rates published and the threads that inform how we perceive things. And finally, human biology itself. Hence the necessary look into why the pursuit of accuracy in facial approximations should be "taken with a grain of salt".

2.1 The taphonomic process

Several questions arise before assessing a skull for facial approximation. How old are these bones? Is it a modern human or a more ancient relative? How old was this individual at the time of death? Was it a female? Was it a male? Can we determine its populational affiliation, where he or she came from? Are there any indicators regarding body mass? Are there any visible pathologies or traumas that would affect the face? If there are traumas, were they already healed when this person died? What was the possible cause of death? The answers to these questions create a biological profile that will inform the selection of the methods and specific guidelines to attempt a craniofacial approximation.

Nonetheless, the amount of information that can be retrieved from skeletal remains is also dictated by the biological and environmental processes that occur from the instant a living organism dies to the moment of its recovery or (re)exposure to the elements. When researching archaeological remains, this span of time can go from decades, to hundreds, to thousands of years, but when it comes to extinct hominids the clock goes back millions of lifetimes.

These processes are commonly referred to as "taphonomic" or "taphonomy", a term coined by the Russian paleontologist Ivan Efremov in 1940, in a paper where he defined it as the "science of the laws of embedding", meaning "the study of the transition (in all its details) of animal remains from the biosphere into the lithosphere" (Efremov, 1940). This new branching of Paleontology sought to address the "incompleteness of the geological chronicle" and provide a research scope that allowed to estimate the amount of information lost or deformed in that transition from *bios* to *lithos*. According to Efremov, biological remains undergo a series of macro- and micro-scale transformations, and therefore should be perceived as altered representations of once-living organisms to create a less biased interpretation of the Past. Since Efremov's first (but not pioneering[7]) thoughts, the term has broadened its significance to include the in-between stages of that transition, focusing on how and why it happens the way it does (Lyman, 2010). Neighboring fields such as zooarchaeology, paleobotany, biological anthropology and forensic science also incorporated and adapted these concepts to answer specific concerns. These concepts address questions such as whether modified animal bones were used as prehistoric tools or if the selective preservation of certain animal bones does reflect a pattern of food consumption in a given archaeological community. In this manner, cultural modifications of biological objects become integrated within the range of possible taphonomic processes (Bartosiewicz, 2008; Lyman, 2010).

When a living being finally finds its resting place, whether naturally or because there was an intention of leaving it there, the environment plays a decisive role in preserving the remains. Besides the presence of different agents (bacteria and insects) that actively fasten the process of decay, external factors

---

[7] Efremov's proposal drives inspiration from the previous works of William Buckland (1784–1856), Charles Lyell (1797–1875), and even Charles Darwin (1809–1882). Further information about the earliest investigations that inspired Efremov's work can be found in Pokines and Symes (2013).

such as exposure to elements, humidity, accessibility to scavengers, temperature, type of soil and even embalming practices will influence the preservation of both hard and soft tissues (M. A. Clark et al., 1997; Nawrocki, 2016). Most of the time, bones and teeth are all that is left after a variable period of decomposition and, unlike other animals, humans found within archaeological contexts tend to go through a burial ritual that helps preserve the integrity of their skeletons (Bartosiewicz, 2008; Weber & Bookstein, 2011). Albeit unusual, soft tissues may also spontaneously prevail under very cool or arid environments: this is the case, for instance, of Ötzi, the Iceman (Spindler, 1994), the bog body known as Tollund Man (Glob, 1969) and, within our Argaric latitudes, the Mummy of Galera (Molina et al., 2003).

As organic decay interferes directly with the material evidence, which is our primary reference for producing facial approximations, it can also permeate the subsequent steps with error. Thus, understanding the taphonomic processes that might have affected the decay of an organism after death marks the beginning of the path to bring it "back to life". The first step in the taphonomical analysis of a human skeleton is quite straightforward because the comparative framework is well-known. Unlike more ancient fossil examples, which are often limited to only one specimen, having a comparative model and knowing how a "normal" *Homo sapiens* skeleton should look is a significant advantage to retrieve these bones to their original state (Lyman, 2010). However, if face morphology is so highly dependent on specific skull shapes and minor variations, then these generalizations should be addressed carefully because they might have a major impact on the final results. Is it safe to assume that any and all deformations will present a significant challenge to produce an unbiased craniofacial approximation? That said, is it possible to retrieve a skull to its original shape and work from a less subjective reference?

2.1.1 Working from dry skulls

Even with the best-preserved remains, it is impossible to overcome the fact that an approximation attempts to build a "living face" from a dry skull. In-vivo bone contains a percentage of water that varies from bone to bone and is also dependent on age, state of nutrition, rate of growth, and species (Huggins, 1937). When

a living organism dies, the body enters a series of decomposition stages during which soft tissues break down, body fluids escape, and all that remains is dry skin, cartilage and bones (Weber & Bookstein, 2011). The level of preservation of these remains will, as mentioned before, depend on the setting in which they rest and will likely undergo dimensional changes in response to humidity conditions. In fact, a number of earlier studies already demonstrate that hydration-related alterations can introduce a variable amount of error in skull measurements both in animal and human bones (Table 2.1).

Table 2.1 - Studies reporting on the impact of humidity on skull measurements (human and non-human samples).

Studies	**(N) and sample**	**General conclusions**
Broca (1874)	(13) Human.	Skulls exhumed from a humid soil may shrink considerably (up to 20 cc of their cranial capacity). If left out in a humid environment, skulls can absorb up to three to four percent of their weight in water. Dry skulls immersed in water can experience an increase that goes up to 50 cc.
Todd (1923a, 1923b)	(24) Human.	Shrinkage is not scalable and does not depend on sex, age, ancestry, cranial thickness, shape and condition of sutures. Average reductions are 1.8 mm in length, 2.1 mm in breadth, and 1.7 mm in auricular height. Calculating capacity from linear dimensions taken in the natural state of the skull might result in higher values owing to the fact that the formula has been constructed from measurements upon dried skulls.
Todd (1925)	(49) Human.	Shrinkage equals between 0.6 and 0.8 percent of the final mummified cranial dimensions. These dimensions come at least to within 0.3 mm of the green state after maceration. After maceration, shrinkage owed to drying varies from 0.8 to 1 percent in relation to the dimensions of the green state.
Todd (1926)	(75) Human.	Shrinkage in mummification and expansion after maceration bear results consistent with Todd (1925). After maceration, shrinkage related with drying varies from 1.1 and 1.2 percent. Amount of shrinkage on drying depends on the atmospheric conditions and on the size or thickness of the bone itself. Shrinkage is not related with sex or ancestry.
(Albrecht, 1976, 1978, 1983)	(825) Non-human. Macaque skulls.	Increased skull size seems to be associated with increased humidity, but intra-observer measurement error cannot be completely discarded either.
Utermohle et al. (1983)	(2) Human. One treated and one untreated.	Evidence of cranial expansion as relative humidity increased in 32 out of 40 measurements, with an average of 1.5 mm. Some measurements like nasal height, orbital breadth, midorbital breadth and nasion-frontale subtense were invariant in all comparisons made.

Lindsten (2002)	(17) Non-human. Pig dental arches.	The results indicate that the crania in skeletal samples can be expected to be 0.3–1.7 percent smaller than in vivo.
Adams and Stephan (2005)	(12) Non-human. Rabbit.	Variation of two to three percent in measurements as humidity increased. Visible changes to the nasal bone morphology.

Broca (1874) and Todd (1923a) detected this occurrence when assessing cranial capacity, while Todd (1923b, 1925, 1926) also reported increases and shrinkage in linear measurements that were related to humidity fluctuations. Albrecht (1976, 1978, 1983), who examined and measured a large sample of 825 macaque skulls, also accounts for significant differences in cranial dimensions that may be attributed to external humidity changes.

Utermohle et al. (1983) experimented on one treated[8] and one untreated human cranium and found that out of 40 measurements, 32 presented variations when the skulls were subjected to different humidity conditions. The total increase in relative humidity between the testing periods was >80%, and the untreated specimen displayed an average increase of 1.5 mm in 31 of the 40 measurements. Table 2.2 shows the values gathered by Utermohle et al. (1983) and the most relevant measurements for craniofacial approximation in bold.

Table 2.2 - Humidity effects on craniometric measurements in an untreated skull, in mm. *I* <18% relative humidity; *II* 36% r.h.; *III* 98% r.h.; *IV* 44% r.h. (1) Invariant measurements in all the comparisons. Adapted from Utermohle et al. (1983). Measurements definition from Howells (1973), as per the original study.

Abr.	**Definition**	**I**	**II**	**III**	**IV**
GOL	Maximum cranial length	190	191	193	191
NOL	Nasio-occipital length (maximum length in the mid-sagittal plane)	186	187	188	187
BNL	Basion-nasion length	108	109	110	109

[8] One of the specimens was previously treated with a coating of polyvinylacetate (PVA).

BBH	Basion-bregma length	141	141	143	141
XCB	**Maximum cranial breadth**	**140**	**141**	**142**	**141**
ZYB	**Bizygomatic breadth**	**136**	**137**	**138**	**137**
AUB	Biauricular breadth	126	126	128	127
ASB	Biasterionic breadth	105	106	107	106
BPL	Basion-prosthion length	103	103	104	103
NPH	**Upper facial height (nasion-prosthion distance)**	**79**	**79**	**80**	**79**
JUB	**Bijugal breadth**	**121**	**122**	**123**	**122**
NLB	**Nasal breadth**	**22**	**22**	**23**	**22**
XML	**Maximum malar length**	**61**	**61**	**62**	**61**
ZMB	**Bimaxillary breadth**	**112**	**112**	**114**	**112**
SSS	**Zygomaxillary subtense**	**29**	**29**	**31**	**30**
FMB	**Bifrontal breadth**	**93**	**93**	**94**	**93**
EKB	**Biorbital breadth**	**97**	**98**	**98**	**98**
WNB	**Simotic chord (least breadth across the nasal bones)**	**6**	**7**	**7**	**7**
GLS	**Glabella projection (from nasion-supraglabellare chord)**	**7**	**7**	**7**	**7**
FRC	Nasion-bregma chord	113	114	115	114
PAC	Bregma-lambda chord	113	114	115	114
OCC	Lambda-opisthion chord	100	100	101	100
BRR	Bregma radius	122	123	124	123
LAR	Lambda radius	109	109	110	109
NAR	**Nasion radius**	**102**	**103**	**103**	**103**
PRR	**Prosthion radius**	**111**	**111**	**112**	**111**
SSR	**Subspinale radius**	**104**	**105**	**106**	**105**
ZOR	**Zygoorbitale radius**	**90**	**90**	**91**	**90**
FMR	**Frontomalare radius**	**89**	**89**	**90**	**89**
EKR	**Ectoconchion radius**	**80**	**80**	**81**	**80**
ZMR	**Zygomaxillary radius**	**76**	**76**	**77**	**77**

NLH	**Nasal height**	**(1)**
OBH	**Orbital height**	**(1)**
WZH	Minimum height of the zygomatic	(1)
FOL	Foramen magnum length	(1)
NAS	**Nasion-frontale subtense**	**(1)**
ZOB	**Zygoorbital breadth**	**(1)**
OSR	Opisthion radius	(1)
BAR	Basion radius	(1)

While some studies (Todd, 1925, 1926) mention that macerated skulls approximate the dimensions of the green state, it is worth pointing out that the numbers from Utermohle et al. (1983) refer to the effects of external humidity on a dried cranium. It is not clear whether the impact of extreme external humidity also approximates the values of the green state, but it is worth noting that some measurements do present a variation of 2 mm (Figure 2.1). Whether these variations in measurements can become significant impairments to a positive identification, by altering drastically the appearance of someone, it is something that remains to be tested.

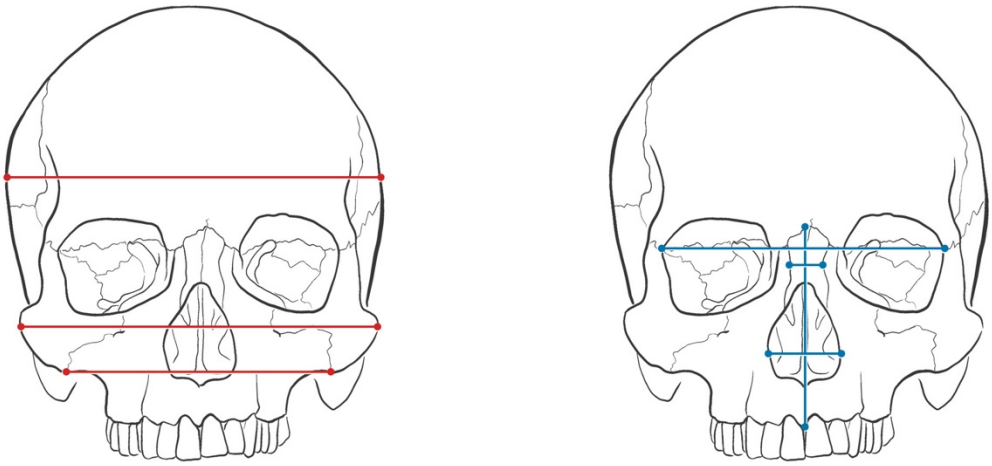

Figure 2.1 - Humidity related variations affecting the facial bones.

In red, up to 2 mm and in blue to 1 mm. After Utermohle et al. (1983).

Adams and Stephan (2005) examined the effects of maceration, drying and re-hydration on a sample of twelve rabbit skulls (*Oryctolagus cuniculus*). Rabbits were chosen as a pilot study for humans due to their relatively delicate nasal bones, prone to deformation under different environmental conditions. Their observations conclude that the measurement variation between the green and the dry state was small, from two to three per cent of the original metrics, and that nasal morphology suffered relevant transformations. The authors also agree that re-hydration of the skulls after drying approximates measurement values similar to those of the green state.

As previously noted by Adams and Stephan (2005), if the guidelines used in craniofacial approximation derive from living individuals and if humidity affects the dimensions of bone, then there might be significant errors when those rules are applied to dried skulls. Even though the differences in the reported skull dimensions seem to be relatively small, we agree that facial approximation should rely on the least possible biased reference. However, further research with human data is necessary to provide a better insight on the impact of humidity on cranial measurements and, subsequently, on facial approximations. Although humidity might play a significant role in the variation of craniometric measurements, we also agree with Albrecht (1983) when he states that it is rather difficult "to precisely delineate the effects of humidity from those possibly related to intra-observer measurement error". The use of high precision scanning devices in future investigations may contribute to this effort while also limiting the introduction of intra-observer measurement errors.

2.1.2 Addressing missing data and plastic deformation

Besides humidity related issues, the bone record is exposed to deformations such as shearing, bending, compression, among others (Weber & Bookstein, 2011). Then, to our already long list of queries required to determine a biological profile of an individual, we need to add a few more to access the amount of information lost due to taphonomical processes. Is the skull fragmented or disarticulated? If so, which bones are absent? Can they be mirrored using the bilateral symmetry axis? Are we falsifying the skull's natural asymmetry by mirroring bones? Is there any plastic deformation that modified the original skull shape and how? Are the alterations in the bones the result of a traumatic event that occurred when this person was alive, or were they caused postmortem? Is it possible to articulate the mandible with the skull to a seemingly faultless teeth occlusion?

Addressing missing data and reversing plastic deformation requires submitting the bone to a process referred to as "reconstruction" in the specialized literature. We examined the conjectural nature of these representations in chapter 1. Any attempt to reinstate missing bone morphology through virtual or

traditional methods requires making assumptions about constraints, integration, symmetry, sex and taphonomy (Gunz et al., 2009). More often than not, there are no unique solutions to a hypothetical reconstruction and our choices might ultimately affect the assessment of a given shape and, consequently, the outcome of the analysis.

So, what happens when we revert to building faces from skulls? If facial approximation is so reliant in individualized skull shapes, how legitimate is it to produce them on top of crania that may not be a faithful representation of the original anymore? I believe it depends on how we approach and present these depictions.

Regarding the approach, the attempt to investigate the original bone morphology is a requisite that goes much beyond bioarcheology or forensic sciences. The search for the visual representation of the original cranial shape has become essential in the fields of paleoanthropology and evolution (see Weber, 2001; Weber & Bookstein, 2011; Zollikofer & Ponce de León, 2005, to name just a few), and disciplines such as orthodontics and maxillofacial surgery, where restoring the original form (for aesthetical purposes) is as important as reestablishing the function (occlusion and articulation, for instance) (Senck et al., 2013). In recent years, an array of computer-based tools have been developed to virtually manipulate skeletal material in paleoanthropology (Benazzi et al., 2011; Grine et al., 2010; Neubauer et al., 2004; Ponce De León & Zollikofer, 1999, to cite just a few), along with medical research and computer assisted surgery (e.g. Fuessinger et al., 2019; Semper-Hogg et al., 2017). These parallel developments created a synergy between various scientific domains, which resulted in more robust protocols to replace the missing geometries. Such computer-based applications allow experimenting with data without manipulating the original objects, and enhance repeatability and provide tools to perform quantitative estimations of accuracy. For instance, Senck et al. (2013) devised a sample-based system to reconstruct very large defects on the sagittal region of skulls and reported an accuracy assessment that stands roughly between 2,5 and 10 mm (Figure 2.2). Other protocols allow handling taphonomically deformed subjects without neglecting the local asymmetries (Ghosh et al., 2010; Schlager et al., 2018; Tallman et al., 2014). Most authors agree that computerized tools, some of which are provided as open-source software (e.g. Morpho and Rvcg packages for R, Schlager, 2017), are instrumental in reducing the subjectivity associated with traditional methods (Senck et al., 2013).

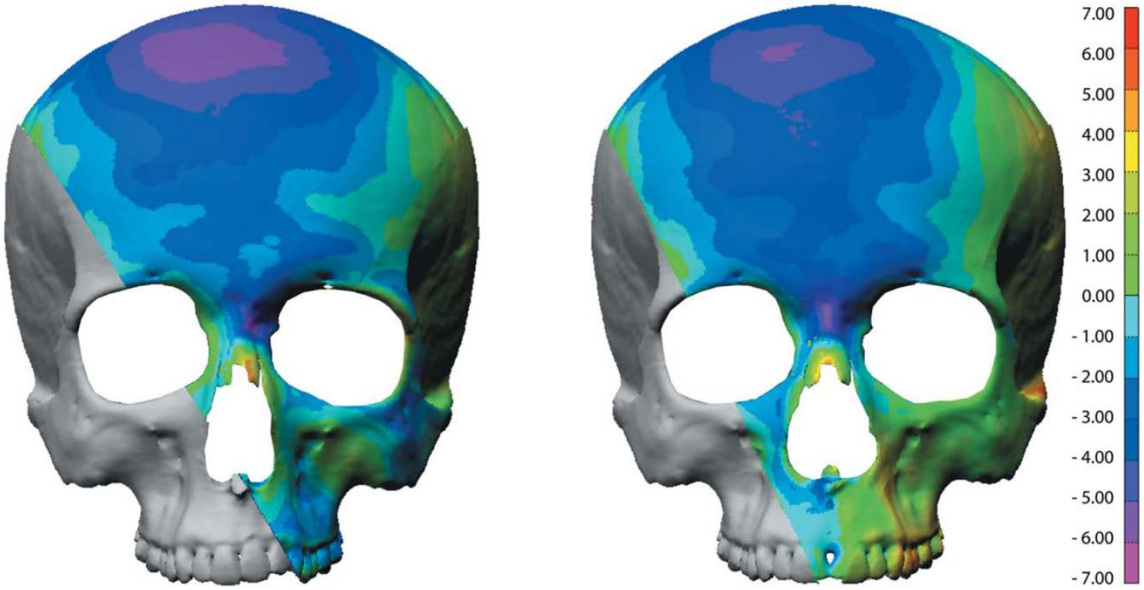

Figure 2.2 - Color coded deviation maps[9] representing the accuracy assessment for the protocol devised by Senck and colleagues. The scale on the right presents both positive and negative values, which relate to how the generated skull overestimates and underestimates the original morphology, respectively. Adapted from Senck et al. (2013).

Thus, incorporating these virtual tools in a facial approximation routine may increase the confidence level of these representations while ensuring repeatability. It will not solve the error that permeates the methods used to estimate features (which we will examine later), but at least it will ensure that the face is being built from a less subjective reference that represents the closest possible alternative to the original skull morphology. A few authors are already applying these resources to their facial approximations (it is the case of the facial approximation of Ferrante Gonzaga, published at Benazzi et al., 2010; or the face of Dante, performed by Benazzi et al., 2009).

[9] Also known as a "heat map", which is a color-coded visualization of the morphological differences between two three-dimensional models.

Occasionally, even if the access to virtual tools allows us to create less biased cranial reconstructions, there are cases where the lack of bone data is so extensive that any attempt to recreate a face from them should be regarded very carefully if not completely dismissed. A curious example is the case of the facial approximation of *Elba*, an adult woman between 20-40 years that died from a fall about 10,000 years ago in Lugo, Spain (Sanín Matías & Serrulla Rech, 2017; Serrulla Rech & Sanin Matias, 2017). Despite having a fairly complete braincase, the facial portion of the skull and mandible are absent. In this case, the anthropological report of the skeleton, together with radiocarbon dating, allows the outline of a general biological profile (an adult woman from an ancient Mesolithic population). However, there are very few intrinsic cranial constraints to the range of variation in a possible representation of the skull, and no indication about the use of a reference sample. The authors acknowledge the highly speculative nature of their "facial approximation" in the original paper (Sanín Matías & Serrulla Rech, 2017), but such considerations are not usually addressed openly in public media.[10]

So, the case of *Elba* also raises different questions, and it relates to how we present facial approximations (especially in the broader circuits of science dissemination). How inclusive should the concept of "facial approximation" be? Before, we have seen that the word "approximation" lends itself to tolerate flexible concepts and narratives of convenience (Lull, 1988), and I have also argued that keeping well-defined boundaries between art and science does not always work in favor of the latter. While creating a visual representation of *Elba* based on the archaeological data is fundamental to enrich the musealization of the remains and motivate the dialogue with the public, a facial approximation is a procedure that cannot be separated from the specificity of a particular skull. Overlooking that aspect not only hinders the recognition of face approximation methods as a science-based endeavor, but also pervades the discourse with the false assumption that it is possible to "know" someone's face irrespective of the amount of data available, which is not the case.

While the mediatic nature of facial approximation sometimes makes room for these gray areas, I believe it is important to create a framework where faces represented from skeletal remains can be allocated

[10] See, as an example, the press report concerning the remains of *Elba* in *El País*, accessed on the 15th of December 2020: https://elpais.com/politica/2017/05/10/diario_de_espana/1494406591_973226.html.

to a specific level of uncertainty, based on the material evidence that sustain them. This project uses a classification scheme that considers the state of preservation of each skull to categorize the uncertainty that is expected to permeate a given facial representation (see Chapter 4 for the rationale underlying this classification). Therefore, accessing accuracy in a facial approximation requires considering two possible dynamic error origins. First, the inaccuracies that originate from the quality of the preserved remains and, secondly, the error that pervades facial approximation guidelines and methods, which may be further magnified by the former. In the future, this (now preliminary) classification system will be freely accessible online so that both scholars and non-researchers alike can make their simulations and derive their conclusions.

2.2 Recognition rates and visual perception

Much has been written about this intangible subject known as human visual perception. Questions such as *how we perceive things* or *what makes something recognizable* can be nearly as vast as the universe. These wonderings are deeply connected with facial approximations because, ultimately, these representations create a stimulus that demands a sensory response which, ideally, will result in recognition.[11]

The published disparities in recognition rates reinforce the ranks of the argument base that deems facial approximation as a highly subjective endeavor (Stephan, 2003a; Stephan & Henneberg, 2001, 2006). Recognition rates have been extensively used as the measuring device that quantifies success and became

[11] At this point, it is important to add a note that clarifies the operational differences between the concepts of "recognition" and "identification" in a forensic facial representation context. Recognizing means that there is some correspondence with an already-known instance, and, for that reason, success usually depends on the exposure of the target face to a family member or an acquaintance. It is a procedure that aims to isolate possible resemblances in order to narrow a list of names and facilitate identification. A positive identification implies a match with a specific individual, confirmed through accepted methods such as a DNA test or a dental record analysis (Wilkinson et al., 2006b).

almost a synonym of methodical accuracy. In fact, I remember this was one of the very first questions I was asked when I started studying facial approximations: *How do you measure success with these techniques? How close, or how similar, is the "approximated face" compared to the "real face"? Out of 10 facial approximations, how many can provide a successful identification? Nine? Three? None?* I did not have a single answer back then, and now I fear I may have found too many.

The questions regarding the accuracy of facial approximations arose almost as early as the first experiences with the techniques. Among the earliest approaches, Kollman and Bückly (1898), Von Eggeling (1913), and Stadtmüller (1922) compared facial approximations with death masks and concluded there was no resemblance between them. Krogman (1946) and Snow et al. (1970) showed more promising results. Snow and colleagues tested two facial approximations of a woman and a man, using volunteers to identify the correct person from face pools with photographs of seven individuals. Regarding the face approximation of the female, only one-quarter of the participants were able to identify the correct picture, possibly influenced by the age difference between the photograph and the individual at death (25 years). The male scored a success rate of 68%. Helmer et al. (1993) conducted a double-blind study with two artists tasked to sculpt 24 faces on 12 skulls each. Then, a group of three examiners would classify the resemblance with a scale where 1 = none, 2 = slight, 3 = approximate, 4 = close, and 5 = strong. The comparison between both facial approximations revealed that 50% had an approximate resemblance, while the comparison between the faces and the photographs of the individuals scored 38% of close resemblance.

Besides these examples, other practitioners have reported all sorts of different percentages. Gerasimov (1971) claimed a success of 100%, and while his results are indeed impressive (Figure 2.3), a flawless rate is hard to accept even for someone as experienced as the Russian anthropologist. The quantification of success differs wildly among published reports: Wilkinson (2004b) has claimed an accuracy rate of 75% for the method pioneered by Richard Neave; Gatliff and Snow (1979) report 70% of positive identifications; and Prag and Neave (1997) remain more cautious at 50–60%. Others, such as Haglund and Reay (1991), stated that none of the 24 facial approximations made to identify the victims in the Green River Serial Murder were able to provide a successful identification. A study by Stephan and Henneberg (2001) also showed less optimistic results when only 1 out of 16 face approximations was identified at a significant rate above chance.

Figure 2.3 - Two of Gerasimov's forensic cases: on the left, facial approximation of Valentina Kosova, followed by her picture. The rightmost images: picture and facial approximation of Nina Z. Adapted from Gerasimov (1971).

Sometimes there are disparities in the percentages depending on who is reporting them too. Wilkinson reports that Gatliff only achieved a 65% success rate (Wilkinson, 2004b), while Prag and Neave (1997) attribute her 72%. These fluctuations may reflect method reevaluations made over the years, but it is unclear from the sources which criteria dictate these percentages.

So, what is failing? Did some practitioners overlook and underreported failed cases, making the rates seem substantially better than what they really are (Stephan, 2003a)? Are these percentual differences motivated by distinctive methodical approaches? Or are positive identifications enabled only by other external factors, such as contextual information (Haglund & Reay, 1991), exposing the images to the "right person" (Haglund, 1998) or simple chance (Stephan & Henneberg, 2001)? As many of these previous accounts rely on the participants' or practitioner's subjective assessments, where accuracy is measured from pooled tests or one-to-one comparisons, less biased approaches are necessary. Proceeding from the same technical principles as the virtual techniques that aim to reinstate the original shapes of bones, quantitative methods based on three-dimensional mesh comparisons, landmarked distances and biometric datasets became the core of accuracy evaluations in recent years.

Wilkinson et al. (2006a) developed a blind test study using two skulls of living subjects and showed that the applied methodology could predict 60% of the male face and 52% of the female with a deviation error below ± 2.5 mm. These results were comparable to those of a study with a sample of three Korean

adults, where each showed a deviation of less than ± 2.5 mm in 54%, 65%, and 77% of the face, respectively (W. J. Lee et al., 2012). Using a bigger sample size of 10 cone-beam computed tomographies (adult individuals with a mean age of 23 years, five female and five male), Short et al. (2014) further expanded on the assessment of techniques and concluded that the percentage of faces with less than ± 2.5 mm error ranged from 56% to 90%. All the individuals from the previous sample present skeletal discrepancies that required surgical correction (six are diagnosed with Class III pattern, with an underdeveloped maxilla, and four with Class II pattern, with an underdeveloped mandible), which is a factor that might influence the evaluation of the accuracy patterns. Miranda et al. (2018) performed tests on four subjects with facial representations generated with different software from the one used on the previous three tests. The results were similar (Table 2.3), suggesting that despite the different workflows, software and practitioners, facial approximation methods might be moving towards standardization and stability. Another recent study by Simmons-Ehrhardt et al. (2020) performed the most extensive quantitative assessment of accuracy on facial depictions predicted from the skull. The authors generated 388 facial approximations (through an automated computational method named *ReFace*[12],– refer to Chapter 4 for a few notes on the differences between approximation approaches) on a sample of North Americans, male and female, of African, Asian, European and Latin American ancestry. The face approximations were not adjusted to reflect weight variations or the age of the subjects. The biometric comparison with the surfaces extracted from the medical images resulted in average absolute differences inferior to 5.37 mm in 66 distances measured from 12 facial landmarks. Simmons-Ehrhardt et al. (2020) study shows that the measurements associated with the mouth width are the least accurate to predict with the current methods, and the results suggest that the relationship between this feature and the anterior dental area is more complex than traditionally assumed by facial approximation guidelines.

Except for Simmons-Ehrhardt et al. (2020), who made landmark-based comparisons, the similarity rate in previous research (Table 2.3) was measured through the generation of a "heat map". While landmark-based assessments offer a quantification of possible error in-between the facial features,

[12] ReFace is the proprietary software of the Federal Bureau of Investigation (FBI) (Turner et al., 2005). It is not publicly released and is not available to the scientific community.

providing clues to which guidelines need to be reviewed or updated, "heat map"-based analyses (also known as surface-to-surface comparisons) provide a valuable tool to evaluate errors in facial tissue depth estimators. W. J. Lee et al. (2015) conducted another reassessment of facial approximation methods based on the same protocol as their previous study (W. J. Lee et al., 2012), but using updated soft tissue datasets derived from a sample of 100 Korean adults (Hwang et al., 2012). Their results for the facial approximations of three Korean subjects show that using more robust datasets does have a significant impact in reducing the deviation errors and approaching the original morphology of the test subjects (Table 2.3 for results). The recognition rates of the faces generated from the Korean sample were further tested with a qualitative assessment (face-pool comparison) (S. Kim et al., 2020). Their results concluded that the recent dataset also performs better in face-pool comparison tests, with the mean recognition rates at 22% and 31% for the old and the recent datasets, respectively.

Table 2.3 - Quantitative accuracy studies using surface-to-surface comparisons. Data after the respective authors.

Study	Image	(n), Sample	Subject	± 2.5 mm	Areas above ± 5.0 mm
Wilkinson et al. (2006a)	CT scans	(2), white North American	1	60%	Right temple, upper cheek, portions of the ears and nasal tip.
			2	52%	Nasal alae, upper lip and ears.
W. J. Lee et al. (2012)	CT scans	(3), Korean	A	54%	Small portions on the lateral part of the forehead, small portion of the nose, and both cheeks.
			B	65%	Minor portions on the lateral forehead, both endocanthi, small parts of lateral and lower cheeks.
			C	77%	Both endocanthi, left side of the upper eyelid, and partial temples.
Short et al. (2014)	Cone beam CT scans	(10), patients from the Glasgow Dental Hospital	1	81%	Right and left eyelid, lower lip, right and left cheek and zygoma region.
			2	71%	Right and left eyelid, tip of nose, right and left zygoma, right and left alar crease, left commisure.
			3	61%	Right and left cheek, right and left eye.

			4	58%	Right and left eyelid, lower lip, right and left cheek and zygoma region.
			5	56%	Right and left eye, left supraorbital region, tip of nose, right and left ala, philtrum, upper and lower lip, right and left commisure, right temporal region.
			6	90%	Right and left temporal region, right and left supraorbital region, right and left upper eyelid, left lower eyelid, lower lip, right and left commisure region.
			7	64%	Right and left eye, dorsum and tip of nose, right and left cheek and zygoma region.
			8	68%	Right and left temporal region, tip of nose, right and left ala, right and left cheek.
			9	80%	Upper lip.
			10	80%	Tip of nose and right commisure region.
W. J. Lee et al. (2015)	CT Scans	(3) Korean	D	88%	Small portions on the lateral part of the forehead, tip of the nose, left mouth corner and a portion of the cheek area.
			E	79%	Minor portions of the lateral forehead, nasal tip, and both lower cheeks.
			F	87%	Small portions of the mouth corners, nasal tip and temple area.
Miranda et al. (2018)	CT Scans	(4), Brazilian	A	63%	In all cases the cheek and eyes were underestimated while the chin and zygomatic were overestimated.
			B	64%	
			C	65%	
			D	74%	

As for the practical application of these methods to evaluate accuracy in forensic or archaeological cases, it is always dependent on having an image of the target person to compare with the facial representation from the skull, a circumstance that becomes exponentially more problematic the older the remains are. A relatively recent case is that of the facial approximation of a young woman discovered in Australia's Belanglo State Forrest in 2010. The representation of the (then) unknown woman was released

in the public media to try and motivate a recognition from someone related to her, and there is a full report on the methods that informed the completion of the facial depiction (Hayes, 2014). After the woman was positively identified by a lead unrelated to those generated by the facial approximation, Hayes (2016) used a geometric morphometrics approach to evaluate the similarity between the face representation from the skull and three antemortem images of the identified individual. While the inaccurate prediction[13] of some characteristics did not facilitate familiar recognition, the morphometric analyses show that the facial approximation is statistically similar to the original face, suggesting that an automated face recognition system could have produced a positive identification (Hayes, 2016).

Despite the quantitative assessments that measure morphological similarities between the representation of the face and the target individual, cases like the facial approximation of the Belanglo woman illustrate that the weaves between likeness and recognition do not create a consistent pattern. Landmark-based analyses provide a means to quantify differences between shapes and distances between features, but they do not transcend them. Morphometrics alone do not explain the spaces that exist between the face and the one who sees it, nor how an image or a sculpture becomes relatable enough to be identified as a living (or dead) person. That is a task for the realms of neuroscience, cognitive psychology, philosophy, and face perception. Otherwise, if the process of identifying a face by a human observer[14] was solely dependent on the metric relations between points, how could visually different faces still be recognized as the same individual (Figure 2.4)?[15] Or how would it be possible that a caricature, which is either an over-

---

[13] It is interesting to observe that the author attributes the inaccuracies present in the facial approximation not only to the limitations of the methods, but also to a practitioner misapplication of these same methods (Hayes, 2016).

[14] As face recognition systems powered by deep-learning and Artificial Intelligence become more and more effective (despite the reported gender and racial biases), this is an important aspect to emphasize. Concerning this subject, I refer to *The Gender Shades project* (available online at: http://gendershades.org) for more information regarding the performance of AI technology focused on human subjects (Buolamwini & Gebru, 2018).

[15] Interestingly enough, morphometric-based and deep learning techniques are also being employed to identify uncertain subjects in ancient paintings and sculptures (see, for instance, Gupta et al., 2018; Srinivasan et al., 2015), or to evaluate the most realistic representation of someone by comparing the existing portraits with the death-mask (Sequenzia et al., 2020).

simplified or exaggerated representation of someone's facial features, is identified as a specific person (Smith, 2018)?

Figure 2.4 - Four portraits of Mary Stuart, Queen of the Scots (1542–1587). From left to right: watercolor by François Clouet (1555), © Ossolineum/National Ossoliński Institute; two paintings by Clouet (c. 1558 and c. 1560, respectively), both images © Royal Trust Collection; painting by an unknown artist, after Clouet (17th-century), © Victor and Albert Museum Collections.

Any figurative representation implies a translation of natural forms into abstract shapes and concepts. Through this conversion, a drawing or a sculpture of a face becomes a hierarchy of lines, edges, values and planes that "read" as the real thing without ever becoming it. What is created is an "illusion" of form and texture because the paint is not skin, and clay (including virtual clay) is not flesh.

Following these ideas, we are obliged to refer to another disputed topic in facial depictions produced in forensic or archaeological contexts: the visual style and aesthetic appeal associated with these visual representations (Wilkinson, 2004b). Multidisciplinary sources suggest that photo-realism is not a prerequisite for human recognition. George (1993), the same proponent for the use of the expression "facial approximation" instead of "reconstruction", suggested that the general shape of the face and its proportions are the most critical factors and that any added detail may hinder the perception of the overall impression. This assumption is in concordance with the thoughts of art historian Michael Podro, who believed that too

much detail might be less convincing than a balanced visual representation containing both a well-described structure and more open areas for interpretation. Achieving a representation that seamlessly merges these two conditions will allow the observer to mentally fill in what is missing and increase its potential recognition (Podro, 1998).

Susan Hayes conducted a series of interesting experiments where the hypothetical dichotomy between likeness and recognition was put to the test, while comparing the differences between familiar and unfamiliar face assessment (Hayes, 2014, 2016; Hayes & Milne, 2011). Her studies explore the relationship between anatomical accuracy and likeness judgements using visual assessments, anthropometric measurements and geometric morphometrics analysis. The results show that an anatomically accurate likeness does not mean a better recognition rate for viewers, as both familiar and unfamiliar observers tend to prefer some sort of exaggeration of distinctive facial features.

On another level, shapes (and how they are perceived) may also be affected by other factors that generate different viewing conditions. The literature on face recognition systems reports that successful biometric identifications depend on factors such as the pose or viewing angle, expression, aging, and illumination, provided that the face is fully visible (see, as an example, Moses et al., 1994; Ramanathan et al., 2004; Tolba et al., 2006). Lighting, for instance, has a well-known lasting effect on the appearance of objects in still images and motion pictures alike. In a particularly illustrative example, Nacho Guzman synthetized this premise in his music video of the song 'Sparkles and Wine' by the music band Opale (accessible online at https://vimeo.com/67356505). The changes between high and low-key illumination, associated with the light's temperature, make the same actress seem like a different person throughout the video, changing the mood of the scene and how we perceive her. So, it is safe to assume and easy to demonstrate (Figure 2.5) that the same will hold true for facial representations made from bone.

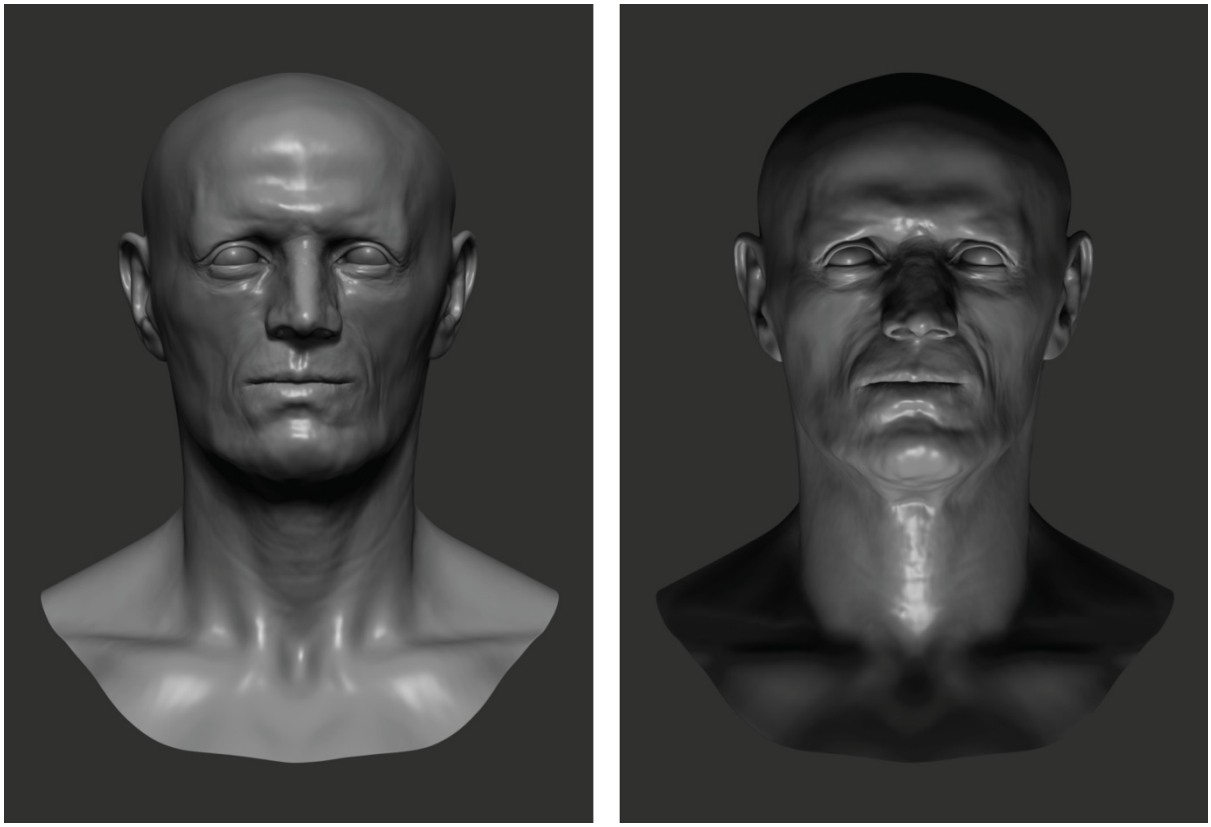

Figure 2.5 - Facial representation of AY5 in different lighting conditions.

So, let us return to the question formulated at the beginning of this section. How do we measure success with these techniques? It depends on how we define *success*.

If success is having a match correspondence between two images (a capture of the real face and a facial representation based on the cranium), then the mean average based on the published quantitative studies approaches 70% correspondence with less than ± 2.5 mm deviation (Table 2.3). Assuming external or taphonomical conditions have not deformed the bone, that is how approximate a facial representation from the skull can be at present. More tests are required to evaluate the impact that the most recent guidelines and datasets may have on these numbers. Further testing is also necessary to assess the integration of facial approximations in automated face recognition routines to identify missing persons, but current results suggest that achieving positive matches is a possibility.

If differently, success is synonymous with achieving a positive identification by a human observer, then it is more difficult to measure. There is no clear reply regarding the amount of precision needed for a facial approximation to result in a positive identification (Guyomarc'h et al., 2014). The prevailing theory postulates that the human brain processes the face in a holistic manner, detecting the shape of the face and the position of the features simultaneously, along with other attributes such as color, or texture (Gold et al., 2012). However, a few experiments indicate that, besides external factors such as the illumination or the position of the head, there are also other dynamics that affect the production and recognition of face representations from the skull. Choosing a photo-realistic rendering in a facial depiction may hinder the process of recognition (Hayes & Milne, 2011) and the unfamiliar face effect[16] was proved to impact the modeling faces from a different ancestry than those familiar to the practitioner (W. J. Lee & Wilkinson, 2016). It is not unreasonable to think that a similar effect might occur when depicting faces from past populations.

Coming back to Podro (1998), a materialization of something, or someone, in a visual representation is a complex interaction between how one apprehends the features and structure internal to the image[17], –how the representation of the face is created–, and how one's perceptions of things and situations influence the interpretation of the viewed image–how a face is recognized. Disentangling these processes is a multidisciplinary effort that proves to be an exciting line of research for the next years.

[16] Research indicates that people are excellent at identifying familiar faces but require a lot of effort to recognize, or even match, unfamiliar faces (Hancock et al., 2000).

[17] When it comes to the specificity of producing a face approximation from the skull, there is another parameter to add to Podro's equation, which is taking into account the methods, the guidelines and the scientific standards.

2.3 Finding the big culprit

There is much to consider when studying facial anatomy and its significance in facial approximation. At first, it seems quite simple: everyone has two eyes, one nose, one mouth and two ears (providing that there are no congenital disabilities or traumatic events that led to their loss or deformation). These features have a well-studied morphology, and through them, our faces concentrate our abilities to see, to smell, to breathe, to ear, to eat, to taste and to communicate both silently, using a network of elaborated expressions and reactions, or out loud, voicing sounds and speech.

There are some limitations regarding the location and relative proportions of features inside what we could call the "edges" of a face: all of them are bilaterally distributed within the lower two-thirds of this space and, except for the ears, placed in the most anterior part of it. Furthermore, both eyes are expected to be more or less the same size, with the nose occupying the center of the face and the mouth roughly placed halfway between the base of the nose and the chin. While all faces share this same basic configuration (known as first-order relational properties), all faces bear subtle differences (second-order relational properties) in this prototypic pattern that will ultimately allow individuals to be identified (Diamond & Carey, 1986).

Much has been written about why faces differ so much across the world. Since the days of Darwin, researchers have tried to unravel why and how this happens, attributing differences to genetic drift, local adaptations and sexual selection. There seems to be a generalized consensus that neurocranial morphology acts as an indicator of population/phylogenetic history, while the face and cranium appear to be under selective pressures related to the climate (Hubbe et al., 2009). The hypotheses postulating that local adaptations modeled a few craniofacial features are especially observable if we zoom out to look at the broad evolutionary scale. Research with fossil hominins (Oyen et al., 1979) and modern humans (Russell et al., 1985) seems to support the notion that mechanical loads during biting and food-processing impact the

eyebrow area, hinting at different dietary adaptations.[18] Also, the correlations found between the nasal index (ratio of nose height/breadth) and temperature and humidity (Davies, 1932; Franciscus & Long, 1991; Weiner, 1954, to name a few), have suggested that climatic adaptation was perhaps the main selective force behind the shape of the nose. These hypotheses have been further corroborated by airflow dynamics simulations which have shown that the shape of the nose might influence the heating and humidification of the air (Churchill et al., 2004). There is also extensive documentation on how selective mate choice based on facial appearance is a universal condition in global human populations (Wells et al., 2009). But only a few studies research the role of non-neutral forces in shaping human soft-tissue morphology (Guo et al., 2014; Zaidi et al., 2017).

Our common denominator is human variation. Ontogeny, genetics, pathology, and environment, they all have a say in how our faces look and age. And when we consider all the actors in this play, predicting something as complex and intricate as the soft tissues layered on top of the skull can be overwhelming at the very least.

Travelling from the outside to the inside, from the surface to the bone, we find the epidermis and dermis, followed by the subcutaneous fat, superficial fascia, musculature, and deep facial fascia (Larrabee et al., 2004). Thus, a large percentage of the face is formed by these tissues preserve only under exceptional circumstances and leave minimal traces of their attachments to the bony surface. A few craniofacial muscles have no direct relationship with the skull because their origins and insertions are within soft tissue (e. g., orbicularis oris, risorius), thus making it rather complicated to determine their accurate placement and shape. Other muscles, like the ones that control many of the facial expressions (e. g., zygomaticus major and minor, mentalis, levator labii superioris, among others) do originate from bone but insert into other soft tissues, also shedding doubts into their original configuration. And even though humans have generally the same mimetic musculature, dissections have shown us that this is not always the rule. Pessa et al. (1998a) found that the risorius muscle, a thin bundle of fibers that causes the lips to flatten and stretch laterally,

[18] On a curious side note, it has been hypothesized that the softer diets characteristic of our industrialized societies, along with global warming effects, will have a considerable impact on human facial appearance in the millennia to come (Lacruz et al., 2019).

was missing in 22 of 50 dissected specimens. Besides the risorius, other muscles of the face vary in presence, form, location and control, which can ultimately influence the movements each individual can create and, consequently, the appearance (Burrows & Cohn, 2009). For the purpose of facial approximation, only the masseter and the temporalis present well-demarcated origin and insertion points and contribute significantly to the overall morphology of the face (something already posited by Gerasimov, as we saw in the previous chapter).

The collagen fibers present in the superficial fascia, along with the facial fat deposits, deteriorate with age and contribute to the sagging of the face (Burrows & Cohn, 2009; Larrabee et al., 2004). But aging is a complex multifactorial process (Mangino, 2014) that depends on genetics, lifestyle and nutrition and reflecting it on a facial approximation may be problematic, especially considering the increase in life expectancy in recent years. The advances in medical science, better hygiene and nutrition habits and a considerable decline in mortality rates among younger people are pointed as the main causes of this phenomenon (Mangino, 2014). Therefore, would a 40-year-old now look as young (or as old) as a 20-year-old then?

And to what extent engaging in certain facial expressions can affect the seeming aging of the face? That is another seldom studied aspect, along with the impact of muscle variation in facial expression. As muscles contract, lines and furrows appear perpendicular to the direction of the movement, creating deformations on the facial skin. In the widely cited review by Schmidt and Cohn (2001), the authors argue that muscle variation may cause individual differences in expression. They cite a study where the variation of the insertion points of the zygomaticus major, which appears as a bifid version in 17 of 50 specimens, is believed to cause a dimple during the contraction of the muscle when smiling (Pessa et al., 1998a; Pessa et al., 1998b). Even less studied than the links between muscle variation and individualized facial expressions, is the impact that these differences might have in diverse cultural backgrounds and the evolutionary interplay between form and function, or facial myology and communication (Schmidt & Cohn, 2001). As time passes and the skin elasticity decreases, these "expression lines" become somehow permanently imprinted on our faces (Burrows & Cohn, 2009), almost as if anatomy found a funny way of mocking us for how much we laughed or cried throughout our lives.

This immensity began to unravel as soon as anatomists and researchers began collecting all sorts of anthropometric measurements, angles and proportion indexes to define what would be the "normal" dimensions of the head, its features and the skull underneath. These measurements are usually organized by age, sex and populational affinity and assist plastic surgeons in detecting defective elements that are involuntarily acquired or that stand out as outliers that slip away from that conceptualized "normality". It seems that beauty is not always in the eye of the beholder, and knowing the average and the relative dimensions of the head and face is fundamental for planning corrective surgeries without disrupting the overall proportions (Farkas, 1994).

However, if we leave the averages aside for a moment and look at the raw anthropometric data, we reencounter human variation. We, scientists, researchers, humans, with our constant need to recognize patterns and bring order to chaos, tend to average out a diversity that often cannot be completely tamed within our artificial criteria. We create endless databases, collect measurements that we classify into groups and try to extract the rules. Then, we come up with proportions, standards and equations that might be representative for most but surely do not represent each and all. As argued in a previous chapter, it is commonly accepted that these restraints permeate the field of facial approximation and turn results into averages that cannot be expected to fulfil the role of an accurate portrait, no matter how skilled the practitioner is or how complete our data is.

Yet, at the same time, human variation is the cornerstone of these facial representations. The range of possibilities, in this case, can be both a blessing and a curse. Human variation hinders our rate of success but also validates the need to keep pursuing better recognition rates. If all faces were exactly the same, there would be no point in trying to understand the differences, to distinguish one face from another, to recognize and to identify someone against everyone else. In this manner, and further beyond the initial goals of assisting forensic investigations or satisfying our curiosity concerning our ancestors' appearance, a facial approximation is also a way to investigate human biological diversity and understand how the different components of our faces interact and correlate.

Personally, the realization of the complexity of these matters resonated the most when I was learning to make portraits in clay from a live model. Making a clay portrait from a living person can perhaps be considered a kind of reverse engineering to performing a facial representation from the skull. A sculptor

needs to "guess" how the skull of the model is without ever seeing it if the portrait is going to convey any sense of internal structure. While at it, I realized that the best approach would be to first engage with everything I knew about anatomy and then forget anatomy existed. This seemingly contradictory statement is just meant to show a substantial difference between modeling *a* face and modeling *that* face. Anatomy sets the standards by which *a* face can be represented convincingly. It follows a known morphological architecture, a complex network of different components made of bone, muscle and other tissues that can be puzzled together to create a seemingly physiological organism. But looking at a sitting model for hours also makes one wonder how much life is behind all that stillness.

We just saw that science attributes the variation we encounter in those anatomical components to an array of genetic and environmental dynamics. How much of *a* face (or skull) can be determined by what our genes carry? Or by our behavior throughout mundane tasks such as eating and sleeping?[19] Or by the climate conditions of where we decided to settle in? What about medical conditions, both hereditary and acquired? As we have just seen, all these factors contribute, in different proportions that vary throughout our life. Despite the advances in recent years, there are still many questions surrounding phenotypic variance that will continue to be slowly unveiled in the decades to come. Yet, *that* face is still much more than that. It results from many cumulative and unpredictable factors and experiences that cannot be accounted for just by running an analysis on a DNA sample or by looking at its separated components and understanding how they relate. Our faces exist on their own as biological matter but also on a multitude of dimensions such as cultural, ethnic and, of course, personal. How much of *that* face is the result of socio-cultural inputs and change, as well as both individual and collective aesthetic values? Most of the times, there are no clear or straightforward answers.

Hence the importance of defining the possibilities, laying out the limitations and acknowledging the unknowns while putting them into a context.

---

[19] A study by Sundelin et al. (2013) has shown how sleep deprivation can affect facial features, leading to side-effects such as hanging eyelids, paler skin, more wrinkles and more droopy corners of the mouth.

3 Shaping faces from skulls

~

The features of the face correlate, more or less strongly, with the bone structures that support them: the eyes with the orbital cavities, the nose with the nasal bones and the piriform aperture, the mouth with the dental arches and the ears with the external acoustic meatus and the temporal bone. There is an extensive body of research concerning these correlations, which form the pillars of facial approximation. However, disentangling the relationships between bone and flesh is a complex enterprise.

The following pages review the research that led to the contemporary methods used in the facial representations included in this thesis.

3.1 The eye region

The literature on the anatomy of the human eye is extensive. This section offers an overview of the anatomy of the eye region, focusing on significant aspects to consider when modeling a face from its skull. The different methods to estimate its placement within the orbit are also discussed, as well as the methods to approximate the position of the corners of the eye, the palpebrae and the eyebrows.

3.1.1 The eyeball: anatomy, proportions, and position

The eyeball is positioned within the orbital cavity, a rigid bone structure that protects the organ of vision and provides origin points for the six extrinsic muscles and the palpebral ligaments. Overall, the globe is not a perfect sphere and the three diameters of the eye present variable measurements. These values differ marginally in the many available sources: for instance, Snell and Lemp (2013) echo Bron et al. (1997) in stating that the anteroposterior diameter measures about 24 mm, the mediolateral diameter about 23.5 mm and the superoinferior 23 mm. Guyomarc'h et al. (2012) inform that the means for the same diameters are 23.7 mm, 24.3 mm, and 24.6 mm, respectively. Although there is no strong correlation between the volume of the eyeball and the orbital height and breadth, males do present a slightly larger volume (<0.5 mm in diameter) when compared to females (Bron et al., 1997; Guyomarc'h et al., 2012). Since these differences seem negligible, the eyeballs modeled for this dissertation project have a diameter of 24 mm and take into account the remaining proportions and values reported in the literature (see Figure 5.3, in Chapter 5).

The eyeball is generally modeled with two simplified spheres, one for the sclera and a smaller one for the cornea, and a planar disc for the iris (Lefohn et al., 2003; Ruhland et al., 2014). While this simplification may be justified by the fact that the visible portion of the eye is not significantly affected by the variations in the diameters of the eyeball, others have argued that generic eye models only roughly approximate the actual physiology of the eye and are insufficient for describing the individual identity of a digital human (Bérard et al., 2014). Although Bérard et al. (2014) approach relies on capturing and modeling real eyes from real people and cannot be fully extrapolated for facial approximation purposes, some of the authors' considerations are worth considering the final stages in the representation of a face. Aspects such as surface detail and vascularization in the sclera, the micro-geometry of the iris and the non-circular transition between the sclera and the iris, may help simulate the variation found in the living human eye and attain a more natural appearance for the visual representation of faces. Since we have argued that too much detail may hinder the purpose of identification (Chapter 2), this situation should be evaluated on a case-by-case basis, especially when the goal of the face representation is to prompt a recognition.

Concerning the growth of the whole globe (cornea and sclera), different sources report that it takes place mainly before birth and reaches full development in the first three years of life (Augusteyn et al., 2012; Duke-Elder, 1961; Weale, 1982), contradicting the previously accepted view that scleral growth would continue throughout childhood and be completed around 14–18 years (Duane et al., 1982). According to these studies, the eye reaches its full development much earlier in life than the head, whose circumference continues to grow at least until late adolescence or early adulthood (Eichorn & Bayley, 1962; Nellhaus, 1968). Therefore, the eyes appear to be much larger during childhood, contributing to the "wide-eye appeal" of young individuals,[20] well-recognized in humans and other species. For this reason, the eyeballs used in the younger individuals in are the same used for adult facial approximations.

Aging also produces noticeable changes in the eyeball. Conditions such as *arcus senilis*, an opaque ring that develops around the peripheral cornea, or cataracts that produce a clouding of the eye lens are common among older individuals (Salvi et al., 2006). However, such conditions cannot be predicted from the skull alone and might be more useful as distinguishing characters in forensic cases where visual witnesses can contribute to the facial approximation process.

Earlier practices in facial approximation (Gatliff, 1984; Taylor, 2001) placed the eyeball centrally within the orbit and determined its projection by aligning the cornea with an imaginary tangent dropped from the mid-superior to the mid-inferior orbital margin. Although the central position of the eyeball has been applied by some practitioners in the past, recent research contradicts the central position of the eyeball and resonates with guidelines from the beginning of the 20-th century (Whitnall, 1921; Wolff, 1933), which placed the eye closer to the roof and lateral margins of the orbit. These conclusions were reiterated by an earlier review of the exophthalmometry literature (Stephan, 2002a), and have also been confirmed by MRI-based research (Wilkinson & Mautner, 2003), dissection (Stephan & Davidson, 2008; Stephan et al., 2009) and, more recently, lateral head cephalograms (Mala & Veleminska, 2018).

[20] Children also have a lower nasal bridge which emphasizes this circumstance. As the individual grows, the nasal bridge becomes higher, the vertical dimensions of the face increase and the cheekbones widen, making the eyes of the adult appear closer to each other (Enlow & Hans, 1996).

As demonstrated by Stephan (2002a) and restated by Wilkinson and Mautner (2003), the previous guideline for estimating the eyeball projection does not have scientific support either. Drawing an imaginary tangent from the mid-superior to the mid-inferior orbital margin underestimates the projection of the eyeball by approximately 4 mm. Gerasimov's eye projection method, as reported in Ullrich and Stephan (2011, 2016), follows a similar guideline but modifies it by moving the eyeball 1–2 mm in front of the tangent connecting the supra and infra-orbital margins and thus providing a better estimate.

Guyomarc'h et al. (2012) propose a set of guidelines based on regression equations that are, at present, the most efficient way to position the eyeball within the orbit (see Figure 5.4, Chapter 5). The authors measured 375 computerized tomography scans of living individuals and confirmed the superolateral placement of the eyeball, according to previous observations on a population of 140 subjects (Guyomarc'h et al., 2010) and earlier research. Rather than estimating eyeball position based on empirical distances (Stephan & Davidson, 2008; Stephan et al., 2009), the hypothesis of Guyomarc'h et al. (2012) relies on the specific morphology of each individual and is not influenced by age or sex. Recent studies concerning the relative position of the eye within the orbit agree with Guyomarch's hypothesis (Dorfling et al., 2018; Mala & Veleminska, 2018) but do advise the need for wider samples and population-specific databases.

3.1.2 Eye canthi, eyelid patterns and eyebrows

The eye canthi location is an essential step during the skull assessment for facial approximation, as they provide landmarks to place the palpebrae and define the eye fissure. There are several studies concerning palpebral anatomy, but published research shows very different results.

The most consensual guideline refers to the relation of the malar (or Whitnall's) tubercle with the outer canthus (exocanthus) of the eye. The malar tubercle is a small elevation on the surface of the zygomatic bone, on the lateral wall of the orbit and is located about 11 mm below the frontozygomatic suture (Whitnall, 1911). Dissection studies have shown that this tubercle serves as the insertion point to

the check ligament of the lateral rectus muscle, the suspensory ligament of the eyeball (Lockwood's ligament), the lateral canthal tendon and the aponeurosis of the levator palpebrae superioris muscle (Fries et al., 2016). It is generally accepted that the outer corner of the eye is located at the same height as the midpoint of the malar tubercle, but the reported distances between the outer canthus and the bone insertion vary between authors (Table 3.1). If the malar tubercle is absent, the exocanthus may be positioned 8–11 mm below the frontozygomatic suture. It is yet to be confirmed whether the ligament runs directly horizontal from the bony insertion to the corner of the eye (Stephan & Davidson, 2008). According to previous scholarship and in agreement with Anastassov and van Damme (1996), the lateral canthus projects ca. 10 mm anterior to the deepest recess of the lateral orbital margin and lies in close contact with the globe.

Table 3.1 - Position of the eye canthi in published studies. Adapted and updated from Stephan and Davidson (2008). Measurements in mm, taken from the respective orbital wall. *

References	**(n), sample**	**Mean age, ancestry**	**Lateral canthus**	**Medial canthus**	**Relative height of medial canthus**
Whitnall (1932)					4 mm lower
Couly et al. (1976)			8–10		
Wolff (1976)			5–7		2 mm lower
Angel (1978), apud *Stephan and Davidson (2008)*			3–4	2	2 mm lower
Stewart (1983)					Same
*Krogman and İşcan (1986)**			5*	3*	
George (1993)					Lower
Sills (1994)			1		
Anastassov and van Damme (1996)	(10), dissection		13.3		
Van den Bosch et al. (1999)					2 mm lower
Yoshino and Seta (2000)				3–5	
Rosenstein et al. (2000)	(21), dissection	Caucasian	7.5		
Stephan and Davidson (2008)	(4), dissection	83 years	4.5	4.8	
S. R. Kim et al. (2016)	(100), CT-scans	27 years, Korean	4.6	9.8	2.6 mm lower

(Dorfling et al., 2018)	(49), dissection. (30), CT-scans	44,5 years, SA (African)	5.0	4.8	1.8 mm higher

There is general agreement that the medial corner (endocanthus) of the eye is placed 2–5 mm lateral to the anterior lacrimal crest, except for the reported values in the Korean sample (S. R. Kim et al., 2016). It extends 5–7 mm away from the globe and towards the nose (Damas et al., 2020). According to the review of Stephan and Davidson (2008), the published data shows discrepancies as to where the exact measurement is taken from, but there is a general agreement that the medial canthus is slightly lower than the lateral eye corner. In spite of that, the study of Dorfling et al. (2018) contradicts this data and indicates that the angle of the palpebral fissure might vary between different populations.

The position of the canthi influences the angle of the palpebral fissure, which may have a horizontal, downward slanting or upward slanting configuration, and is shown to be sexually dimorphic and asymmetric (Guyomarc'h, 2011). Several authors report that the length of the palpebral fissure stands between 26 and 30 mm (Anastassov & van Damme, 1996; Farkas, 1994; Whitnall, 1932; Wolff, 1976), or between 60–80% of the orbital width (Fedosyutkin & Nainys, 1993). Van den Bosch et al. (1999) indicated that the palpebral fissure length appears to be smaller in older when compared to younger individuals. These measurements are consistent with the study by Stephan and Davidson (2008), who report an average of 24,5 mm for the length of the eye fissure, which corresponded to ca. 74% of the total orbital width in the dissected specimens.

As S. R. Kim et al. (2016) and Dorfling et al. (2018) include samples of particular groups (Korean and South African, of African descent, respectively), in this study I chose to follow the guidelines presented by Stephan and Davidson (2008) (see Figure 5.5, Chapter 5). It is not clear if the disparate distances given in the literature result from different measuring protocols, variations in the quality of the data, or both. In any event, the accurate placement of the corners of the eye cannot be fully guaranteed at the moment due to the lack of more extensive data samples. More studies are required to gain better insight and stabler guidelines for the relationships between the canthal ligaments and the orbital cavity.

According to Balueva et al. (2009), Fedosyutkin and Nainys (1993) and Rynn et al. (2012), the supraorbital rim defines the structure of the eyelid fold. A thick lateral orbital rim that is slanted upwards and posteriorly will create a more pronounced fold laterally. A thick lateral orbital rim that is slanted upwards and posteriorly, will create a fold that is more pronounced laterally. The natural eyelid crease can be located between 8 and 10 mm from the lid margin in women and 7 to 9 mm in men (Straka & Foster, 2018).

The same authors and Whitnall (1921) state that a flatter nasal bridge, combined with a thick anterior lacrimal crest and projecting maxillary bones, suggests the an epicanthic fold, a trait commonly associated with individuals of Asian ancestry. Other authors have also reported variations related to age, sex and ancestry in the morphology of the eye region (Sforza et al., 2009b; Van den Bosch et al., 1999).

The eyebrow pattern is supposed to echo the shape of the supraciliary arch, and the relationship has been noticed by palpation and craniograph research (Balueva et al., 2009; Fedosyutkin & Nainys, 1993). According to the same researchers, the lower outline of the eyebrow sits on top of the upper orbital edge and follows the same shape. If the brow ridge is strongly developed, the eyebrows will shift downwards 1–2 mm below the upper rim, causing what has been referred to as "overhanging" eyebrows (Fedosyutkin & Nainys, 1993). Conversely, a weakly developed nasal and brow ridge will make the inner third of the eyebrow turn inwards into the orbit while the remaining part will gradually rise to meet the contour of the orbital margin. If the outer part of the supraorbital rim is thick and the brow ridge developed, the eyebrow will describe an angle. Following the same authors, the outline of the eyebrow is also supposed to match the outline of the superciliary arch.

Taylor (2001) reported that the superciliare point is directly above the lateral margin of the iris. Stephan (2002b) tested this guideline and observed that while it might be approximate for females, the superciliare point is more laterally positioned in males. A recent study measured the eyebrow shape in a total of 244 Caucasian individuals and, in accordance with Stephan (2002b), concluded that visible sexual dimorphism and age-related changes occur (Kraus et al., 2019). Their results show that the highest point in the eyebrow (HBP) is located higher and more laterally in males than in young females, indicating that the brow is more angled in males and more curved in females. The same authors also suggest that the eyebrows become more similar with age, as the characteristic curvature seen in young females starts to converge with

the typical appearance of the male eyebrows. Another age-related change observed by them, and contrary to the behavior of most tissues in the body, is the upward movement of the upper brow line in older individuals, especially females.

The eyebrows can be a problematic feature to assess due to their volatile character. They are subject to personal aesthetic taste, social trends, or even ritualistic practices and can easily be plucked or painted to alter the natural shape or completely removed.

3.2 The nose

The nose is a central piece in establishing the contour line of the profile of an individual. The nose is located in the middle third of the face, relates to all other facial features and plays an essential role in recognizing the profile view.

The human nose is a complex structure that presents a significant amount of individual variation within muscles, skin and fat, as well as asymmetrical cartilages and intricate anatomical relationships between hard and soft tissues (Anderson et al., 2008; Steele & Thomas, 2009). While some bones of the skull do contribute to underline the overall framework of the nose, by supporting the nasal cartilaginous skeleton, most of the external morphology is shaped by soft tissues. Of all these tissues, the musculature is the one with less impact on the shape of the profile (Macho, 1989). The nasals, maxillae, ethmoid and vomer bones provide support for the cartilaginous skeleton, which is composed of the septal cartilage, the lateral cartilages, the greater alare, and a variable number of lesser alar and sesamoid cartilages (Anderson et al., 2008). The septal cartilage divides the piriform aperture in the sagittal plane and is sustained by the vomer bone and the anterior nasal spine. The lateral cartilages are triangular structures that are continuous with the septal cartilage and attach to the inferior surface of the nasal bones. The greater alar cartilages contribute to form the exterior walls of the nostrils, as well as the columella and the tip of the nose. The lesser alar cartilages, together with the fibro-areolar tissue, help shape the inferior part of the walls of the nostrils (Anderson et al., 2008; Drake et al., 2017). The skin that covers the nose is usually thinner at the

mid-third, over the dorsum and rhinion, and thicker at the nasal tip and nasofrontal groove (1.25 mm) (according to dissection data published by Lessard & Daniel, 1985).

Several techniques for estimating nasal morphology from the bone anatomy have been presented throughout the years, making the nose the most studied feature of the face. The first studies to assess the relationships between bone and the soft nose were conducted early in the 20th century by Birkner (1907); His (1895); Schultz (1918); Tandler (1909); and Virchow (1912), but have been contradicted by more recent research. Despite the marked differences in the nasal shape between distinct populations, sexual dimorphism manifests in a similar way (Aung et al., 2000; He et al., 2009; Ngeow & Aljunid, 2009; Ozdemir et al., 2009; Pazos et al., 2008; Schlager & Rüdell, 2015; Sforza et al., 2011), with males showing larger noses than females, and different growth patterns for each sex have been reported. The growth of the nasal tissues occurs earlier in adolescent females (see, for instance, Sforza et al., 2011; or Van der Heijden et al., 2008) and reaches the majority of adult dimensions around 16 years of age for both men and women (Prahl-Andersen et al., 1995; Sforza et al., 2011). Age-related changes have also been reported for the nasal anatomy (Schlager, 2013; Schlager & Rüdell, 2015; Sforza et al., 2011), as increments in the nose dimensions continue well-beyond skeletal maturity and tend to be more visible in males than in females (Farkas, 1994; Sforza et al., 2011; Zankl et al., 2002). These increments make the nose become more prominent and, as the septum tends to sink downwards (likely amplified by maxillary resorption after teeth loss), the tip also descends (Macho, 1986, 1989). These changes interfere with applying the published methods in individuals above 50 years of age, increasing the chance for less accurate predictions (Guyomarc'h, 2011; Rynn et al., 2010).

Maxillary and mandibular disorders also seem to impact nasal dimensions. Glanville (1969) reports that maxillary prognathism seems to correlate with broad and shorter noses. Other authors state that a vertical deficiency in the maxilla results, consequently, in insufficient support for the nose cartilages and might be the underlying cause for nasal dorsal humps and overhanging nasal tips (Peacock et al., 2014).

As the literature on nose morphology is extensive, Table 3.2 and Table 3.4 collect the most relevant studies that proposed methods to predict the soft anatomy from the nasal bones.

Table 3.2 - Published guidelines to determine the anatomy of the nose profile from the skull.

LC = lateral cephalograms; CT = computer tomography; CBCT = cone beam computer tomography.

References	(n), sample	Guidelines according to the authors
Gerasimov (1955, 1971)		Two-tangent method: one line extends from the "last third of the nasal bone", and the other follows the general direction of the anterior nasal spine. The point where the two intersect dictates the position of the pronasale. This guideline was interpreted literally in Stephan et al. (2003), and more freely in Rynn and Wilkinson (2006), who used the distal end of the nasal bones.
Gerasimov as described by Ullrich and Stephan (2011, 2016)		Later variant of the two-tangent method: One line extends from the distal end of the nasal bones (last 1–2 mm), and the other follows the general direction of the floor of the anterior part of the nasal aperture (on the maxillary bone) adjacent to the anterior nasal spine and vomer bone. The intersection dictates the position of the pronasale. The outline of the infero-lateral rim of the nasal aperture was used to approximate the outline of the tip of the nose.
Krogman and İşcan (1986), first described in Krogman (1962)		A line is projected following the direction of the nasal spine. The pronasale point is located at three-times the depth of the soft tissue marker at the mid-philtrum point, along the projected line.
George (1987)	(54), LC. North Americans aged between 14 and 36 years.	A line (A) extends from nasion to the point of most flexion beneath the nasal spine (B). A second line (C) is placed parallel to Frankfort Horizontal Plane and passes halfway along the inferior slope of nasal spine. Projection is estimated from a percentage of the distance between nasion and point B. In profile, the alar groove is anterior and inferior to the nasal notch.
Macho (1986, 1989)	(353), LC. Austrian subjects between 21 and 83 years.	Measurements are taken perpendicular to nasion-sella plane (NSP) and regression equations are used to predict height, length and depth of the nose.
Prokopec and Ubelaker (2002)	Explanation of a method originally developed by Gerasimov.	A line is drawn crossing the nasion and prosthion (A) and transfer it to intersect the foremost point on the nasal bone (B). Four to six equidistant parallel lines are placed perpendicular to B to the base of the piriform aperture. Those lines are then mirrored to the other side of line B to obtain the outline of the nose profile. 2 mm are added to the contour to simulate the mean thickness of the skin.
Stephan et al. (2003)	(59), LC. Australian of European ancestry between 32 and 82 years.	Nasal bone angle measured from nasion to rhinion. Measurements taken from cranial landmarks and regression equations are used to predict the pronasale.
Utsuno et al. (2008)	(128), LC. Japanese male children between 7 and 18 years old.	Measurements are taken from cranial landmarks, and regression equations are used to estimate the nasal tip.
Rynn et al. (2010)	(79), CT. North American adults below 50.	Measurements taken from cranial landmarks and regression equations are used to estimate the nose's projection and predict the height, length, and depth of the nasal profile. The equations are sex-specific. Also, in profile, the alar crease is placed approximately 5 mm anterior and inferior to the aperture border.

*Guyomarc'h (2011)***	(119), CT. European, aged between 18 and 87	Measurements are taken from cranial landmarks and regression equations are used to estimate the projection of the nose and predict height, length and depth of the nasal profile.
K. M. Lee et al. (2014)	(437), CBCT. Korean. Young adults.	Measurements are taken from cranial landmarks and regression equations are used to estimate the pronasale and the subnasale.
Utsuno et al. (2016)	(55), LC. Japanese males between 20 and 40 years old.	Measurements are taken from cranial landmarks and regression equations are used to estimate the nasal tip.
Tedeschi-Oliveira et al. (2016)	(600) LC, Brazilian adults between 24 and 77 years.	Proposal of a new guideline that establishes the pronasale within a 90º angle with the rhinion and the prosthion points.
Sarilita et al. (2018)	(335), LC. Indonesian adults between 17 and 51 years.	Recalibration of the method of Rynn et al. (2010) to achieve better results for an Indonesian population.
Ridel et al. (2018)	(120), CBCT. SA, European and African ancestry, between 18 and 30	Measurements are taken from cranial landmarks and regression equations are used to estimate the pronasale and the subnasale.
Bulut et al. (2019)	(90), CT. Turkish, between 20 and 49 years old.	Recalibration of the method of Rynn et al. (2010) to achieve better results for a Turkish population.
Chu et al. (2020)	(240), CBCT. Chinese between 20 and 30 years.	Measurements are taken from cranial landmarks and regression equations are used to estimate the nasal profile. The equations are sex specific.
U. Y. Lee et al. (2020)	(437), CT. Korean aged between 20 and 85 years.	Measurements are taken from cranial landmarks and regression equations are used to estimate the nasal profile. The equations are sex and age specific.

*According to the authors, after the publication of *Vosstanovlenie lica po cerepu* (1955), Gerasimov continued to update his methods for 15 years prior to his death. This reference offers the most up-to-date account of the method, as experimented directly by Herbert Ullrich, who was a pupil of Gerasimov.

**Unpublished PhD thesis.

Table 3.2 shows that methods are currently moving towards standardization and improvement, materialized in the development of prediction techniques that rely on larger datasets and population-specific regression equations. As shown in Table 3.3, some of the methods defined in Table 3.2 were put to the test independently by several researchers, sometimes with contradicting results that might stem from different interpretations of the recommended guidelines. Mala (2013) tested the methods of Stephan et al. (2003)

and Rynn et al. (2010) and concluded that the latter performed slightly better and should be preferred for statistical and practical reasons, at least for populations of European ancestry. Regarding the estimation of the pronasale tip using Gerasimov's two-tangent methods, Maltais Lapointe et al. (2016) put the existing variables to the test and concluded that the one proposed by Ullrich and Stephan (2011, 2016) performs better than the others but, contrary to previous studies, cannot accurately approximate the position of the pronasale. However, it is worth emphasizing that Maltais Lapointe et al. (2016) used postmortem CT scans taken in supine position. Thus, it is difficult to evaluate if the flattening of relevant soft tissue caused by the effect of gravity introduced a bias in the results.

Rynn et al. (2010) also confirmed earlier suggestions that a deviation on the bony septum represents an opposite lateral deviation of the nose (Gray, 1965; Seltzer, 1944) and that the shape of the anterior nasal spine (sharp, spatulate or split) translates into the shape of the tip in frontal view (normal/rounded, bifid columella or full bifid nasal tip, respectively) (Weaver & Bellinger, 1946). Davy-Jow et al. (2012) suggest a simple method to approximate the shape of the nose tip, using a sample of 25 full head CT scans. They propose that the shape of the nose tip mimics the curvature of the superior portion of the nasal aperture when the soft tissue pronasale superimposes the hard-tissue-rhinion. In practice, the pronasale tip can be approximated from the cranium by tilting the head dorsally ca. 60º, but this cannot be used for individuals with snub noses.

Table 3.3 - Published assessments of accuracy for nasal projection performed independently by various researchers. Measurements in mm.

Methods tested	**Stephan et al. (2003) (1)**	**Rynn and Wilkinson (2006) (2)**	**Mala (2013) (3)**	**Maltais Lapointe et al. (2016) (4)**
Gerasimov (1955, 1971)	Overestimated nasal projection by 6.2 in males and 4.3 in females.	Predicted the position of a point on the tip of the nose within 1.		Overestimated two reference points by 19.37 and 11.93.
Gerasimov after Ullrich and Stephan (2011, 2016)				Overestimated two reference points by 8.85 and 5.44.
Krogman and İşcan (1986)	Underestimated by 1.9 in males and 4.1 in females.	Underestimated by 9.3 in males and 8.9 in females.		

George (1987)	Underestimated nasal projection by 1.5 in males and 2.8 in females.	Overestimated nasal projection by 1.4 in males and 0.9 in females.	
Macho (1986, 1989)		Overestimated all measurements, except female nose length.	
Prokopec and Ubelaker (2002)	Overestimated nasal projection by 1.4 in males and 2.2 in females.		
Stephan et al. (2003)	Overestimates nasal projection by 0.2 in males and underestimates by 0.1 in females.*	Underestimates nasal projection by 2.2 in males and 1.1 in females.	Underestimates nasal projection by 2.4 in males and 0.8 in females. Vertical placement is overestimated by 1.1
*Rynn et al. (2010)***			Underestimates nasal projection by 1.3 and overestimated vertical position by 0.04.

* It is worth noting that these results may be biased because the regression equations were tested on the same sample they were derived from.

** Also tested by the authors on a small sample of five subjects with European ancestry from Belgium, where the largest estimated error does not exceed 2.5 mm.

(1) Tested on a sample of 59 lateral head cephalograms of Australian individuals of European ancestry between 32 and 82 years.

(2) Tested on a variable sample of 122 lateral head cephalograms of adult individuals of European ancestry from Great Britain.

(3) Tested on a sample of 86 lateral head cephalograms of individuals between 19 and 43 years old from Central European descent.

(4) Tested on a sample of 137 postmortem CT scans of individuals between 21 and 87 years old from a modern Danish population.

Although less studied than the nose profile, a few guidelines were proposed to predict the nasal width from the measurements of the piriform aperture (Table 3.4).

Table 3.4 - Published guidelines to determine the alar width from the piriform aperture.

CT = computer tomography; CBCT = cone beam computer tomography.

References	(n), sample	Guidelines according to the authors
Gerasimov (1955, 1971)		The width of the bony nasal aperture at its widest point is 3/5 of the overall width of the soft nose. The height of the upper alae is aligned with the *crista conchalis* inside the piriform aperture. Rynn et al. (2010) later tested both guidelines and found them to be accurate. The base of the nose is in line with the direction of the nasal spine. Asymmetry in the alar height will be apparent in the shape of the lateral nasal bones.
Hoffman et al. (1991)	(182), North American of African and European descent	Corrected an earlier guideline by Krogman (1962) and proposed a simple equation using the bony alar width to estimate the soft distance.
*Guyomarc'h (2011)**	(422), CT. European aged between 18 and 95	Measurements are taken from cranial landmarks and regression equations are used to estimate the alar width.
K. M. Lee et al. (2014)	(60), CBCT. Korean. Young adults.	Measurements are taken from cranial landmarks and regression equations are used to estimate the alar width.
Strapasson et al. (2017)	(96) CBCT. Brazilian, aged between 18 and 65 years.	Measurements are taken from cranial landmarks and regression equations are used to estimate the alar width. Method further tested with a larger sample (246 CT scans of Brazilian adults) and deemed accurate by Strapasson et al. (2019a).
Ridel et al. (2018)	(120), CBCT. SA, European and African ancestry, between 18 and 30	Measurements are taken from cranial landmarks and regression equations are used to estimate the alar width.
Chu et al. (2020)	(240), CBCT. Chinese between 20 and 30 years.	Measurements are taken from cranial landmarks and regression equations are used to estimate the alar width and angle. The equations are sex-specific.
U. Y. Lee et al. (2020)	(389), CT. Korean aged between 20 and 85 years.	Measurements are taken from cranial landmarks and regression equations are used to estimate the alar width. The equations are sex- and age-specific.

*Unpublished PhD thesis.

Despite the number of existing studies, a recent systematic review of the literature has highlighted problems still entailed by predicting the nose from skeletal morphology (Strapasson et al., 2019b). Many guidelines presently in use are derived from relatively small samples ($n < 100$) and require more testing to be further validated. Published data also makes it apparent that nose anatomy varies among different groups and needs specific equations to reduce the estimation error (Chu et al., 2020; Ridel et al., 2018; Sarilita et al., 2018; Utsuno et al., 2016). Thus, besides age and sex, populational affinity is also an essential parameter to consider when selecting guidelines to perform facial approximations.

3.3 The mouth

The placement of the mouth is essential for a correct evaluation of the facial proportions. The oral aperture is bound by the upper and lower lips and opens to the oral cavity. The superior border of the upper lip connects to the columella of the nose through the philtrum, and the inferior limit of the lower lip is the mentolabial sulcus (Carey et al., 2009). Both lips connect at the labial commissures, also known as the corners of the mouth (Carey et al., 2009), and the size and curvature of the red portion (the vermilion) present individual, sex and populational variation.

Compared to the nose, the relationships between the soft tissues of the mouth and the skeletal structure are fairly understudied. Most of the earlier research on this area of the face was developed within the fields of orthodontics and surgery, but these are not concerned with the relationships between bone and soft tissue. Instead, they focus on aesthetic standards (e. g. Broadbent & Mathews, 1957) or offer correlations between other facial features (Nanda & Ghosh, 1995). Some of the earlier recommended guidelines propose an estimation based on a feature-to-feature correlation, potentially increasing the amount of error if the first feature is incorrectly placed (e. g. Krogman & İşcan, 1986; Prag & Neave, 1997). However, and despite the more "mobile" nature of the mouth and limited connection to bone structures, research suggests that at least some of its characteristics can be predicted from skeletal anatomy. Table 3.5

and Table 3.6 contain an overview of the published guidelines for the general morphology of the mouth and thickness of the lips, respectively.

Table 3.5 - Published guidelines for the general morphology of the mouth area (mouth canthi, oral line, nasolabial fold, width of the philtrum). LC = lateral cephalograms; P = Photographs; CT = computer tomography; CBCT = cone beam computer tomography.

References	**(n), sample**	**Guidelines according to the authors**
Wilder (1912)		The oral line in repose matches the occlusion line of the teeth.
Gerasimov (1955, 1971)		The teeth occlusion, the dental pattern, the morphology of the mandible and the facial profile define the shape of the mouth. The nasolabial fold starts from the lateral border of the nasal aperture above the *crista conchalis* and ends just below the second molar in the direction of the inner angle of the mandible.
Gerasimov as described by Ullrich and Stephan (2011, 2016)		The width of the mouth equals the distance between the upper second molars. The oral fissure follows the line of occlusion, but it is set above it (the stomion point is halfway down the central incisors).
Fedosyutkin and Nainys (1993); Gatliff (1984); Krogman (1962)		The mouth width is approximately the distance between two lines radiating from the junction of the canine and first premolar on each side.
Angel (1978), apud Wilkinson (2004b)		The mouth canthi stand at the first premolar-canine junction and the oral fissure is located at the level of the midpoint of the incisors. The strength of the markings of the levator and depressor anguli oris muscles defines the height of the canthi. The markings of the levator labii superioris and zygomaticus define the curves and depth of the nasolabial fold, along with the possibility of a second lateral crease.
Krogman and İşcan (1986)		The mouth width equals the distance between the pupils and the corners of the mouth correspond to the junction between the upper canine and first premolar on both sides. The radiating lines guideline should be used in three-dimensional facial approximations.
George (1987)	(54), LC. North Americans between 14–36.	The oral fissure cuts across the lower third (female) or quarter (male) of the maxillary central incisor.
Fedosyutkin and Nainys (1993)		The nasolabial fold extends from the upper edge of the nostril to the first maxillary molar. It is more pronounced when the canine fossa is deep (5 mm), and when the teeth are absent. The width of the philtrum matches the distance between the midpoints of the upper central incisors.
Prag and Neave (1997)		Distance between the medial borders of the iris equals the mouth width.
Lebedinskaya (1998), apud Mala and Veleminska (2016)		Recommends placing the oral fissure opposite to the cutting edge of the upper central incisors.
Taylor (2001)		The oral fissure is slightly above the edges of the upper central incisors.

Stephan (2003b); Stephan and Henneberg (2003)	(93), P. Mixed population. Young adults.	Inter-canine width is about 75% of the actual mouth width.
Song et al. (2007)	(50), Dissection. Korean, from 31–101 years.	The infraorbital foramina and the corners of the mouth lie in the same sagittal plane.
Dias et al. (2016)	(430), CBCT. Brazilian between 11 and 81 years old.	Proposes that the 75% rule, originally published by Stephan and Henneberg (2003) is the most accurate guideline to estimate mouth width in males, while females achieve a better approximation with an 80% rule.
Mala and Veleminska (2016)		Reports an unpublished guideline by Balueva and Veselovskaya: the oral line relates to incisor occlusion. If the upper incisors overbite the lower ones, the oral fissure is placed at the level of the cutting edge of the lower incisors. If the maxillary incisors occlude with the mandibular ones, the oral fissure is opposite to the cutting edge of the upper incisors.

Table 3.6 - Published guidelines for the morphology of the lips. LC = lateral cephalograms; P = Photographs; CT = computer tomography; CBCT = cone beam computer tomography.

References	**(n), sample**	**Guidelines according to the authors**
Gerasimov (1955, 1971)		The height of the enamel of the middle incisor equals the thickness of the vermilion, but this is not a constant factor as it changes with age and varies within the same racial group. The lip thickness derives from the prognacy of the teeth, the incisors, and alveolar parts of both the maxilla and mandible. Prominent big teeth associate with thick lips and prognathism. Small straight teeth relate to thin lips and orthognathism. Maxillary and mandibular prognathism suggest procheilia of the upper and lower lip, respectively.
Gerasimov as described by Ullrich and Stephan (2011, 2016)		With strong prognathism the lips are thick and the philtrum deep. Large incisors also mean thick lips. Weak prognathism and average-sized teeth produce a feminine lip form. If the central incisor is broad with a small lateral incisor, then the upper lip is strongly curved. If both incisors are broad, the upper lip is less curved. A deep mentolabial sulcus with a projecting chin, then the lower lip is thick.
Krogman (1962); Krogman and İşcan (1986)		Both African and European ancestries have a well-developed philtrum and show a cupid's bow in the upper lip. In individuals of European ancestry, the vermilion shows a smooth junction with the upper lip, whereas in Africans it is elevated to form what Krogman described as the "lip seam".
Angel (1978), apud Wilkinson (2004b)		Lip thickness is influenced by the projection of the teeth, racial group, and the strength of incisive and buccinator muscles. The line of the lower edge of the lower lip is just above the middle of the incisor crowns.

Gatliff (1984); Gatliff and Snow (1979); Taylor (2001)		The vertical thickness of the lips is measured from gum line to gum line on the teeth.
George (1987)	(54), LC. North Americans aged 14–36 years.	The border of the upper lip stands opposite to the upper quarter of the maxillary central incisor in both males and females. The lower lip is opposite to the lower three-quarter mark of the mandibular central incisor.
Fedosyutkin and Nainys (1993)		With maxillary prognathism, the upper lip projects further than the lower one. The lower lip projects if there is mandibular prognathism or if the frontal edge of the alveolar arc of the mandible is well-developed. Other characteristics of the mouth and lips have to be derived from an "educated guess".
Wilkinson et al. (2003)	(95), Direct measurements. European and Asians descent aged 20–60.	Regression equations based on teeth dimensions for a European population and for Asians of the Indian subcontinent.
*Guyomarc'h (2011)**	(157), CT. European aged 18–88 years.	Regression equations based on teeth dimensions.
Dias et al. (2016)	(430), CBCT. Brazilian aged between 11 and 81 years old.	The height of the vermillion borders corresponds to approximately 26% of the width of the mouth.
Mala and Veleminska (2016)	(96), LC. European aged between 19 and 43 years.	Reports on an unpublished guideline by Balueva and Veselovskaya, according to which the upper lip margin is placed at the upper margin of the maxillary central incisors, and the lower lip margin is opposite to the lower margin of mandibular central incisors.
Houlton et al. (2020)	(124) CBCT. SA of African and European ancestry, aged between 20–87.	Estimates upper, lower, and total lip height through regression equations best suited to individuals of Sub-Saharan African origin.

*Unpublished PhD thesis.

The earliest guideline by Wilder (1912) seems to be contradicted by more recent arguments that the line of contact between the lips, the oral fissure, lies just above the incisal edges of the anterior maxillary teeth (Fedosyutkin & Nainys, 1993; George, 1987; Mala & Veleminska, 2016; Standring, 2016; Taylor, 2001; Ullrich & Stephan, 2011, 2016).

A few studies have addressed the accuracy of mouth and lip prediction guidelines (Table 3.7). Stephan (2003b) tested three guidelines, two of them based on measurements related to another feature

(the eye), and one focusing on the relations of the mouth with the teeth. The author found that, among the tested guidelines, the most accurate is the one that predicts mouth width from the medial borders of the iris. Wilkinson et al. (2003) tested the width of the mouth in a sample of 96 individuals and found no correlation between mouth width, bizygomatic width, interpupillary, and interalar distances. Following Stephan (2003b), these authors concluded that the most reliable guideline to predict mouth width is the interlimbus (medial borders of the iris) distance. To achieve a guideline that is not dependent on the placement of other predicted features, Stephan and Henneberg (2003) proposed that mouth width corresponds to approximately 75% of the distance between the canines. This assessment was later confirmed by other independent studies (Dias et al., 2016; Stephan & Murphy, 2008).

Stephan and Murphy (2008) tested the "radiating lines" method,[21] the inter-mental and inter-orbital foramina distances (Song et al., 2007), the 75% rule, and the inter-canine distance (Stephan & Henneberg, 2003). Despite the small sample made up of nine dissected individuals, the authors propose that the inter-orbital foramina distance can be used as an alternative to predict mouth width in edentulous crania. Mala and Veleminska (2016) tested a sample of 96 individuals and reported that the oral fissure was in 99 percent of the cases above the cutting edge of the upper incisors and is not sex specific. They sustain that the lower central incisors can be used to guide the placement of the oral line if the central incisors are missing. According to Mala and Veleminska (2016), Wilkinson et al. (2003) provides the best approximation to estimate the thickness of the lips in females. For males, the best guideline for the upper lip is that of George (1987) and, for the lower lip, Wilkinson et al. (2003) should be followed.

[21] This is the guideline first proposed by Krogman (1962), as interpreted by Wilkinson (2004a, 2004b), who establishes that the angle of the lines radiating from the canines should be perpendicular to the contour of the dental arcade.

Table 3.7 - Accuracy assessments for guidelines for the prediction of mouth width. Measurements in mm.

Methods tested	Stephan (2003b) (1)	Wilkinson et al. (2003) (2)	Stephan and Murphy (2008) (3)
Interpupillary distance	Overestimates by 11 (SD 4).	Overestimates by 10.5.	
Interlimbus distance	Underestimates by 2 (SD 4).	Overestimates by 2.6.	
Canine width	Underestimates by 13 (SD 3).		
75% rule			Underestimates by 2.4.
Radiating lines			Underestimates by 7.3.
Infraorbital foramina distance			Underestimates by 3.3.
Mental foramina distance			Underestimates by 12.9.

(1) Tested on a sample of 146 photographs of a mixed population made up of young adults.

(2) Tested on a sample of 96 direct measurements and photographs of adult individuals of European ancestry and Asian (from the Indian subcontinent), aged between 20 and 60 years old.

(3) Tested on a sample of 9 embalmed cadavers of European extraction, ranging from 62 to 94 years. Canine width, 75% rule and radiating lines were tested on a sample of 3; infraorbital and mental foramina distance in samples of 9 and 8, respectively.

Anthropometric studies show that mouth width displays significant differences between male and female. Latta (1988) measured one hundred patients (between 32 to 87 years) and found that the width of the mouth and the width of the philtrum were correlated irrespective of age, sex or racial group. In Latta (1988), none of these distances was affected by age, and the size of the mouth and philtrum was larger in men than women and larger for African when compared to European descent. Ferrario et al. (2000b) measured mouth widths in adults from northern Italy and found that the distances were greater in men, showing similar values to other studies (Farkas, 1994; Nanda & Ghosh, 1995). Other anthropometric studies show that there is significant variation across different ages and populations. Like the nose, all lip dimensions seem to be larger in males than in females (Ferrario et al., 2000a) and reaches adult size between 16 and 18 years (Gonçalves et al., 2011). Populational differences can also be observed. African individuals

present thicker lip heights compared to those of European ancestry (Houlton et al., 2020; Schmidlin et al., 2018; Sforza et al., 2010). However, a recent study by Houlton et al. (2020) found no support for the relationship between incisor and lip height, suggesting that the canon employed by Gatliff and Snow (1979), Gatliff (1984), and Taylor (2001) is inaccurate for individuals of Sub-Saharan African origin. This circumstance had already been reported by Wilkinson et al. (2003), who emphasized the need for population-specific equations.

Aging also interferes with the shape of the mouth and lips, causes dental wear (Sperber, 2017), and increased distances in mouth width for males. Moreover, it leads to a decrease in the lip height that is observable in different populations (Dias et al., 2016; Houlton et al., 2020; Schmidlin et al., 2018; Sforza et al., 2010; Wilkinson et al., 2003).

3.4 The chin

The chin has been a subject of interest for more than two centuries. It is regarded as a significant morphological trait within the scope of evolutionary studies and relevant for identifying hominid fossils. Schwartz and Tattersall (2000) provide an extensive overview of this feature, including developmental and morphological data on the skeletal chin of *Homo sapiens* and a review of the Neanderthal and the Middle to Late Pleistocene hominid fossils from Europe, the Levant, and northern Africa.

Tandler (1909), cited by Wilkinson (2004b), was the first to address the relationship between the chin and the underlying bone anatomy. He reported that the degree of chin protrusion and the thickness of soft tissues above were not connected.

However, decades later, Gerasimov (1971) suggested that the morphology of the mandible does influence the chin appearance: if the lower border is soft and rounded inwards, and has no crests or roughness, then the muscles will cover the bone and form gentle chin contours. Conversely, if the lower border shows prominent crests, then well-developed muscles will be present and form a more massive chin. Gerasimov (1971) also stated that a cleft chin or dimple would be present if there is a central groove on the

mental eminence and strong muscle attachments for the mentalis muscles. This idea finds resonance in more recent research. Schwartz and Tattersall (2000) refer that, in some individuals, the two mandibular halves fuse, but the symphyseal gap in the midline is not completely obliterated, leaving some reminiscence of a shallower inverted "V" depression. Kumar et al. (2014) link this bony fissure to the Y-shaped deformation that sometimes occurs on the soft chin, a feature they call the "chin dimple".

Gerasimov (1971) also addressed the fact that aging makes the chin protrude. Aging leads to bone resorption at the alveolar processes, and the loss of teeth will ultimately alter the jawline and mouth significantly (Bodic et al., 2005). The bony changes affecting the profile include a reduction in mandibular alveolar ridge height. The resorption rate depends on the shape of the mandibular base: the broader the base, the slower the rate of resorption. Therefore, the mouth will apparently sink into the face, making the nose and the chin appear more prominent, and the distance between these two features will decrease (Neave, 1998). These transformations will also influence the mentalis musculature, the main supporting element of the soft chin (Rubens & West, 1989).

For Fedosyutkin and Nainys (1993), the shape of the lower face echoes that of the mandibular contour. The same authors relate the analysis of the mandible with the shape of the chin: if the gonial angle is over 125º and the coronoid process is high, it is likely that the face narrows towards the chin; a right angle, coupled with a low and wide coronoid process favors a rounded or rectangular shape. They also state that an everted gonial region can be associated with a more squared shape of the lower face, while the chin will be high if the height of the mandibular body diminishes from the chin triangle to the rami.

Other guidelines suggest that, when seen from the frontal view, the chin shape will also be under the influence of the mental spines (otherwise known as genial tubercles): if the genial tubercles are closer, the chin will be more triangular; if wide apart, the chin will be squared; and, if unexpressed, the chin will be round (Damas et al., 2020).

Despite these orientations, the representation of the soft chin from the bone is still based on rather subjective and vague directives (İşcan & Steyn, 2013), and requires more independent testing.

3.5 The ears

Despite the existence of several anthropometric studies, few have investigated the relationship between the ears and the skull. Eye-tracking studies (e. g. Buchan et al., 2007; Iskra & Gabrijelčič, 2016) have shown that when we try to assess identity, emotions, or speech, our gaze is directed primarily at our other features, namely the eyes, nose and mouth. Ears are often covered, either by hair or headgear such as hats, turbans, or veils, and they are immovable features that do not contribute to the complex network of facial expressions. Even so, modeling the ears in a facial approximation is still required to achieve an acceptable *gestalt* appearance of the face.

Welcker (1883) was the first to approach the subject. He upheld that the main axis of the ear is parallel to the ascending ramus of the mandible and that the cartilaginous opening of the ear is placed more superior and posterior than the bone opening, with a mean displacement of 5.3 mm. The first of Welcker's guidelines for ear prediction lacks empirical testing (Guyomarc'h & Stephan, 2012), but the second was later confirmed by Ashley-Montagu (1939). Through a sample of 40 dissections in adults, the latter author established that the opening of the external auditory meatus is located 5 mm below and 2 mm anterior in relation to the porion landmark. The distance between the bone and the cutaneous opening is approximately 9.6 mm.

Gerasimov (1955) states that the ear and the nose share similar heights, based on data collected from 462 Tajiks. Despite minor modifications in later years (Ullrich & Stephan, 2011), Gerasimov's guidelines echo much older rules of proportion. These rules have been repeated and slightly modified by other practitioners (Fedosyutkin & Nainys, 1993; Gatliff, 1984; Jordanov, 2003), but recent testing (Guyomarc'h & Stephan, 2012) shows that even though there is a weak positive correlation between nose height and ear height, the height of the nose usually underestimates ear height. This circumstance is already stressed by the measurements published in Farkas' (1994) and Farkas et al. (1985), according to which the ears are, on average, ca. 10 mm larger than the nose.

Gerasimov also placed the angle of the ear parallel to the jawline and reported a relationship between the mastoid processes and the earlobes: (1) if the mastoid processes are directed downwards, in relation to the Frankfort Horizontal Plane (henceforth FHP), then the earlobe is attached to the soft tissue

of the cheek; (2) if the mastoid processes point forward, the earlobe is separated from the cheek. These relationships were later supported by Fedosyutkin and Nainys (1993). While Renwick (2012), *apud* Damas et al. (2020) agrees with Gerasimov's statement concerning earlobe attachment, Guyomarc'h and Stephan (2012) found no relationship between the mastoid processes and the earlobes in a sample of 78 CT scans of living subjects collected at French hospitals.

Despite recognizing a large magnitude of error permeating ear prediction guidelines, Guyomarc'h and Stephan (2012) published the most complete validation study on these features so far, and their findings set the current standards for modeling the ears in a facial approximation. The authors present a regression equation that may be used to predict ear length, as it provides the greatest generalization verified by cross-validation, whereas the width of the ear should follow the published means (Table 3.8 and Table 3.9).

Table 3.8 - Mean ear height and width (mm) in adult males in the literature, adapted and expanded from Guyomarc'h and Stephan (2012). Left ear measurements reported where the original study does not combine both.

Study	**Method**	**Sample**	**n**	**Age range (years)**	**Mean height**	**SD**	**Mean width**	**SD**
Bozkir et al. (2006)	Sliding caliper	Turkish	191	18–25	63.1	3.6	33.3	2.2
Jordanov (2003)	n/a	Bulgarians	53	Adults	62.9	2.8	-	-
Farkas (1994)	Sliding caliper	U. S. Caucasoids	109	19–25	62.9	3.5	36.4	2.4
		Chinese	30	18	60.7	2.8	34.7	2.4
		African American	50	18–25	59.8	4.0	36.2	3.2
Brucker et al. (2003)	Sliding caliper	Rhode Island Hospital	34	18–61	65.2	-	-	-
Ferrario et al. (1999)	3D digitizer	Italians	126	18–30	63.2	4.0		
			99	31–56	65.3	4.1		

Meijerman et al. (2007)	Photogrammetry	Dutch	911	20–90	71.0	5.5	35.0	3.3
Sforza et al. (2009a)	3D digitizer	White Italians	126	18–30	62.2	4.1	36.7	3.5
			99	31–80*	65.8	4.7	39.1	3.7
Alexander and Laubach (1968), apud Guyomarc'h and Stephan (2012)	Photogrammetry	USAF Flight Personnel	500	22–34	67.1	4.5	-	-
Purkait and Singh (2007)	Sliding caliper	Indian (South East Asian)	121	18–30	57.7	2.2	31.1	1.8
			294	30–70**	61.2	3.5	34.3	2.2
Guyomarc'h and Stephan (2012)	CT scans and sliding caliper	French hospitals (mixed ancestry)	43	18–84	64.3	5.5	38.5	3.2
Modabber et al. (2018)	3D Scans	Caucasians	40	21–35	62.7	3.7	32.7	3.3
			40	36–50	66.2	3.6	34.1	2.8
			40	51–65	68.2	4.0	36.3	2.8
Faakuu et al. (2020)	Sliding caliper	Dagaaba (Upper West Region of Ghana)	116	15–75	58.3	3.8	32.8	2.2

(* Weighted mean calculated by combining original samples of 30–40, 40–50, 50–60, and 60–70 years; ** Weighted mean and standard deviation calculated by combining the original samples of 31–40, 41–50, 51–64, and 65–80 years)

Table 3.9 - Mean ear height and width (mm) in adult females in the literature, adapted and expanded from Guyomarc'h and Stephan (2012). Left ear measurements reported where the original study does not combine both.

Study	**Method**	**Sample**	**n**	**Age range (years)**	**Mean height**	**SD**	**Mean width**	**SD**
Bozkir et al. (2006)	Sliding caliper	Turkish	150	18–25	59.7	3.0	31.1	2.2
Jordanov (2003)	n/a	Bulgarians	108	Adults	58.5	3.9	-	-
Farkas (1994)	Sliding caliper	U. S. Caucasoids	200	Female, 19–25	59.9	3.5	33.7	2.2
		Chinese	30	Female, 18	57.6	3.6	32.4	2.4

		African American	50	Female, 18–25	57.0	3.3	34.2	2.9
Brucker et al. (2003)	Sliding caliper	Rhode Island Hospital	89	Female, 19–65	59.7	-	-	-
Ferrario et al. (1999)	3D digitizer	White Italians	73	Female, 18–30	57.4	3.5		
			38	Female, 31–56	60.3	3.2		
Meijerman et al. (2007)	Photogrammetry	Dutch	431	Female, 20–90	64.0	5.4	33.0	2.9
Sforza et al. (2009a)	3D digitizer	White Italians	66	Female, 18–30	56.4	4.1	34,4	3.1
			64	Female, 31–80*	61.6	4.2	36.1	3.3
Guyomarc'h and Stephan (2012)	CT scans and sliding caliper	French hospitals (mixed ancestry)	35	Female, 18–84	59.1	4.3	35.2	3.3
Modabber et al. (2018)	3D Scans	Caucasians	40	Female, 21–35	58.9	3.0	31.6	2.6
			40	Female, 36–50	61.7	4.4	33.1	2.8
			40	Female, 51–65	63.1	4.4	33.8	2.3
Faakuu et al. (2020)	Sliding caliper	Dagaaba (Upper West Region of Ghana)	147	Female, 15–75	56.1	4.0	31.5	2.5

(* Weighted mean calculated by combining original samples of 30–40, 40–50, 50–60, and 60–70 years).

A first glance at Table 3.8 and

Table 3.9 shows that the range of variation for ear height is between ca. 55 and 65 mm for females, and is slightly wider for males, at ca. 57–70 mm. Moreover, the range of variation for ear width is between ca. 30 and 40 mm for both sexes. Studies have also shown that there is a positive correlation between ear length and age (Asai et al., 1996; Heathcote, 1995).

As the equations that predict ear shape rely on the age parameter, it is important to stress that any inaccuracies in estimating the age of the skeleton will inflate the amount of error in the calculations of ear

length. Also, according to Guyomarc'h and Stephan (2012), there are no valid skeletal indicators to determine whether someone has attached or free earlobes. Thus, only the faces of Asian individuals should be modeled with attached earlobes because this feature tends to be less common in other human populations, and supramastoid crests seem to be associated with free earlobes.

At present, and always according to Guyomarc'h and Stephan (2012), all remaining ear characteristics cannot be predicted from the analysis of the skull alone, and it is likely that the limited interrelationships between the soft tissues of the ear and underlying bone anatomy will hinder future efforts in producing more accurate guidelines.

3.6 General morphology of the face

3.6.1 The thickness of soft tissues

The measurements taken from various points on the face to establish the distances between bone and skin surface are commonly known as soft tissue depths. Even though the techniques to collect them have varied throughout the years,[22] their aim has remained constant: to define the distances between the surface of the skin and the underlying bone, including a variety of organs and tissues in between, in order to "map" how the face fits on top of the skull at different craniofacial landmarks. This means that these measurements do not include discriminative information about the isolated components that make up the facial architecture of tissues (such as muscle, fat or other organs), nor do they provide precise estimations of specific individuals (Stephan & Simpson, 2008a). Instead, these measurements represent averages of sample sets of variable sizes, which belong to groups of individuals of a given age, sex, population and stature (body mass index).

[22] The first measurements were taken using needle punctures (Gerasimov, 1955; His, 1895; Kollman & Bückly, 1898; Welcker, 1883), while later techniques include clinical calipers (K. D. Kim et al., 2005), radiographs (Garlie & Saunders, 1999; George, 1987; Rhine & Moore, 1984, cited in Taylor, 2001), ultrasound (De Greef et al., 2006; Manhein et al., 2000), CT scans (Phillips & Smuts, 1996), and MRI (Pluym et al., 2007; Sahni et al., 2002).

Until now, research on the depth of soft tissues has been extensive and not always consistent. These studies have reported data for several age ranges and focused on diverse population groups (see Almeida et al., 2013; Bulut et al., 2014; Cavanagh & Steyn, 2011; Chung et al., 2015; Codinha, 2009; Domaracki & Stephan, 2006; Drgáčová et al., 2016; Hwang et al., 2012, to cite just a few), but the overall lack of standardization concerning landmark nomenclature, sample type (cadaver or living subjects), subcategorization of the mean values, and the use of different measurement techniques, sometimes undermine the selection of the adequate dataset to apply in facial approximations.

In recent years, there has been an effort towards standardization with the creation of three Tallied Facial Soft Tissue Depth Tables, now commonly referred to as the T-Tables (Stephan, 2014, 2017; Stephan & Simpson, 2008a, 2008b). The T-Tables compile weighted means (or grand means) both from raw data and mean values extracted from published studies and establish the average thickness of soft tissue depth for subadults (between 0–11 years and 12–17 years) and adults (above 18 years). This procedure reduces noise in data (by averaging out errors) obtained from a large sample size that is more representative of the whole population, and increases practicality in selecting and using datasets (Stephan, 2014). They rely on well-established principles that postulate that (1) a large sample is more likely to have the characteristics of the whole than a smaller one (Law of Large Numbers); and that (2) the distribution of the means (from multiple samples) will approximate the normal distribution as the size of the samples increase, making the mean of the sample means converge with the population mean regardless of the underlying population's distribution (Central Limit Theorem) (Moore et al., 2014). The most up to date T-Table compiles data from maximum sample sizes of 10,333 adult individuals older than 18 years, 3145 sub-adults aged between 12 to 17 years, and 3023 children aged between 0 and 11 years (Table 3.10 and Table 3.11).

Table 3.10 - 2018 T-Table with total weighted means. Mean was calculated from all published studies reporting a soft tissue depth mean for the corresponding landmark. *n* is the sample size used to calculate each weighted mean. Adapted from Stephan (2017).

Landmarks	**Adults > 18 years**		**Sub-adults (0 – 11 years)**		**Sub-adults (11 – 17 years)**	
	Mean	*n*	Mean	*n*	Mean	*n*
Median landmarks						

op–op0	6.0	2273				
v–v0	5.0	2272				
g–g0	5.5	9876	5.5	3023	5.5	1949
n–se0	6.5	10,333	8.0	4995	7.5	3145
mn–mn0	4.5	2072	4.0	433	4.0	472
rhi–rhi0	3.0	9553	2.5	1971	2.5	1005
sn–sn0	13.0	3283	10.5	1756	13.0	1480
mp–mp0	11.5	8920	12.0	4254	15.0	2617
pr–ls0	12.0	8485	13.0	2567	14.5	2177
id–li0	13.5	8046	14.0	2385	15.5	2018
sm–sm0	11.0	9342	10.5	2791	11.5	2078
pg–pg0	11.0	10,297	10.5	5192	12.0	3411
gn–gn0	7.5	1585	6.5	1347	7.5	833
me–me0	7.5	7515	7.0	1052	8.0	377
Bilateral landmarks						
mso–mso0	7.0	5639	5.0	469	6.0	246
mio–mio0	7.0	5700	6.0	521	7.0	251
ac–ac0	10.0	2559	7.5	410	8.0	104
go–go0	12.0	7028	13.0	657	13.5	239
zy–zy0	7.0	7489	7.5	110	8.0	147
sC–sC0	10.5	5303			11.0	104
iC–iC0	10.5	2770			10.5	104
ecm2–sM20	25.0	3784			27.0	104
ecm2–iM20	20.0	3038			23.0	104
mr–mr0	19.0	4927	18.0	108	19.5	142
mmb–mmb0	13.0	3598	10.5	411	12.5	104

Table 3.11 - 2018 T-Table with total weighted means calculated from studies that reported standard deviations (*s*). *n* is the sample size used to calculate each weighted mean. Adapted from Stephan (2017).

Landmarks	Adults > 18 years			Sub-adults (0 – 11 years)			Sub-adults (11 – 17 years)		
	Mean	*s*	*n*	Mean	*s*	*n*	Mean	*s*	*n*
Median landmarks									
op–op0	6.5	2.0	1992						
v–v0	5.0	1.5	1941						
g–g0	5.5	1.0	8439	5.5	1.5	3005	5.5	1.0	1930
n–se0	6.0	1.5	8519	6.5	1.5	3009	7.0	1.5	2142
mn–mn0	4.5	1.5	1718	4.0	1.0	415	4.0	1.0	454
rhi–rhi0	3.0	1.0	8279	2.5	1.0	1953	2.5	0.5	986
sn–sn0	13.0	3.0	2685	10.0	2.0	1556	12.5	2.0	1263
mp–mp0	11.0	2.5	7227	12.0	2.5	2286	15.0	2.5	1632
pr–ls0	12.0	3.0	7455	13.0	2.5	2367	14.5	2.0	1960
id–li0	13.5	3.0	7037	14.5	2.5	2185	15.5	2.0	1801
sm–sm0	11.0	2.0	7978	10.5	2.5	2573	11.5	1.5	1842
pg–pg0	11.0	2.5	8333	10.5	2.5	3006	12.0	3.0	2191
gn–gn0	7.5	3.0	1421	6.5	2.0	1329	7.5	2.0	814
me–me0	7.0	2.5	6576	7.0	2.5	1052	8.0	2.0	377
Bilateral landmarks									
mso–mso0	6.5	2.0	5110	5.0	1.0	469	6.0	1.0	245
mio–mio0	7.0	3.0	5172	6.0	1.5	521	7.0	1.5	250
ac–ac0	10.0	2.5	2309	7.5	2.0	410	7.5	2.0	103
go–go0	12.5	6.5	6040	13.0	3.5	657	13.5	4.5	238
zy–zy0	7.0	3.0	6279	7.5	1.5	110	8.0	2.0	147
sC–sC0	10.0	2.5	5178				11.0	2.5	103
iC–iC0	10.5	2.0	2643				10.5	2.5	103
ecm2–sM20	25.5	6.0	3451				27.0	4.0	103
ecm2–iM20	20.5	5.0	2705				23.0	4.0	103
mr–mr0	19.0	4.5	4606	18.0	4.0	108	19.5	4.5	142

mmb–mmb0	13.0	3.5	3572	10.5	3.5	411	12.5	3.5	103

When comparing the data from Table 3.10 and Table 3.11 with the previous versions of the T-Table (available at Stephan, 2014; Stephan & Simpson, 2008a, 2008b), we observe that the current version has reached a level of stability (Stephan, 2017). Despite increasing disagreement from other authors (De Greef et al., 2009), the mean values for males and females are reportedly very similar and justify, together with measurement uncertainty, collapsing sex-specific means at least for now (Stephan, 2017; Stephan & Simpson, 2008a). Nonetheless, it is worth stressing that Stephan also advocates that larger sample sizes may be required to fine-tune population means at landmarks showing higher standard deviations (e. g. go–go0; ecm2–sM20; emc2–iM20; mr–mr0; and mmb–mmb0). In this regard, De Greef et al. (2009) developed a study to evaluate the impact of age, sex and body mass on facial depths. They report that the area of the lower face is precisely the most affected by body mass alterations, even if the latter cannot be predicted from the skull alone.

Other recent research highlights the main advantages of using the T-Tables against opting for a smaller dataset based on sex, age or even ancestry. Stephan et al. (2015) advise that significant statistical differences should not be directly interpreted as biological signal since they may be caused by other factors, such as measurement error or the use of small samples, which are prone to display more noise than larger ones. Another factor affecting specific datasets is the difficulty of undertaking random sampling and ensuring reproducibility. Cadaver studies are mostly represented by elder individuals coming from social environments open to body donation, while research conducted at the universities is often derived from data obtained from the student community. This circumstance renders most datasets non-representative of the whole population and is considered a sampling error. In some cases, it is possible to minimize sampling error by increasing the sample sizes, but many of the published datasets are derived from small numbers ($n < 40$) (Stephan, 2015a; Stephan & Simpson, 2008a, 2008b).

Chapter 4

4 Materials, methods and process

~

4.1 The archaeological context: La Almoloya (Pliego/Mula) and La Bastida (Totana)

All facial representations included in this thesis belong to individuals excavated at La Almoloya and La Bastida, two of the most important archaeological sites from the Bronze Age society of "El Argar" (2200–1550 cal. BCE) as well as Late Prehistoric Europe (Lull et al., 2009; Lull et al., 2011b; Lull et al., 2016b). The Argaric society occupied an extensive territory in southeastern Iberia (Figure 4.1) and left persistent traces of their presence in the form of large hill settlements, a peculiar intramural funerary ritual of individual or double tombs, and thousands of objects made of metal, stone, bone and pottery. Seen in their contexts, these features and objects indicate sharp socio-economic contrasts and hint at a state society

organized by classes, where the dominant one exerted control over the exploitation of resources through violence and tributes (see, for instance, Lull et al., 2011a, 2013b).

After being "put back on the map" by Louis and Henry Siret in the late 19th-century, the investigation of the society of El Argar underwent a new period of relative silence after the 1940s, until Vicente Lull presented and published a systematic review on its "culture" (Lull, 1979, 1983). The *La Bastida Project* of the Universitat Autònoma de Barcelona, along with other archaeological interventions such as those of Gatas in Almería (Spain) (Castro et al., 1999), is an ultimate consequence of that first systematic approach to the Argaric archaeology and has since been actively engaged not only with large-scale fieldwork and research at different Bronze Age settlements, but also with interdisciplinary analyses, heritage preservation and public outreach.[23] It is under the scope of this endeavor dedicated to the comprehensive study of the Argaric society that this dissertation project was conceived and developed.

[23] Besides the extensive list of publications, the *La Bastida Project* also cooperated in the creation of the *Ruta Argárica de Sierra Espuña* (accessible at https://www.ruta-argarica.es). This online platform that aims to present Argaric-related content and promote touristic activities and experiences in the region around the Murcian mountain-chain.

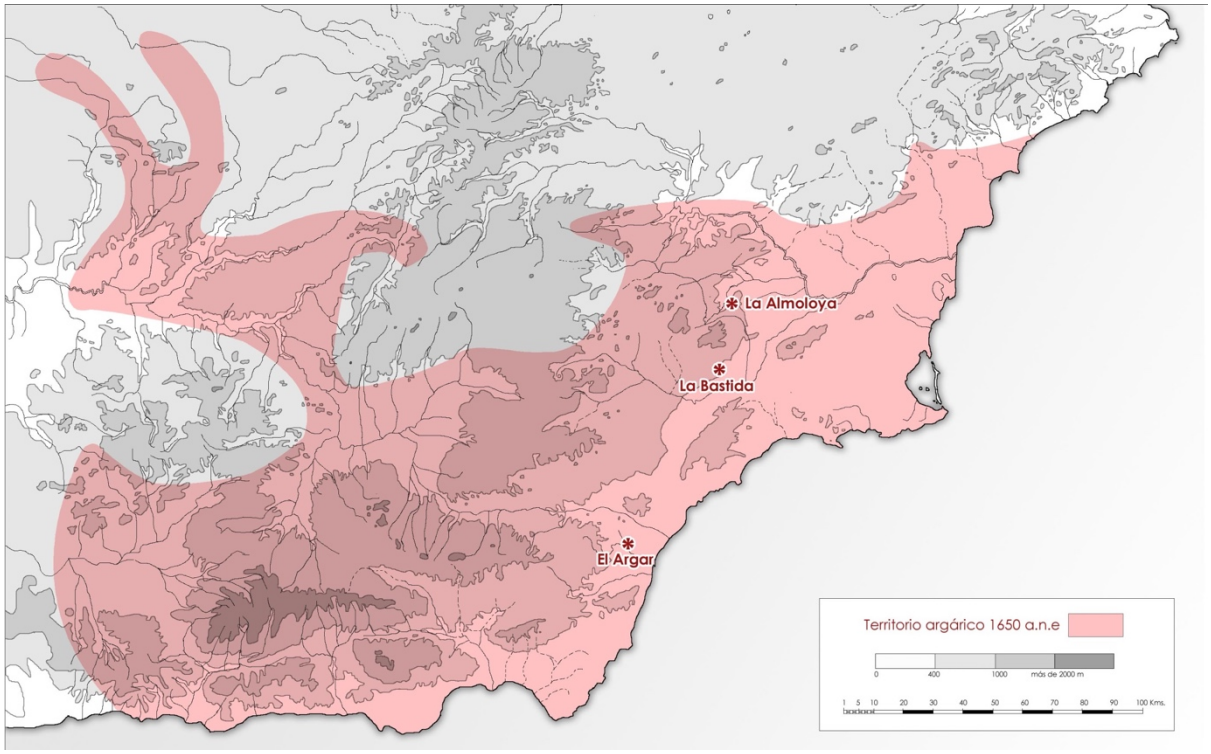

Figure 4.1 - Map of the El Argar's territory in 1650 BCE. © ASOME-UAB.

Both La Bastida and La Almoloya are key settlements to understand the dynamics of the world of El Argar. The recent excavations at La Bastida have unearthed an urban center established on a hilltop between the mountains of Espuña and La Tercia, and shown that the settlement had an impressive fortification and was the largest epicenter of economic and political power (Lull et al., 2014a). The site was inhabited for six hundred years or more (2200–1600/1550 cal. BCE), at times by more than 1000 people, and, since the earliest excavations in the 19th-century, more than two hundred tombs have been documented (Lull et al., 2011b).

La Almoloya occupies a plateau 585m above the sea level in the northern spurs of Sierra Espuña and, like La Bastida, it was occupied over a time span of more than six centuries (2200–1550 cal. BCE). The findings suggest an important center of power, a stage where the Argaric elite would exercise their political dominance over an important part of the Argaric territory, resources and population (Lull et al., 2016b). Four seasons (2013-2016) of archaeological interventions at La Almoloya have yielded 105 tombs with 85 adults and 40 infants (Lull et al., 2016c).

As mentioned above, the Argaric burials follow a particular ritual that differentiated the dead through sets of funerary offerings that distinguished age, sex and social status. Indeed, it has been inferred that the offerings correspond to at least three social classes. Elite burials represent about 10% of the funerary record and are distinguished by the presence of specific metal weapons (halberds and swords), along with ornaments (e. g. diadem) made of silver and gold. Approximately half of the burials belong to "members of full right" within the community, a group of individuals that integrated a second class and were buried with common metal tools, ornaments and ceramic vessels. The remaining 40% correspond to individuals buried with very modest offerings or no grave goods at all and seem to represent the lowest sector composed of servants or slaves (Lull & Estévez, 1986). The socio-economic and political privileges (or lack of them) seem to have been mainly inherited within a society that remembered kinship ties (be they consanguineous or affinal) and imposed strict control on human relationships (Lull et al., 2005, 2013a, 2016a).

This dissertation project aims to produce an independent approach to studying these relationships using the geometric morphometrics toolset to analyze facial morphology represented through the application of facial approximation techniques.

4.2 Research questions and hypotheses

The work hypothesis developed within this project derives from two premises. The first is the notion that it is possible to predict the morphology of the face using cranial shape as a reference and achieve a significant level of accuracy by selecting validated guidelines. Despite the practical and methodological limitations (see Chapter 2 and 3), this circumstance has been demonstrated by recent quantitative tests (see, for instance, Miranda et al., 2018; Short et al., 2014; Simmons-Ehrhardt et al., 2020).

The second premise is the concept that animates recent research on facial and craniofacial genetics, which relies on the possibility of inferring externally visible characteristics from a biological DNA sample, paired with the principle of phenotypic genetic heritability. The transmission of biological information from parents to offspring is a well-established principle in genetic research. In Chapter 2, I have highlighted the effects of both genetic and environmental factors on the morphology of the face and how difficult it has been to disentangle them.

The same premises that drive our research have been put to the test in two previous occasions. In the first, Richard Neave was asked to compare the facial morphology of two Egyptian brothers from the 12th Dynasty whose bones hinted at a seemingly different appearance (Prag & Neave, 1997; Wilkinson, 2004b). Although the genetic relation between Nekht-Ankh and Khnum-Nakht is known from inscriptions on their coffins and was recently verified by aDNA sequencing (Drosou et al., 2018), the morphology of their skulls and postcranium shows substantial differences, ruling out a shared family line.

Musgrave et al. (1995) put a similar attempt in place, with seven facial approximations of individuals from the Late Bronze Age of Grave Circle B in Mycenae. The authors hypothesized that by comparing the faces on a "purely visual base", and how the bodies were positioned within the grave, individuals G55 and G58 shared a family relationship (possibly brother and sister or cousins). Musgrave et al. (1995) also placed skeletons Z59 and G51 in the "long face group" and theorized that the first might have been the father or grandfather of the second, while they were also unrelated to individuals G55 and G58 who had different facial features. Later on, one of the hypotheses of Musgrave et al. (1995) was confirmed by ancient mitochondrial DNA (mtDNA), showing that G55 and G58 are indeed brother and sister and had the same mother. MtDNA also confirmed that individual Z59 has a different haplogroup from G55 and G58, making him unrelated to the second pair, at least on the maternal side. Due to the absence of autosomal DNA or the Y chromosome, the family relationship between Z59 and G51 could not be confirmed or discarded (Bouwman et al., 2008).

The influence of Mendelian inheritance on facial features is well-documented in some historical examples. The Habsburgs, the European royal family that lent their name to mandibular prognathism, are one of those cases in which an extreme facial phenotype was passed on for generations. Besides the mandibular prognathism, the members of the Habsburg House were also afflicted by other facial

deformities usually associated with maxillary deficiencies, including everted lower lips (also known as the "Habsburg lip") and noses with a dorsal hump and an overhanging nasal tip (or, rather unsurprisingly, the "Habsburg nose"). Evidence for these malformations can be found both in clinical diagnoses carried from observing their portraits (Vilas et al., 2019) and in examinations of their skeletal remains (Giuffra et al., 2014; Lippi et al., 2011; Peacock et al., 2014).

While the prevalence of extreme mandibular prognathism among the Habsburgs has been attributed to continuous inbreeding (see, for instance, Álvarez & Ceballos, 2015; Álvarez et al., 2009; Vilas et al., 2019), facial morphology is still characterized by a remarkable similarity among non-consanguineous marriages. Recent research indicates that the facial complex is under strong genetic control (e.g. Claes et al., 2018; Cole et al., 2017; Tsagkrasoulis et al., 2017), as over 50 loci associated with facial traits have been identified to date (see Richmond et al., 2018 for a review).

Taking into account this research scope, the general objective for this project is to evaluate the possibilities of the facial approximation techniques and how much these can contribute to a particular archaeological discourse. It aims to do so by approaching a specific question: can we infer genetic relatedness by analyzing a face representation that relied on the skull as a reference?

4.3 Skull sample

A preliminary selection of the Argaric crania from La Bastida and La Almoloya was prepared after inspecting the photographic inventory curated by the ASOME-UAB team. Then, a second selection was made after a general visual assessment of the preservation state of the skulls and mandibles, ensuring that most of the facial portion was present. To attain a less subjective group of selection criteria, I propose a simple classification system that aims to describe the suitability for facial approximation (henceforth SFA)

of the inspected remains. As mentioned before, a facial approximation is an enterprise that should not be detached from the specifics of a particular skull, nor from applying validated methods, regardless of the final aim (Hayes, 2015).

Therefore, within the classification system presented here, priority is given to the state of preservation of the morphological elements and cranial landmarks necessary to estimate the features of the face that can be predicted using validated guidelines (refer to Table 4.1 and Chapter 3 for a review on the published methods).

Table 4.1 - Bone morphology, cranial landmarks and distances required to estimate surface anatomy in a facial approximation.

Surface anatomy	Morphology	Landmarks and distances
Eye region	Orbital cavity, supraorbital ridge, frontal bone	Dacryon, ectoconchion, supraconchion, orbitale, nasion, frontozygomatic suture (frontomalare orbital)
Nose	Nasal bones, nasal cavity, anterior nasal spine,	Nasion, rhinion, acanthion, subspinale. Preserved width of the piriform aperture.
Mouth and lips	Canine teeth, mandible (to determine occlusion)	Distance between the canine teeth, infraorbital foramina, length of the central incisors
Chin and lower contour of the face	Mental protuberance, lower mandibular border	
Ears	Temporal bone	Porion point

To apply this system, we must consider the "face" and the "head" as two distinct entities to establish a hierarchy in which the particularities of the former are not overwhelmed by the "wholeness" of the latter. This notion echoes the osteological terminology that separates the bones of the head (neurocranium) from the bones of the face (splanchnocranium or viscerocranium). Also, it may be justified by the fact that, even though the cranium is essential to envision the overall shape of the head, all the features and the respective landmarks to estimate them are found in the facial portion. Moreover, Beatty (2015) argued that such division is also crucial for a more exploratory interpretation of the significance of

the face within archaeology and osteoarchaeology, where a more "craniocentric" approach has been the rule so far.

With these concepts in mind, every group and every subgroup were attributed a numeric value according to the presence, absence or degree of fragmentation of each portion (present = 1; 0,75 = fragmented and repositioned/represented using intrinsic information; 0,25 = fragmented and repositioned/represented using extrinsic information from sample-based or manual techniques[24]; absent = 0). The allocation of each skull to a confidence interval is then calculated using the following expression: $(a * 3 + e + f + g + h + i + j + k + l)\ d + (b * 1) + (c * 3)$. The sum of these variables will result in a number between 0 and 16, which can then be allocated to one of the seven levels of confidence (Table 4.2).

Table 4.2 - Confidence intervals for the seven categories of the SFA system.

Range	Category / level of confidence
>15	1
15 to 13	2
13 to 10	3
10 to 8	4
8 to 6	5
6 to 4	6

[24] Based on the two main approaches to aid the reconstruction of biological specimens, according to Zollikofer and Ponce de León (2005). First, the so-called bottom-up approach does not require any external information or prior knowledge about how the object looked before. It relies on intrinsic information only and is achieved by doing a number of small operations (e.g., mirroring bilateral symmetry, putting fragments together…) until we get a representation of how the object was before. The top-down approach uses extrinsic information filtered by parsimony and may introduce reconstruction biases as it relies on more preconceptions than the first.

<4 7

This system can be beneficial to describe archaeological cases where there is no comparative framework to validate the work hypotheses, and poor preservation of the remains hinders the application of the methods. Still, it is important to emphasize that the proposed classification system does not aim to elate on how accurate a facial approximation ultimately is but rather propose confidence intervals for how representative of a specific individual the facial approximation might be.

The final selection includes four skulls from La Bastida[25] and 36 crania from La Almoloya. It comprises 22 females, 16 males and two infants, and all the social classes of El Argar are represented (Figure 4.2) (Lull & Estévez, 1986; Lull et al., 2011a, 2014a). All data concerning the biological characteristics of the individuals (sex, age at death, height…) is extracted from the annual field reports (Lull et al., 2013c, 2014b, 2015b, 2016c). Additional information and updates regarding the anthropological analysis of the skeletons were kindly provided by Cristina Rihuete Herrada, Camila Oliart and Maria Inés Fregeiro, anthropologists of the *La Bastida Project*.

[25] Despite the relevant number of tombs reported in La Bastida (more than two hundred), the smaller sample is due to the variable state of preservation of the tombs found at the settlement. For the most part, this is due to the high intensity of clandestine excavations, along with architectonic remodeling during the Argaric period (Lull et al., 2011b).

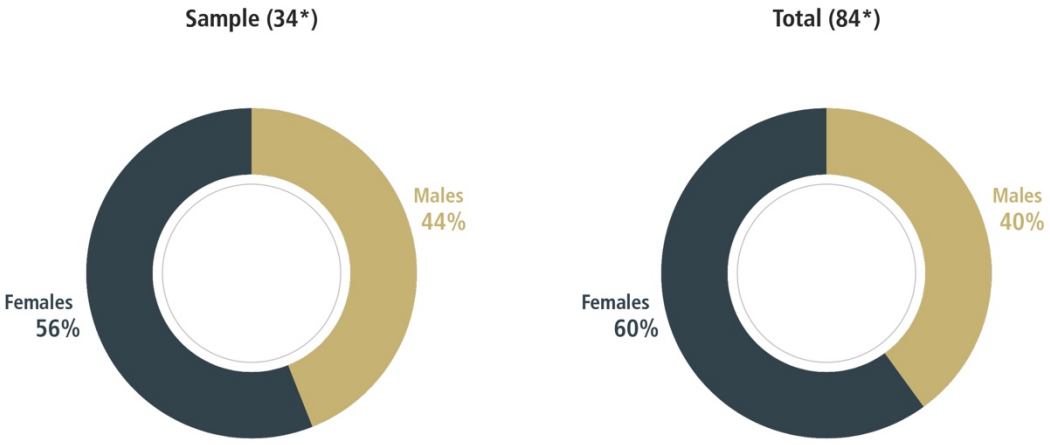

Figure 4.2 - Comparison between the ratio of females vs. males in our sample (left) and the number of individuals excavated at La Almoloya in the end of the fourth campaign (right). *Not including infants and juveniles.

Our sample gathers individuals from 34 different tombs. All four individuals of La Bastida come from different burials. There are six double tombs in the La Almoloya sample where both individuals are represented; nine double tombs represented by only one of the occupants; and 15 single burials.

Table 4.3 presents the classification obtained using the SFA system. All crania ranking under the 3rd level were discarded as it was essential to guarantee that there were enough cranial landmarks to collect measurements from and support the placement of guidelines and soft tissue depth markers.

Table 4.3 - Classification of the Argaric crania used in this project, according to the suitability for facial approximation (SFA) classification system.

1st level	AY5, AY12, AY16, AY24 Female, AY24 Male, AY32, AY38 Male, AY46, AY58, AY67, AY68 Male, AY80 Female, AY80 Male, AY82 Male, AY86, AY90 Female, AY90 Male, AY96 and AY97 Female
2nd level	AY11, AY21, AY22 Female, AY22 Male, AY26 Female, AY30, AY42 Male, AY45, AY47, AY48, AY53, AY82 Female, AY87, BA31, BA33, BA63 and BAM-6
3rd level	AY3, AY38 Female, AY60 Male and AY94 Female

Crania AY29, AY42 Female, AY71 and AY76 were also laser scanned but discarded for being either too close to or in the 4th level (with a SFA score of 10, 7.75, 8.5 and 10 respectively). Three of the previous skulls (AY29, AY71 and AY76) also lack the mandible, a relevant feature whose morphology underlies the contour of the lower face. Appendix A provides a visual reference that compiles digital renderings of all the skulls and mandibles in four canonical views and before any attempt to reconstruct missing elements.

It is often the case in investigations of prehistoric realities, where the given names of individuals are unknown, that human remains and their facial approximations are named after the place where they were found (e. g. Cheddar Man, Tollund Man, among many others). In our case, however, each facial approximation is labelled after the identification number attributed during the excavation campaigns, inventory work, and museum research conducted by the ASOME–UAB team. The materials recovered from both La Almoloya and La Bastida during UAB's field campaigns were kept at the Archaeological Research Center of La Bastida (Totana, Murcia). "AY" stands for the individuals excavated at La Almoloya, and the following number is nothing but the order by which the tombs were identified in the field. "BA" and "BAM" is used for the individuals found at La Bastida, the latter label representing finds from earlier fieldwork which are deposited at the Museo Arqueológico de Murcia. In cases where there is a double tomb with two individuals, these are differentiated according to their sex (e. g. AY38 male, AY22 female).

4.4 Control group

One of the major difficulties for this project was finding a way to test somehow the accuracy of the methods employed. As mentioned before, it is not possible to compare the facial approximations of Argaric individuals with their real faces or other contemporary references.

Previous research with similar face depiction protocols has been published and reveals that approximately 70% of the face (mean average of 22 subjects, published in five different studies) can be predicted with a deviation error below ± 2.5 mm (W. J. Lee et al., 2015; W. J. Lee et al., 2012; Miranda et

al., 2018; Short et al., 2014; Wilkinson et al., 2006a). While the cited research offers an approximated figure for the potential accuracy of these techniques, it also uses a few dated guidelines and less robust soft tissue depth datasets than the ones applied to the Argaric facial representations. For that reason, and considering the limitations inherent to archaeological cases, it was established that the next best option would be to test the applied methodology with a control group of individuals from the same geographic region as the prehistoric settlements.

Besides overcoming the administrative and legal requirements regarding personal data protection, the difficulty in performing these tests stands in finding case studies without visible pathologies (both at the level of the skeleton and soft tissues) or a history of orthognathic treatments. After many unfruitful attempts and contacts, the ASOME Research Group was finally able to establish a collaboration with the Radiological Service at the Morales Meseguer Hospital in Murcia and submit a proposal for a blind-test study using CT-Scans of heads of living subjects. The project entails producing facial approximations of ten living individuals, using the same methods employed for the archaeological data. The three-dimensional models of the patients' crania will be exported from the CT-Scans by an independent researcher, and all facial approximations will be performed without previous access to the real face of the individuals. In a second phase, the facial approximations will be compared with the three-dimensional models of the real faces exported from the patients' medical images. In order to evaluate the accuracy of the method through quantitative and qualitative indicators, the faces will be tested using landmark-based distances, surface-to-surface comparisons and face-pool recognition assessments.

The Ethics Committee of the Morales Meseguer Hospital approved this study on December 5th, 2019. Unfortunately, the final stretch of this doctoral thesis also coincided with the beginning of the Covid-19 pandemic in March 2020, an event that put the healthcare system under extreme pressure in Spain. Like most European countries, Spain went into a three-month lockdown that restricted people's mobility and the hospitals redirected their resources and personnel into taking care of the high number of patients seeking assistance. For this reason, the project with the Morales Meseguer Hospital was put on hold until it was safe to continue collecting the consent forms from the participants.

As the Covid-19 pandemic is still ongoing as I am writing these pages, it was not yet possible to have access to the CT-Scan data sample of our control group, and, as of now, the methodology applied on

this project remains untested. Nevertheless, the ASOME team hopes to continue the collaboration with the Morales Meseguer Hospital, as soon as participants' health and safety can be ensured and publish the results in the near future.

4.5 A handful of possibilities: two and three-dimensions

Since the very first attempt to produce a facial approximation in the 19th century, the act of building a face on top of a skull has seen many different processes and creative solutions that are ultimately materialized in two- or three-dimensions. As technology became more accessible to the everyday consumer, it also broadened the assortment of tools and interfaces available, allowing different exploratory experiences, adaptations and innovative approaches to long-established processes (see, as an example, Mahoney & Wilkinson, 2012; Roughley & Wilkinson, 2019; Smith et al., 2020). Choosing one or the other (or a mix of many) usually comes down to either the available resources or the practitioners' professional background.

Manual approaches include images produced with traditional tools (e.g., pencil drawings or clay sculptures) and digital resources created using Adobe Photoshop® or Zbrush®. Even though computerized tools allow for quick replication of specific tasks,[26] there is sometimes a misunderstanding regarding how computer software is used and the extent of automatization in the operations that can be performed. Creating a drawing using Adobe Photoshop® or a sculpture in Zbrush® does not come "at the push of a button" but rather a manual process performed in a digital environment. In these circumstances, the outcome reflects a similar decision-making process to the one used when working with traditional tools.

Automated or algorithm-based tools refer to those software applications where a computerized system performs a set of pre-programmed operations. These computer-assisted tools rely on more or less

[26] A good example is the possibility of using libraries of muscles or faces that can be imported/exported through different files and projects (Mahoney & Wilkinson, 2012).

limited databases of medical imagery of living individuals and soft tissue depth information. Most tools are based on a process where a three-dimensional generic face (also known as a template) is "deformed" to meet the criteria of a specific target skull (see Claes et al., 2010 for a review on computerized systems; and Guyomarc'h et al., 2014 for a relatively recent automated method that performs with a good level of accuracy). While these approaches have been tagged as less subjective than the manual ones, they also present less flexibility for choosing specific guidelines that might be better suited for a particular cranium (e.g., selecting a specific database of soft tissue depths). Sometimes, upgrading these programs may take a while, and older versions may not be up to date with the recent guidelines. Moreover, these tools do not optimally handle missing data and require a complete skull to produce a face approximation (Guyomarc'h et al., 2018). Although computerized applications may bring facial approximation methods closer to the possibility of standardization, none of them has been widely accepted by the forensic community (Guyomarc'h et al., 2014).

4.5.1 Clay and pixels

The primary approach for this dissertation follows a manual workflow developed in a digital environment, similar to that of Mahoney and Wilkinson (2012). Muscles, tissues and faces were modeled using Maxon's Cinema 4D® together with Zbrush® by Pixologic. The first is a 3D modeling, animation and rendering software, while the second is a digital sculpting application that provides the closest computerized alternative to traditional clay. The reasoning behind choosing digital media instead of traditional clay tools has to do with three main practical factors: storage logistics, flexibility and process reversibility. The first is perhaps the simplest to justify. It is undoubtedly easier to store and transport thousands of megabytes in digital files than 40 life-size clay busts. Yet, flexibility and process reversibility were also determinant factors. As addressed in the previous section, manual methods offer more flexibility in selecting guidelines and when dealing with missing data.

While clay and digital facial approximations follow similar protocols, they also have their pros and cons because both rely on a successive addition of layers of information. First, producing busts in real clay involves some additional steps and maintenance. The skulls and mandibles have to be laser-scanned and prepared to be printed in three dimensions to obtain a support with the same surface morphology of the bones. The printed 3D replicas are then to be anatomically oriented and inserted in a wooden or metal base. There are different types of clay with different properties (e.g., water-based, oil-based, wax-based, and polymer clay), requiring distinct handling techniques and procedures. While water-based clay is soft and more malleable, it also dries fast and cracks easily. Therefore, the long-term preservation of the final result depends on creating a mold and a replica or hollowing the sculpture and firing it in a ceramic kiln. Gerasimov reportedly used a molding mastic whose primary ingredient was beeswax (Ullrich & Stephan, 2011, 2016). This is a type of plastiline clay that can be very difficult to manipulate initially (it becomes more pliable when heated) but yields very fine detail and facilitates precision work. It also reacts to oxygen exposure and becomes harder through oxidization. It cannot be fired, however, and it is not permanent unless a mold is made.

While it is true that any clay has the advantage of providing a tactile surface to work with, it also produces opaque layers. This means that once the surface of the skull is covered in clay, the practitioner loses sight of the bone morphology underneath. To minimize this circumstance, Gerasimov (Gerasimov, 1971; Ullrich & Stephan, 2016) advised working on just one half of the head before covering everything with clay. After that, the other half can be modeled using the finished half as a reference. While this might be a worthy workaround when asymmetry is relatively slight, once the bone surface is covered, there is no way to visualize the skull inside the head. And, having that possibility is valuable to double-check the anatomical relationships and even introduce new data and corrections to the initial face. This is where a digital workflow presents an important advantage, which is the possibility of applying transparencies to selected objects or hiding layers to access underlying information. It is also rather easy to further manipulate and adjust the face to more recent guidelines and test different facial approximation protocols.

Finally, given that one of the main objectives of this thesis is to produce shape analyses, creating facial approximations through traditional techniques would imply setting up another data acquisition stage.

The clay sculptures of the facial approximations would have to be laser-scanned and post-processed to be compatible with the geometric morphometrics software.

4.6 Digital scanning and anatomical orientation of three-dimensional models

The available resources allowed us to establish a non-invasive protocol for three-dimensional data acquisition. All three-dimensional models of the skulls and mandibles were acquired using a Faro Laser ScanArm® V3 with its plugin for Geomagic® and edited within Geomagic® and Zbrush® (Pixologic, LA, USA). The scanning sessions were run at the Archaeological Research Center of La Bastida in Totana and the ASOME installations at the Universitat Autònoma de Barcelona.[27]

The process begins with the acquisition of a variable number of laser scan passes for each skull and mandible until all the surface morphology of the bones is properly covered and registered (Figure 4.3). Each scan is composed of "points", and each point represents a coordinate in the three-dimensional space (along X, Y, and Z axes) that was registered when the laser met the surface of the object. All scan passes have to include areas of overlapping morphology in-between them to perform the alignment of the various scanned portions of the surface. At this stage, a "raw" version of the laser scans is kept separately, and all subsequent operations are performed in a duplicate file to safeguard the data (in case there is an unwanted and unreversible edition or if the digital file somehow gets corrupted).

[27] Permission to access and laser scan cranium BAM-6 was kindly granted by Luis de Miquel Santed, museum curator at Museo Arqueológico de Murcia.

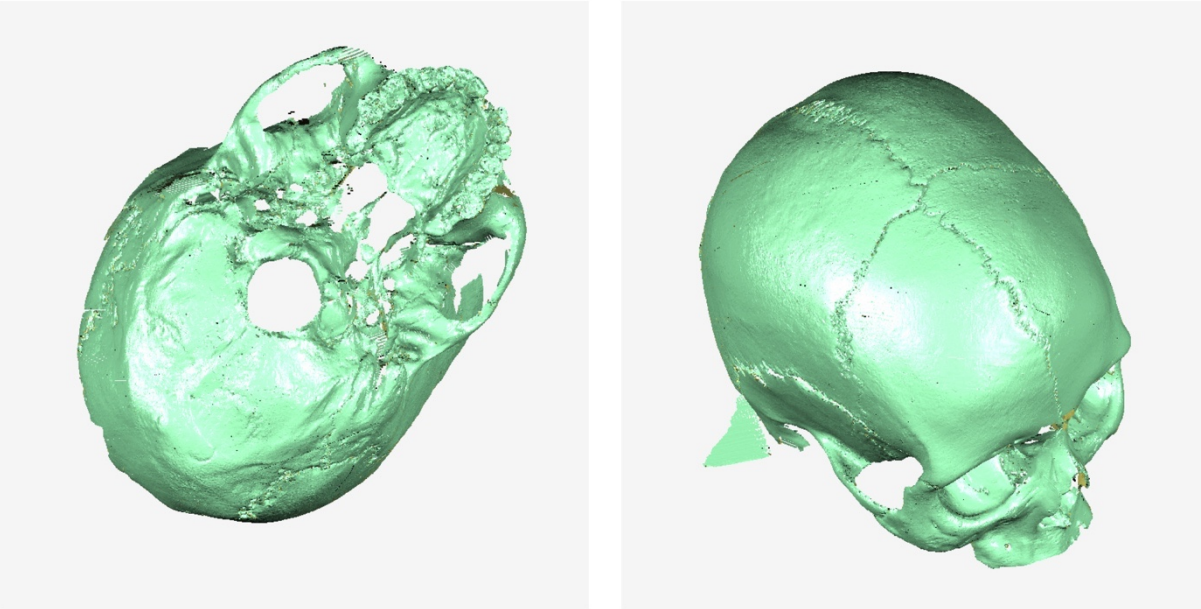

Figure 4.3 - Two different scan passes of the cranium of AY24 Female.

Next, the alignment of the multiple scans begins by using a manual registration process that is progressively refined until a high precision fit of the scans is achieved. Working with several scan passes can quickly make up a very "crowded" workspace, but Geomagic® allows the user to work in "object layers", making it possible to toggle on or off the visibility of the scans as needed. Occasionally, the laser scan might capture external data (referred to as "noise") that is not part of the desired object (Figure 4.4, on the left). These circumstances are minimized by adding a cutting plane to limit the laser's reach whenever possible. The model is then carefully examined again, and all noise that made it through the cutting plane (e.g., single or isolated groups of points in the digital space, with no connection to the main object) is manually selected and deleted. Once the whole object is aligned correctly and noise-free, all scan passes are merged into a single point cloud (Figure 4.4, on the right).

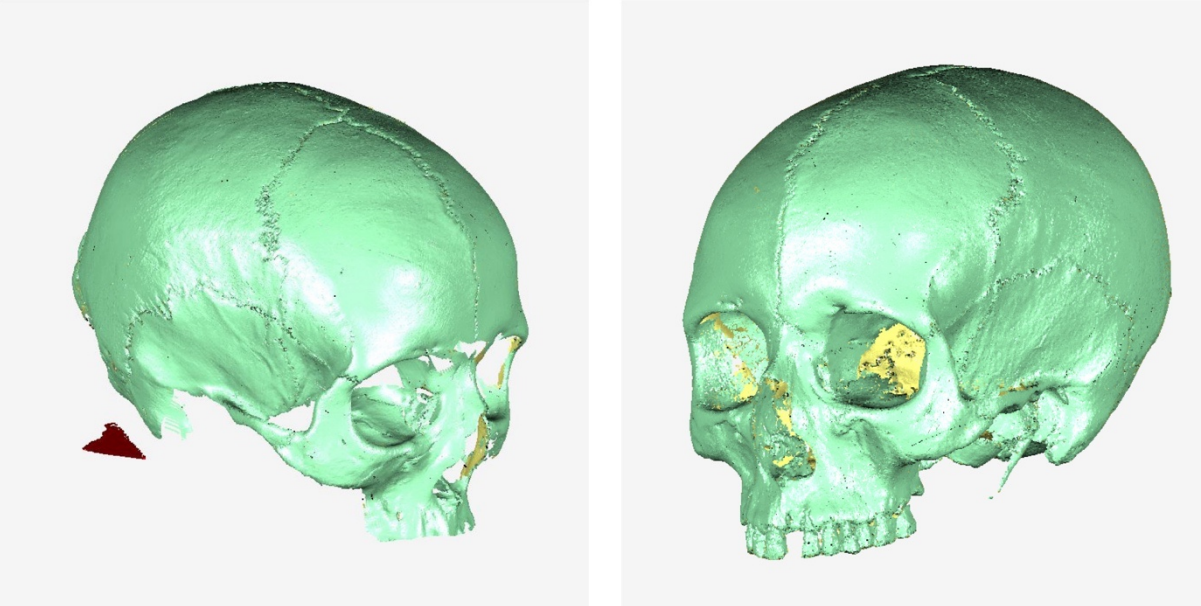

Figure 4.4 - On the left, cleaning up external noise. On the right, the cleaned point cloud.

Once the different scan passes have been merged, and the digital object is a precise replica of the original, we are left with a cloud made up of millions of points. To optimize the post-processing time, a progressive reduction of the number of points (a function called decimation) is performed to decrease the number of unnecessary overlaps and facilitate the creation of the surface. Afterwards, the decimated point cloud is ready to be converted to a polygon mesh through a triangulation process. Several operations are then performed to check mesh integrity to repair any topological error that might generate imperfections or noise in the final visualization of the three-dimensional object. These operations include repairing non-manifold edges (geometry that cannot exist in three-dimensional space), eliminating self-intersections, and closing mesh holes that are not part of the original object (Figure 4.5). Finally, the mesh is exported as a .obj file and imported into Zbrush® for an optimized polygon reduction using the decimation plugin. At the same time, the model is closely inspected to guarantee that all the important surface details are not lost or overwritten by an averaging algorithm (Figure 4.6).

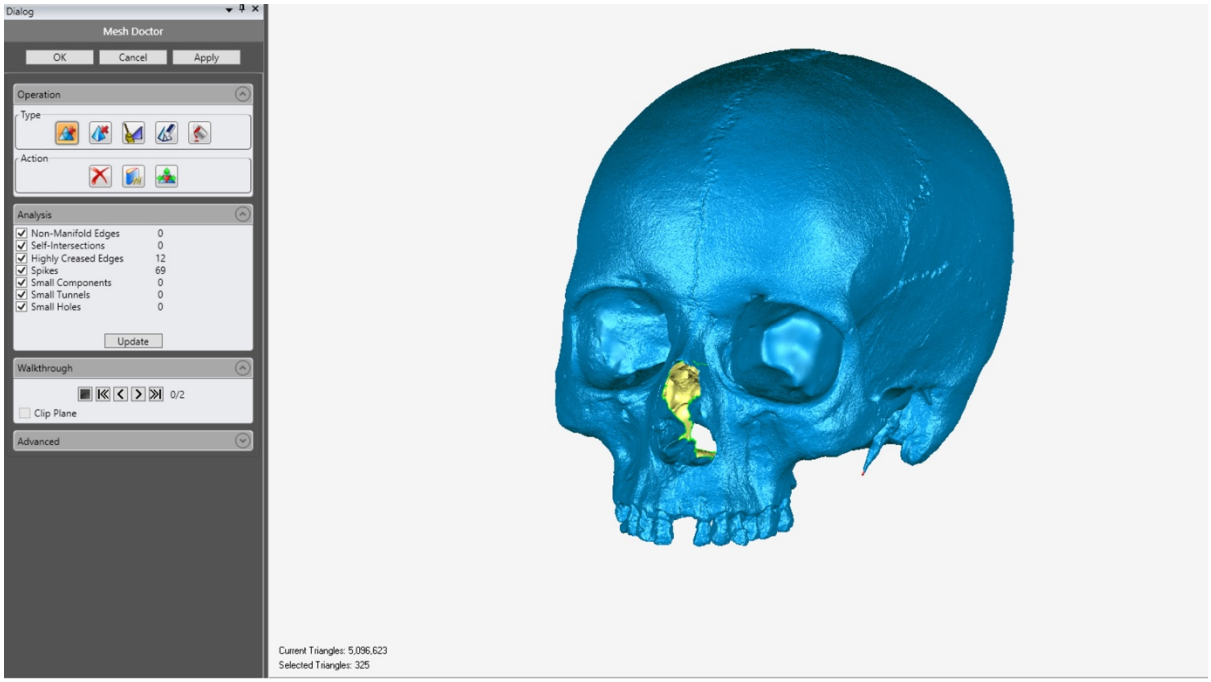

Figure 4.5 - Using the repair tools inside Geomagic®.

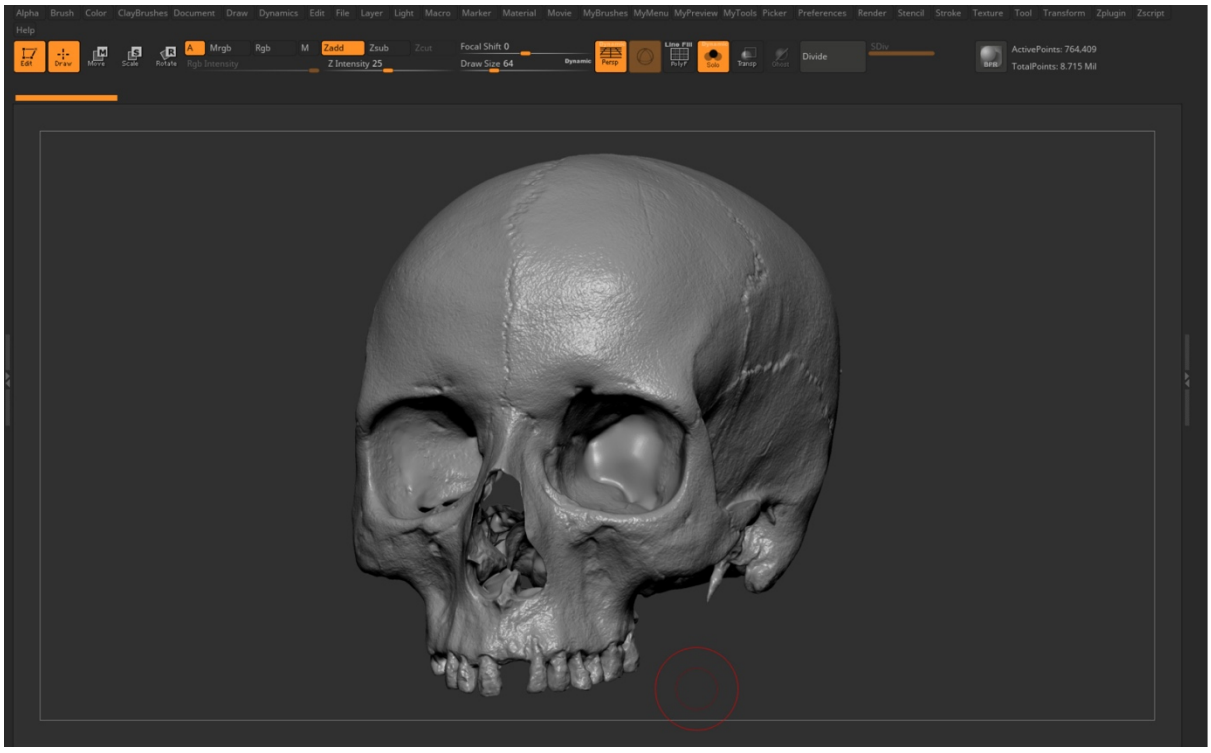

Figure 4.6 - Final mesh of the skull that belongs to AY24 Female.

After this first phase of data acquisition and processing, both skull and mandible must be oriented in the digital space. For that purpose, each three-dimensional skull is visually checked against the real bones to ensure that all the main features are accurately captured, and that no accidental operation changed the surface geometry and interfered with the facial approximation process. Then, the surface mesh is aligned to the center of the digital Euclidean space (point 0, 0, 0) to ensure that all skulls share approximately the same three-dimensional space and match real-life units.

All skulls are oriented using the Frankfort Horizontal Plane (FHP). The FHP is a horizontal reference line or plane that extends from the lowest point in the inferior border of the left orbital rim (orbitale) to the highest point on the upper margin of both left and right external auditory meatus (porion) (Figure 4.7).

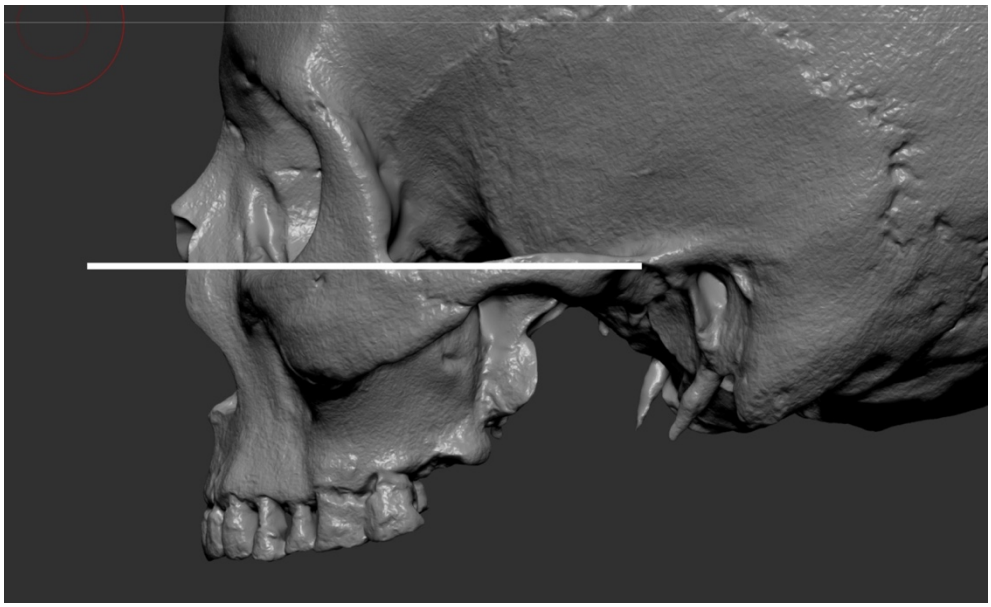

Figure 4.7 - Orientation of the cranium in the Frankfurt Horizontal Plan.

Once the skull is oriented, the mandible is then imported into the main file to be placed in an anatomical position. Plastic deformation may displace the original position of the glenoid fossae and introduce error if we attempt to place the mandible by articulating the condyles. For that reason, the preferrable way to align the mandible is by checking teeth occlusion. Since handling digital files removes

the tactile dimension of studying bones, occlusion is also double-checked against the osteological remains (Figure 4.8). Whenever necessary, reference pictures are taken to aid digital placement.

Figure 4.8 - Double-checking the occlusion against the osteological remains.

Chapter 5

5 Forty faces

~

Implementing a procedure that can be uniformly applied to a group of crania can be a challenge, mainly due to the different preservation states of the bone references. Sometimes the material or biological evidence justifies choosing an alternative parameter to guide the visual representation or using multiple strategies to double-check the position of a specific point. Chapter 5 provides a report on the decision-making behind each facial approximation included in this thesis. The anthropological analysis of a few individuals motivated a reflection on certain difficulties found along the process, such as the visual representation of pathological or traumatic events that affected the face or the facial approximation of sub-adults.

5.1 Methods and guidelines

The general description of the osteological material focuses on those elements that are the most relevant to estimate the facial features. The preservation state of the internal bony structures that do not directly impact the overall shape of the face is not reported. Nonetheless, Appendix A offers a visual account of the osteological material when it was laser-scanned.

Almost every skull and mandible present a variable degree of missing elements which have to be visualized to enable the facial approximation process. Time constraints imposed on this project led me to omit from the representation(s) those areas that only contribute marginally to the morphology of the face

(such as the bones in the *norma basalis* of the cranium), unless they provided some control for the anatomical placement of the facial bones or mandible. The protocol for assessing missing regions relevant for facial approximation followed a three-step assessment based on the principles posited by Zollikofer and Ponce de León (2005, and see discussion in Chapters 2 and 3). First, priority was given to the information contained in each skull. This means that, whenever it was possible, the extant geometry was duplicated and mirrored along the sagittal plane. These functions were done using the registration tools of Geomagic®, which enable the integration of the mirrored duplicate by interpolating it with the preserved parts of the cranium or mandible. This protocol allows for the most accurate representation possible because it considers bilateral symmetry to guide the reposition of missing elements while using information extrapolated from the skull itself. The statistics panel in Geomagic® was examined each time to ensure that the aligned fragments converged (Figure 5.1) and were placed in close anatomic correspondence to each other.

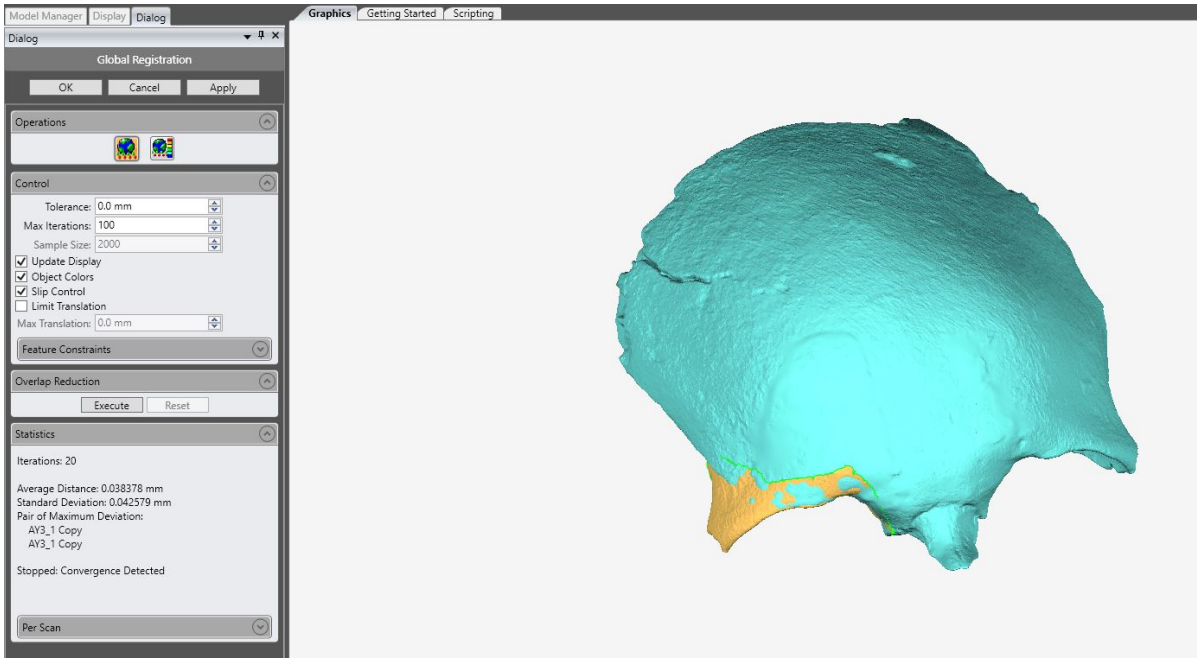

Figure 5.1 - Alignment of fragments within Geomagic®. The alignment process ends once convergence is detected.

Second, for those regions that lack anatomic evidence from both sides, the visual representation of the skull followed three-dimensional morphing procedures using data from the Argaric sample. Considerations regarding the crania that required this approach and correction of plastic deformation are explained in detail for each case.

Finally, in those cases where it was necessary to recreate anatomical components that show significant intraspecific variation (e.g., anterior nasal spine), I opted to perform a parsimonious representation that follows the adjacent anatomy. It is likely that this method generates morphologies that are more hypothetical than the previous approaches. Appendix A depicts the skulls after the protocol for readdressing missing data and uses the same canonical views as the images of the crania in their original state. Crucially, the preservation of the original scan data will allow for future reassessments of the process and the proposal of alternative visualizations to test the impact of different protocols on the representation of faces from the skull. As previously noted, all facial representations are categorized according to our "suitability for facial approximation" (SFA) classification system (see Chapter 3). This dissertation includes nineteen facial approximations allocated to the 1st level of the SFA classification system, seventeen in the 2nd and four within the 3rd (Table 5.1).

Table 5.1 - Classification of the Argaric crania used in the project,
according to the suitability for facial approximation (SFA) classification system.

1st level	AY5, AY12, AY16, AY24 Female, AY24 Male, AY32, AY38 Male, AY46, AY58, AY67, AY68 Male, AY80 Female, AY80 Male, AY82 Male, AY86, AY90 Female, AY90 Male, AY96 and AY97 Female
2nd level	AY11, AY21, AY22 Female, AY22 Male, AY26 Female, AY30, AY42 Male, AY45, AY47, AY48, AY53, AY82 Female, AY87, BA31, BA33, BA63 and BAM-6
3rd level	AY3, AY38 Female, AY60 Male and AY94 Female

The measuring tools from Cinema 4D® were used to collect the lengths and widths from the virtual skulls (Table 5.2), and the craniometric measurements were used to calculate the position and morphology of the facial features are highlighted. Cinema 4D® allows the user to create "objects" out of measured distances (Figure 5.2). This tool provides an opportunity to keep track of the precise locations where the measurements were taken from, which is a valuable resource to ensure repeatability and measurement consistency.

Table 5.2 - Measurements used in this study. Definitions after Buikstra and Ubelaker (1994) (1), Rynn et al. (2010) (2), Guyomarc'h et al. (2012) (3), and Stephan and Henneberg (2003) (4).

Measurement	Abr.	Definition	Estimate	Study
Cranial measurements				
Maximum cranial length	g-op	Maximum distance (instrumentally determined) between glabella and opisthocranium in the midsagittal plane, measured in a straight line.		(1)
Maximum cranial breadth	eu-eu	Maximum width of skull perpendicular to midsagittal plane wherever it is located (instrumentally determined), with the exception of the inferior temporal lines and the area immediately surrounding them.		(1)
Bizygomatic diameter	zy-zy	Direct distance between most lateral points on the zygomatic arches.		(1)
Basion-bregma height	ba-b	Direct distance from the lowest point on the anterior margin of foramen magnum to bregma.		(1)
Cranial base length	ba-n	Direct distance from nasion to basion.		(1)
Basion-prosthion length	ba-pr	Direct distance from basion to prosthion.		(1)
Maxillo-alveolar breadth	ecm-ecm	Maximum breadth across the alveolar borders of the maxilla measured on the lateral surfaces at the location of the second maxillary molars.		(1)
Maxillo-alveolar length	pr-alv	Direct distance from prosthion to alveolon.		(1)
Biauricular breadth	au-au	Least exterior breadth across the roots of the zygomatic processes, wherever found.		(1)
Upper facial height	n-pr	Direct distance from nasion to prosthion.		(1)
Minimum frontal breadth	ft-ft	Direct distance between the two frontotemporale.		(1)

Upper facial breadth	fmt-fmt	Direct distance between the two external points on the frontomalar suture.		(1)
Nasal breadth	al-al	Maximum breadth of the nasal aperture.	Soft nose width	(1)
Nasion to acanthion	n-a	Direct distance between nasion and acanthion.	Pronasale	(2)
Rhinion to subspinale	rhi-ss	Direct distance between rhinion and subspinale.	Pronasale and nasal depth	(2)
Nasion to subspinale	n-ss	Direct distance between nasion and subspinale.	Nasal length and height	(2)
Orbital breadth	d-ec	Laterally sloping distance from dacryon to ectoconchion.	Orbital breadth	(1), (3)
Orbital height	Perp to d-ec	Direct distance between the superior and inferior orbital margins. Measurement is taken perpendicular to orbital breadth and similarly bisects the orbit.		(1)
Orbital height	sk-or	Projected vertical distance between supraconchion and orbitale.	Orbital height	(3)
Nasion to frontomalare orbitale	n-fmo	Direct distance between nasion and frontomalare orbitale.	Eyeball projection	(3)
Biorbital breadth	ec-ec	Direct distance between right and left ectoconchion.		(1)
Interorbital breadth	d-d	Direct distance between right and left dacryon.		(1)
Intercanine width	c-c	Direct distance between the most lateral aspects of the canines.	Mouth width	(4)
Frontal chord	n-b	Direct distance from nasion to bregma taken in the midsagittal plane.		(1)
Parietal chord	b-l	Direct distance from bregma to lambda taken in the midsagittal plane.		(1)
Occipital chord	l-o	Direct distance from lambda to opisthion taken in the midsagittal plane.		(1)
Foramen magnum length	ba-o	Direct distance from basion to opisthion.		(1)
Foramen magnum breadth	Perp to ba-o	Distance between the lateral margins of foramen magnum at the points of greatest lateral curvature.		(1)
Mastoid length	-	Vertical projection of the mastoid process below and perpendicular to the Frankfurt Horizontal Plane (FHP).		(1)
Mandible measurements				
Chin height	id-gn	Direct distance from infradentale to gnathion.		(1)

Height of the mandibular body	-	Direct distance from the alveolar process to the inferior border of the mandible perpendicular to the base of the mental foramen.	(1)
Breadth of the mandibular body	-	Maximum breadth measured in the region of the mental foramen perpendicular to the long axis of the mandibular body.	(1)
Bigonial width	go-go	Direct distance between right and left gonion.	(1)
Bicondylar breadth	cdl-cdl	Direct distance between the most lateral points on the two condyles.	(1)
Minimum ramus breadth	-	Least breadth of the mandibular ramus measured perpendicular to the height of the ramus.	(1)
Maximum ramus breadth	-	Distance between the most anterior point on the mandibular ramus and a line connecting the most posterior point on the condyle and the angle of the jaw.	(1)
Maximum ramus height	-	Direct distance from the highest point on the mandibular condyle to gonion.	(1)

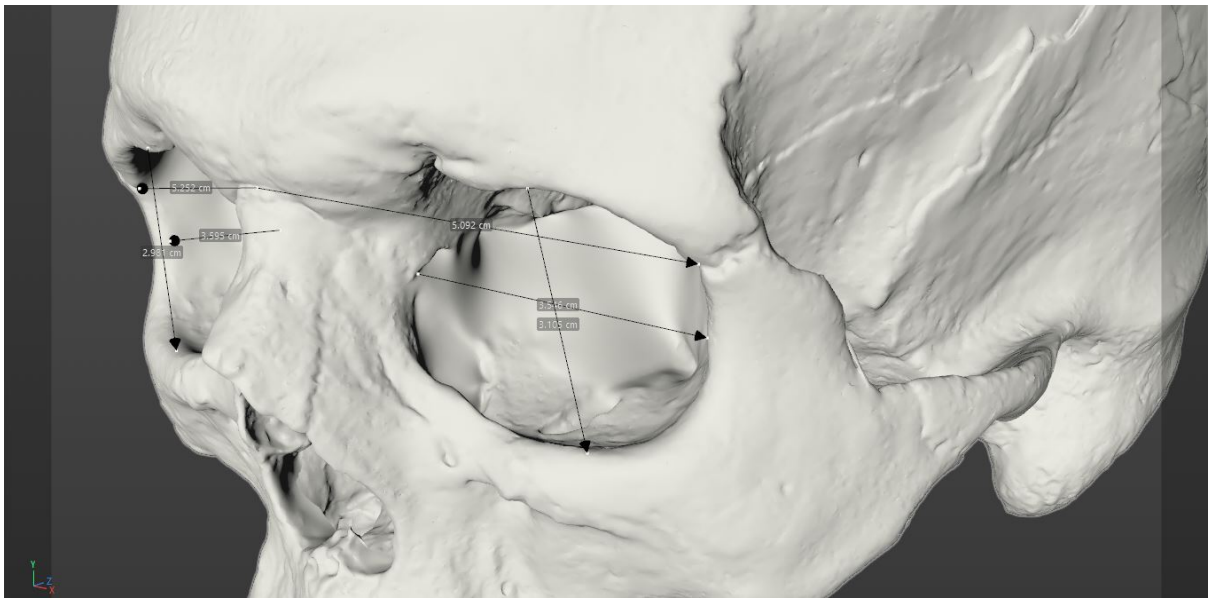

Figure 5.2 - Measurements taken within Cinema4D®.

In addition to the digital craniometric measurements, a subset of nine crania using breadth calipers and straight digital calipers was also measured. The main objective of this procedure was to verify the suitability of the three-dimensional models acquired with the Faro Laser ScanArm® V3 and determine

whether they represented an accurate digital replica of the physical object. Both physical and digital craniometric measurements were then subjected to a Paired Samples T-test using IBM SPSS®. The differences were found to be non-significant in all measured individuals (Table 5.3).

Table 5.3 - Difference between the physical (P) and digital (D) measurements on the cranium.

N = number of measurements taken.

			Paired Differences			
	N	Correlation	Mean	Std. Deviation	Std. Error Mean	*p* value
AY5P & AY5D	27	1.000	.00778	1.35394	.26056	.976
AY12P & AY12D	23	1.000	-.44304	1.08699	.22665	.063
AY16P & AY16D	28	1.000	-.06250	1.04911	.19826	.755
AY22P & AY22D	15	.999	-.17400	1.03652	.26763	.526
AY38P & AY38D	28	1.000	.14107	.96781	.18290	.447
AY46P & AY46D	27	1.000	-.35407	1.19073	.22916	.134
AY47P & AY47D	20	.999	-.71300	2.02246	.45224	.131
AY48P & AY48D	26	1.000	-.25769	1.23473	.24215	.297
AY67P & AY67D	23	.999	-.07304	1.41171	.29436	.806

Preference was given to those guidelines that rely on individual cranial anatomy and allow the estimation of features through regression equations with a known SEE (standard error of the estimate). However, it should be noted that regression equations and their SEE are derived from a specific sample and sometimes do not achieve exactly the same results on different populations (see, for instance, the evaluation of the methods to estimate the nasal shape by Rynn & Wilkinson, 2006). Chapter 3 provides a review of the published methods and was instrumental to inform the following selection. Any divergence from the general approach is justified by the morphological assessment of a particular set of bones and further explained in the respective section. The mandible was placed with a small gap of around 3 mm

between the upper and lower teeth to account for the physiological position of the mandible at rest (referred to as the vertical dimension of the occlusion at rest) (Bhattacharya et al., 2006; Fayz & Eslami, 1988).

As mentioned before, a single eye globe was modeled after published proportions (Figure 5.3) and used consistently in all facial approximations. The position and projection of the eyeball within the orbit were estimated using the guidelines posited by Guyomarc'h et al. (2012) (Table 5.4, Figure 5.4), which seem to be relatively consistent and stable across different populations.

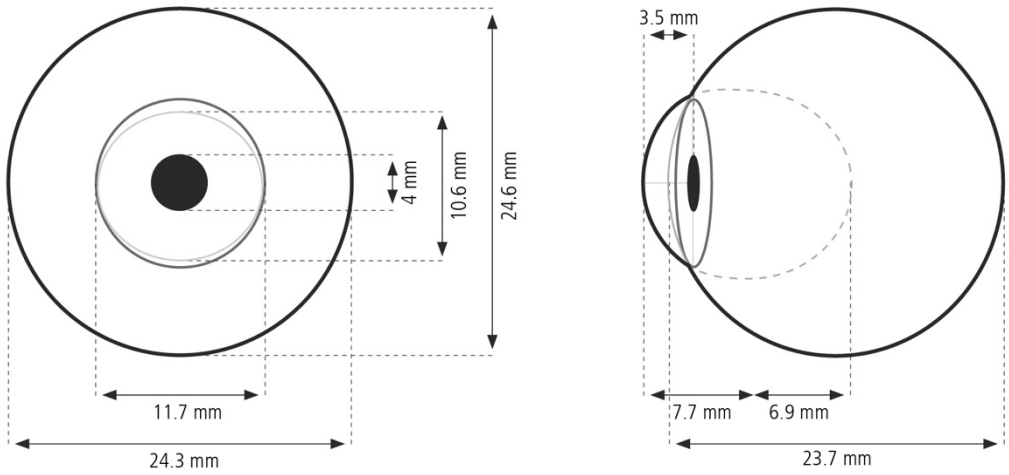

Figure 5.3 - Measurements of the eyeball.

Table 5.4 - Prediction equations used for the placement of the eyeball in the orbit.

Tested on a sample of 375 individuals of mixed ancestries, aged between 18 and 95 years.

SEE = Standard error of the estimate. Adapted from Guyomarc'h et al. (2012).

Eyeball position	**Equation**	**SEE (mm)**
Superoinferior (a)	0.54 * OBH—3.5	1.4
Mediolateral (b)	0.59 * OBB—0.4	1.3
Anteroposterior (c)	0.23 * OBH + 0.26 * n-fmo—3.5	2.1

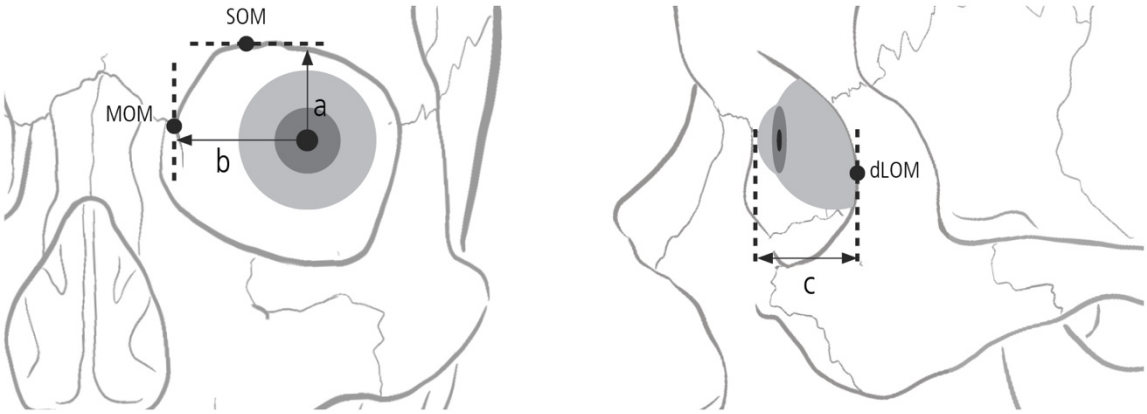

Figure 5.4 - Placement of the eyeball. Adapted from Guyomarc'h et al. (2012).

The eye canthi placement followed the guidelines published by Stephan and Davidson (2008), with the medial canthus located 4.8 mm lateral to the medial orbital margins and the lateral canthus 4.5 mm medial to the lateral orbital margins (Figure 5.5). The height of the lateral corner was determined after assessing the position of the Whitnall's tubercle or 10 mm below the frontozygomatic suture, and the medial canthi was placed 1 mm below the relative position of the former. The anteroposterior position of the lateral corner projects ca. 10 mm from the deepest point on the lateral orbit viewed in profile (Figure 5.5). As highlighted in Chapter 3, the placement of the eye canthi is rather problematic and further studies are necessary to produce better estimates in the future.

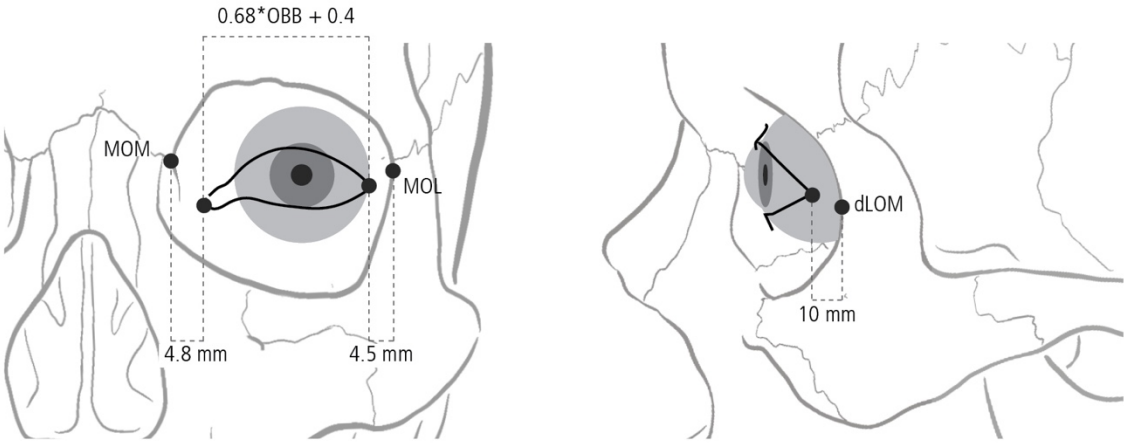

Figure 5.5 - Placement of the eye canthi and estimation of the palpebral length.

After Stephan and Davidson (2008) and Guyomarc'h (2011).

The palpebral length, which corresponds to the distance between the medial and lateral canthi, was double-checked against the regression equation published at Guyomarc'h (2011) (Table 5.5, Figure 5.5). These two orientations do not always coincide in practice, which is expectable if we consider the small sample that informs the method proposed by Stephan and Davidson (2008) and the significant SEE of 3.6 mm in the equation by Guyomarc'h (2011).

Table 5.5 - Prediction equations for the length of the palpebral fissure. Tested on a sample of 374 individuals of mixed ancestries, aged between 18 and 95 years. SEE = Standard error of the estimate. After Guyomarc'h (2011).

Palpebral length	**Equation**	**SEE (mm)**
Right	0.71 * OBB + 3.2	3.6
Left	0.68 * OBB + 0.4	3.6

The dimensions of the external nose profile were estimated through the regression equations published by Rynn et al. (2010) for adults and sub-adults alike (Table 5.6, Figure 5.6 and Figure 5.7). Besides independent evaluations performed on adult samples (Guyomarc'h, 2011; Mala, 2013), the same equations were also tested on a Scottish sub-adult group (age range between 8–16 years) and produced results similar to those of the adult population (Sarilita et al., 2018). Both Rynn et al. (2010) and Guyomarc'h (2011) warn that applying this method to individuals above 50 and edentulous persons increases the SEE's, likely due to the dropping of the nasal tip and the morphological changes caused by the alveolar resorption in the prosthion point. The nose width was calculated following the regression equations presented by Guyomarc'h (2011) (Table 5.7).

Table 5.6 - Prediction equations to estimate the nose profile. Derived from a sample of 79 North American adults aged below 50. Adapted from Rynn et al. (2010). (1) SEE calculated by Guyomarc'h (2011), who tested the equations on a sample of 119 individuals between 18 and 87 years old, and 72 individuals aged 18 to 49. (2) As calculated by Mala (2013) on a sample of 34 females, aged between 19 and 39, and 52 males, aged 21 to 43.

Predicted dimension	**Equation**	**<2.5 mm (%)**	**<5 mm (%)**	**SEE (mm) (1)**		**SD of difference (2)**	
				18-87 y	18-49 y	Females	Males
Pronasale anterior (1)	0.83 * Y—3.5	68.9	86.2	3.4	2.9	2.47	2.54
Pronasale vertical (2)	0.9 * X—2	82.8	96.6	2.6	2.3	1.93	2.32
Pronasale pFHP (3)	0.93 * Y—6	65.5	86.2	2.9	2.9	2.60	2.77
Nasal length (4)	0.74 * Z + 3.5	87.0	97.3	5.6	5.2	3.00	3.10
Nasal height (females) (5)	0.63 * Z + 17	81.8	100.0	4.3	4.0	2.47	
Nasal height (males) (5)	0.78 * Z + 9.5	76.4	96.4	4.0	2.9		2.62
Nasal depth (females) (6)	0.5 * Y + 1.5	92.8	98.6	2.5	2.3	1.65	
Nasal depth (males) (6)	0.4 * Y + 5	78.5	100.0	2.5	1.5		2.29

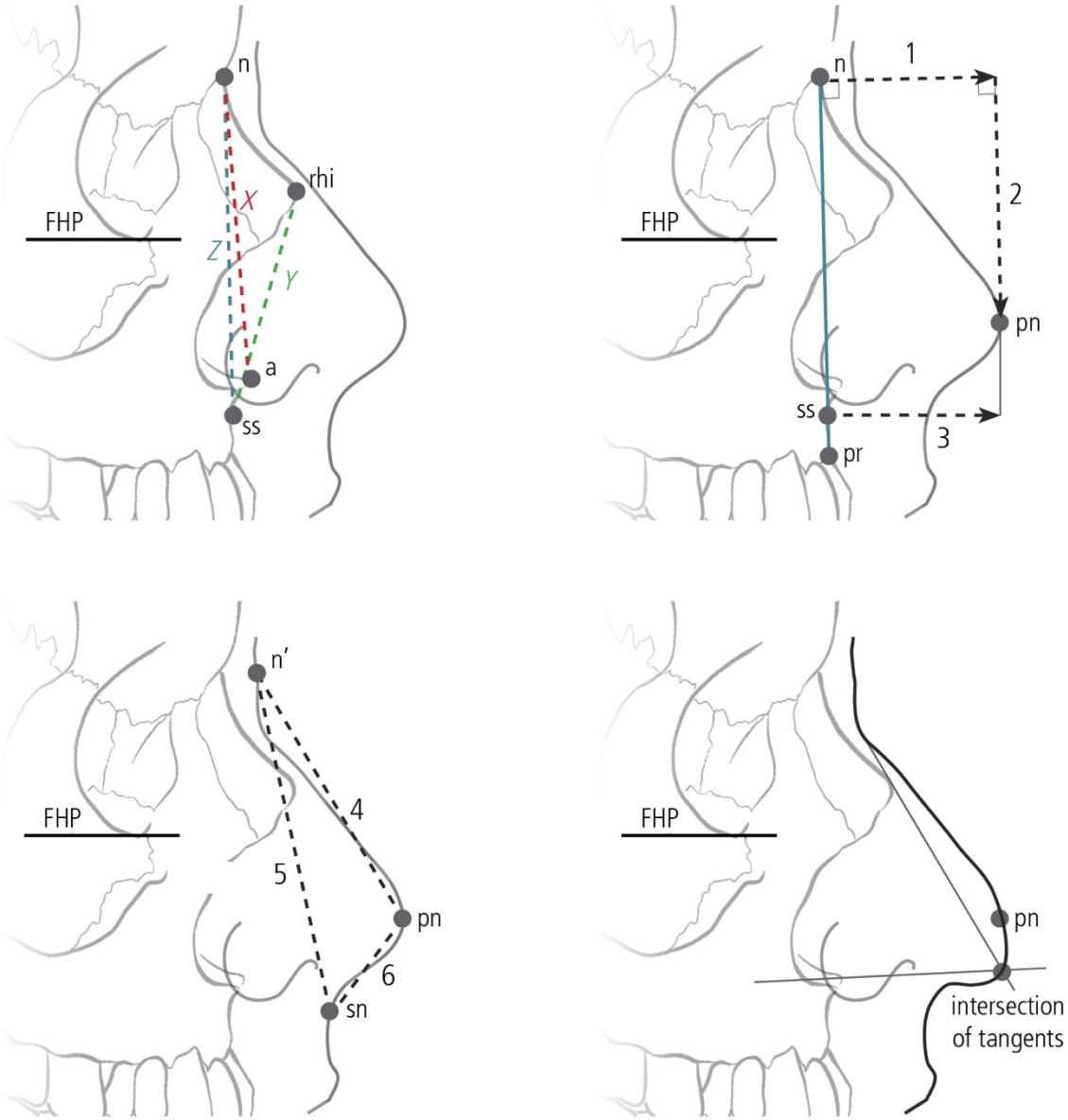

Figure 5.6 - Prediction of the nose profile. Adapted from Rynn et al. (2010). The figure on the bottom right corner depicts the addition of Gerasimov's Two-Tangent method to the process of Rynn and colleagues.

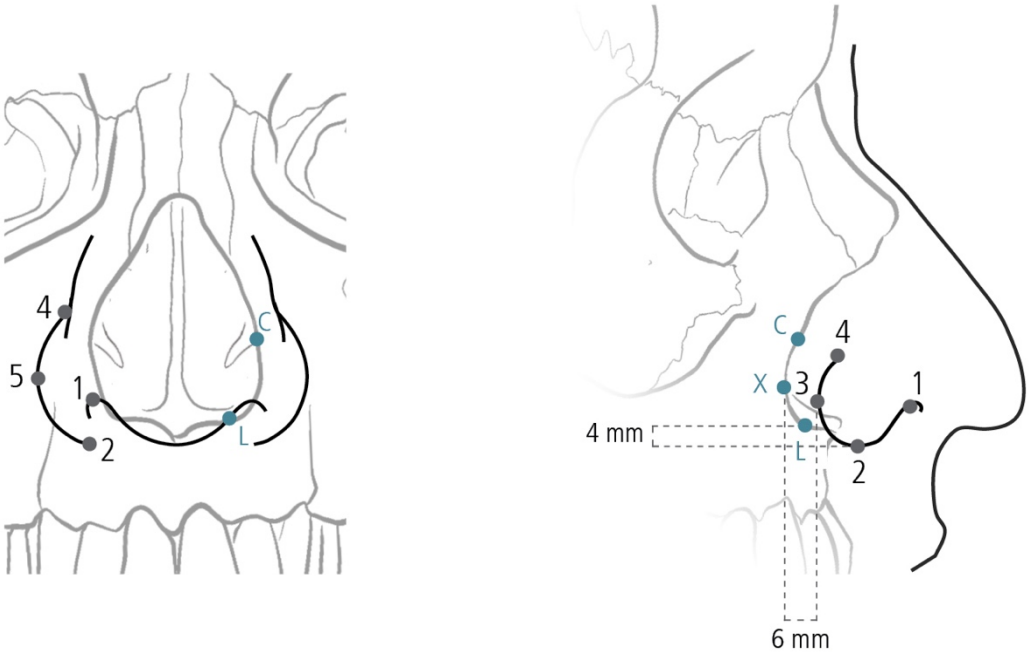

Figure 5.7 - Position of the alar landmarks in relation to the bone, in frontal and profile view. 1 = most superior point on the nostril border; 2 = most inferior point on the alar curvature (subalare); 3 = most posterior point on the alar groove (ac); 4 = most superior point on the alar groove; 5 = most lateral point on the ala. C = inferior turbinate or *concha*; X = most posterior point on the lateral border of the piriform aperture; L = the lowest point on the aperture border. Adapted from Rynn et al. (2010).

Table 5.7 - Prediction equations to estimate the nasal width. Derived from a sample of 422 adults between 18 and 95 years. Adapted from Guyomarc'h (2011).

Predicted dimension	**Equation**	**r^2**	**SEE (mm)**
Nose width	(0.62 * al-al) + (3.51 * sex) + (0.04 * age) + 18	0.43	3.0

The prediction of the mouth width has relied on two guidelines. Whenever the maxillary canines were present, we applied the 75% rule published by Stephan and Henneberg (2003), which posits that canine width accounts for 75% of the total width of the mouth. As mentioned previously in Chapter 3, the 75% rule is reportedly the most accurate to estimate the width of the mouth (Dias et al., 2016; Guyomarc'h, 2011; Stephan & Henneberg, 2003; Stephan & Murphy, 2008). If the canines are missing, or if the subject is edentulous, the guideline followed is the one presented by Song et al. (2007), which aligns the corners of the mouth in a straight line with the infraorbital foramina.

The height of the lips was estimated following the recommendations of Mala and Veleminska (2016). The guidelines presented by George (1987) were used for estimating the oral fissure in both sexes and the upper lip thickness in males, and the recommendations of Wilkinson et al. (2003) for European individuals were employed to calculate lip thickness in females and lower lip thickness in males (Table 5.8). Despite the existing method errors, Mala and Veleminska (2016) report that the current standards allow estimating a restricted space above the teeth where the lips may be positioned with a certain degree of accuracy. However, it is worth mentioning that many of the calculations used to estimate the lip thickness in this project are derived from individuals that present different degrees of tooth wear and, for that reason, the results are likely biased towards thinner lips.

Table 5.8 - Prediction equations to estimate the height of the lips, calculated from a sample of 80 adults between 18 and 95 years. Adapted from (1) SEE calculated by Guyomarc'h (2011), who tested the equations on a sample of 157 individuals between 18 and 88 years old. (2) As calculated by Mala and Veleminska (2016), tested on a sample of 86 adults, aged between 19–43.

Predicted dimension	**Equation**	**SEE (mm) (1)**	**SD of difference (2)**
Upper lip thickness	0.4 + 0.6 * upper teeth height	2.6	1.4
Lower lip thickness	5.5 + 0.4 * lower teeth height	3.0	2.1

The ears were positioned according to the recommendations extracted from Ashley-Montagu (1939) (Figure 5.8). Despite the availability of regression equations for ear length and width prediction, they are permeated with significant amounts of error (Table 5.9) (Guyomarc'h & Stephan, 2012). For that reason, the ear shape was modeled after general anatomical and artistic principles and within the average values indicated in Chapter 3 (length between 55–65 mm for females and 60–70 mm males, and 30–40 mm width for both), as a means to ensure the *Gestalt* appearance of the face.

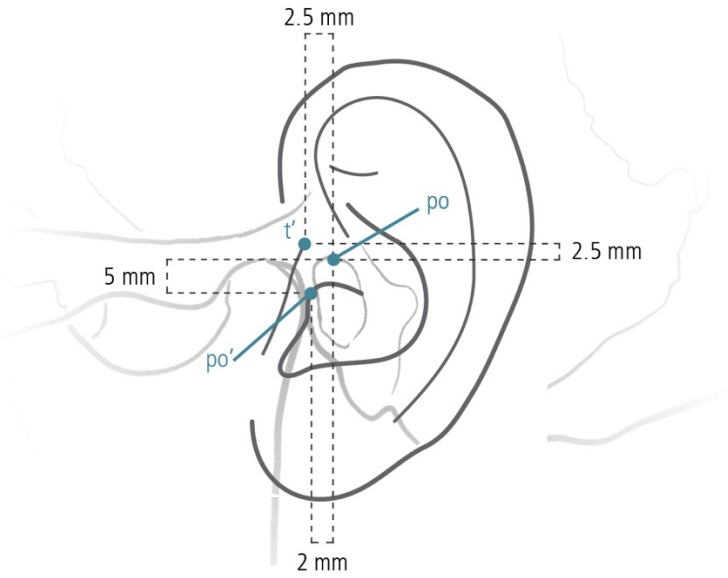

Figure 5.8 - Position of the tragion (t) and cutaneous porion (po') in relation to the bony porion (po). Laterally, the po' is located 9.6 mm from po. After Ashley-Montagu (1939).

Table 5.9 - Prediction equations to estimate the dimensions of the ear. Ear length tested on a sample of 4653 individuals from various samples and width tested on a sample of 78 French individuals. Adapted from Guyomarc'h and Stephan (2012).

Ear dimension	**Equation**	**SEE**
Length	(4.95 * sex) + (0.19 * age) + 53.05	5.1
Width	(3.20 * sex) + (0.05 * age) + 33.02	3.1

The representation of facial wrinkles was kept conservative for two main reasons. First, and as explained in Chapter 2, it is problematic to estimate the visible effects of aging in an ancient population exposed to a particular lifestyle and environment. Second, according to Hadi and Wilkinson (2016), most facial creases seem to have little relationship to the morphology of the underlying skull. The study reports that only the infraorbital crease seemed to follow the morphology of the orbital border in approximately half of the subjects (see Table 5.10).

Table 5.10 - Visually detected creases and their relationship with the underlying skeletal features. Study based on a sample of 83 antemortem photographs and surface scans of the skulls from the William Bass skeletal collection of the University of Tennessee. Adapted from Hadi and Wilkinson (2016).

Type of crease	**Presence in photograph**	**Relation with the skeletal features**	**Creases related with the skull (%)**
Nasolabial fold	79	0	0
Infraorbital crease	48	25	52.08
Horizontal forehead lines	39	3	7.69
Vertical glabellar line	35	8	22.86
Mandibular folds (marionette lines)	31	0	0
Corner of mouth lines (marionette lines)	30	0	0
Chin crease	25	4	16.00
Periorbital lines (crows feet)	22	1	4.55
Lower eyelid	18	0	0
Transverse nasal line	18	4	22.22
Mental pit/crease	10	2	20.00
Cheek fold/wrinkle	7	0	0
Lower lip lines	7	0	0
Unclassified crease	7	2	28.57
Perioral wrinkles/upper lip lines	5	0	0
Periauricular lines	1	0	0
Bifid nose	0	0	0

The characteristics that cannot be predicted from the skull were not added to the facial representations at this stage. They include eye and skin pigmentation, hair, facial hair, eyebrows and eyelashes, and other references for color and texture. The mummified remains from Tomb 121 of the Argaric settlement of Castellón Alto (Galera, Granada) preserves soft tissues, including a particular hairstyle, facial hair and skin (Molina et al., 2003), but other than that, there are no traces that could bring some insight on the Argaric grooming habits or whether they used body decoration such as face painting. The grave goods found in the Argaric tombs include adornments such as earrings, earplugs, beads or linen fragments (Lull et al., 2013c, 2014b, 2015a, 2015b, 2016c) but, other than that, there is no data for other deliberate body modification practices such as tattooing or scarification. However, it is very likely that future iterations of these faces include interpretations of how these elements were used and inferences regarding their phenotype from the upcoming aDNA analyses.

As the published archaeogenetic studies regarding the Argaric populations are still limited (Szécsényi-Nagy et al., 2017), choosing a particular dataset that compiles soft-tissue data from modern-day populations might introduce a specific populational bias. For that reason, considering the available data and following the arguments laid out in Chapter 3, I selected the soft tissue means published by Stephan and Simpson (2008a, 2008b), and later updated at Stephan (2014) and Stephan (2017), (see Chapter 3 for a discussion on soft tissue depth systems). The minimum depths from Stephan's (2017) weighted means for S studies (Table 5.11) were selected as being more likely to reflect the body mass of prehistoric individuals with slight statures.[28] Recent work by Oliart (2021) has established that males from La Bastida would stand below 1.70 m tall, with an average height of 1.61 m, while females were approximately 7 cm smaller (average of 1.54 m).

[28] To represent body mass, the best option would be to use shorths and 75-shormaxes of pooled data but, as of now, the available means rely on very small sample sets (min n = 13 and max n = 397) (Stephan et al., 2013). Results from rolling means have shown that a sample of at least 2000 individuals is required before soft tissue depths begin producing stabilized values (Stephan, 2017).

Table 5.11 - Soft tissue depths (bold) used for the Argaric faces. After T-table published by Stephan (2017).

Landmarks	Adults > 18 years			Sub-adults (0 – 11 years)		
	Mean	*s*	Used mean	Mean	*s*	Used mean
Median landmarks						
op–op0	6.5	2.0	**4.5**			
v–v0	5.0	1.5	**3.5**			
g–g0	5.5	1.0	**4.5**	5.5	1.5	**4.0**
n–se0	6.0	1.5	**4.5**	6.5	1.5	**5.0**
mn–mn0	4.5	1.5	**3.0**	4.0	1.0	**3.0**
rhi–rhi0	3.0	1.0	**2.0**	2.5	1.0	**1.5**
sn–sn0	13.0	3.0	**10.0**	10.0	2.0	**8.0**
mp–mp0	11.0	2.5	**8.5**	12.0	2.5	**9.5**
pr–ls0	12.0	3.0	**9.0**	13.0	2.5	**11.5**
id–li0	13.5	3.0	**10.5**	14.5	2.5	**12.0**
sm–sm0	11.0	2.0	**9.0**	10.5	2.5	**8.0**
pg–pg0	11.0	2.5	**8.5**	10.5	2.5	**8.0**
gn–gn0	7.5	3.0	**4.5**	6.5	2.0	**4.5**
me–me0	7.0	2.5	**4.5**	7.0	2.5	**4.5**
Bilateral landmarks						
mso–mso0	6.5	2.0	**4.5**	5.0	1.0	**4.0**
mio–mio0	7.0	3.0	**4.0**	6.0	1.5	**4.5**
ac–ac0	10.0	2.5	**7.5**	7.5	2.0	**5.5**
go–go0	12.5	6.5	**6.0**	13.0	3.5	**9.5**
zy–zy0	7.0	3.0	**4.0**	7.5	1.5	**6.0**
sC–sC0	10.0	2.5	**7.5**			
iC–iC0	10.5	2.0	**8.5**			
ecm²–sM²0	25.5	6.0	**19.5**			
ecm$_2$–iM$_2$0	20.5	5.0	**15.5**			
mr–mr0	19.0	4.5	**14.5**	18.0	4.0	**14.0**
mmb–mmb0	13.0	3.5	**9.5**	10.5	3.5	**7.0**

This decision is further supported by a recent publication that brings some insight into the diet of the inhabitants of La Bastida and Gatas, another Argaric hilltop settlement (Knipper et al., 2020). Stable nitrogen and carbon isotope analysis performed on botanical, faunal and skeletal remains from both sites show that local diets were primarily based on barley and supplemented with a certain amount of animal resources (meat and dairy products). Williams et al. (2008) literary review reports that there is extensive evidence supporting that a diet high in whole grains is associated with a lower body mass index, smaller waist circumference, and reduced risk of being overweight. Moreover, studies on potential indicators of activity such as osteoarthritis, musculoskeletal stress markers and traumatisms suggest that the Argaric populations were subjected to intensive physical efforts (Jimenez et al., 2014; Oliart, 2021). Considering that physical activity is linked to energy expenditure which, together with food intake, is the second part of the equation to achieve weight loss and maintenance (Cox, 2017), we established that it is likely that most of the Argaric population had a slender physique. Still, it is worth noting that these assumptions require a certain degree of caution, not only due to the role that individual metabolisms might play but also the social position each of these individuals occupied within their community (which may imply more or less labor-intensive tasks or privileged access to specific resources). With these criteria in mind, the tissue depth markers were positioned in their respective anatomical points on the three-dimensional models of the crania, at an angle of 90 degrees to the bone surface.

Considering the samples from which these guidelines derive, it is likely that the face approximations in this study have some sort of bias towards the facial morphology of recent populations. For practical reasons, it is impossible to overcome this trend. Further anthropometric studies comparing the average facial dimensions of these prehistoric faces with data from contemporary groups might provide some insight into the suitability of the present guidelines to represent past populations.[29]

[29] The facial approximation of the "Tham Lod" woman uses a similar approach (Hayes et al., 2017). The authors used a statistical approach to compare the facial dimensions of a female individual from an ancient Thai population with contemporary groups from around the world. They concluded that, despite relying on a subset of guidelines tailored for European individuals, the approximated face is not overly influenced by contemporary facial characteristics.

The areas of origin and insertion of the facial muscles were noted for each skull, and a database of pre-modeled soft tissues was created to aid in the approximation process. These muscles can be imported across several digital files and may be modified to meet the specifications of each individual morphology. Due to the time-consuming nature of this task and the elusive character of mimetic musculature (see Chapter 2 for a reflection on the variation observed in human myology), the facial approximations only include the masseter and the temporalis muscles. This realization is neither new nor recent. Ullrich and Stephan (2011) reviewed Gerasimov's methodology and highlighted that the Russian anthropologist only represented the two muscles of mastication and considered the remaining ones to be dubious. Still, the remaining soft tissues of the face (muscles, glands, fat pads and skin thicknesses) were thoroughly researched and examined both in the literary references and empirically.

Generic face and neck models were used in a manner similar to that of the muscle database. These models provide a practical way to apply a "skin coating" on top of the skull and the subsequent layers of information while also allowing individual modifications and adjustments. Extra care was taken to avoid any morphological generalization derived from applying a common "skin" model to avoid biasing the appearances and the results. The features were further refined following the published relationships for the eye region, nose, and mouth (Balueva et al., 2009; Fedosyutkin & Nainys, 1993; Rynn et al., 2012), and the faces were finished after a round of extensive revisions performed together with the anthropologists from the "La Bastida Project". Appendix B gathers the visual documentation of all the facial approximations produced for this project.

5.2 Faces of La Almoloya

5.2.1 First level facial approximations

5.2.1.1 AY5

Tomb AY5 belongs to an adult male of about 30-40 years old at the time of death, buried just below the floor of La Almoloya's "Great Hall" (Lull et al., 2013c, 2015a). Both the skull and mandible are almost complete and present no traces of plastic deformation. The anterior nasal spine (ANS) is missing, and so are some of the maxillary and mandibular teeth. The distance between the nasion and acanthion, used to estimate the vertical tangent of the pronasale point, was measured from a representation of the ANS based on the adjacent anatomy. For that reason, the precise location of the vertical pronasale point cannot be securely estimated (Table 5.12 and Figure 5.9).

Table 5.12 - Summary of the methods used in the facial representation of AY5.

Preservation state	Skull	Excellent overall state. Anterior nasal spine is missing, and so are the central and lateral incisors, and the second premolar on the right quadrant of the maxilla.
	Mandible	Excellent overall state. Lateral incisor and first premolar are missing on the left quadrant.
Representation of missing components	Skull	Missing components mirrored using bilateral symmetry.
	Mandible	Missing components mirrored using bilateral symmetry.
Confidence level	15,25	1st Level
Facial approximation	Soft tissue depths	Stephan (2017); Stephan and Simpson (2008a)
	Eye placement	Guyomarc'h et al. (2012); Stephan and Davidson (2008); Stephan et al. (2009)
	Eye canthi	Stephan and Davidson (2008)
	Nose profile	Rynn et al. (2010); Ullrich and Stephan (2011, 2016)

Nasal tip	Davy-Jow et al. (2012)
Nose width	Guyomarc'h (2011)
Mouth width	Song et al. (2007); Stephan and Henneberg (2003)
Lip thickness	George (1987); Wilkinson et al. (2003)
Ear placement	Ashley-Montagu (1939); Guyomarc'h and Stephan (2012)

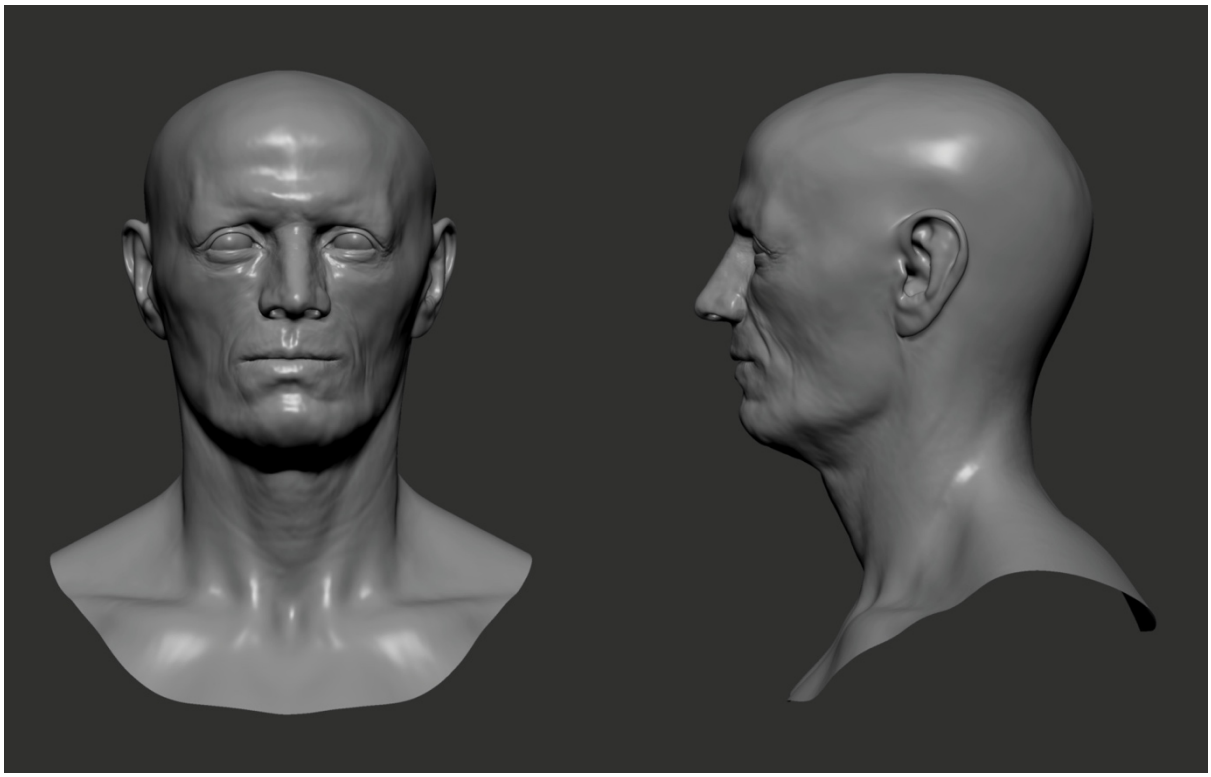

Figure 5.9 - Facial representation of AY5.

5.2.1.2 AY12

Tomb AY12 is the burial place of a man who passed away between 40 and 55 years old and was buried in the "Great Hall" of La Almoloya (Lull et al., 2013c, 2015a). Both cranium and mandible are mostly complete and in a good overall state. Since the nasal bones are missing, the profile of the bony part of the nose and

the height of the pronasale point should be considered tentative. AY12 likely had a snub nose (a nose that is short and slightly turned upwards) and, for that reason, the shape of the tip cannot be predicted using the method of Davy-Jow et al. (2012) (Table 5.13 and Figure 5.10). The individual buried at AY12 lost most maxillary teeth premortem, and the alveolar resorption in the arcades makes the placement of the ecm^2 and ecm_2 tissue depth markers more problematic.

Table 5.13 - Summary of the methods used in the facial representation of AY12.

Preservation state	Skull	Good overall state. The nasal bones are missing, along with the right frontal incisor, both lateral incisors and canines.
	Mandible	Excellent overall state.
Representation of missing components	Skull	The nasal bones were represented after assessing the adjacent anatomy.
	Mandible	None.
Confidence level	15,25	1st Level
Facial approximation	Soft tissue depths	Stephan (2017); Stephan and Simpson (2008a)
	Eye placement	Guyomarc'h et al. (2012); Stephan and Davidson (2008); Stephan et al. (2009)
	Eye canthi	Stephan and Davidson (2008)
	Nose profile	Rynn et al. (2010); Ullrich and Stephan (2011, 2016)
	Nasal tip	Cannot be predicted.
	Nose width	Guyomarc'h (2011)
	Mouth width	Song et al. (2007)
	Lip thickness	George (1987); Wilkinson et al. (2003)
	Ear placement	Guyomarc'h and Stephan (2012)

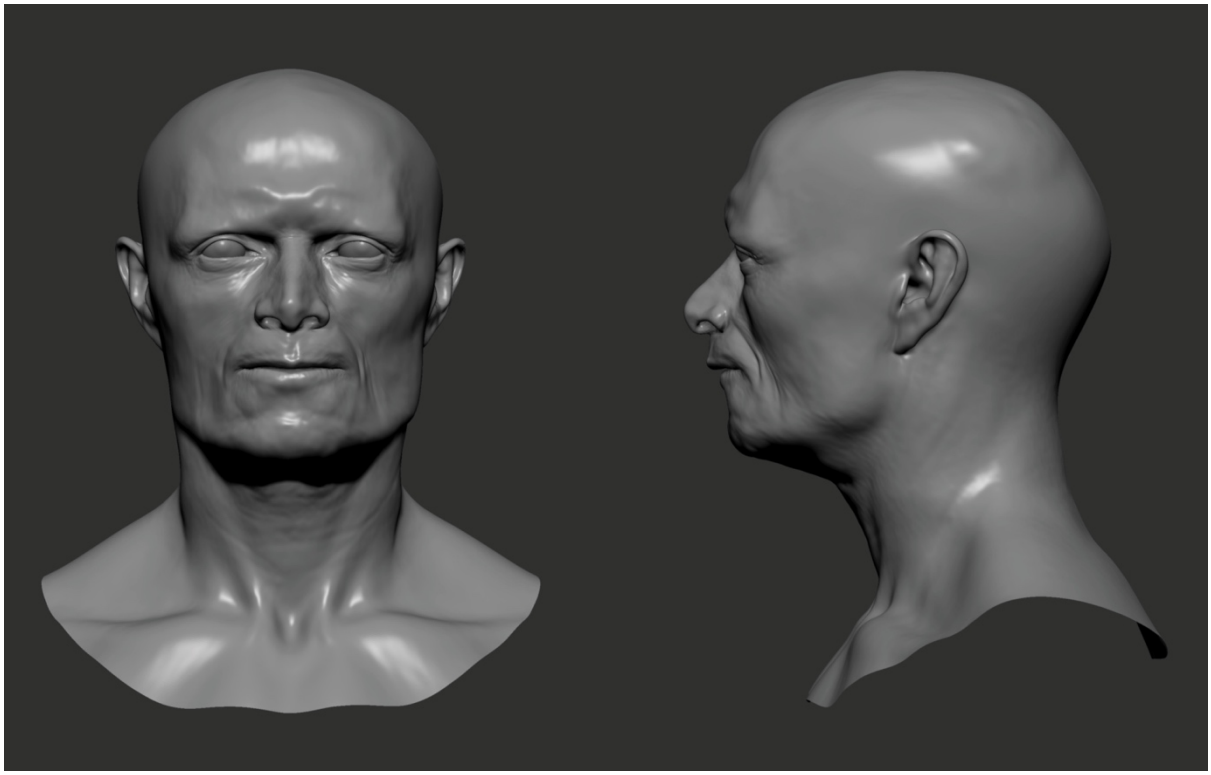

Figure 5.10 - Facial representation of AY12.

5.2.1.3 AY16

The man buried in Tomb AY16 died between 45 and 50 years old (Table 5.14 and Figure 5.11). Both the skull and mandible are nearly complete. A mirroring operation of the skull provided elements for the visual representation of the right portion of the nasal bone, central left incisor, right lateral incisor, and the adjacent portion of the maxilla. The ANS is absent and was represented in a parsimonious manner and taking into account the adjacent anatomy. For that reason, the columella and the precise location of the vertical pronasale might have a considerable amount of error. The same process of reflecting the anatomy of the preserved bones provided the basis for the representation of the right frontal incisor and the missing portion of the left coronoid process of the mandible.

Table 5.14 - Summary of the methods used in the facial representation of AY16.

Preservation state	Skull	Excellent overall state. Anterior nasal spine is missing, and so are the central left incisor and the right lateral incisor.
	Mandible	Excellent overall state. Central right incisor is absent.
Representation of missing components	Skull	Missing components mirrored using bilateral symmetry.
	Mandible	Missing components mirrored using bilateral symmetry.
Confidence level	15,25	1st Level
Facial approximation	Soft tissue depths	Stephan (2017); Stephan and Simpson (2008a)
	Eye placement	Guyomarc'h et al. (2012); Stephan and Davidson (2008); Stephan et al. (2009)
	Eye canthi	Stephan and Davidson (2008)
	Nose profile	Rynn et al. (2010); Ullrich and Stephan (2011, 2016)
	Nasal tip	Davy-Jow et al. (2012)
	Nose width	Guyomarc'h (2011)
	Mouth width	Song et al. (2007); Stephan and Henneberg (2003)
	Lip thickness	George (1987); Wilkinson et al. (2003)
	Ear placement	Ashley-Montagu (1939); Guyomarc'h and Stephan (2012)

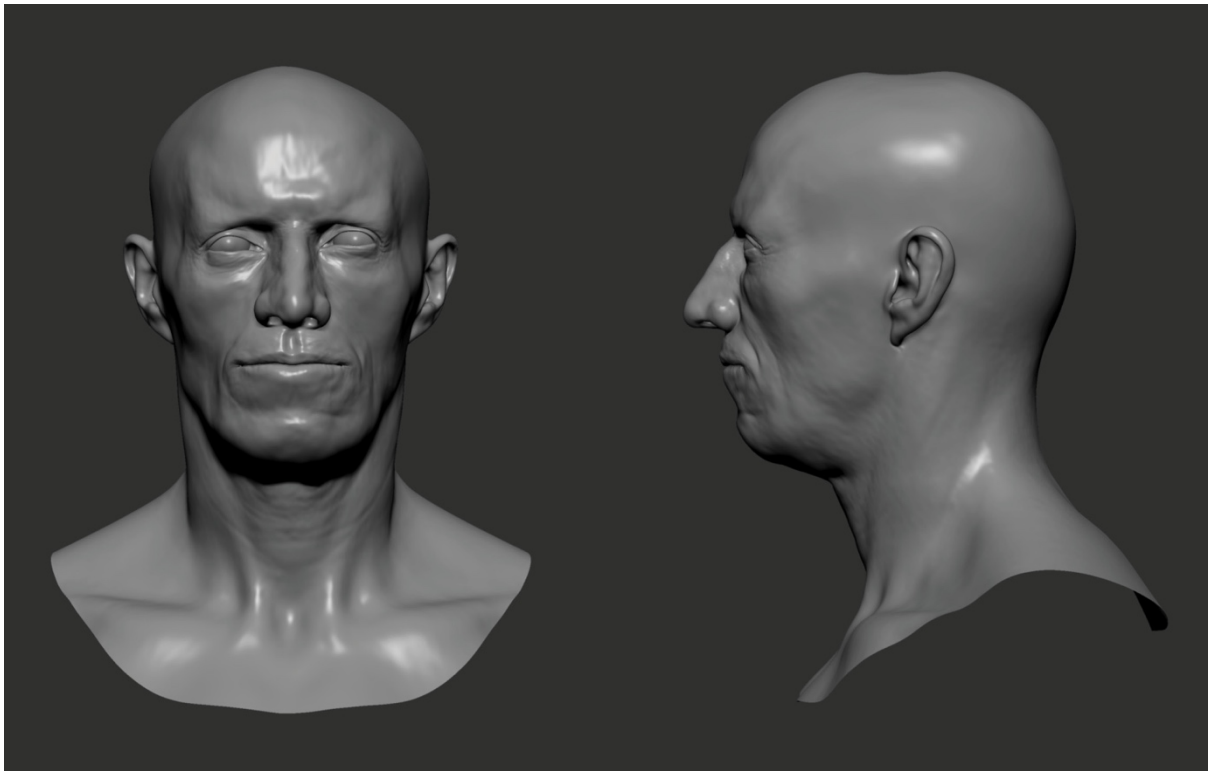

Figure 5.11 - Facial representation of AY16.

5.2.1.4 AY24 Female

The woman from Tomb AY24 was approximately 30 years old at death (Table 5.15 and Figure 5.12). The skull is nearly complete and exceptionally well-preserved, missing only the central left maxillary incisor and the two premolar teeth on the right quadrant. The missing teeth were represented using mirrored symmetry of the preserved parts. The mandible is fragmented at the mental area and was reassembled in a virtual environment using teeth occlusion as the anatomical constraint to assess the correct placement. The lower lip thickness cannot be predicted due to the missing central incisors on the mandible.

Table 5.15 - Summary of the methods used in the facial representation of AY24 Female.

Preservation state	Skull	Excellent overall state. The central left incisor and the right premolar teeth are not preserved.
	Mandible	Excellent overall state but fragmented at the mental area. Central incisors, right incisor and canine are missing.
Representation of missing components	Skull	Missing components mirrored using bilateral symmetry.
	Mandible	Reassembled using teeth occlusion as the anatomical constraint. Missing components mirrored using bilateral symmetry.
Confidence level	15,25	1st Level
Facial approximation	Soft tissue depths	Stephan (2017); Stephan and Simpson (2008a)
	Eye placement	Guyomarc'h et al. (2012); Stephan and Davidson (2008); Stephan et al. (2009)
	Eye canthi	Stephan and Davidson (2008)
	Nose profile	Rynn et al. (2010); Ullrich and Stephan (2011, 2016)
	Nasal tip	Davy-Jow et al. (2012)
	Nose width	Guyomarc'h (2011)
	Mouth width	Song et al. (2007); Stephan and Henneberg (2003)
	Lip thickness	George (1987); Wilkinson et al. (2003)
	Ear placement	Ashley-Montagu (1939); Guyomarc'h and Stephan (2012)

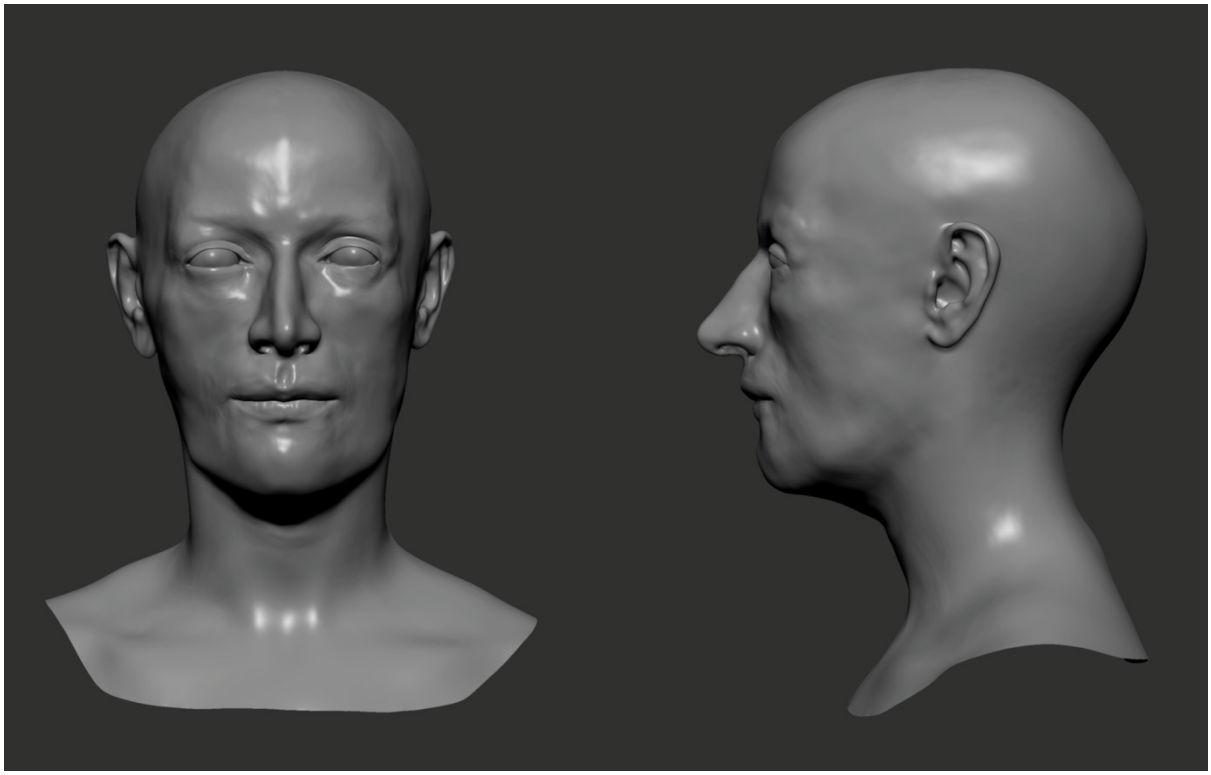

Figure 5.12 - Facial representation of AY24 Female.

5.2.1.5 AY24 Male

This skull belongs to a male aged 35-40 years old at death (Table 5.16 and Figure 5.14). The cranium was laser-scanned after the manual reassembling of the fragments. There are missing bone fragments on the posterior portion of the left parietal that were filled using the function "fill hole" in Geomagic®. The left frontal incisor was lost premortem, and the remaining incisors and both canines are missing. The mandible is complete.

Considering the fragmentation along the frontozygomatic sutures and zygomatic arches, it is hypothesized that there is a slight rotation/misalignment of the neurocranium in relation to the facial portion. For that reason, the left temporal was rotated slightly inwards to compensate for the observed detachment along the temporoparietal suture, and the neurocranium was rotated and moved using the zygomatic arches as an anatomical constraint (Figure 5.13).

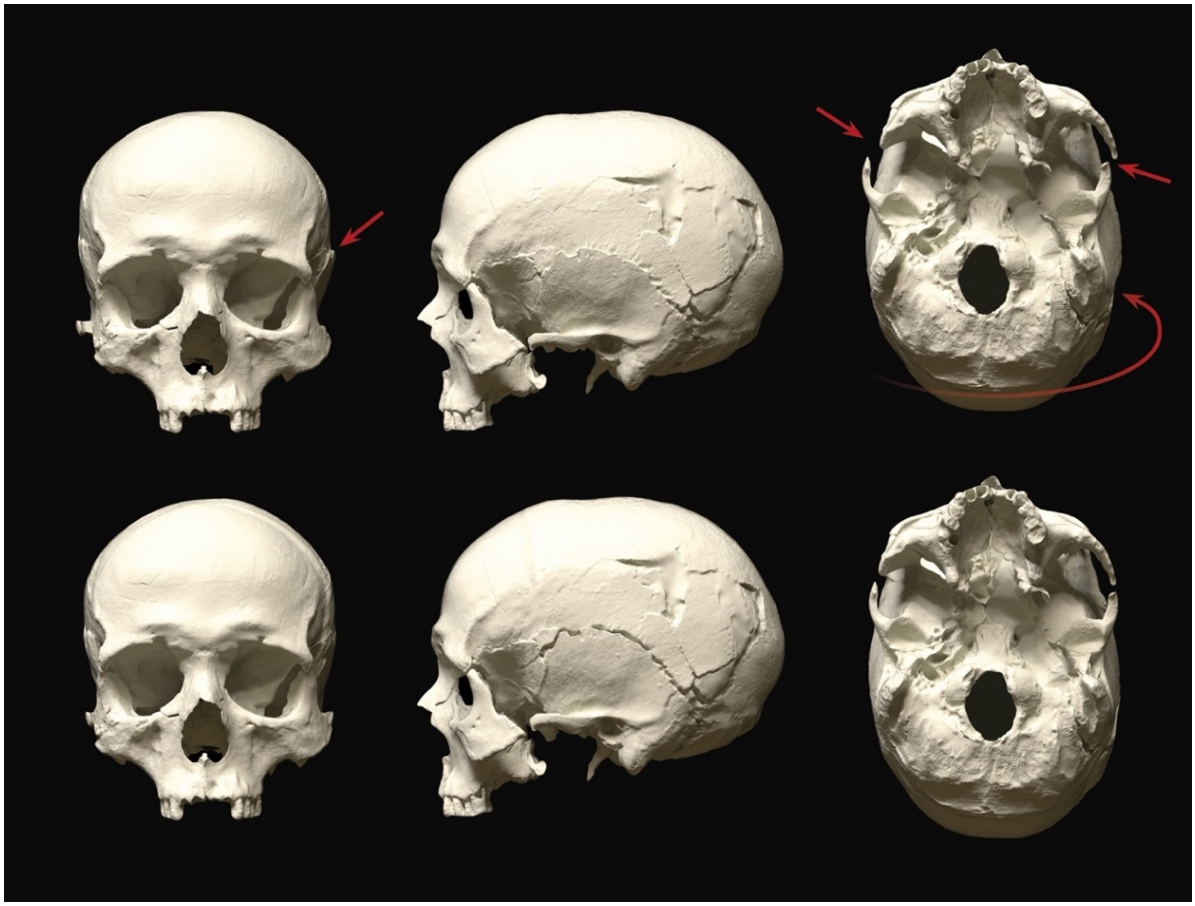

Figure 5.13 - Correcting plastic deformation on AY24 Male cranium.

The alveolar resorption in the maxilla does not allow for the placement of the *ecm*[2] tissue depths, and the estimation of the upper lip thickness is not possible due to the absence of maxillary incisors.

Table 5.16 - Summary of the methods used in the facial representation of AY24 Male.

Preservation state	Skull	Good overall state. Missing portions on the left parietal bone.
	Mandible	Excellent state.
Representation of missing components	Skull	Rotation of the neurocranium using the zygomatic arches as anatomical constraint. Missing components mirrored using bilateral symmetry.
	Mandible	None.

Confidence level	15,50	1st Level
Facial approximation	Soft tissue depths	Stephan (2017); Stephan and Simpson (2008a)
	Eye placement	Guyomarc'h et al. (2012); Stephan and Davidson (2008); Stephan et al. (2009)
	Eye canthi	Stephan and Davidson (2008)
	Nose profile	Rynn et al. (2010); Ullrich and Stephan (2011, 2016)
	Nasal tip	Davy-Jow et al. (2012)
	Nose width	Guyomarc'h (2011)
	Mouth width	Song et al. (2007)
	Lip thickness	Wilkinson et al. (2003)
	Ear placement	Ashley-Montagu (1939); Guyomarc'h and Stephan (2012)

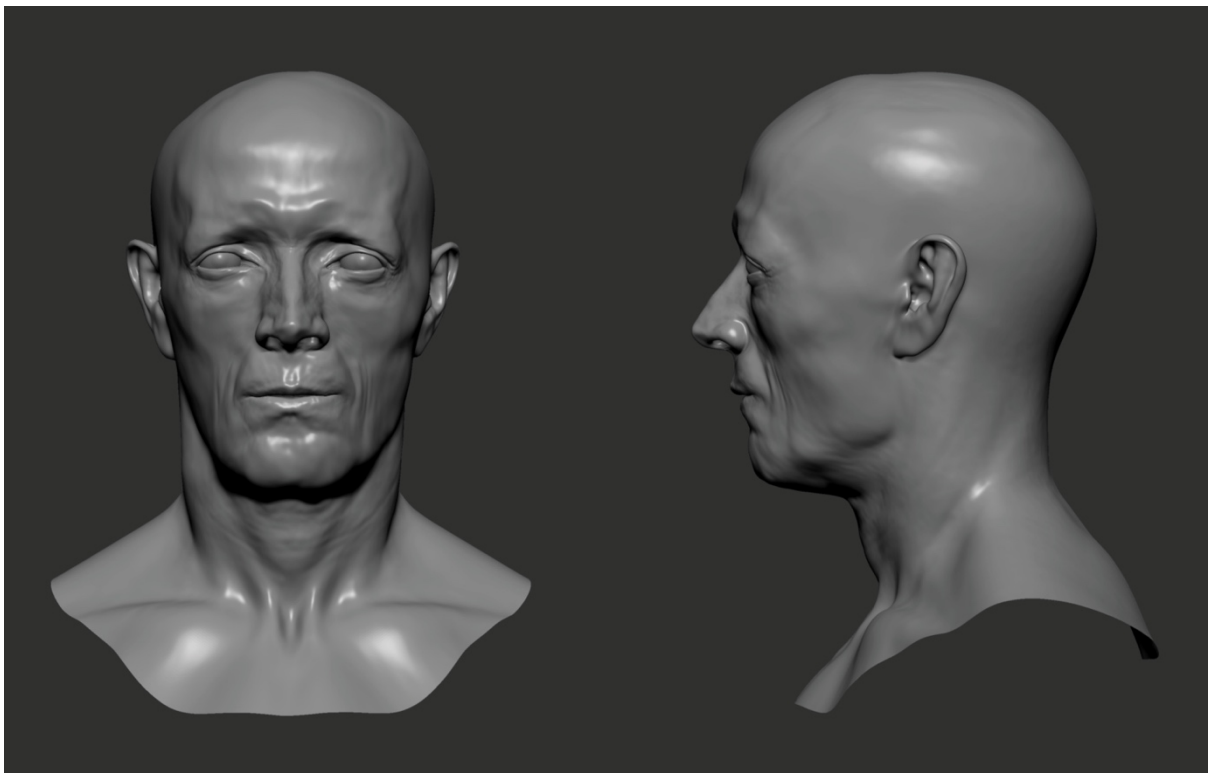

Figure 5.14 - Facial representation of AY24 Male.

5.2.1.6 AY32

Tomb AY32 is the burial place of a male individual aged between 35 and 45 years old (Table 5.17 and Figure 5.15). The skull is complete, and therefore no representation of missing elements was necessary. The missing fragment on the most posterior part of the occipital was filled within Geomagic® using the "fill hole" function.

Table 5.17 - Summary of the methods used in the facial representation of AY32.

Preservation state	Skull	Excellent overall state.
	Mandible	Excellent overall state.
Representation of missing components	Skull	None.
	Mandible	None.
Confidence level	16	1st Level
Facial approximation	Soft tissue depths	Stephan (2017); Stephan and Simpson (2008a)
	Eye placement	Guyomarc'h et al. (2012); Stephan and Davidson (2008); Stephan et al. (2009)
	Eye canthi	Stephan and Davidson (2008)
	Nose profile	Rynn et al. (2010); Ullrich and Stephan (2011, 2016)
	Nasal tip	Davy-Jow et al. (2012)
	Nose width	Guyomarc'h (2011)
	Mouth width	Song et al. (2007); Stephan and Henneberg (2003)
	Lip thickness	George (1987); Wilkinson et al. (2003)
	Ear placement	Ashley-Montagu (1939); Guyomarc'h and Stephan (2012)

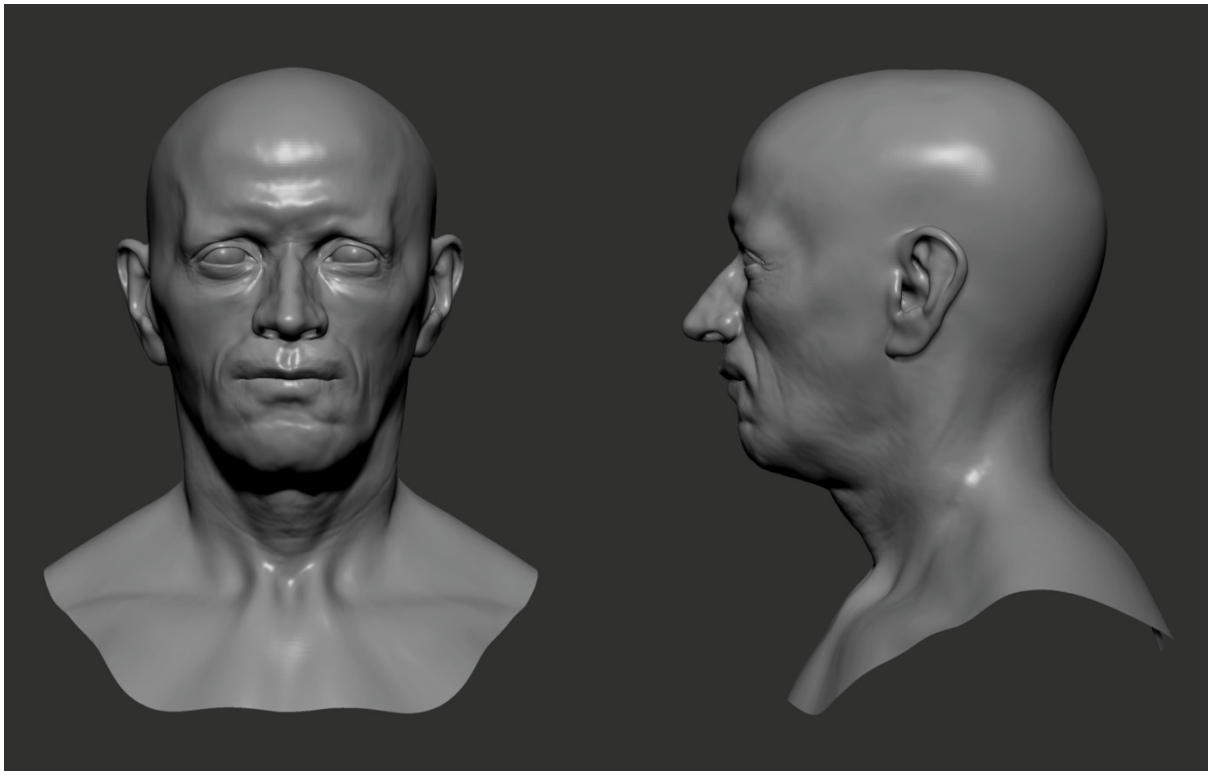

Figure 5.15 - Facial representation of AY32.

5.2.1.7 AY38 Male

The male from Tomb AY38 died between 35 and 40 years of age, and both the skull and mandible are complete (Table 5.18 and Figure 5.16). The frontal bone has a healed blunt force wound that was surely visible in life. This individual presents robust features and a pronounced retrognathic mandible, justifying his representation with the upper teeth exposed.

Table 5.18 - Summary of the methods used in the facial representation of AY38 Male.

Preservation state	Skull	Excellent overall state.
	Mandible	Excellent overall state.

Representation of missing components	Skull	None.
	Mandible	None.
Confidence level	16	1st Level
Facial approximation	Soft tissue depths	Stephan (2017); Stephan and Simpson (2008a)
	Eye placement	Guyomarc'h et al. (2012); Stephan and Davidson (2008); Stephan et al. (2009)
	Eye canthi	Stephan and Davidson (2008)
	Nose profile	Rynn et al. (2010); Ullrich and Stephan (2011, 2016)
	Nasal tip	Davy-Jow et al. (2012)
	Nose width	Guyomarc'h (2011)
	Mouth width	Song et al. (2007); Stephan and Henneberg (2003)
	Lip thickness	George (1987); Wilkinson et al. (2003)
	Ear placement	Ashley-Montagu (1939); Guyomarc'h and Stephan (2012)

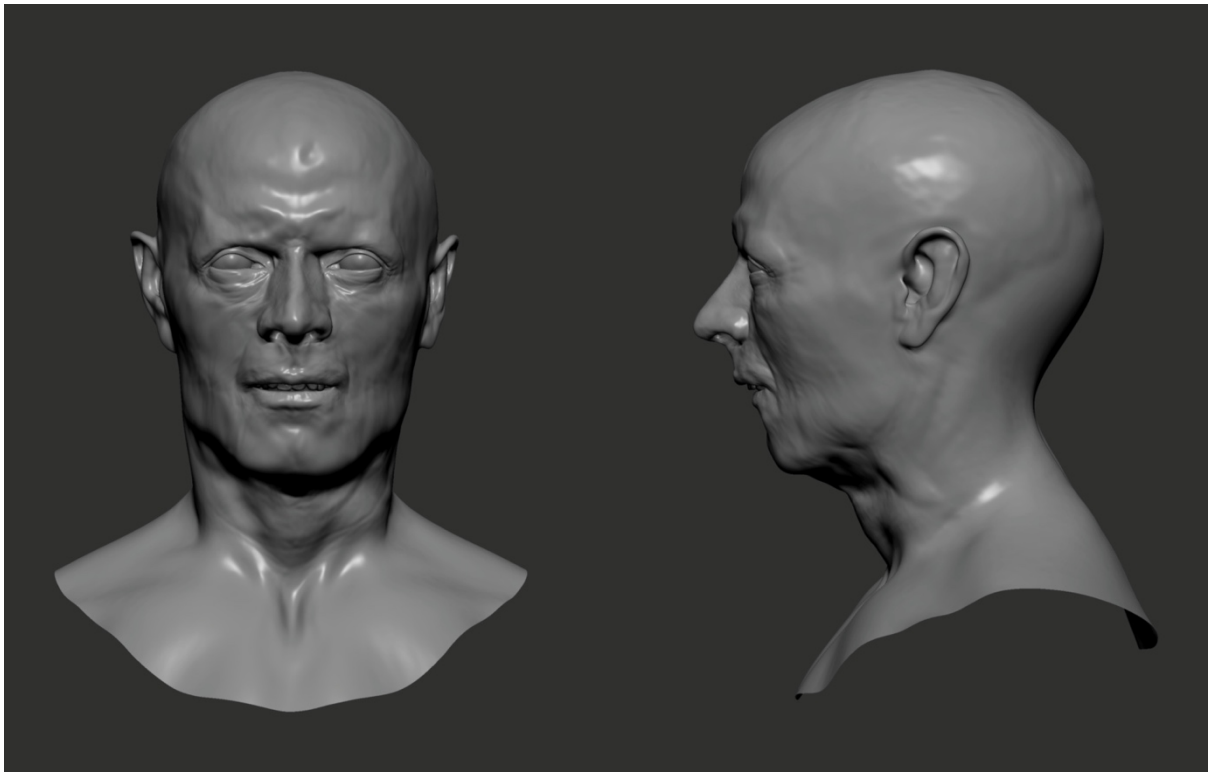

Figure 5.16 - Facial representation of AY38 Male.

5.2.1.8 AY58

AY58 designates the tomb of an adult female aged between 30 and 35 years old at the time of death (Table 5.19 and Figure 5.17). Both cranium and mandible are complete, but the missing incisors hinder the prediction of the thickness of the lips. Like to AY12, the individual from tomb AY58 had a snub nose. All molar teeth on the mandible were lost antemortem and, therefore, the *ecm2* soft tissue markers cannot be placed on the mandible.

Table 5.19 - Summary of the methods used in the facial representation of AY58.

Preservation state	Skull	Good overall state.
	Mandible	Good overall state.
Representation of missing components	Skull	Missing components mirrored using bilateral symmetry.
	Mandible	Missing components mirrored using bilateral symmetry.
Confidence level	15,00	1st Level
Facial approximation	Soft tissue depths	Stephan (2017); Stephan and Simpson (2008a)
	Eye placement	Guyomarc'h et al. (2012); Stephan and Davidson (2008); Stephan et al. (2009)
	Eye canthi	Stephan and Davidson (2008)
	Nose profile	Rynn et al. (2010); Ullrich and Stephan (2011, 2016)
	Nasal tip	Cannot be predicted.
	Nose width	Guyomarc'h (2011)
	Mouth width	Song et al. (2007)
	Lip thickness	Cannot be predicted.
	Ear placement	Ashley-Montagu (1939); Guyomarc'h and Stephan (2012)

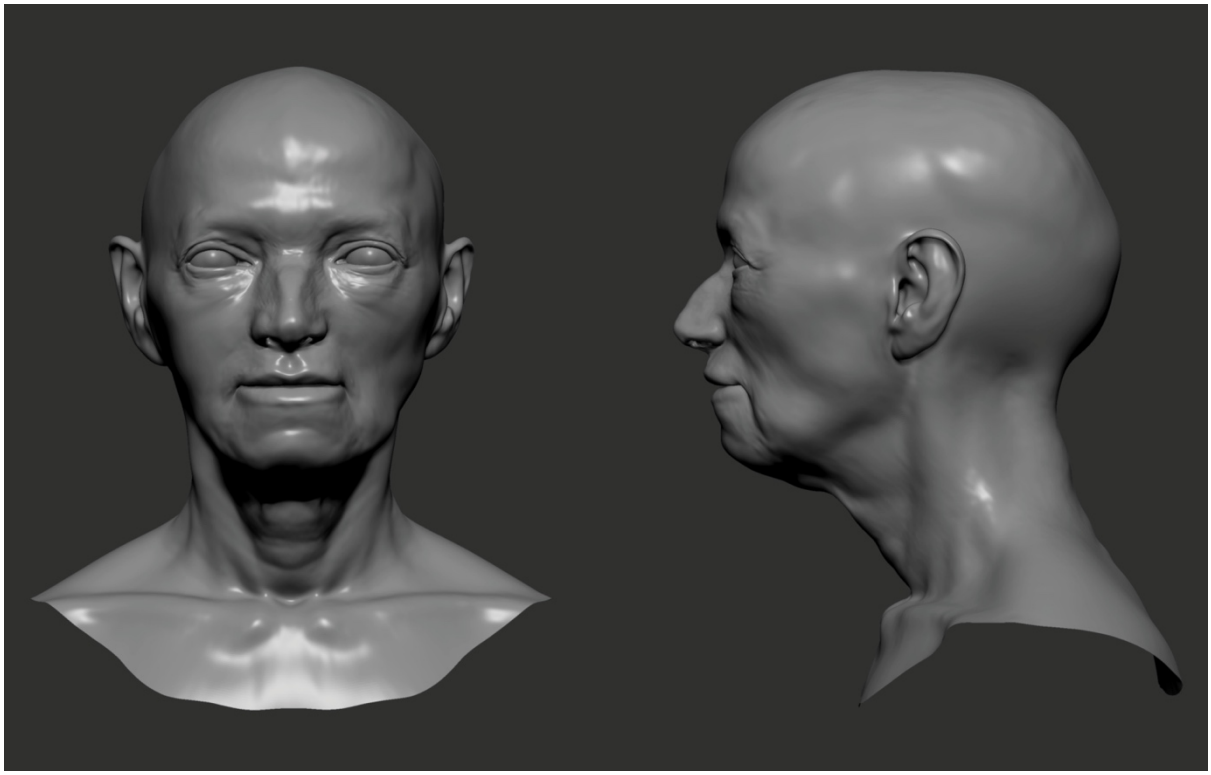

Figure 5.17 - Facial representation of AY58.

5.2.1.9 AY67

The individual buried in Tomb AY67 is a man aged 35 and 40 at the time of death (Table 5.20 and Figure 5.18). The skull is very well preserved overall, but the right mastoid process is fragmented, and the right lateral incisor is absent. The mandible is nearly complete, lacking only the central left incisor and the first molar on the right quadrant. The right temporal bone shows some detachment from the original position, and it is possible that the calvarium has distorted slightly towards the right side too, due to the pressure of the sediment on top of the body, which was resting on its right side. Since this aspect does not interfere directly with the facial portion, there was no attempt to correct it.

Table 5.20 - Summary of the methods used in the facial representation of AY67.

Preservation state	Skull	Excellent overall state. Right mastoid process is absent. It is possible that the calvarium presents some plastic distortion towards the right side, likely due to the position of the individual within the tomb.
	Mandible	Excellent overall state, central left incisor and first right molar missing.
Representation of missing components	Skull	None.
	Mandible	None.
Confidence level	15,25	1st Level
Facial approximation	Soft tissue depths	Stephan (2017); Stephan and Simpson (2008a)
	Eye placement	Guyomarc'h et al. (2012); Stephan and Davidson (2008); Stephan et al. (2009)
	Eye canthi	Stephan and Davidson (2008)
	Nose profile	Rynn et al. (2010); Ullrich and Stephan (2011, 2016)
	Nasal tip	Davy-Jow et al. (2012)
	Nose width	Guyomarc'h (2011)
	Mouth width	Song et al. (2007); Stephan and Henneberg (2003)
	Lip thickness	George (1987); Wilkinson et al. (2003)
	Ear placement	Ashley-Montagu (1939); Guyomarc'h and Stephan (2012)

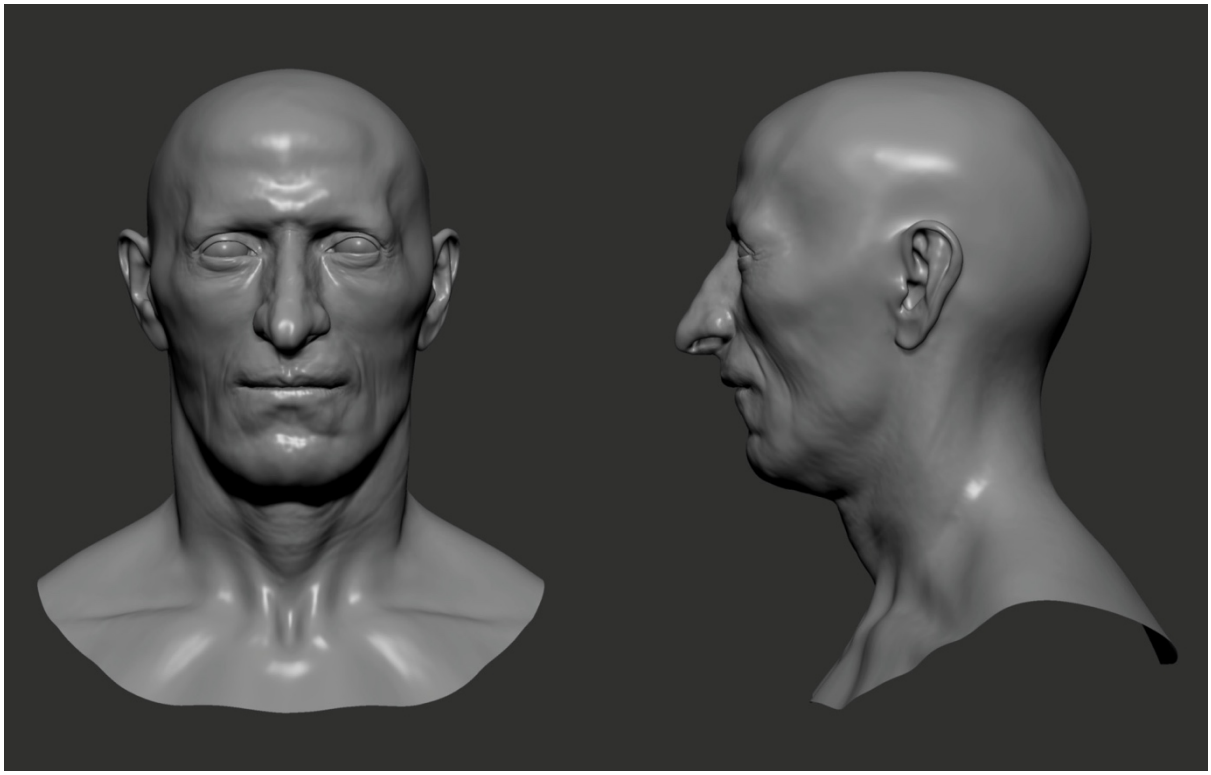

Figure 5.18 - Facial representation of AY67.

5.2.1.10 AY68 Male

AY68 is a double tomb. Here, we represent the face of the male, who died between 25 and 30 years old. The skull is virtually complete, but all maxillary incisors are missing, and all molars were lost antemortem. The upper lip thickness cannot be accessed due to the absence of the incisors, and the *ecm²* soft tissue depths cannot be placed. The left ramus of the mandible was reassembled digitally using the alignment and interpolation tools in Geomagic® (Table 5.21 and Figure 5.19).

Table 5.21 - Summary of the methods used in the facial representation of AY68 Male.

Preservation state	Skull	Excellent overall state. All incisors are missing.
	Mandible	Excellent overall state.

Representation of missing components	Skull	None.
	Mandible	None.
Confidence level	15,00	1st Level
Facial approximation	Soft tissue depths	Stephan (2017); Stephan and Simpson (2008a)
	Eye placement	Guyomarc'h et al. (2012); Stephan and Davidson (2008); Stephan et al. (2009)
	Eye canthi	Stephan and Davidson (2008)
	Nose profile	Rynn et al. (2010); Ullrich and Stephan (2011, 2016)
	Nasal tip	Davy-Jow et al. (2012)
	Nose width	Guyomarc'h (2011)
	Mouth width	Song et al. (2007); Stephan and Henneberg (2003)
	Lip thickness	George (1987); Wilkinson et al. (2003)
	Ear placement	Ashley-Montagu (1939); Guyomarc'h and Stephan (2012)

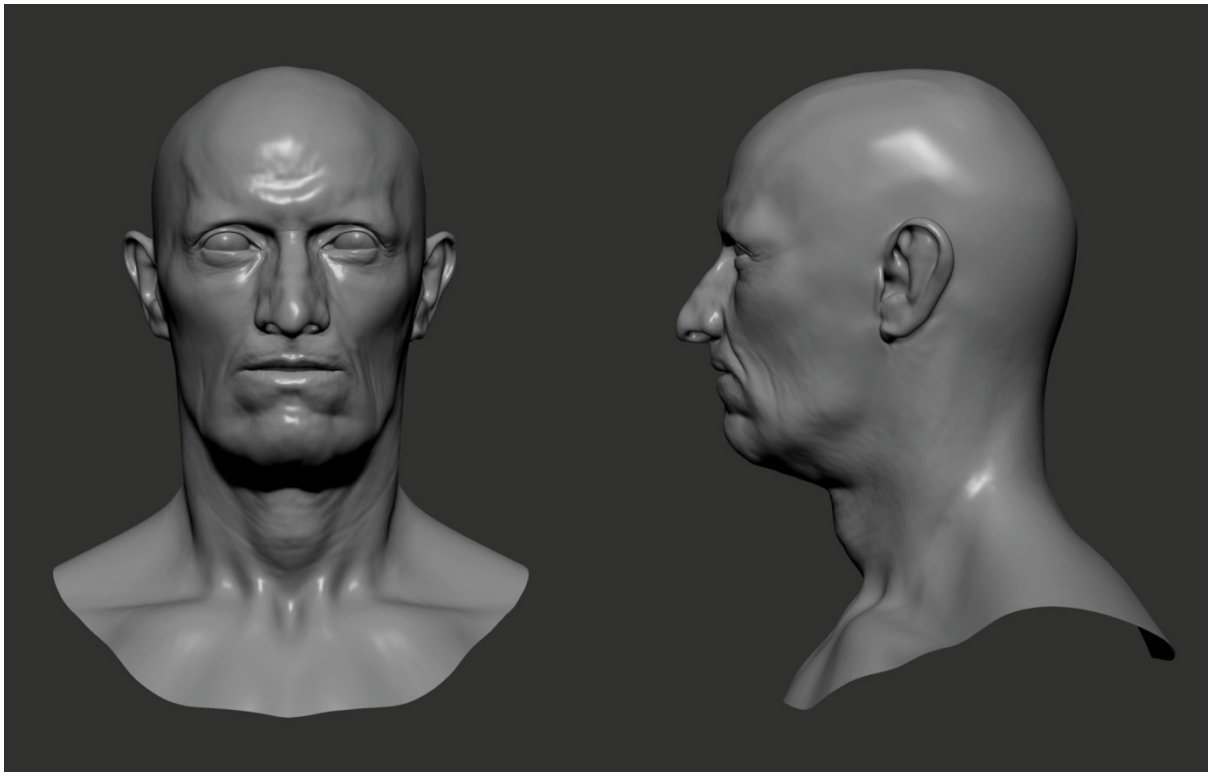

Figure 5.19 - Facial representation of AY68 Male.

5.2.1.11 AY80 Female

AY80 is a double inhumation. The female was between 30 and 35 years old at the time of death (Table 5.22 and Figure 5.20). The occipital portion of the cranium is fragmented, and both frontal incisors and canines are missing. For that reason, the thickness of the upper lip cannot be predicted. The mandible is almost complete, missing only the second premolar and third molar on the left quadrant, and the right lateral incisor and both premolars on the right quadrant.

Table 5.22 - Summary of the methods used in the facial representation of AY80 Female.

Preservation state	Skull	Good overall state. The occipital is fragmented, and the frontal incisors and canines are missing.
	Mandible	Excellent overall state.
Representation of missing components	Skull	Missing components mirrored using bilateral symmetry.
	Mandible	Missing components mirrored using bilateral symmetry.
Confidence level	15,50	1st Level
Facial approximation	Soft tissue depths	Stephan (2017); Stephan and Simpson (2008a)
	Eye placement	Guyomarc'h et al. (2012); Stephan and Davidson (2008); Stephan et al. (2009)
	Eye canthi	Stephan and Davidson (2008)
	Nose profile	Rynn et al. (2010); Ullrich and Stephan (2011, 2016)
	Nasal tip	Cannot be predicted.
	Nose width	Guyomarc'h (2011)
	Mouth width	Song et al. (2007)
	Lip thickness	George (1987); Wilkinson et al. (2003)
	Ear placement	Ashley-Montagu (1939); Guyomarc'h and Stephan (2012)

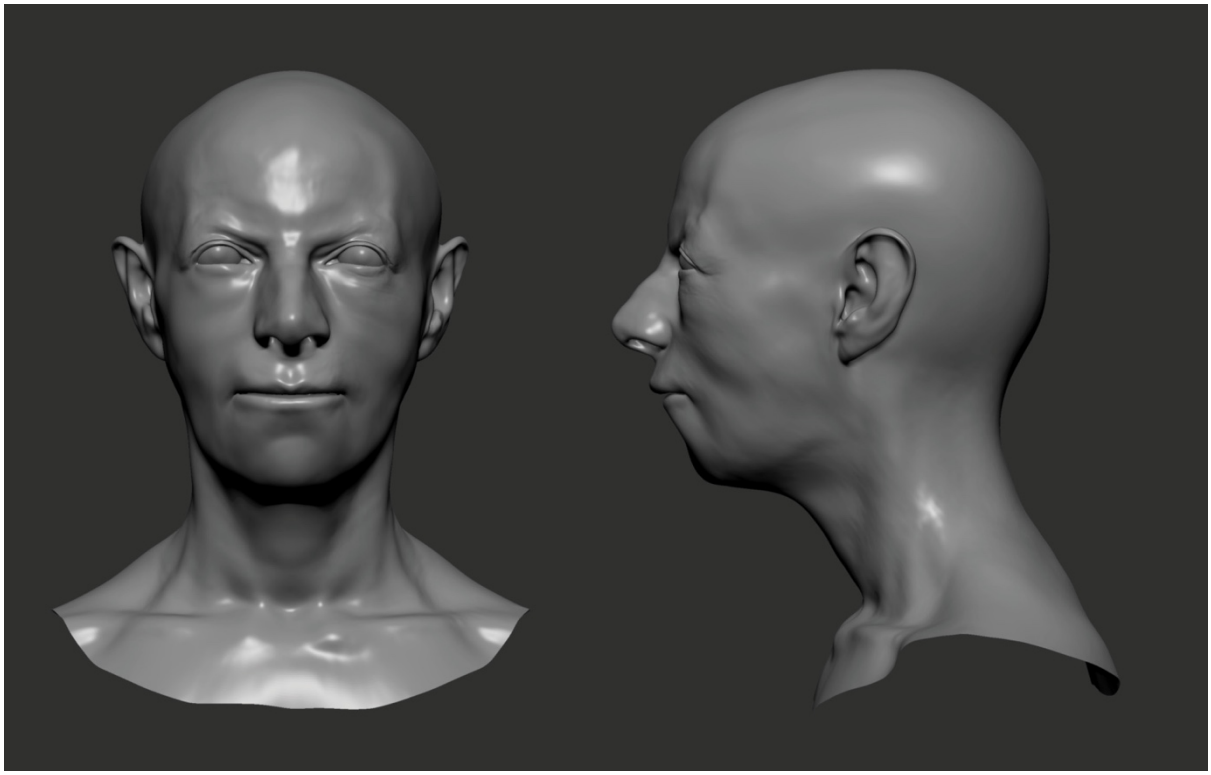

Figure 5.20 - Facial representation of AY80 Female.

5.2.1.12 AY80 Male

The skull and mandible of the male of Tomb 80 are complete (Table 5.23 and Figure 5.21). He died around 30 years old. The central left and the lateral right incisors are missing, and the first left molar on the mandible was lost premortem.

Table 5.23 - Summary of the methods used in the facial representation of AY80 Male.

Preservation state	Skull	Excellent overall state. Left central and right lateral incisors are missing, along with the two right molars.
	Mandible	Excellent overall state, with only the central and lateral incisors missing in the right quadrant. First left molar lost premortem.

Representation of missing components	Skull	Missing components mirrored using bilateral symmetry.
	Mandible	Missing components mirrored using bilateral symmetry.
Confidence level	16,00	1st Level
Facial approximation	Soft tissue depths	Stephan (2017); Stephan and Simpson (2008a)
	Eye placement	Guyomarc'h et al. (2012); Stephan and Davidson (2008); Stephan et al. (2009)
	Eye canthi	Stephan and Davidson (2008)
	Nose profile	Rynn et al. (2010); Ullrich and Stephan (2011, 2016)
	Nasal tip	Davy-Jow et al. (2012)
	Nose width	Guyomarc'h (2011)
	Mouth width	Song et al. (2007); Stephan and Henneberg (2003)
	Lip thickness	George (1987); Wilkinson et al. (2003)
	Ear placement	Ashley-Montagu (1939); Guyomarc'h and Stephan (2012)

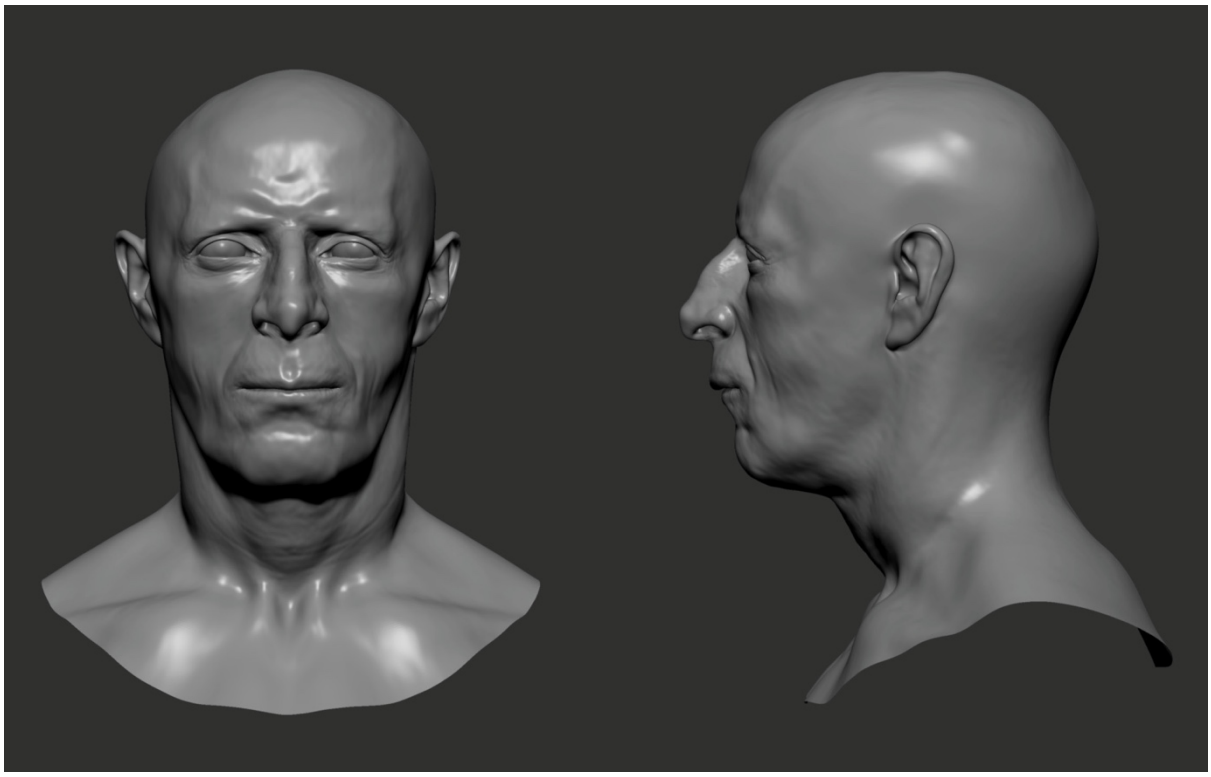

Figure 5.21 - Facial representation of AY80 Male.

5.2.1.13 AY82 Male

This individual came from a double tomb and was between 40 and 44 years old at the time of his death (Table 5.24 and Figure 5.22). The cranium is complete, missing only the lateral incisor and canine on the left side of the maxilla. The frontal incisors of the mandible were lost antemortem. The alveolar resorption on both maxilla and mandible hinders the placement of the *ecm²* and *ecm₂* soft tissue depth markers.

Table 5.24 - Summary of the methods used in the facial representation of AY82 Male.

Preservation state	Skull	Good overall state. The left lateral incisor and canine are missing.
	Mandible	Good overall state.
Representation of missing components	Skull	Missing components mirrored using bilateral symmetry.
	Mandible	Missing components mirrored using bilateral symmetry.
Confidence level	15,50	1st Level
Facial approximation	Soft tissue depths	Stephan (2017); Stephan and Simpson (2008a)
	Eye placement	Guyomarc'h et al. (2012); Stephan and Davidson (2008); Stephan et al. (2009)
	Eye canthi	Stephan and Davidson (2008)
	Nose profile	Rynn et al. (2010); Ullrich and Stephan (2011, 2016)
	Nasal tip	Davy-Jow et al. (2012)
	Nose width	Guyomarc'h (2011)
	Mouth width	Song et al. (2007); Stephan and Henneberg (2003)
	Lip thickness	George (1987)
	Ear placement	Ashley-Montagu (1939); Guyomarc'h and Stephan (2012)

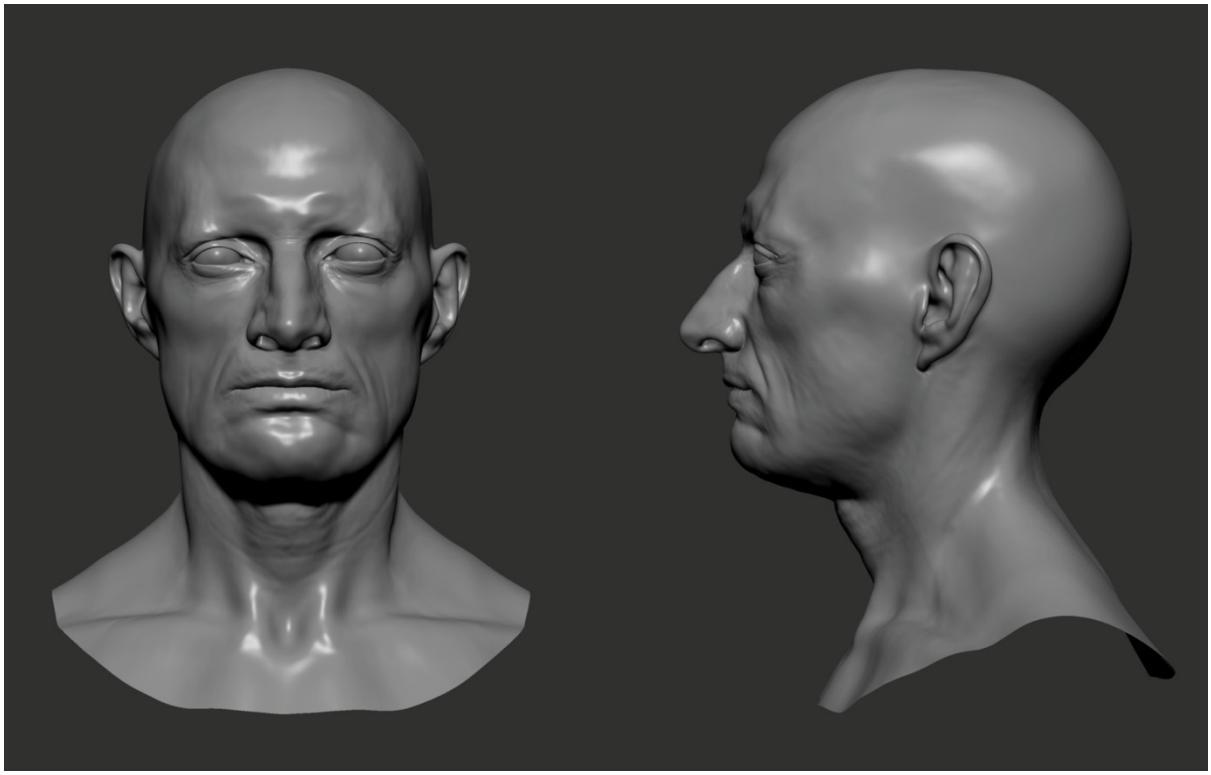

Figure 5.22 - Facial representation of AY82 Male.

5.2.1.14 AY86

The female buried in Tomb AY86 was between 30 and 40 years old at the time of death (Table 5.25 and Figure 5.23). Both the cranium and mandible are virtually complete, and the missing fragments on the right temporal and parietal bones were filled using the "fill hole" function in Geomagic®. Since most frontal teeth are missing, the thickness of the lips cannot be estimated. The alveolar resorption on the left side of the maxilla does not allow the placement of the *ecm²* soft tissue depth marker.

Table 5.25 - Summary of the methods used in the facial representation of AY86.

Preservation state	Skull	Good overall state. All frontal teeth are missing.
	Mandible	Good overall state. All incisors are missing.

Representation of missing components	Skull	None.
	Mandible	None.
Confidence level	15,00	1st Level
Facial approximation	Soft tissue depths	Stephan (2017); Stephan and Simpson (2008a)
	Eye placement	Guyomarc'h et al. (2012); Stephan and Davidson (2008); Stephan et al. (2009)
	Eye canthi	Stephan and Davidson (2008)
	Nose profile	Rynn et al. (2010); Ullrich and Stephan (2011, 2016)
	Nasal tip	Davy-Jow et al. (2012)
	Nose width	Guyomarc'h (2011)
	Mouth width	Song et al. (2007); Stephan and Henneberg (2003)
	Lip thickness	Cannot be estimated.
	Ear placement	Ashley-Montagu (1939); Guyomarc'h and Stephan (2012)

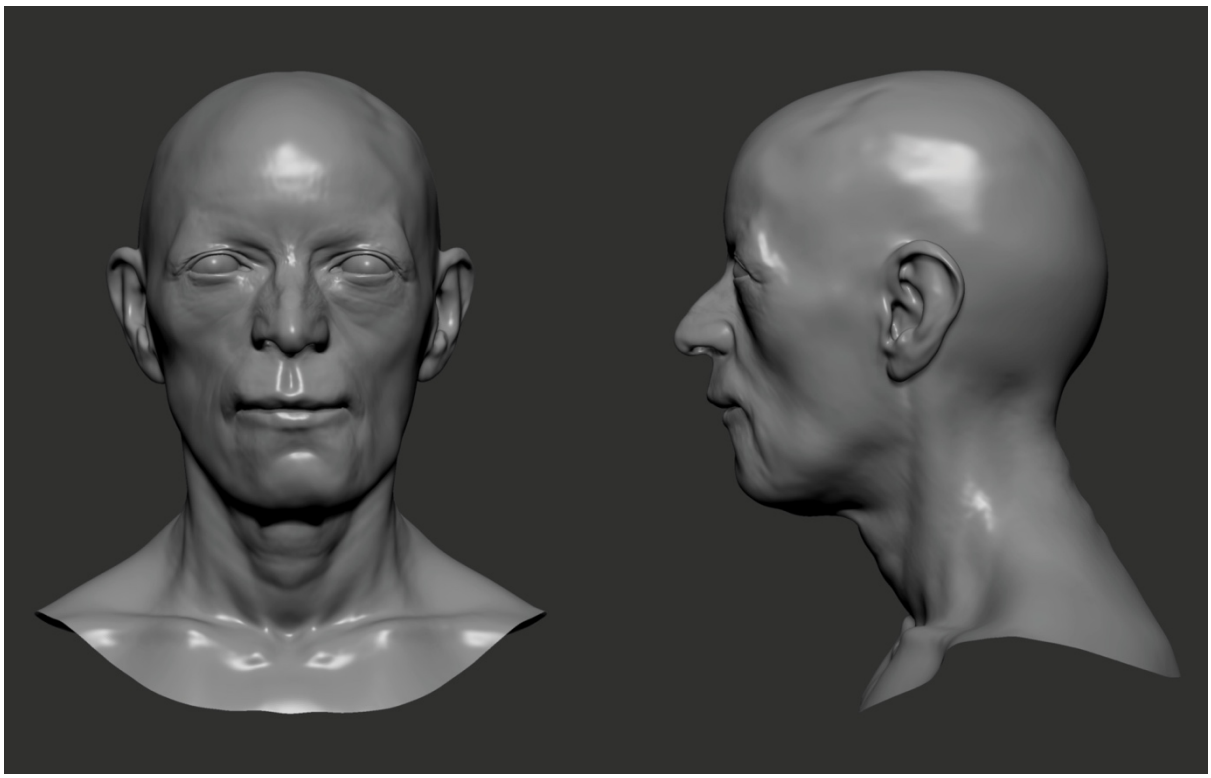

Figure 5.23 - Facial representation of AY86.

5.2.1.15 AY90 Female

Tomb AY90 contained two individuals. The female died between the age of 35 and 45 (Table 5.26 and Figure 5.24). Both cranium and mandible are in a good overall state. All molars on the maxilla, except for the second molar on the left side, were lost antemortem. This circumstance, along with the alveolar resorption on the mandible, hinders the placement of the *ecm²* and *ecm₂* tissue depths. The thickness of the lips cannot be estimated due to the missing incisors.

Table 5.26 - Summary of the methods used in the facial representation of AY90 Female.

Preservation state	Skull	Good overall state. All frontal teeth are missing.
	Mandible	Good overall state. Front incisors are missing.
Representation of missing components	Skull	Missing components mirrored using bilateral symmetry.
	Mandible	Missing components mirrored using bilateral symmetry.
Confidence level	15,00	1st Level
Facial approximation	Soft tissue depths	Stephan (2017); Stephan and Simpson (2008a)
	Eye placement	Guyomarc'h et al. (2012); Stephan and Davidson (2008); Stephan et al. (2009)
	Eye canthi	Stephan and Davidson (2008)
	Nose profile	Rynn et al. (2010); Ullrich and Stephan (2011, 2016)
	Nasal tip	Cannot be predicted.
	Nose width	Guyomarc'h (2011)
	Mouth width	Song et al. (2007); Stephan and Henneberg (2003)
	Lip thickness	Cannot be estimated.
	Ear placement	Ashley-Montagu (1939); Guyomarc'h and Stephan (2012)

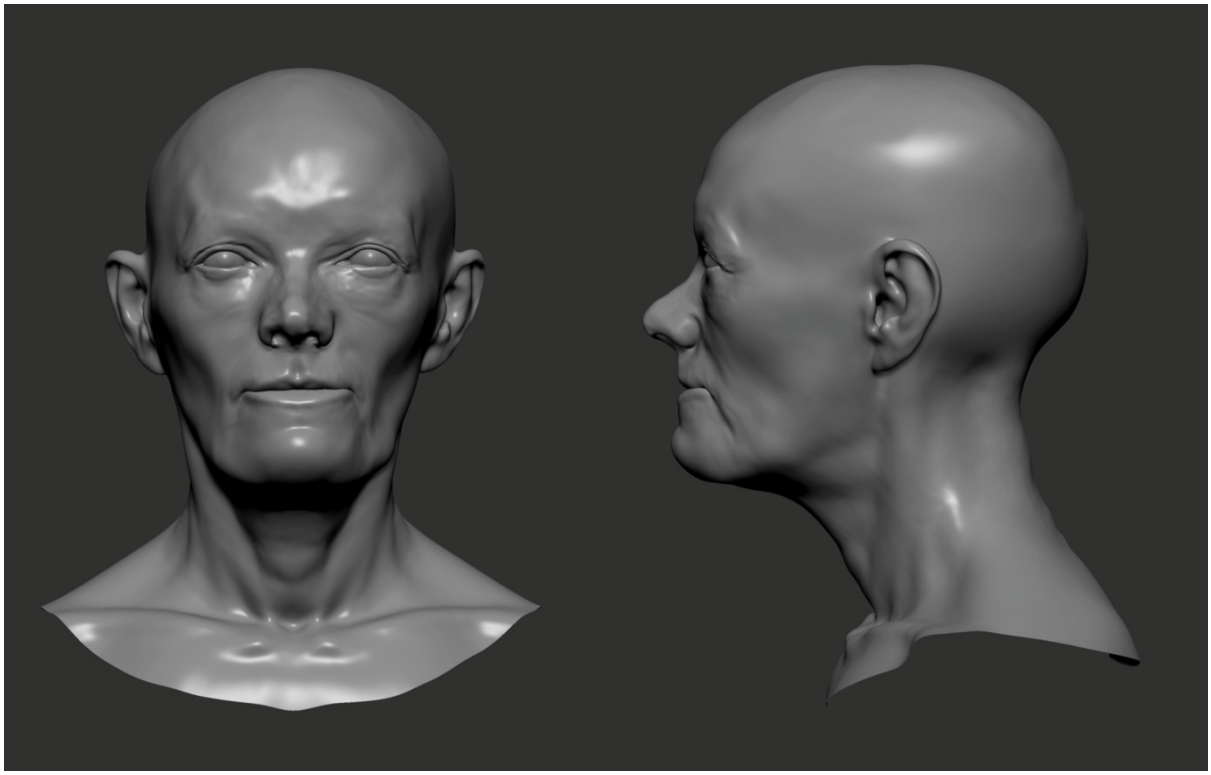

Figure 5.24 - Facial representation of AY90 Female.

5.2.1.16 AY90 Male

The male from Tomb AY90 presents a nearly complete cranium and mandible (Table 5.27 and Figure 5.25). He was between 35 and 40 years old at the time of death. All incisor and canine teeth of the maxilla are missing, and consequently, the superior lip thickness should be considered approximate. On the mandible, the central left incisor was mirrored using its right counterpart, along with the first molar on the left side. The alveolar resorption on the left side of the mandible shows that the second molar was lost premortem, and, for that reason, it is not possible to place the ecm_2 soft tissue depth. The upper lip thickness could not be estimated due to the absence of the upper incisors.

Table 5.27 - Summary of the methods used in the facial representation of AY90 Male.

Preservation state	Skull	Excellent overall state. The incisors and canines are missing.
	Mandible	Excellent overall state. The central left incisor, first left molar and right condyle missing.
Representation of missing components	Skull	None.
	Mandible	Missing components mirrored using bilateral symmetry.
Confidence level	15,00	1st Level
Facial approximation	Soft tissue depths	Stephan (2017); Stephan and Simpson (2008a)
	Eye placement	Guyomarc'h et al. (2012); Stephan and Davidson (2008); Stephan et al. (2009)
	Eye canthi	Stephan and Davidson (2008)
	Nose profile	Rynn et al. (2010); Ullrich and Stephan (2011, 2016)
	Nasal tip	Davy-Jow et al. (2012)
	Nose width	Guyomarc'h (2011)
	Mouth width	Song et al. (2007)
	Lip thickness	Wilkinson et al. (2003)
	Ear placement	Ashley-Montagu (1939); Guyomarc'h and Stephan (2012)

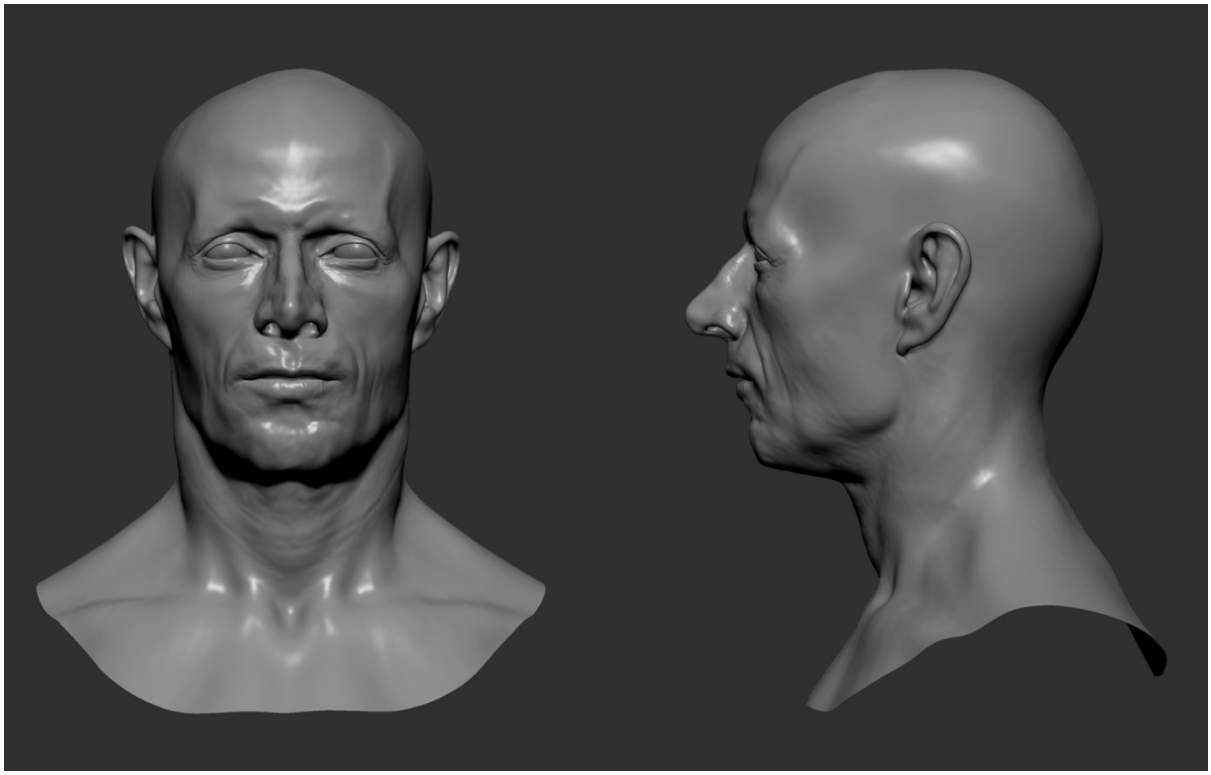

Figure 5.25 - Facial representation of AY90 Male.

5.2.1.17 AY96

AY96 presents a complete cranium and mandible. It belongs to a female individual who passed away between 35 and 40 years old (Table 5.28 and Figure 5.26). The loss of the front teeth led to resorption of the prosthion, which may cause a higher degree of error when estimating the profile of the soft nose. The front teeth of the mandible are missing. In this case, both the mouth placement and the estimation of the lip thickness are somewhat problematic. The bone resorption in the mandible does not allow for the placement of the *ecm*$_2$ soft tissue depth markers.

Table 5.28 - Summary of the methods used in the facial representation of AY96.

Preservation state	Skull	Good overall state.
	Mandible	Good overall state. All front teeth are missing.
Representation of missing components	Skull	None.
	Mandible	None.
Confidence level	15,00	1st Level
Facial approximation	Soft tissue depths	Stephan (2017); Stephan and Simpson (2008a)
	Eye placement	Guyomarc'h et al. (2012); Stephan and Davidson (2008); Stephan et al. (2009)
	Eye canthi	Stephan and Davidson (2008)
	Nose profile	Rynn et al. (2010); Ullrich and Stephan (2011, 2016)
	Nasal tip	Davy-Jow et al. (2012)
	Nose width	Guyomarc'h (2011)
	Mouth width	Song et al. (2007)
	Lip thickness	Cannot be predicted.
	Ear placement	Ashley-Montagu (1939); Guyomarc'h and Stephan (2012)

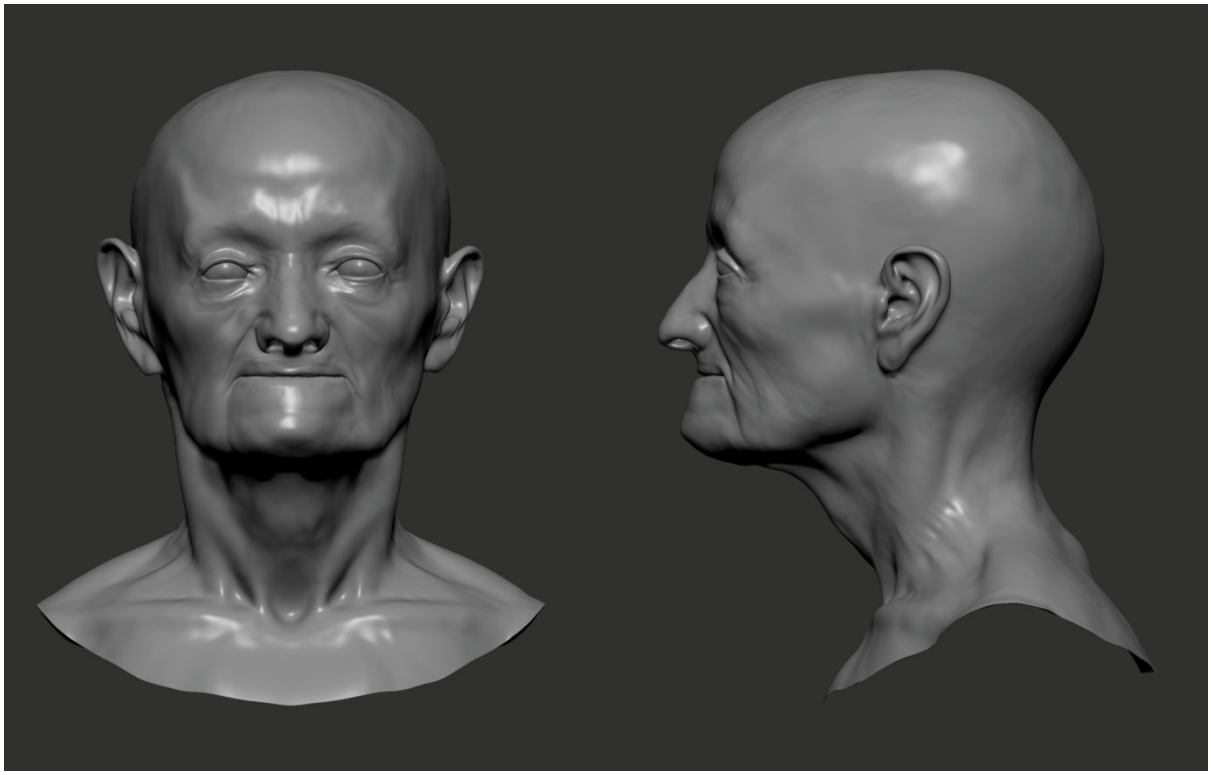

Figure 5.26 - Facial representation of AY96.

5.2.1.18 AY97 Female

AY97 is a double tomb. This facial representation belongs to a female who lived a six-decade-long life (Table 5.29 and Figure 5.27). Both cranium and mandible are relatively complete, but the thickness of the lips cannot be estimated due to the absence of front teeth.

Table 5.29 - Summary of the methods used in the facial representation of AY97 Female.

Preservation state	Skull	Good overall state.
	Mandible	Good overall state.
	Skull	None.

Representation of missing components	Mandible	None.
Confidence level	15,00	1st Level
Facial approximation	Soft tissue depths	Stephan (2017); Stephan and Simpson (2008a)
	Eye placement	Guyomarc'h et al. (2012); Stephan and Davidson (2008); Stephan et al. (2009)
	Eye canthi	Stephan and Davidson (2008)
	Nose profile	Rynn et al. (2010); Ullrich and Stephan (2011, 2016)
	Nasal tip	Davy-Jow et al. (2012)
	Nose width	Guyomarc'h (2011)
	Mouth width	Song et al. (2007)
	Lip thickness	Cannot be predicted.
	Ear placement	Ashley-Montagu (1939); Guyomarc'h and Stephan (2012)

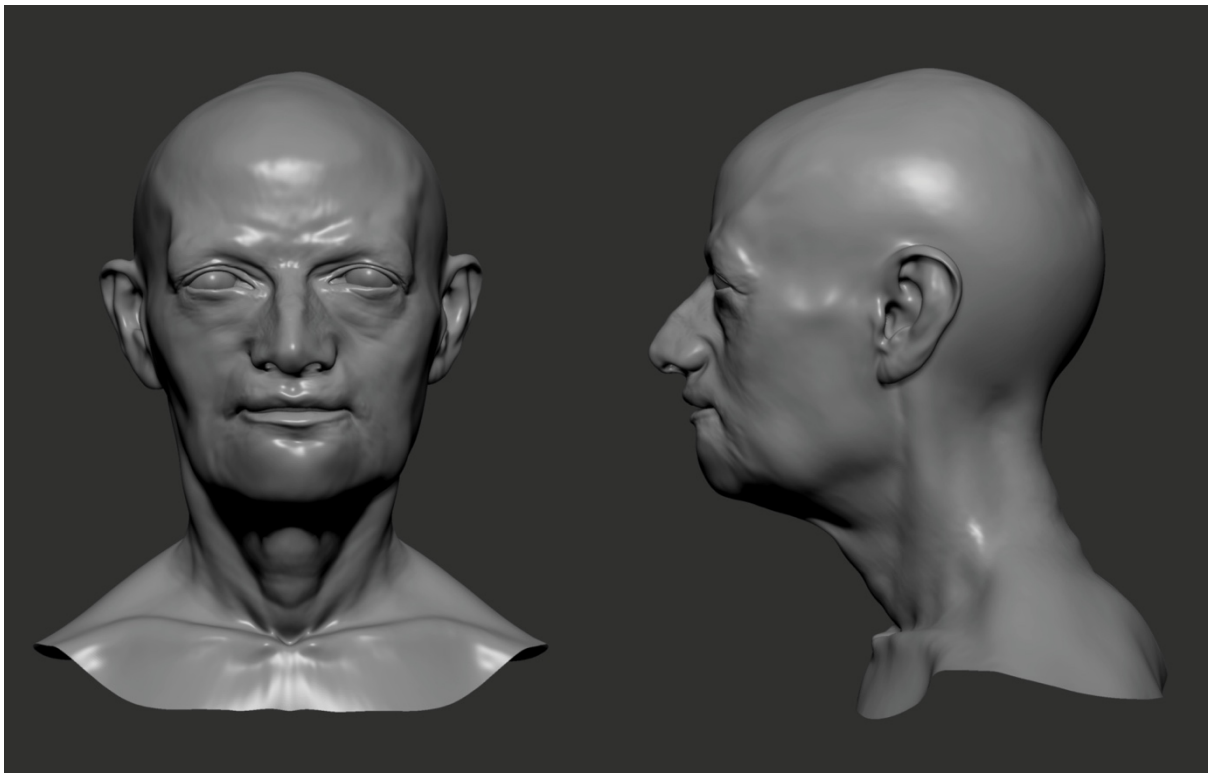

Figure 5.27 - Facial representation of AY97 Female.

5.2.2 Second level facial approximations

5.2.2.1 AY11

The individual buried in Tomb AY11 is a female who died around the age of 30–35 years old (Table 5.30 and Figure 5.28). The facial portion of the skull is almost complete, but the calvarium is far too fragmented to be manually reassembled. For that reason, the maximum width of the face and the general contour of the head is unknown. The mandible is complete, missing only the incisors, canine and first premolar on the right quadrant. The representation of the overall shape of the head and the maximum width of the face should be considered tentative.

Table 5.30 - Summary of the methods used in the facial representation of AY11.

Preservation state	Skull	The facial bones are good overall state. The neurocranium is too fragmented and cannot be manually reassembled.
	Mandible	Excellent overall state. Both incisors and canine on the right quadrant are missing.
Representation of missing components	Skull	Missing components mirrored using bilateral symmetry. The neurocranium is not visually represented.
	Mandible	Missing components mirrored using bilateral symmetry.
Confidence level	14,75	2nd Level
Facial approximation	Soft tissue depths	Stephan (2017); Stephan and Simpson (2008a)
	Eye placement	Guyomarc'h et al. (2012); Stephan and Davidson (2008); Stephan et al. (2009)
	Eye canthi	Stephan and Davidson (2008)
	Nose profile	Rynn et al. (2010); Ullrich and Stephan (2011, 2016)
	Nasal tip	Davy-Jow et al. (2012)
	Nose width	Guyomarc'h (2011)
	Mouth width	Song et al. (2007); Stephan and Henneberg (2003)

Lip thickness	George (1987); Wilkinson et al. (2003)
Ear placement	Guyomarc'h and Stephan (2012)

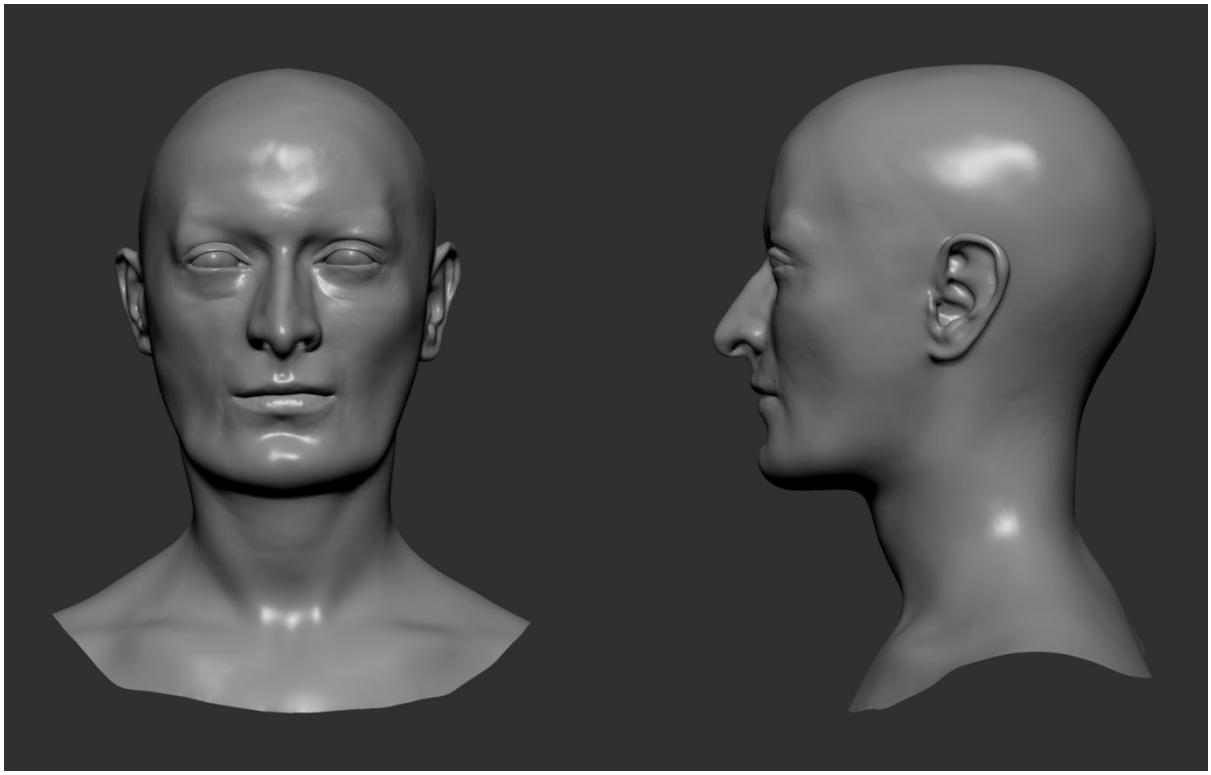

Figure 5.28 - Facial representation of AY11.

5.2.2.2 AY21 Female

This skull belongs to an adult female aged 30-35. Due to the fragmentation along the nasal and zygomatic sutures, the skull's facial portion began detaching and bending forward. This instance was corrected in a digital environment by positioning the skull and mandible in anatomical position and subsequently rotating the facial bones along a horizontal axis centered at the frontozygomatic sutures. Dental occlusion was assumed as the anatomical constraint to reduce the degree of freedom during the rotation of the facial bones (Figure 5.29).

Figure 5.29 - Correction of the position of the facial bones in AY21, using the mandible as the anatomical constraint.

The orbital rims and sockets also required a considerable degree of intervention. This process began with the mirroring of the skull using the bilateral axis. Afterwards, the "best-fit alignment" operation provided the best possible correspondence by interpolating the mirrored portion with the preserved parts of the skull. The right temporal also presents a slight detachment from the parietal, which hinders the prediction of the widest facial points. The missing portions on the parietal and occipital bones were refilled using the "fill hole" operation within Geomagic®. There was no attempt at representing the missing bone portions around the foramen magnum. The general shape of the calvarium bends towards the left side and, because it might be the result of post-mortem fragmentation and deformation, it was not represented in the facial approximation. The lower lip thickness could not be estimated due to the absence of the lower mandibular incisors (Table 5.31 and Figure 5.30).

Table 5.31 - Summary of the methods used in the facial representation of AY21.

Preservation state	Skull	Good overall state. Missing portions on the eye sockets and fragmentation along the nasal and zygomatic bones.
	Mandible	Excellent overall state. Central incisors missing.
Representation of missing components	Skull	Missing components mirrored using bilateral symmetry. Rotation of the facial bones using the dental occlusion as an anatomical constraint.
	Mandible	None.
Confidence level	14,00	2nd Level
Facial approximation	Soft tissue depths	Stephan (2017); Stephan and Simpson (2008a)
	Eye placement	Guyomarc'h et al. (2012); Stephan and Davidson (2008); Stephan et al. (2009)
	Eye canthi	Stephan and Davidson (2008)
	Nose profile	Rynn et al. (2010); Ullrich and Stephan (2011, 2016)
	Nasal tip	Davy-Jow et al. (2012)
	Nose width	Guyomarc'h (2011)
	Mouth width	Song et al. (2007); Stephan and Henneberg (2003)
	Lip thickness	George (1987); Wilkinson et al. (2003)
	Ear placement	Ashley-Montagu (1939); Guyomarc'h and Stephan (2012)

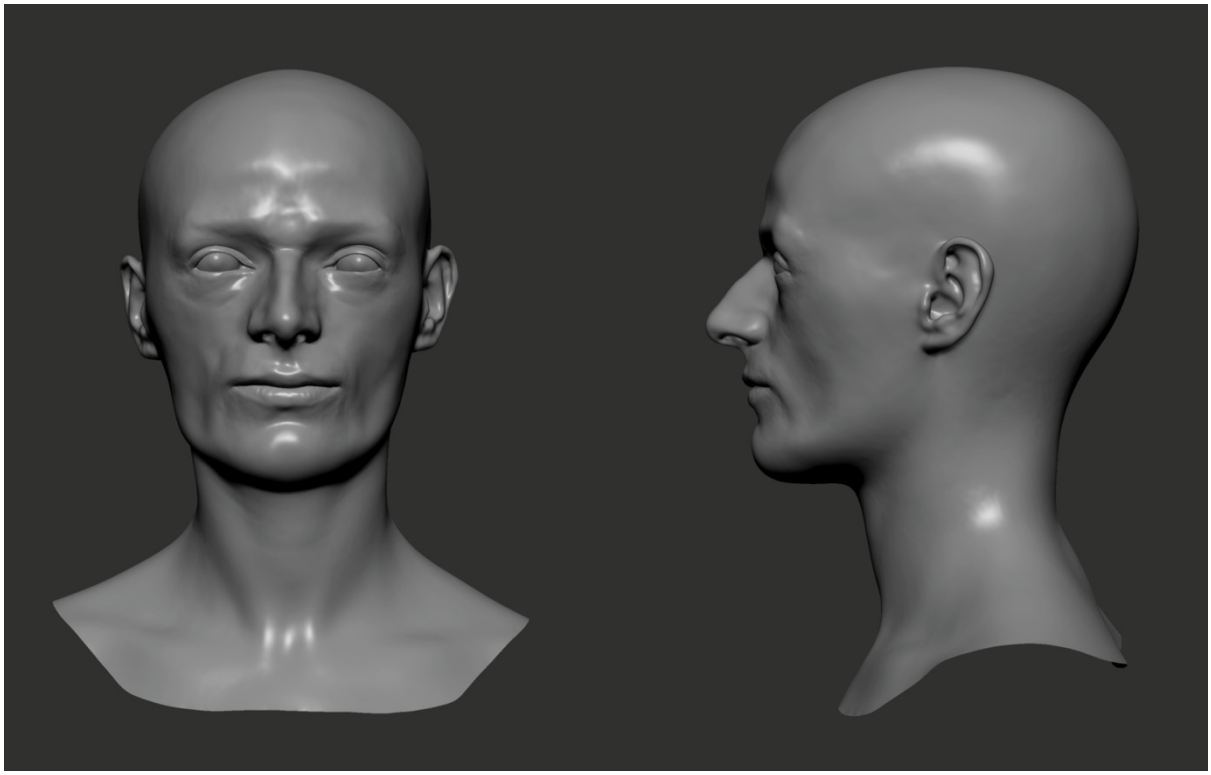

Figure 5.30 - Facial representation of AY21.

5.2.2.3 AY22 Female

This female skull belongs to an adult individual (Table 5.32 and Figure 5.31). The skull is missing a considerable portion of the left parietal and temporal bones. The left zygomatic arch is absent as well, along with both maxillary canines, the first molar on the left side and the frontal incisor on the right. Loss of the left frontal incisor was premortem due to the noticeable resorption of the alveolus. The right central incisor, both canines and the first molar on the maxilla's left quadrant are missing. The right ramus of the mandible is absent and all teeth, except for the molars, are missing. To illustrate the missing parts on the left side of the skull, the right parietal and temporal bones were mirrored and matched with the left side in Geomagic® to achieve an optimal alignment. The representation of the right ramus of the mandible followed a similar process, and after mirroring the left mandibular ramus, I also considered the articulation of the condylar process with the fossa. The lip thickness cannot be predicted.

Table 5.32 - Summary of the methods used in the facial representation of AY22 Female.

Preservation state	Skull	Good overall state. The temporal and a portion of the parietal bones are absent on the left side, along with the zygomatic arch. Right central incisor, both canines and the first molar on the left maxillary quadrant are missing.
	Mandible	Good overall state. Right ramus of the mandible is missing. All teeth except the molars did not preserved.
Representation of missing components	Skull	Missing components mirrored using bilateral symmetry.
	Mandible	Missing components mirrored using bilateral symmetry.
Confidence level	14,00	2nd Level
Facial approximation	Soft tissue depths	Stephan (2017); Stephan and Simpson (2008a)
	Eye placement	Guyomarc'h et al. (2012); Stephan and Davidson (2008); Stephan et al. (2009)
	Eye canthi	Stephan and Davidson (2008)
	Nose profile	Rynn et al. (2010); Ullrich and Stephan (2011, 2016)
	Nasal tip	Davy-Jow et al. (2012)
	Nose width	Guyomarc'h (2011)
	Mouth width	Song et al. (2007)
	Lip thickness	Cannot be predicted.
	Ear placement	Ashley-Montagu (1939); Guyomarc'h and Stephan (2012)

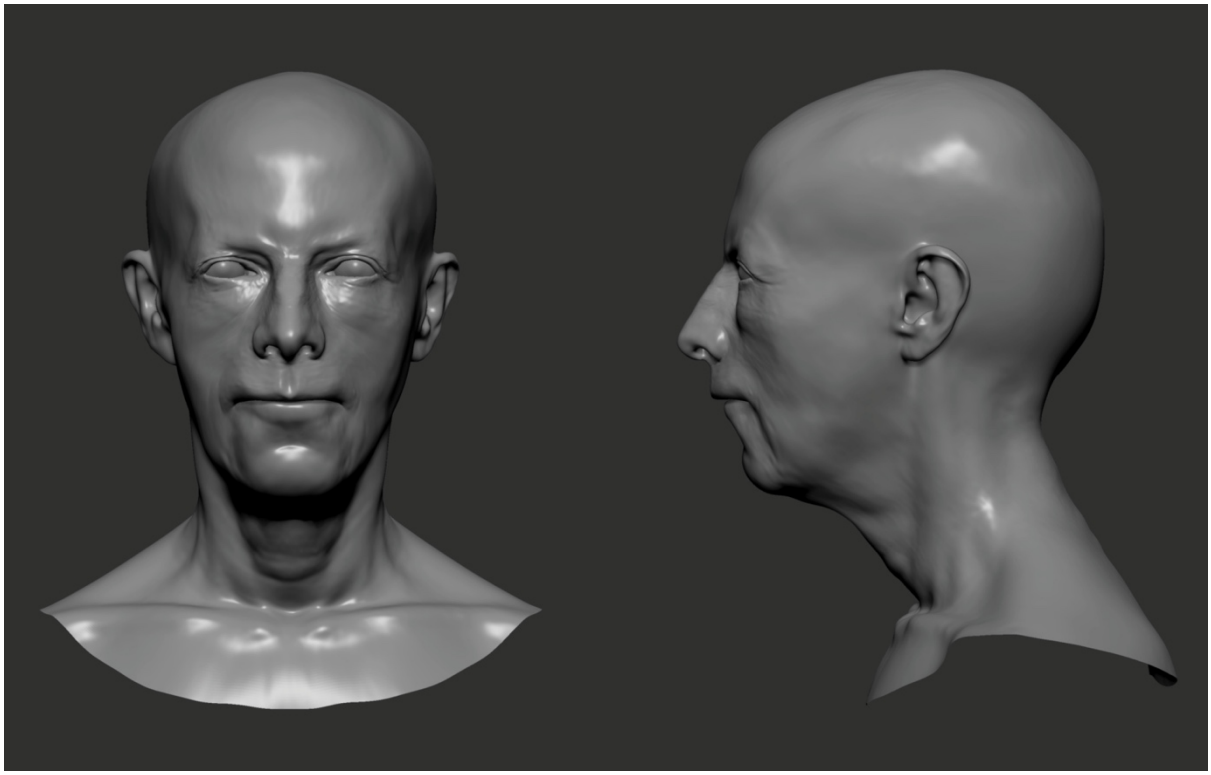

Figure 5.31 - Facial representation of AY22 Female.

5.2.2.4 AY22 Male

The male from Tomb AY22 was an adult between 35 and 45 years at death (Table 5.33 and Figure 5.32). The calvarium is fragmented and was manually reassembled before laser scanning. After being laser-scanned separately, the calvarium and the facial portion were placed in anatomical position in a virtual environment. The lateral wall of the left orbit is absent and was represented by mirroring the right portion of the facial bones and interpolating it with the existing morphology. The left zygomatic bone and both zygomatic arches are missing. Thus, the maximum width of the face should be considered tentative. Both maxillary central incisors are absent, along with all the molars on the right maxilla. The mandible also lacks a few teeth and the right condyle. The thickness of the upper lip cannot be predicted.

Table 5.33 - Summary of the methods used in the facial representation of AY22 Male.

Preservation state	Skull	Fragmented calvarium. Left zygomatic bone and both zygomatic arches are missing, along with the central maxillary incisors.
	Mandible	Right condyle absent and a few missing teeth.
Representation of missing components	Skull	Manual and virtual reassembly of fragments. Missing components mirrored using bilateral symmetry.
	Mandible	Missing components mirrored using bilateral symmetry.
Confidence level	13,00	2nd Level
Facial approximation	Soft tissue depths	Stephan (2017); Stephan and Simpson (2008a)
	Eye placement	Guyomarc'h et al. (2012); Stephan and Davidson (2008); Stephan et al. (2009)
	Eye canthi	Stephan and Davidson (2008)
	Nose profile	Rynn et al. (2010); Ullrich and Stephan (2011, 2016)
	Nasal tip	Davy-Jow et al. (2012)
	Nose width	Guyomarc'h (2011)
	Mouth width	Song et al. (2007); Stephan and Henneberg (2003)
	Lip thickness	Cannot be predicted.
	Ear placement	Ashley-Montagu (1939); Guyomarc'h and Stephan (2012)

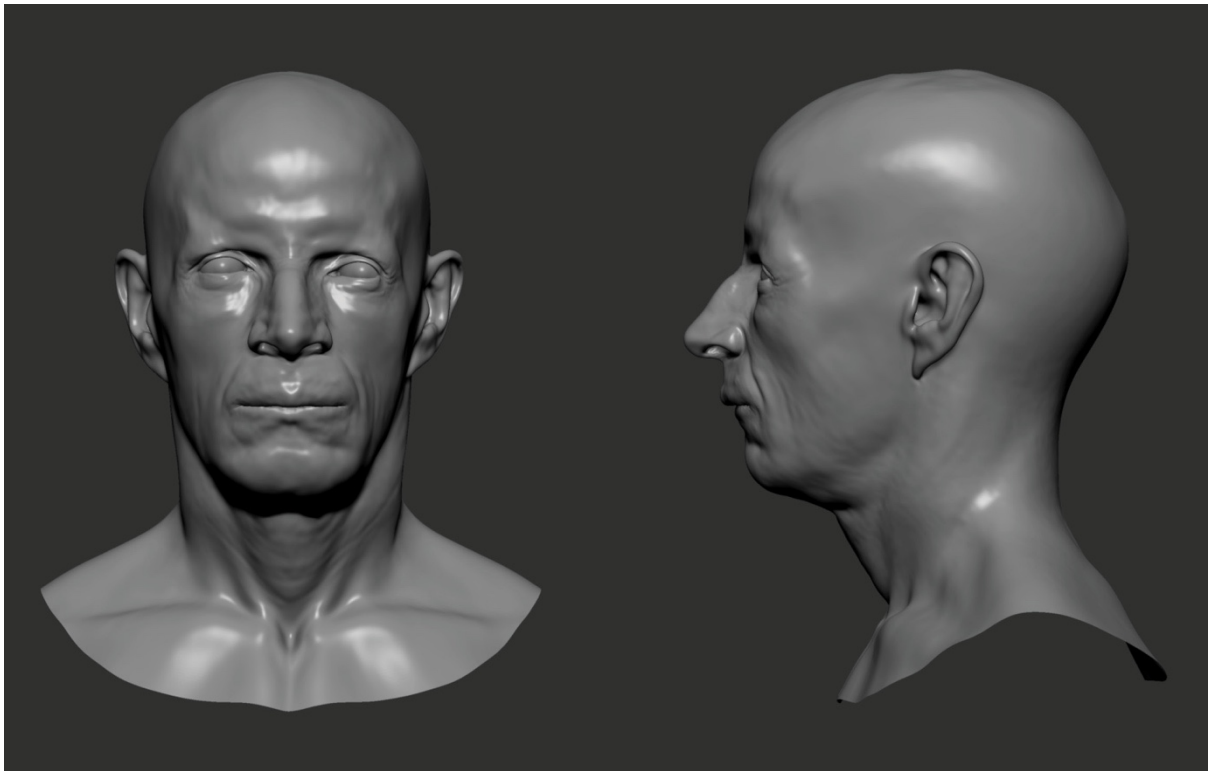

Figure 5.32 - Facial representation of AY22 Male.

5.2.2.5 AY26

AY26 is the tomb of an older woman who died beyond 60 years old (Table 5.34 and Figure 5.33). The cranium is missing a substantial portion of the left temporal and occipital bones. The frontal incisors and right lateral incisor of the maxilla are missing, along with the frontal incisors of the mandible. The left ramus of the mandible is fragmented, and part of the right mandibular body is missing as well. The absent portions were represented using the mirroring and interpolating function within Geomagic®. The shape of the nasal tip and the thickness of the lips cannot be predicted.

Table 5.34 - Summary of the methods used in the facial representation of AY26 Female.

Preservation state	Skull	Missing portions on the left temporal and occipital bones. Frontal incisors and right lateral incisor are missing.
	Mandible	The left ramus and a portion of the right mandibular body are missing.
Representation of missing components	Skull	Missing components mirrored using bilateral symmetry.
	Mandible	Missing components mirrored using bilateral symmetry.
Confidence level	13,00	2nd Level
Facial approximation	Soft tissue depths	Stephan (2017); Stephan and Simpson (2008a)
	Eye placement	Guyomarc'h et al. (2012); Stephan and Davidson (2008); Stephan et al. (2009)
	Eye canthi	Stephan and Davidson (2008)
	Nose profile	Rynn et al. (2010); Ullrich and Stephan (2011, 2016)
	Nasal tip	Cannot be predicted.
	Nose width	Guyomarc'h (2011)
	Mouth width	Song et al. (2007); Stephan and Henneberg (2003)
	Lip thickness	Cannot be predicted.
	Ear placement	Ashley-Montagu (1939); Guyomarc'h and Stephan (2012)

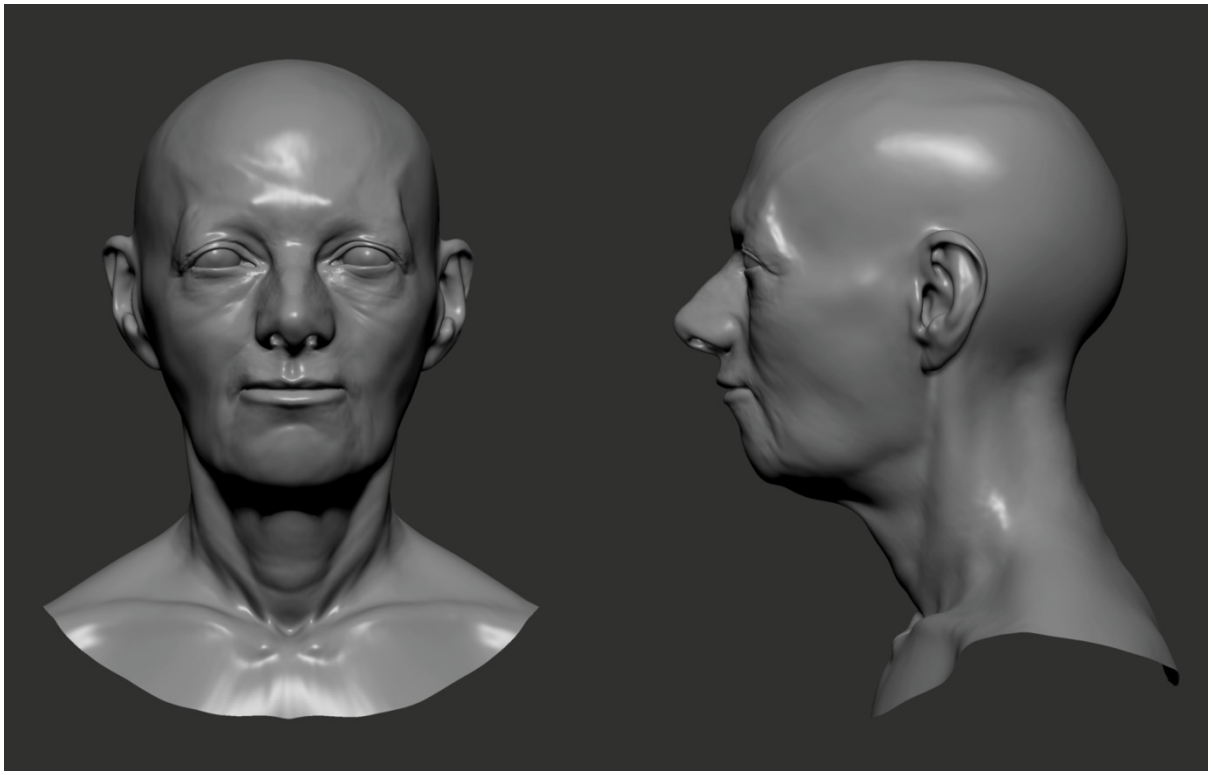

Figure 5.33 - Facial representation of AY26 Female.

5.2.2.6 AY42 Male

The male skull found in Tomb AY42 shows very robust features and belongs to an adult that died between 35 and 45 years old (Table 5.35 and Figure 5.34). The cranium was manually reassembled before being laser scanned and is nearly complete, missing only the right zygomatic arch, the right nasal bone, the ANS and the frontal left incisor. The second premolar was lost premortem. The distance between the nasion and acanthion, used to estimate the vertical tangent of the pronasale point, was measured from a representation of the ANS based on the adjacent anatomy, hindering a more precise placement of the vertical pronasale point. The mandible is fragmented along the alveoli of the central incisors, hindering the placement of the *id* soft tissue depth and the estimation of the lower lip thickness.

Table 5.35 - Summary of the methods used in the facial representation of AY42 Male.

Preservation state	Skull	Good overall state. Missing portions on the eye sockets and fragmentation along the nasal and zygomatic bones.
	Mandible	Good overall state. Central incisors missing.
Representation of missing components	Skull	Missing components mirrored using bilateral symmetry.
	Mandible	None.
Confidence level	14,25	2nd Level
Facial approximation	Soft tissue depths	Stephan (2017); Stephan and Simpson (2008a)
	Eye placement	Guyomarc'h et al. (2012); Stephan and Davidson (2008); Stephan et al. (2009)
	Eye canthi	Stephan and Davidson (2008)
	Nose profile	Rynn et al. (2010); Ullrich and Stephan (2011, 2016)
	Nasal tip	Davy-Jow et al. (2012)
	Nose width	Guyomarc'h (2011)
	Mouth width	Song et al. (2007); Stephan and Henneberg (2003)
	Lip thickness	George (1987)
	Ear placement	Ashley-Montagu (1939); Guyomarc'h and Stephan (2012)

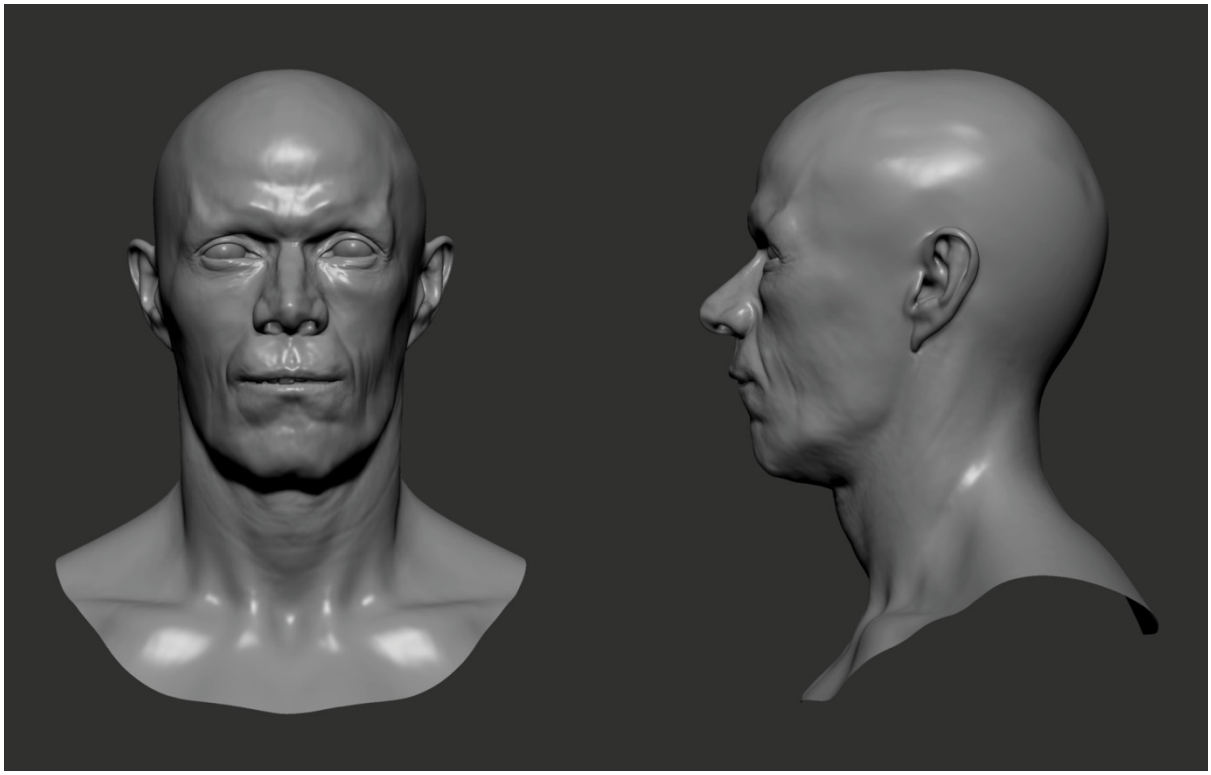

Figure 5.34 - Facial representation of AY42 Male.

5.2.2.7 AY45

AY45 contained a robust male individual aged between 25 and 35 years old at the time of death (Table 5.36 and Figure 5.35). The cranium is split from the maxilla and, for that reason, both parts were laser scanned separately and placed in anatomical position in a virtual environment. The cranium also shows some fragmentation along the malar bones, and a portion of the left nasal bone and orbit is missing. The neurocranium suffered plastic deformation, possibly due to the position of the individual inside the tomb. In this instance, no attempt was made to correct it. The right mandibular condyle is separated from the remaining of the mandible and was virtually positioned in place using the "best fit" tools inside Geomagic®. The teeth show a substantial amount of wear and, therefore, it is possible that the lip thickness is underestimated.

Table 5.36 - Summary of the methods used in the facial representation of AY45.

Preservation state	Skull	Missing portions on the malar bones, left nasal and orbit. Neurocranium shows plastic deformation.
	Mandible	Good overall state.
Representation of missing components	Skull	Missing components mirrored using bilateral symmetry.
	Mandible	Missing components mirrored using bilateral symmetry.
Confidence level	13,00	2nd Level
Facial approximation	Soft tissue depths	Stephan (2017); Stephan and Simpson (2008a)
	Eye placement	Guyomarc'h et al. (2012); Stephan and Davidson (2008); Stephan et al. (2009)
	Eye canthi	Stephan and Davidson (2008)
	Nose profile	Rynn et al. (2010); Ullrich and Stephan (2011, 2016)
	Nasal tip	Davy-Jow et al. (2012)
	Nose width	Guyomarc'h (2011)
	Mouth width	Song et al. (2007); Stephan and Henneberg (2003)
	Lip thickness	George (1987); Wilkinson et al. (2003)
	Ear placement	Ashley-Montagu (1939); Guyomarc'h and Stephan (2012)

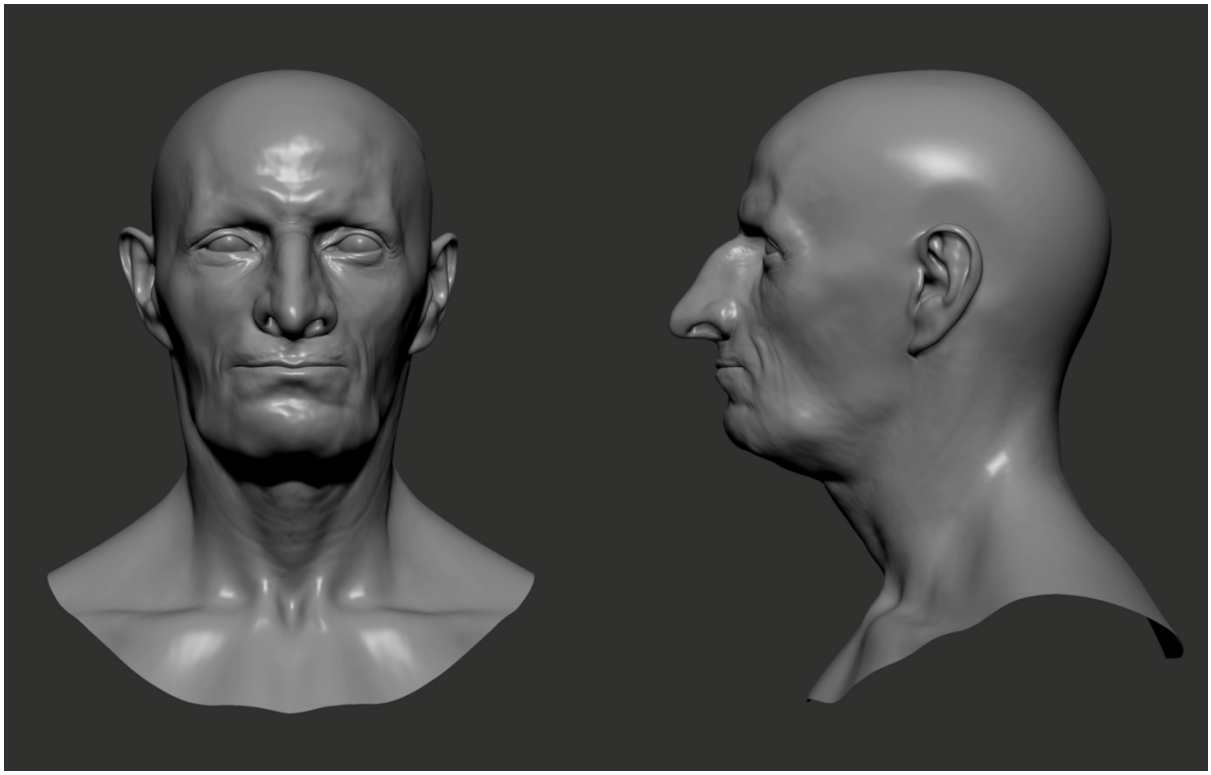

Figure 5.35 - Facial representation of AY45.

5.2.2.8 AY47

AY47 is the burial of an adult female. The maxilla is separated from the remaining cranium and was placed in an anatomical position using the mandibular occlusion as a constraint. Both left nasal and left malar bone are fragmented and were represented by mirroring the morphology on the right side. The lateral maxillary incisor and all the molars on the right quadrant were lost premortem, and the right canine and second premolar were lost postmortem. The mandible has good preservation overall, but several teeth are missing as well. On the right quadrant, the central right and lateral incisors from both sides are missing, and the third left molar is absent as well. The central left incisor and first molar were lost premortem. All teeth present considerable wear and hinder the application of the equations to estimate the thickness of the lips (Table 5.37 and Figure 5.36).

The woman buried in tomb AY47 presents an interesting case of a healed depressed fracture of the frontal bone, which would have been visible in life.

Table 5.37 - Summary of the methods used in the facial representation of AY47.

Preservation state	Skull	Maxilla is separated from the cranial vault. Fragmented portions on the nasal and malar area. Various teeth were lost premortem and others missing due to taphonomical processes.
	Mandible	Good overall state. Also presents pre- and postmortem teeth loss.
Representation of missing components	Skull	Virtual alignment of the maxilla using the mandible as an anatomical constraint. Missing components mirrored using bilateral symmetry when available.
	Mandible	Missing components mirrored using bilateral symmetry.
Confidence level	13,50	2nd Level
Facial approximation	Soft tissue depths	Stephan (2017); Stephan and Simpson (2008a)
	Eye placement	Guyomarc'h et al. (2012); Stephan and Davidson (2008); Stephan et al. (2009)
	Eye canthi	Stephan and Davidson (2008)
	Nose profile	Rynn et al. (2010); Ullrich and Stephan (2011, 2016)
	Nasal tip	Cannot be predicted.
	Nose width	Guyomarc'h (2011)
	Mouth width	Song et al. (2007); Stephan and Henneberg (2003)
	Lip thickness	George (1987); Wilkinson et al. (2003)
	Ear placement	Ashley-Montagu (1939); Guyomarc'h and Stephan (2012)

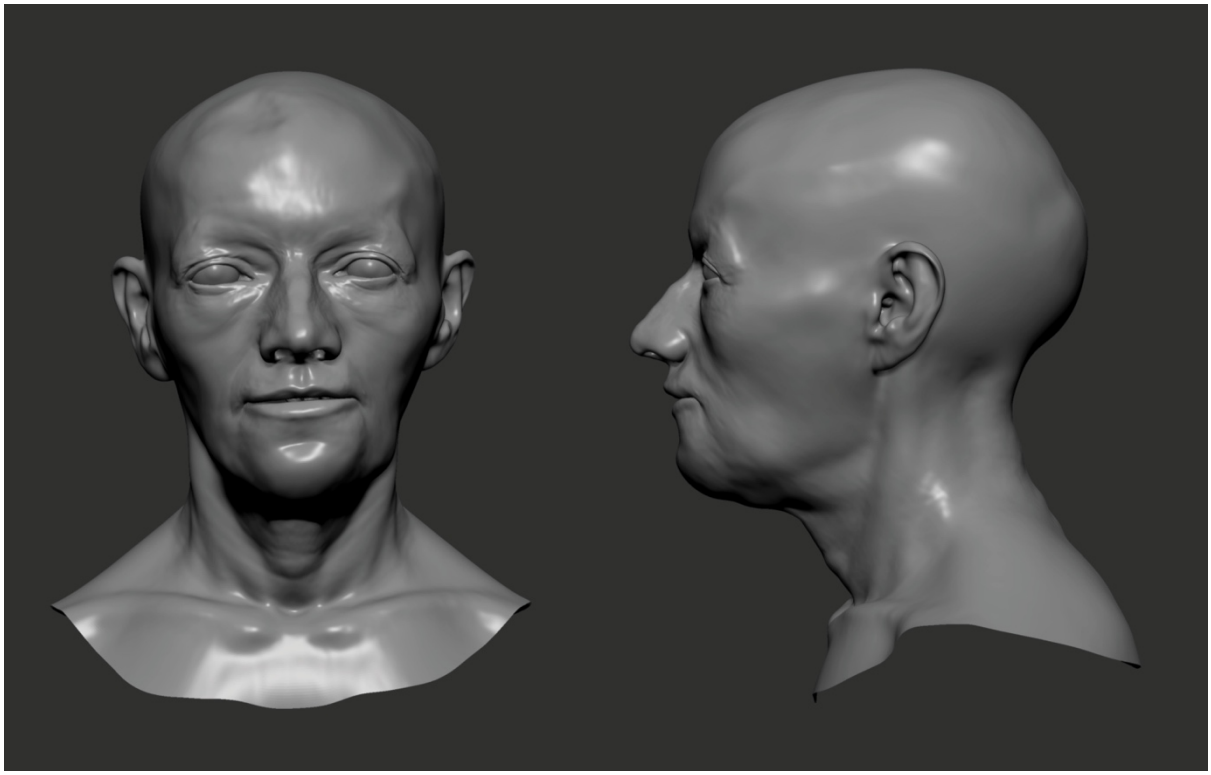

Figure 5.36 - Facial representation of AY47.

5.2.2.9 AY48

AY48 is the tomb of an aged female that lived beyond five decades (Table 5.38 and Figure 5.37). The cranium is almost complete, and all but one molar teeth on each side of the maxilla are preserved. The remaining teeth were lost antemortem, as evidenced by the resorption of the alveoli. As mentioned previously and noted by Rynn et al. (2010), this circumstance might interfere with the application of the methods to estimate the nose profile and produce higher margins of error. The thickness of the lips cannot be estimated. The mandible is almost complete, with some fragmentation along the right ramus. All mandibular molars were lost antemortem.

Table 5.38 - Summary of the methods used in the facial representation of AY48.

Preservation state	Skull	Good overall state. The right zygomatic is fragmented.
	Mandible	Good overall state. The right ramus is fragmented.
Representation of missing components	Skull	Missing components mirrored using bilateral symmetry.
	Mandible	Missing components mirrored using bilateral symmetry.
Confidence level	14,00	2nd Level
Facial approximation	Soft tissue depths	Stephan (2017); Stephan and Simpson (2008a)
	Eye placement	Guyomarc'h et al. (2012); Stephan and Davidson (2008); Stephan et al. (2009)
	Eye canthi	Stephan and Davidson (2008)
	Nose profile	Rynn et al. (2010); Ullrich and Stephan (2011, 2016)
	Nasal tip	Davy-Jow et al. (2012)
	Nose width	Guyomarc'h (2011)
	Mouth width	Song et al. (2007)
	Lip thickness	Cannot be estimated.
	Ear placement	Ashley-Montagu (1939); Guyomarc'h and Stephan (2012)

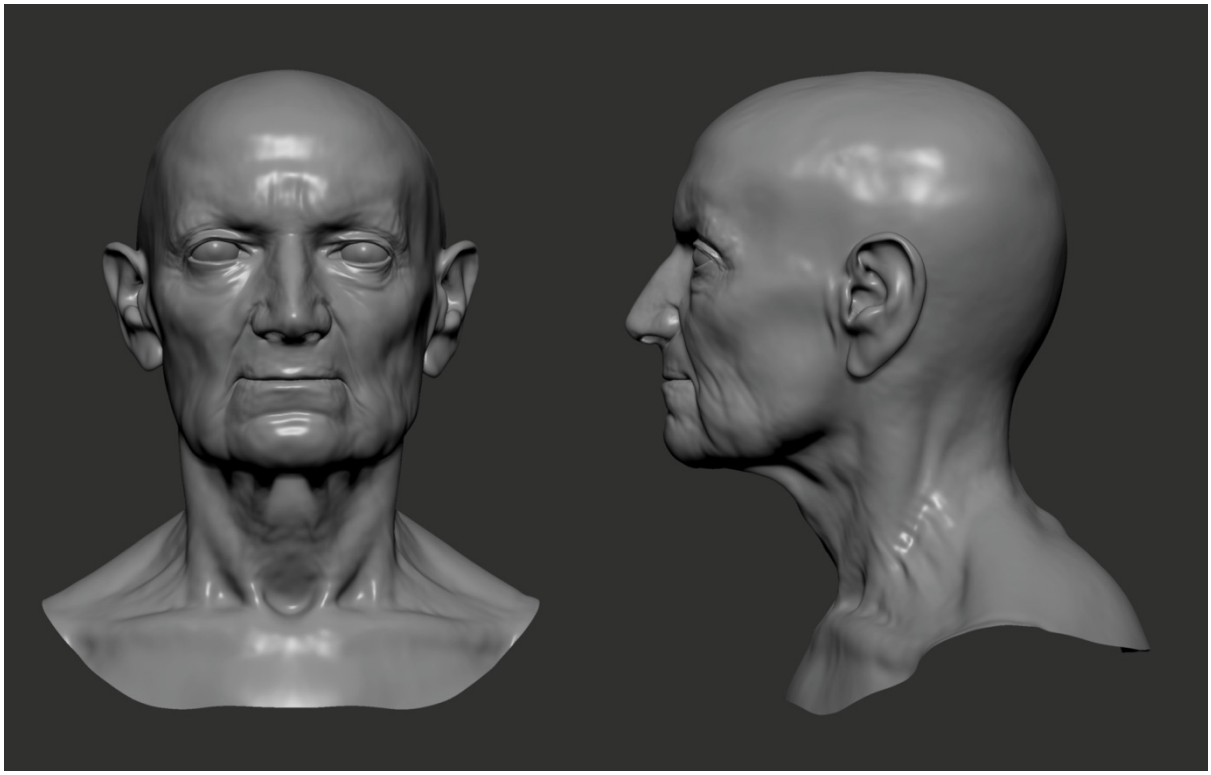

Figure 5.37 - Facial representation of AY48.

5.2.2.10 AY53

AY53 was the resting place of a female individual aged between 40 and 45 years at the time of death (Table 5.39 and Figure 5.38). The facial portion of the cranium is nearly complete, but the neurocranium is quite fragmented and presents some plastic deformation. It is missing the left temporal bone and also lacks portions of the right parietal and temporal bones. The pronasale position was estimated from a reconstructed ANS, and the missing frontal incisors hinder the estimation of the upper lip thickness. The *ecm2* soft tissue depth markers cannot be placed. The mandible is almost complete, albeit showing some teeth loss that occurred antemortem, and is missing a portion of the right ramus, which was reconstructed by mirroring the existing symmetry.

Table 5.39 - Summary of the methods used in the facial representation of AY53.

Preservation state	Skull	Good overall state. The neurocranium is fragmented along the sagittal suture and there are missing portions of both temporal bones and on the right parietal bone.
	Mandible	Excellent overall state. The right ramus is fragmented.
Representation of missing components	Skull	Missing components mirrored using bilateral symmetry.
	Mandible	Missing components mirrored using bilateral symmetry.
Confidence level	14,75	2nd Level
Facial approximation	Soft tissue depths	Stephan (2017); Stephan and Simpson (2008a)
	Eye placement	Guyomarc'h et al. (2012); Stephan and Davidson (2008); Stephan et al. (2009)
	Eye canthi	Stephan and Davidson (2008)
	Nose profile	Rynn et al. (2010); Ullrich and Stephan (2011, 2016)
	Nasal tip	Davy-Jow et al. (2012)
	Nose width	Guyomarc'h (2011)
	Mouth width	Song et al. (2007); Stephan and Henneberg (2003)
	Lip thickness	George (1987); Wilkinson et al. (2003)
	Ear placement	Ashley-Montagu (1939); Guyomarc'h and Stephan (2012)

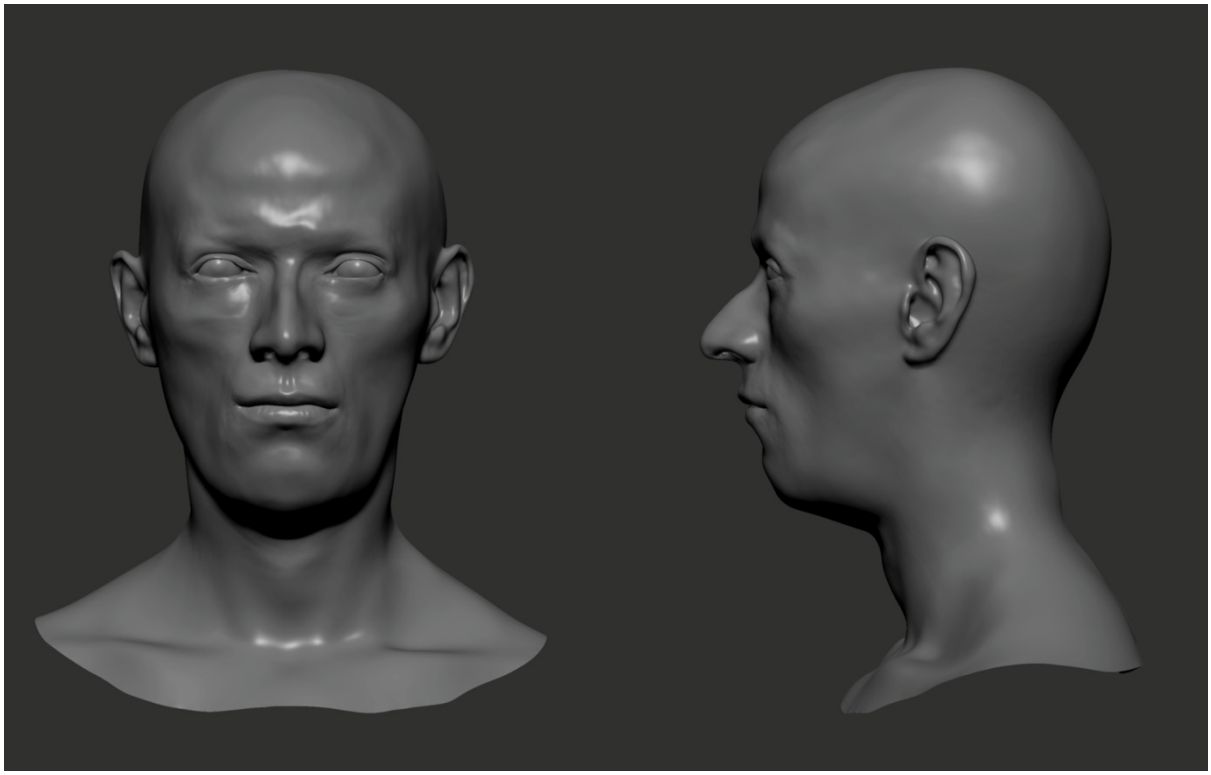

Figure 5.38 - Facial representation of AY53.

5.2.2.11 AY82 Female

This female individual occupied a double tomb and died between 35 and 40 years old (Table 5.40 and Figure 5.39). The right frontal process of the maxilla is damaged and was represented using the mirroring and interpolation tools within Geomagic®. Both zygomatic arches are missing, making the estimation of the width of the face tentative. The right mastoid is fragmented. The maxilla only preserves two premolar teeth on the left quadrant, and the remaining dentition was lost antemortem. The thickness of the upper lip cannot be estimated, and the *ecm2* soft tissue depths cannot be placed. The mandible is complete, and all molar teeth on the left quadrant were lost antemortem.

Table 5.40 - Summary of the methods used in the facial representation of AY82 Female.

Preservation state	Skull	The cranium is missing the frontal process of the maxilla on the right side and both zygomatic arches, and the right mastoid process is fragmented.
	Mandible	Good overall state.
Representation of missing components	Skull	Missing components mirrored using bilateral symmetry.
	Mandible	None.
Confidence level	13,50	2nd Level
Facial approximation	Soft tissue depths	Stephan (2017); Stephan and Simpson (2008a)
	Eye placement	Guyomarc'h et al. (2012); Stephan and Davidson (2008); Stephan et al. (2009)
	Eye canthi	Stephan and Davidson (2008)
	Nose profile	Rynn et al. (2010); Ullrich and Stephan (2011, 2016)
	Nasal tip	Cannot be predicted.
	Nose width	Guyomarc'h (2011)
	Mouth width	Song et al. (2007); Stephan and Henneberg (2003)
	Lip thickness	George (1987); Wilkinson et al. (2003)
	Ear placement	Ashley-Montagu (1939); Guyomarc'h and Stephan (2012)

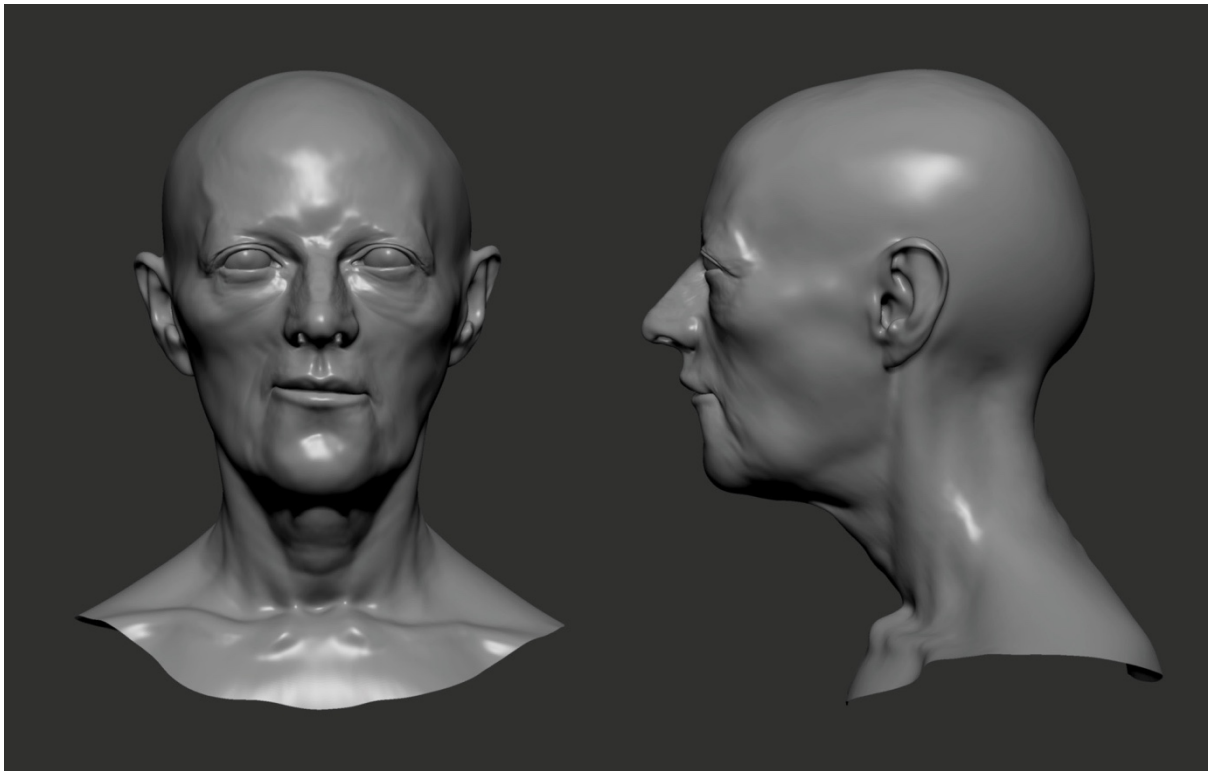

Figure 5.39 - Facial representation of AY82 Female.

5.2.2.12 AY87

AY87 is the final resting place of a female who was 30 to 40 years old when she died (Table 5.41 and Figure 5.40). Both cranium and mandible are complete. All teeth on the maxilla were lost premortem, along with the front incisors and all the mandibular molars. The bone resorption on the prosthion area hinders a more precise estimation of the nasal profile.

Table 5.41 - Summary of the methods used in the facial representation of AY87.

Preservation state	Skull	Excellent overall state.
	Mandible	Excellent overall state.

Representation of missing components	Skull	None.
	Mandible	Missing components mirrored using bilateral symmetry.
Confidence level	14,00	2nd Level
Facial approximation	Soft tissue depths	Stephan (2017); Stephan and Simpson (2008a)
	Eye placement	Guyomarc'h et al. (2012); Stephan and Davidson (2008); Stephan et al. (2009)
	Eye canthi	Stephan and Davidson (2008)
	Nose profile	Rynn et al. (2010); Ullrich and Stephan (2011, 2016)
	Nasal tip	Davy-Jow et al. (2012)
	Nose width	Guyomarc'h (2011)
	Mouth width	Song et al. (2007)
	Lip thickness	Cannot be predicted.
	Ear placement	Ashley-Montagu (1939); Guyomarc'h and Stephan (2012)

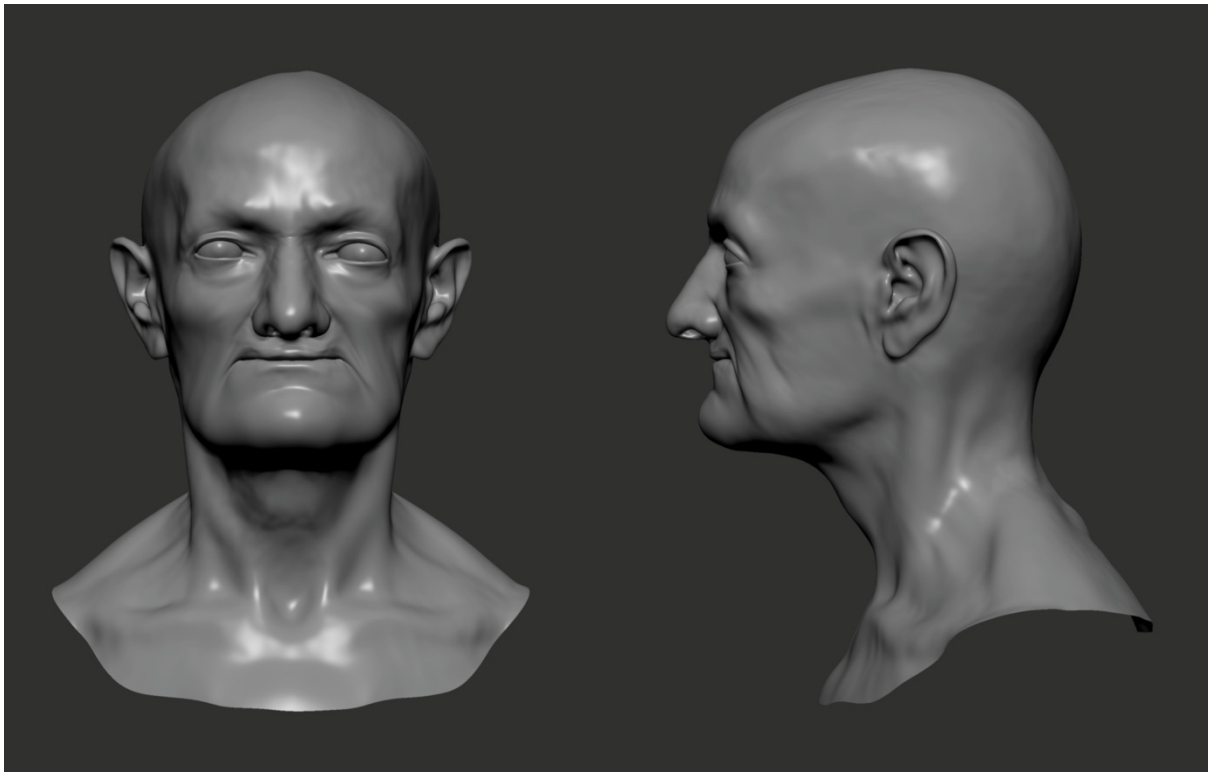

Figure 5.40 - Facial representation of AY87.

5.2.3 Third level facial approximations

5.2.3.1 AY3

AY3 is a double tomb that belonged to a female, aged between 25 and 30 years, and her unborn child. The state of preservation of these remains motivated a different approach to evaluate the precision of a virtual reassembly of fragments without a haptic device to emulate the tactile impression present in the manipulation of the original bones. For that purpose, after all the fragments were laser-scanned separately and placed in anatomical position in a virtual environment, an independent observer proceeded on doing a manual reconstruction of the cranium, which was also laser scanned. Both reconstructions were then superimposed (Figure 5.41) to visualize the differences between both approaches, showing that the virtual reassembly presents a deviation of approximately 2 mm in the facial area and the posterior part of the cranium. After registering the differences, the individual fragments were then aligned in Geomagic®, taking the manually reassembled cranium as a reference. Despite being an extra step, this protocol allows a more precise placement of the fragments in anatomical position by taking advantage of the tactile properties of a manual reassembly.

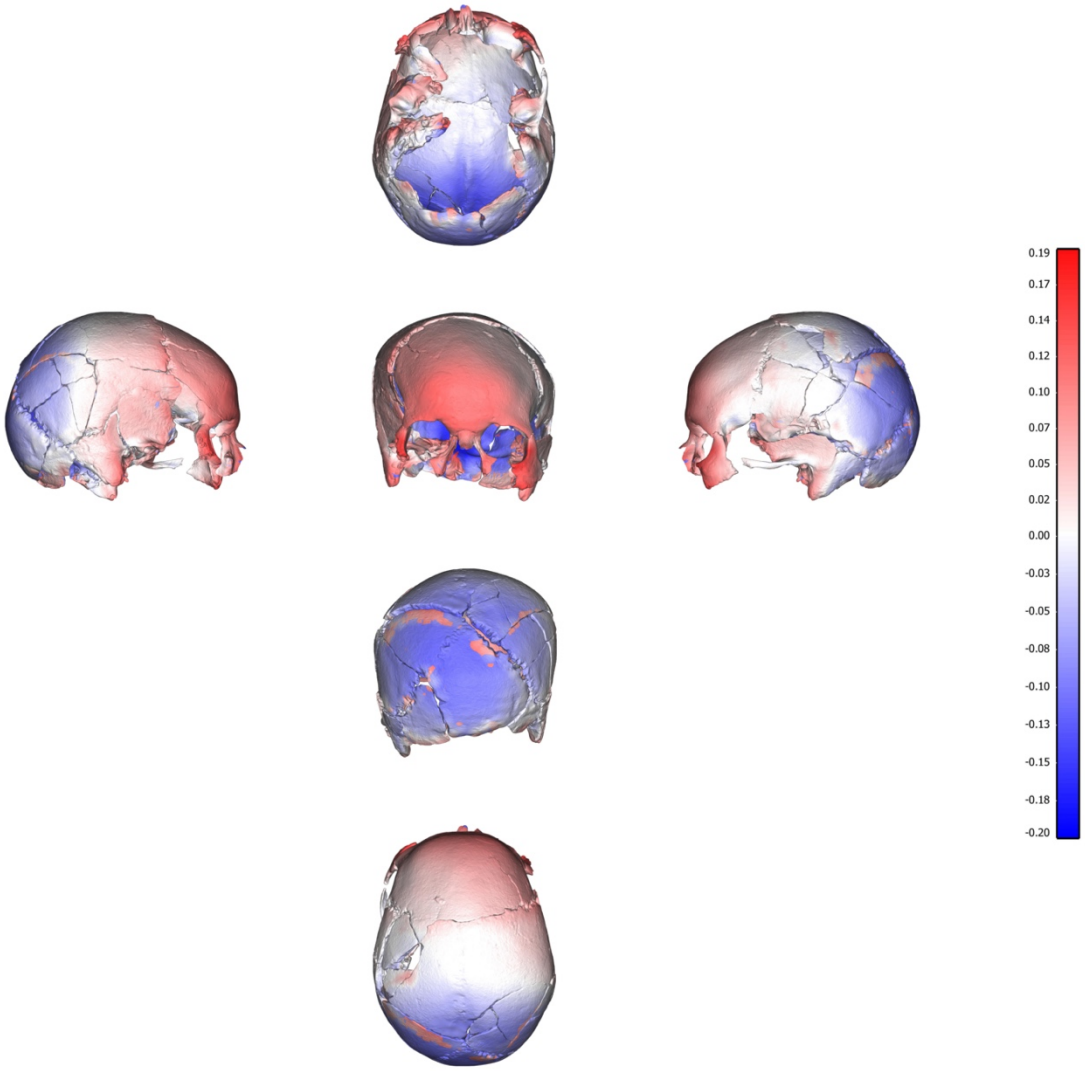

Figure 5.41 - Comparison between the virtual and the manual reconstruction of the cranium of AY3.

Considering the level of fragmentation and deformation present in this individual, applying of the methods for facial approximation can be problematic. Most measurements to estimate the features are taken from reassembled fragments of the cranium and should be considered tentative. Also, it is not possible to predict the thickness of the upper lip (Table 5.42 and Figure 5.42).

Table 5.42 - Summary of the methods used in the facial representation of AY3.

Preservation state	Skull	Very fragmented. There are missing portions on both orbits, on the right malar bone and the frontal part of the maxilla. The neurocranium shows plastic deformation towards the right side.
	Mandible	Very fragmented. Missing portions on the mental area and the right mandibular body.
Representation of missing components	Skull	Missing components mirrored using bilateral symmetry.
	Mandible	Missing components mirrored using bilateral symmetry.
Confidence level	12,25	3rd Level
Facial approximation	Soft tissue depths	Stephan (2017); Stephan and Simpson (2008a)
	Eye placement	Guyomarc'h et al. (2012); Stephan and Davidson (2008); Stephan et al. (2009)
	Eye canthi	Stephan and Davidson (2008)
	Nose profile	Rynn et al. (2010); Ullrich and Stephan (2011, 2016)
	Nasal tip	Davy-Jow et al. (2012)
	Nose width	Guyomarc'h (2011)
	Mouth width	Song et al. (2007); Stephan and Henneberg (2003)
	Lip thickness	Cannot be predicted.
	Ear placement	Ashley-Montagu (1939); Guyomarc'h and Stephan (2012)

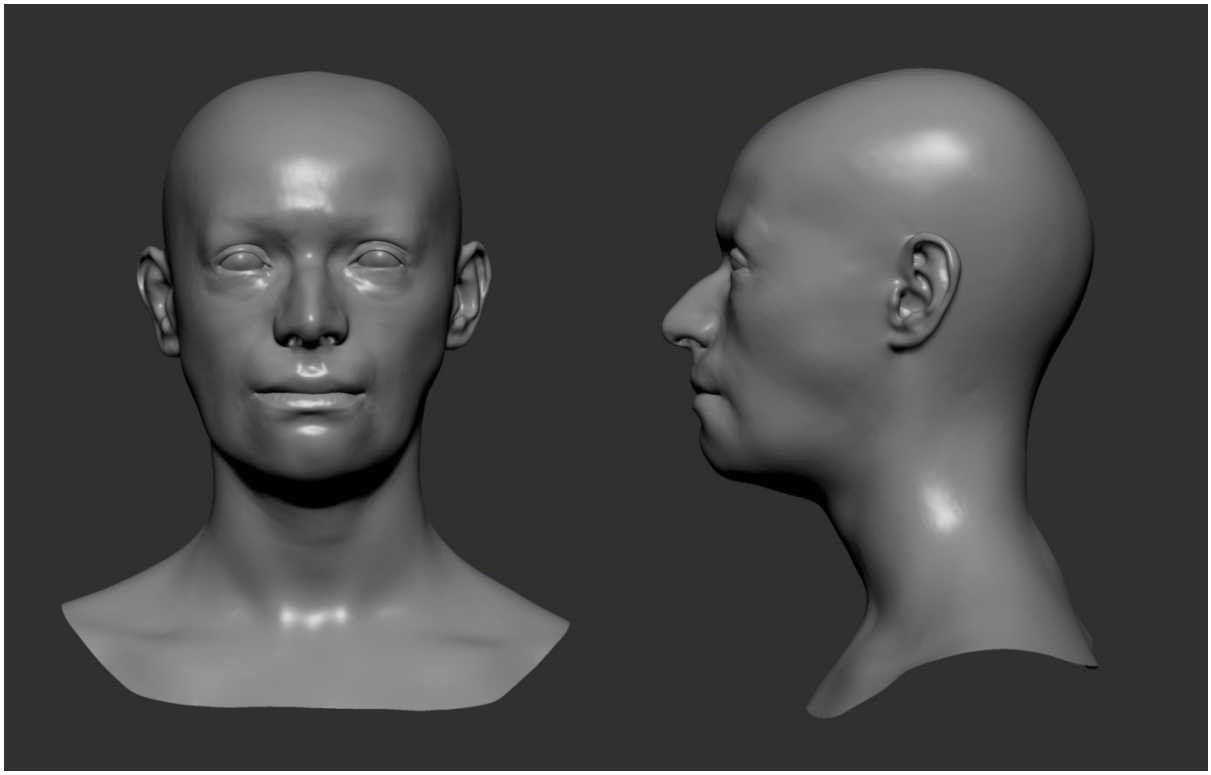

Figure 5.42 - Facial representation of AY3.

5.2.3.2 AY38 Female

This woman, who died when she was between 25 and 30 years old, was the second individual buried in Tomb AY38 (Table 5.43 and Figure 5.44). The skull is missing a large portion of the facial bones. The left parietal, frontal and nasal bones were not preserved, and the right malar and zygomatic are missing. The portion consisting of the inferior and lateral borders of the right orbit, right zygomatic and right temporal bone was mirrored from the left side and positioned on the skull by interpolation with the existent morphology (Figure 5.43). Due to the preservation state of the cranium, most of the upper portion of the face should be considered tentative.

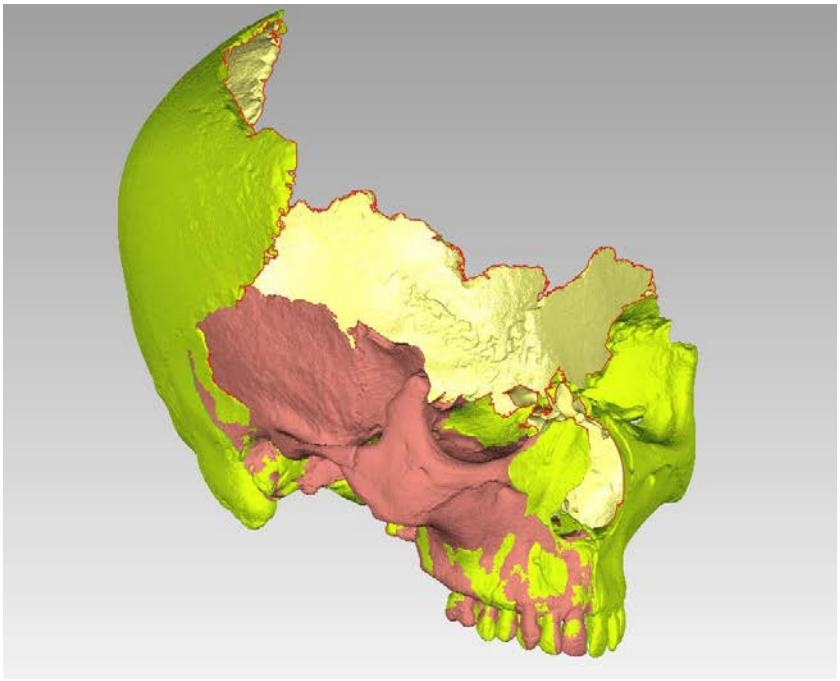

Figure 5.43 - Mirroring and aligning missing bones with the existing parts of the cranium of AY38.

Table 5.43 - Summary of the methods used in the facial representation of AY38 Female.

Preservation state	Skull	Missing a considerable portion of the cranium. Left parietal, frontal and nasal bones are missing, along with
	Mandible	Excellent overall state. Missing the frontal and lateral incisors on the right quadrant.
Representation of missing components	Skull	Missing components mirrored using bilateral symmetry. Tentative reconstruction of the frontal and nasal bones.
	Mandible	Missing components mirrored using bilateral symmetry.
Confidence level	11,50	3rd Level
Facial approximation	Soft tissue depths	Stephan (2017); Stephan and Simpson (2008a)
	Eye placement	Cannot be predicted.
	Eye canthi	Cannot be predicted.

Nose profile	Cannot be predicted.
Nasal tip	Cannot be predicted.
Nose width	Guyomarc'h (2011)
Mouth width	Song et al. (2007); Stephan and Henneberg (2003)
Lip thickness	George (1987); Wilkinson et al. (2003)
Ear placement	Ashley-Montagu (1939); Guyomarc'h and Stephan (2012)

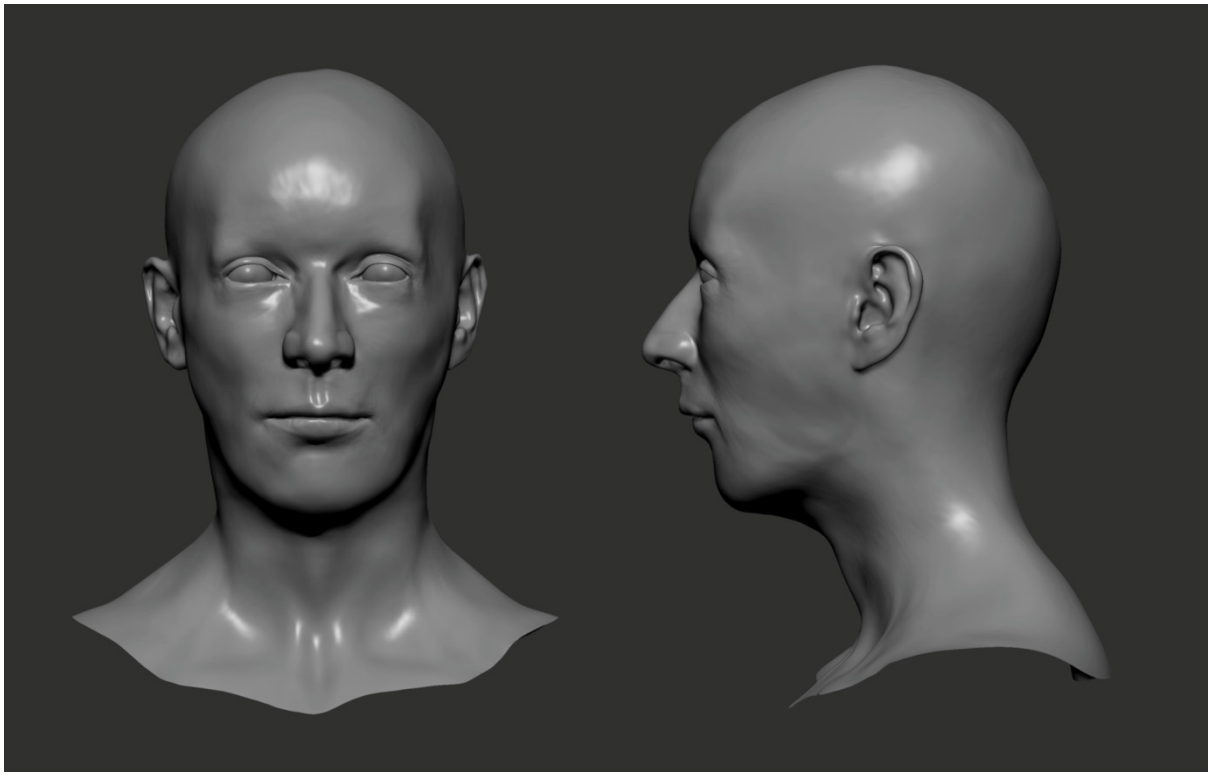

Figure 5.44 - Facial representation of AY38 Female.

5.2.3.3 AY60 Male

AY60 is a double tomb. Here, we applied the facial approximation protocol on the male, who was about 40 years old at the time of his death (Table 5.44 and Figure 5.45). Albeit fragmented, the cranium is mostly

complete. A large portion of the neurocranium shows plastic deformation and, to facilitate the facial approximation process, the distorted bone was manually manipulated using the existing morphology as a constraint. A future improvement to this process consists of using a reference sample to assess the deformation and "remove" it digitally. The upper lip thickness cannot be predicted, and the alveolar resorption in both sides of the maxilla hinders the placement of the *ecm*² soft tissue depths.

Table 5.44 - Summary of the methods used in the facial representation of AY60 Male.

Preservation state	Skull	The cranium is fragmented.
	Mandible	Excellent overall state.
Representation of missing components	Skull	The plastic deformation in the parietal bones was manually adjusted by using the remaining bones as a constraint.
	Mandible	None.
Confidence level	12,75	3rd Level
Facial approximation	Soft tissue depths	Stephan (2017); Stephan and Simpson (2008a)
	Eye placement	Guyomarc'h et al. (2012); Stephan and Davidson (2008); Stephan et al. (2009)
	Eye canthi	Stephan and Davidson (2008)
	Nose profile	Rynn et al. (2010); Ullrich and Stephan (2011, 2016)
	Nasal tip	Davy-Jow et al. (2012)
	Nose width	Guyomarc'h (2011)
	Mouth width	Song et al. (2007); Stephan and Henneberg (2003)
	Lip thickness	George (1987); Wilkinson et al. (2003)
	Ear placement	Ashley-Montagu (1939); Guyomarc'h and Stephan (2012)

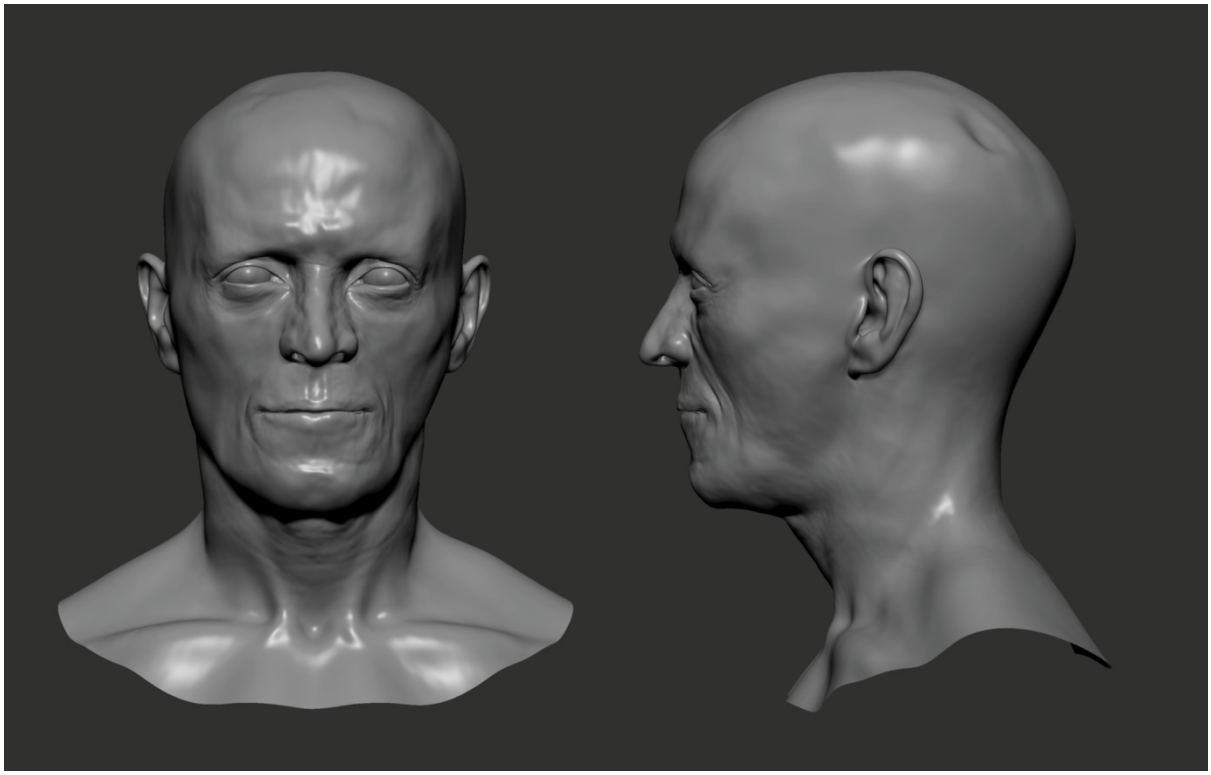

Figure 5.45 - Facial representation of AY60 Male.

5.2.3.4 AY94 Female

AY94 is a double tomb. The female died when she was between 35 and 40 years old (Table 5.45 and Figure 5.46). The cranium is complete, missing only the frontal teeth. The mandible is broken in half, and the left ramus is fragmented. The left gonion is missing and, since the mental portion of the mandible is fragmented, the general contour of the chin both in profile and front views should be considered tentative.

Table 5.45 - Summary of the methods used in the facial representation of AY94 Female.

Preservation state	Skull	Good overall state. The frontal teeth are missing.
	Mandible	The mandible is fragmented. Missing portions on the left ramus, the right gonion and menton.

Representation of missing components	Skull	Missing components mirrored using bilateral symmetry.
	Mandible	Missing components mirrored using bilateral symmetry. Tentative reconstruction of the mental area.
Confidence level	12,50	3rd Level
Facial approximation	Soft tissue depths	Stephan (2017); Stephan and Simpson (2008a)
	Eye placement	Guyomarc'h et al. (2012); Stephan and Davidson (2008); Stephan et al. (2009)
	Eye canthi	Stephan and Davidson (2008)
	Nose profile	Rynn et al. (2010); Ullrich and Stephan (2011, 2016)
	Nasal tip	Davy-Jow et al. (2012)
	Nose width	Guyomarc'h (2011)
	Mouth width	Song et al. (2007)
	Lip thickness	Cannot be predicted.
	Ear placement	Ashley-Montagu (1939); Guyomarc'h and Stephan (2012)

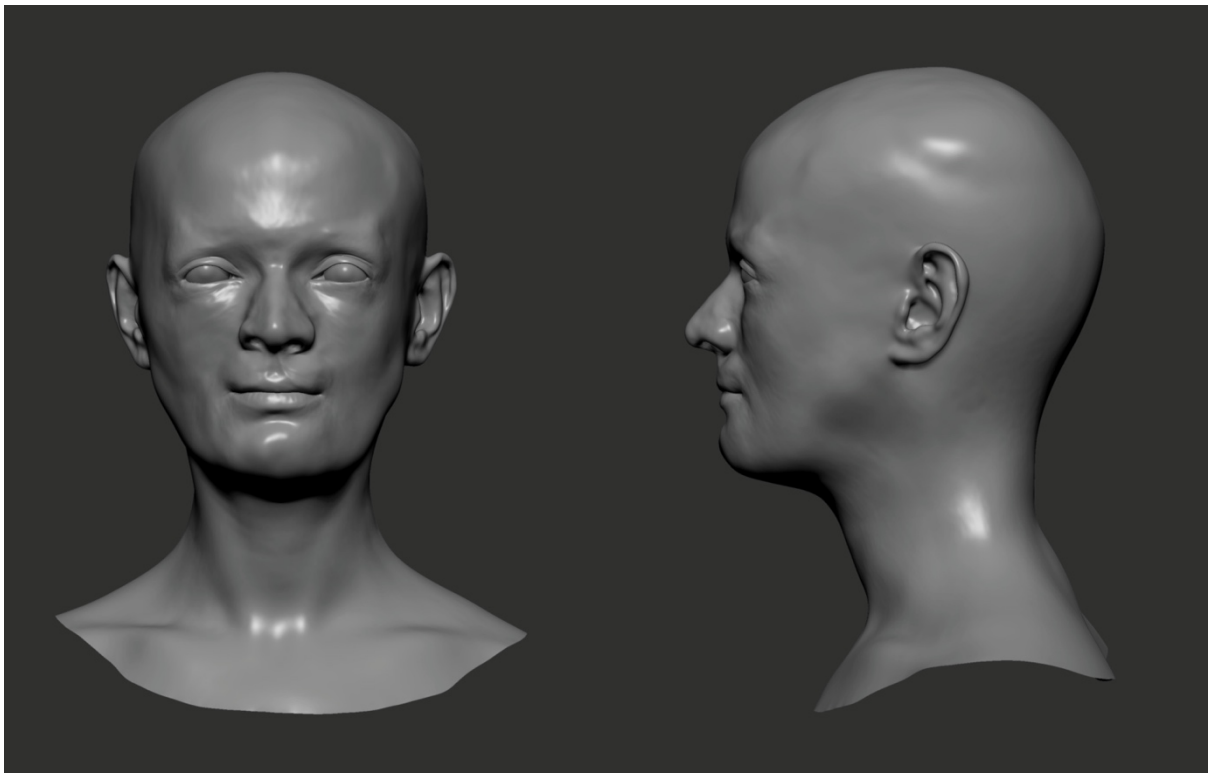

Figure 5.46 - Facial representation of AY94 Female.

5.3 Being young at La Almoloya

5.3.1 AY30

The tomb AY30 of La Almoloya held the remains of two children. Here, we represent the face of the oldest of them, who was between 8 and 9 years of age at the time of death (Table 5.46 and Figure 5.48). The cranium is fragmented and was reassembled manually before being laser-scanned. The fragments that could not be anatomically oriented with the cranium were laser-scanned separately and placed in position with Geomagic®. The process is explained in Figure 5.47.

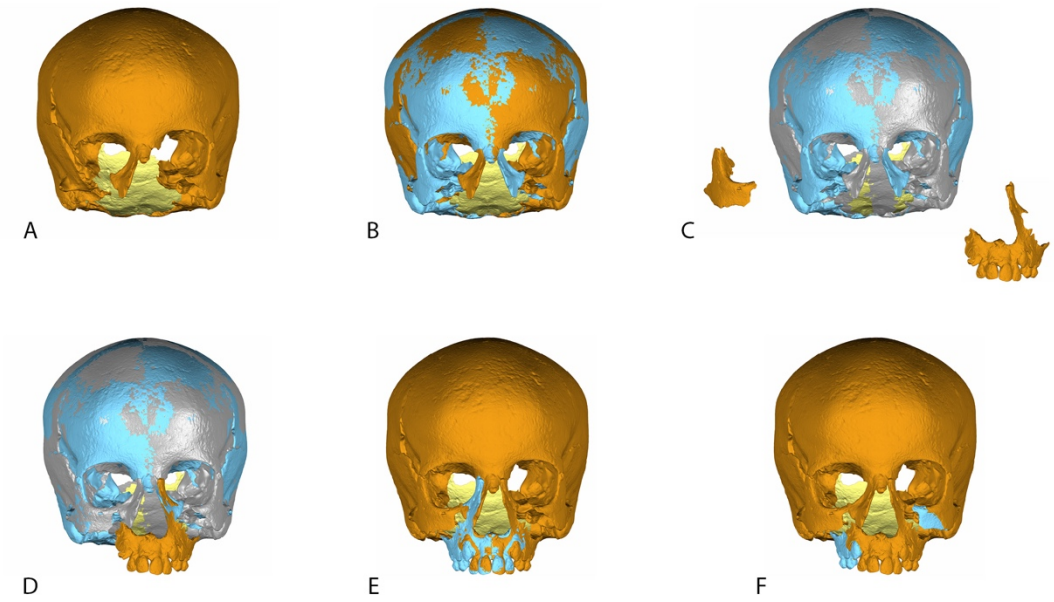

Figure 5.47 - Process of the virtual reassembly of the individual of tomb 30. A = Laser scan of the cranium; B = Mirrored cranium (in blue) superimposing the original; C = Fragments scanned separately (in orange); D = Alignment of the fragments with the cranium; E = Mirrored maxilla superimposing the original; F = Final result of the reassembly process, showing the original cranium (in orange) and the mirrored parts (in blue).

Table 5.46 - Summary of the methods used in the facial representation of AY30.

Preservation state	Skull	Fragmented. Both malar bones are incomplete, and the right portion of the maxilla is absent.
	Mandible	Fragmented but mostly complete. The front incisors are missing.
Representation of missing components	Skull	Missing components mirrored using bilateral symmetry.
	Mandible	Missing components mirrored using bilateral symmetry.
Confidence level	13,00	2nd Level
Facial approximation	Soft tissue depths	Stephan (2017); Stephan and Simpson (2008a)
	Eye placement	Guyomarc'h et al. (2012); Stephan and Davidson (2008); Stephan et al. (2009)
	Eye canthi	Stephan and Davidson (2008)
	Nose profile	Rynn et al. (2010); Ullrich and Stephan (2011, 2016)
	Nasal tip	Davy-Jow et al. (2012)
	Nose width	Guyomarc'h (2011)
	Mouth width	Song et al. (2007); Stephan and Henneberg (2003)
	Lip thickness	George (1987); Wilkinson et al. (2003)
	Ear placement	Ashley-Montagu (1939); Guyomarc'h and Stephan (2012)

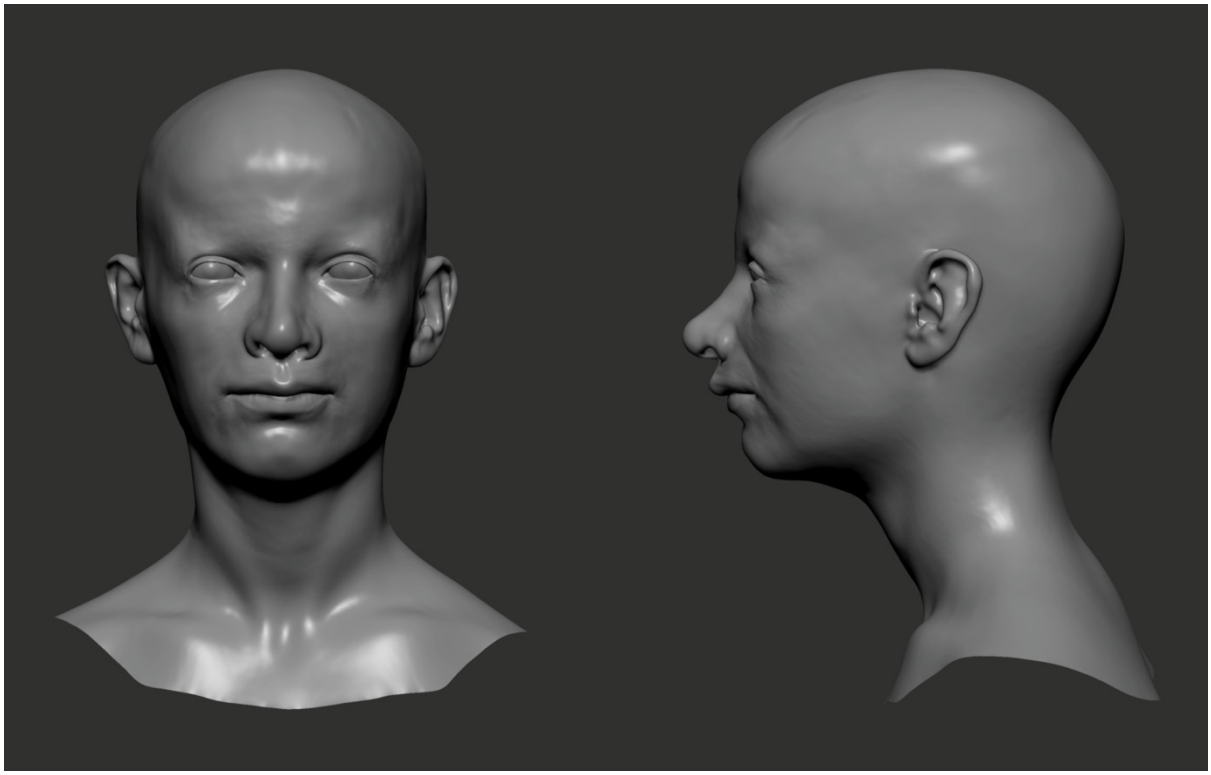

Figure 5.48 - Facial representation of AY30.

5.3.2 AY46

AY46 is the burial of an infant deceased at the age of 6 or 7 (Table 5.47 and Figure 5.49). Both cranium and mandible are complete and in excellent state. The cranium presents a wide nasal bridge, and the estimation of the placement of the eyes indicates that the interpupillary distance (p–p), as measured from the predicted position of the eyeballs, is approximately 69 mm. The intercanthal width (en–en) is approximately 40 mm, and the biocular width (ex–ex) is 86.5 mm, as measured from the estimated canthi of the eyes. All these measurements are considerably above the anthropometric values provided by the literature (Farkas et al., 1989) and are consistent with moderate hyperteloric orbits. The aDNA results may provide some insight on possible syndromes that usually associate with hypertelorism. Should that be the case, this facial approximation will likely undergo a revision in the future.

Table 5.47 - Summary of the methods used in the facial representation of AY46.

Preservation state	Skull	Excellent state.
	Mandible	Excellent state.
Representation of missing components	Skull	None.
	Mandible	None.
Confidence level	16,00	1st Level
Facial approximation	Soft tissue depths	Stephan (2017); Stephan and Simpson (2008a)
	Eye placement	Guyomarc'h et al. (2012); Stephan and Davidson (2008); Stephan et al. (2009)
	Eye canthi	Stephan and Davidson (2008)
	Nose profile	Rynn et al. (2010); Ullrich and Stephan (2011, 2016)
	Nasal tip	Davy-Jow et al. (2012)
	Nose width	Guyomarc'h (2011)
	Mouth width	Song et al. (2007); Stephan and Henneberg (2003)
	Lip thickness	George (1987); Wilkinson et al. (2003)
	Ear placement	Ashley-Montagu (1939); Guyomarc'h and Stephan (2012)

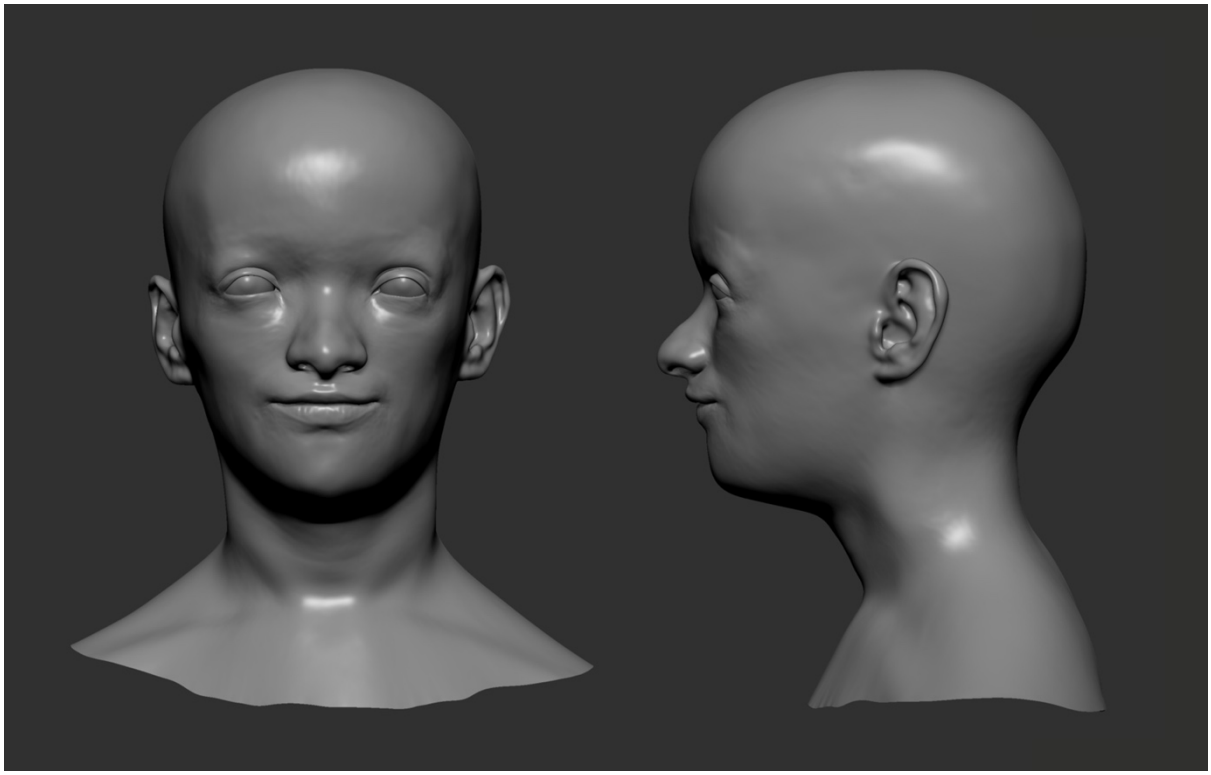

Figure 5.49 - Facial representation of AY46.

5.4 Four faces from La Bastida

5.4.1 BA31 Female

The skull from Tomb BA31 belongs to a female aged between 40 and 50 years old (Table 5.48 and Figure 5.50). The right zygomatic is fragmented, and the lateral wall of the right orbit is detached from the remaining skull. The fragmented portion was realigned in Geomagic® using bilateral symmetry and interpolation with the existing geometry to ensure the most approximate placement. The height of the lips should be considered tentative in this representation.

Table 5.48 - Summary of the methods used in the facial representation of BA31.

Preservation state	Skull	Good overall state. The right zygomatic bone is fragmented. All incisors, canines and first premolars are missing.
	Mandible	Good overall state. Both coronoid processes are broken. All incisors and canines are missing.
Representation of missing components	Skull	Lateral wall of the right orbit positioned virtually through bilateral symmetry. Missing components mirrored using bilateral symmetry when available.
	Mandible	None.
Confidence level	13,00	2nd Level
Facial approximation	Soft tissue depths	Stephan (2017); Stephan and Simpson (2008a)
	Eye placement	Guyomarc'h et al. (2012); Stephan and Davidson (2008); Stephan et al. (2009)
	Eye canthi	Stephan and Davidson (2008)
	Nose profile	Rynn et al. (2010); Ullrich and Stephan (2011, 2016)
	Nasal tip	Davy-Jow et al. (2012)
	Nose width	Guyomarc'h (2011)
	Mouth width	Song et al. (2007)
	Lip thickness	Cannot be predicted due to missing morphology.
	Ear placement	Ashley-Montagu (1939); Guyomarc'h and Stephan (2012)

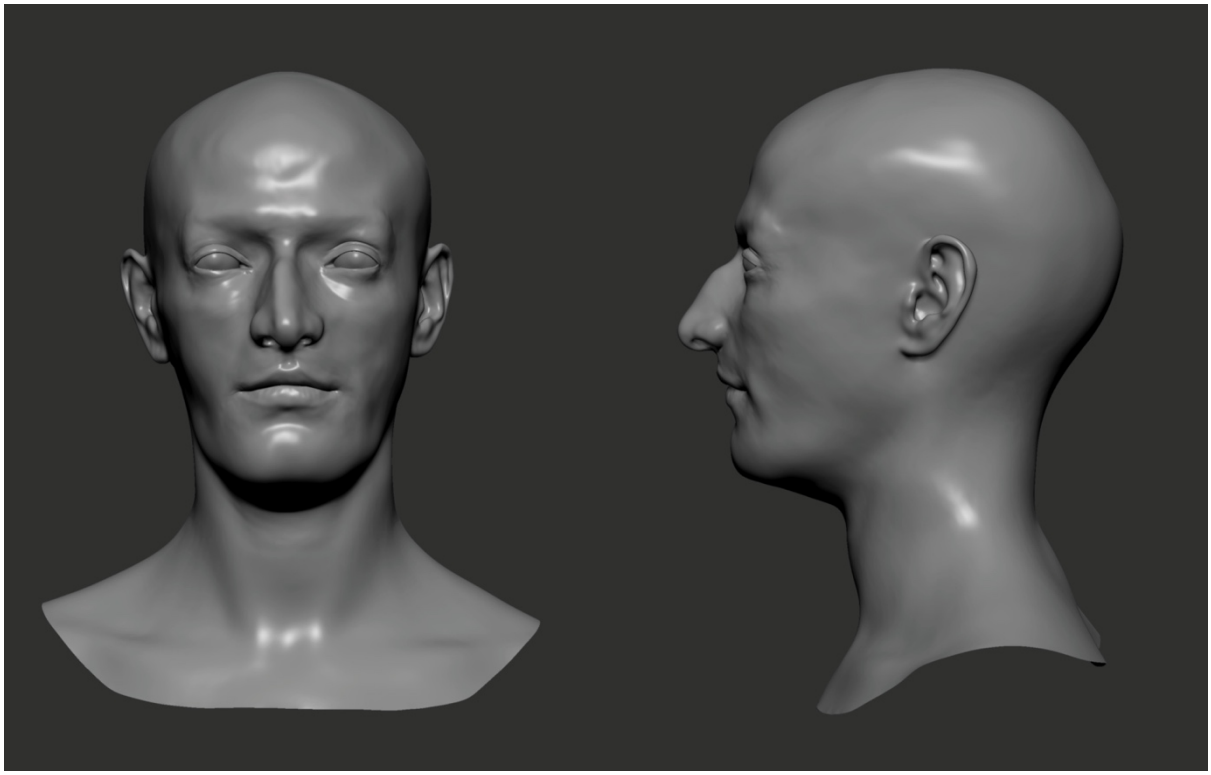

Figure 5.50 - Facial representation of BA31.

5.4.2 BA33

BA33 is a male that died between 45 and 50 years old. The original cranium is fragmented and was temporarily reconstructed to be laser-scanned, but its fragile and brittle condition makes it difficult to stabilize the bones in an anatomical position. For that reason, each fragment was laser-scanned separately and repositioned later in a virtual environment. Then, a rough laser scan of the whole skull with the bones in anatomical position was used as a "map" to aid in the virtual alignment of the fragments, allowing us to set up anatomical constraints that limit the possible angles of variation between fragments (Figure 5.51). As both zygomatic arches are absent, their representation follows the adjacent anatomy, and, as a result, the maximum width of the face should be considered tentative. There is also significant damage to both temporal bones, the left parietal bone, and the occipital suture. BA33 lost all molar teeth on the left quadrant of the maxilla premortem, a circumstance made evident by the alveolar resorption present. As mentioned

before, alveolar resorption hinders the placement of the *ecm²* soft tissue depth in the alveolar ridge. All incisors and both canines are missing and, on the right quadrant of the maxilla, only the first premolar is preserved, thus leaving very few anatomical constraints to position the mandible according to the occlusion of the teeth. The mandible is better preserved than the skull but still has some degree of fragmentation. The coronary process and gonial angle on the left side are fragmented, and both molars are missing on the right quadrant.

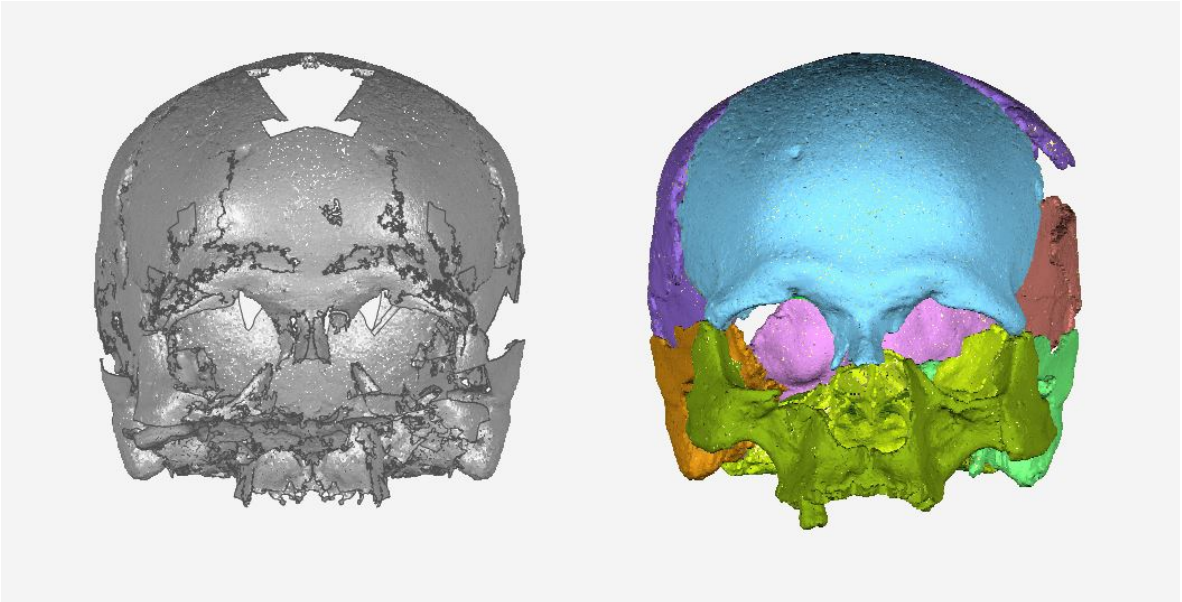

Figure 5.51 - On the left, rough laser scan of BA33.

On the right, all fragments scanned separately and aligned to the rough matrix.

The level of fragmentation present in this individual makes it somewhat problematic to apply facial approximation methods. Some measurements to estimate the features, namely the ones used to position the eyeballs and to predict nose's width, are taken from mirrored parts of the cranium and should be considered tentative. Also, the upper lip thickness cannot be predicted (Table 5.49 and Figure 5.52).

Table 5.49 - Summary of the methods used in the facial representation of BA33.

Preservation state	Skull	Very fragile and brittle. There is relevant damage on both temporal bones, on the left parietal and along the occipital suture. Both zygomatic arches are missing. All incisors and both canines are missing, along with the molar teeth on the right quadrant.
	Mandible	Good overall state. Both left coronoid and gonial angle are fragmented and the molar teeth on the right quadrant are missing.
Representation of missing components	Skull	Virtual alignment of the fragments executed using a rough laser scan of the whole cranium. Zygomatic arches represented according to the adjacent anatomy. Missing components mirrored using bilateral symmetry.
	Mandible	Missing components mirrored using bilateral symmetry.
Confidence level	13,00	2nd Level
Facial approximation	Soft tissue depths	Stephan (2017); Stephan and Simpson (2008a)
	Eye placement	Guyomarc'h et al. (2012); Stephan and Davidson (2008); Stephan et al. (2009)
	Eye canthi	Stephan and Davidson (2008)
	Nose profile	Rynn et al. (2010); Ullrich and Stephan (2011, 2016)
	Nasal tip	Cannot be predicted.
	Nose width	Guyomarc'h (2011)
	Mouth width	Song et al. (2007)
	Lip thickness	Cannot be predicted.
	Ear placement	Ashley-Montagu (1939); Guyomarc'h and Stephan (2012)

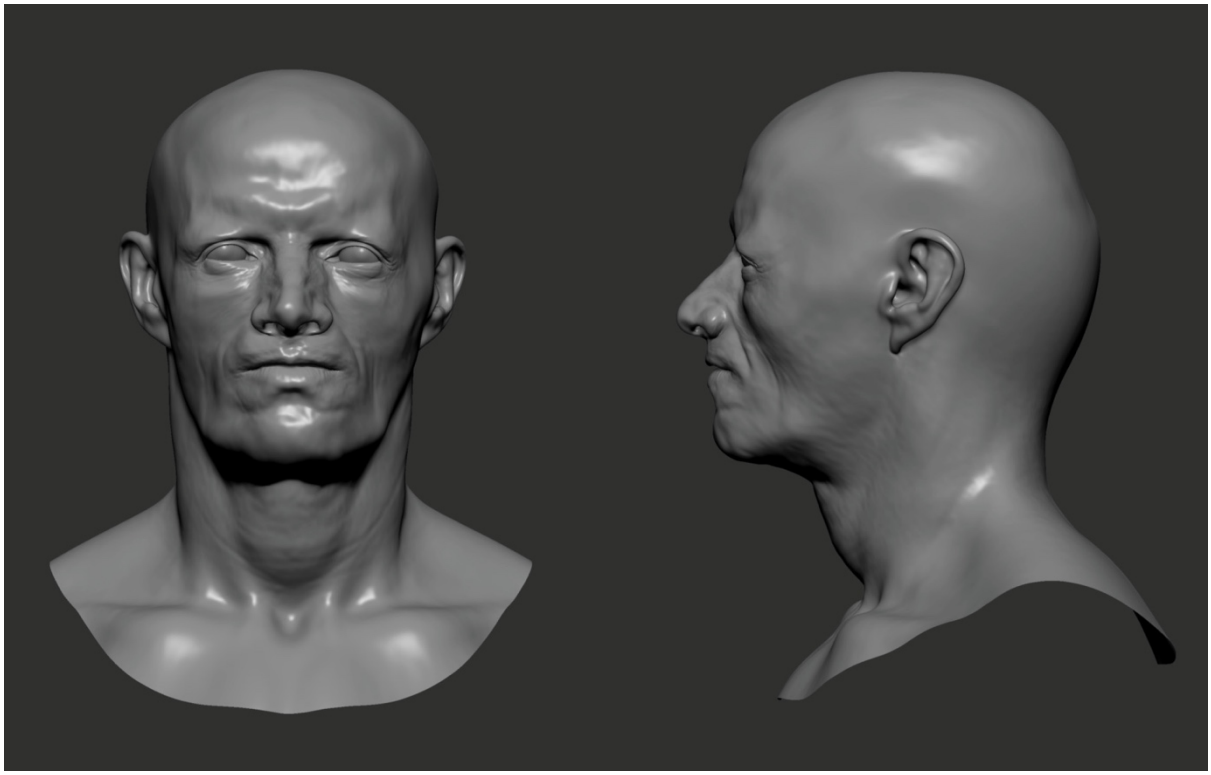

Figure 5.52 - Facial representation of BA33.

1.1.1. BA63

The skull of BA63 belongs to a female aged between 40 and 49 years old (Table 5.50 and Figure 5.53). The cranium is well preserved, but both the nasal bones and the right zygomatic arc are fragmented. All maxillary teeth are missing, except for the first premolar and the first and third molars on the left quadrant. The mandible is missing the right condyle and all teeth, except for three molars. The nasal bones are represented through a manual reconstruction that relies on the adjacent anatomy and, for that reason, the nasal profile should be considered tentative. Since most teeth are missing, the lip thickness cannot be predicted using the recommended methods.

Table 5.50 - Summary of the methods used in the facial representation of BA63.

Preservation state	Skull	Fairly well-preserved, but the nasal bones, the right zygomatic and most teeth are missing.
	Mandible	Good general state, but the right condyle and most teeth are missing.
Representation of missing components	Skull	Manual reconstruction of the nasal bones based on the adjacent anatomy. Missing components mirrored using bilateral symmetry when available.
	Mandible	Missing components mirrored using bilateral symmetry.
Confidence level	13,25	2nd Level
Facial approximation	Soft tissue depths	Stephan (2017); Stephan and Simpson (2008a)
	Eye placement	Guyomarc'h et al. (2012); Stephan and Davidson (2008); Stephan et al. (2009)
	Eye canthi	Stephan and Davidson (2008)
	Nose profile	Rynn et al. (2010); Ullrich and Stephan (2011, 2016)
	Nasal tip	Cannot be predicted.
	Nose width	Guyomarc'h (2011)
	Mouth width	Song et al. (2007)
	Lip thickness	Cannot be predicted due to missing morphology.
	Ear placement	Ashley-Montagu (1939); Guyomarc'h and Stephan (2012)

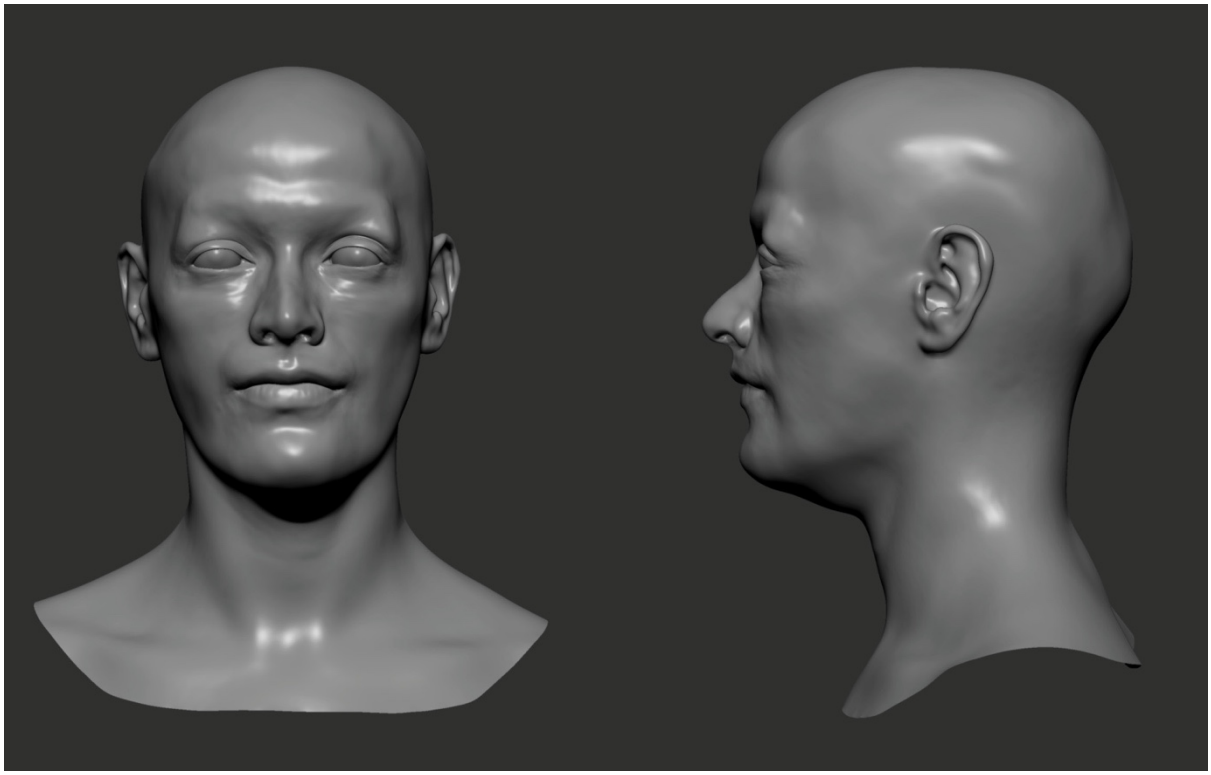

Figure 5.53 - Facial representation of BA63.

5.4.3 BAM-6

BAM-6 contained a female aged between 20 and 35 (Table 5.51 and Figure 5.54). The skull is missing significant portions on the left temporal, parietal and occipital bones, and the left zygomatic arch is fragmented. The pronasale position was estimated from a reconstructed ANS, and the missing frontal incisors hinder the estimation of the lip thickness. The mandible is fragmented along the mental area and was reassembled in a virtual environment. The frontal incisors and all teeth on the right quadrant are missing.

Table 5.51 - Summary of the methods used in the facial representation of BAM-6.

Preservation state	Skull	Missing portions on the left temporal, parietal and occipital bone. Left zygomatic arch is fragmented.
	Mandible	Good general state.
Representation of missing components	Skull	Manual reconstruction of the nasal bones based on the adjacent anatomy. Missing components mirrored using bilateral symmetry.
	Mandible	Missing components mirrored using bilateral symmetry.
Confidence level	13,75	2nd Level
Facial approximation	Soft tissue depths	Stephan (2017); Stephan and Simpson (2008a)
	Eye placement	Guyomarc'h et al. (2012); Stephan and Davidson (2008); Stephan et al. (2009)
	Eye canthi	Stephan and Davidson (2008)
	Nose profile	Rynn et al. (2010); Ullrich and Stephan (2011, 2016)
	Nasal tip	Davy-Jow et al. (2012)
	Nose width	Guyomarc'h (2011)
	Mouth width	Song et al. (2007)
	Lip thickness	Cannot be predicted due to missing morphology.
	Ear placement	Ashley-Montagu (1939); Guyomarc'h and Stephan (2012)

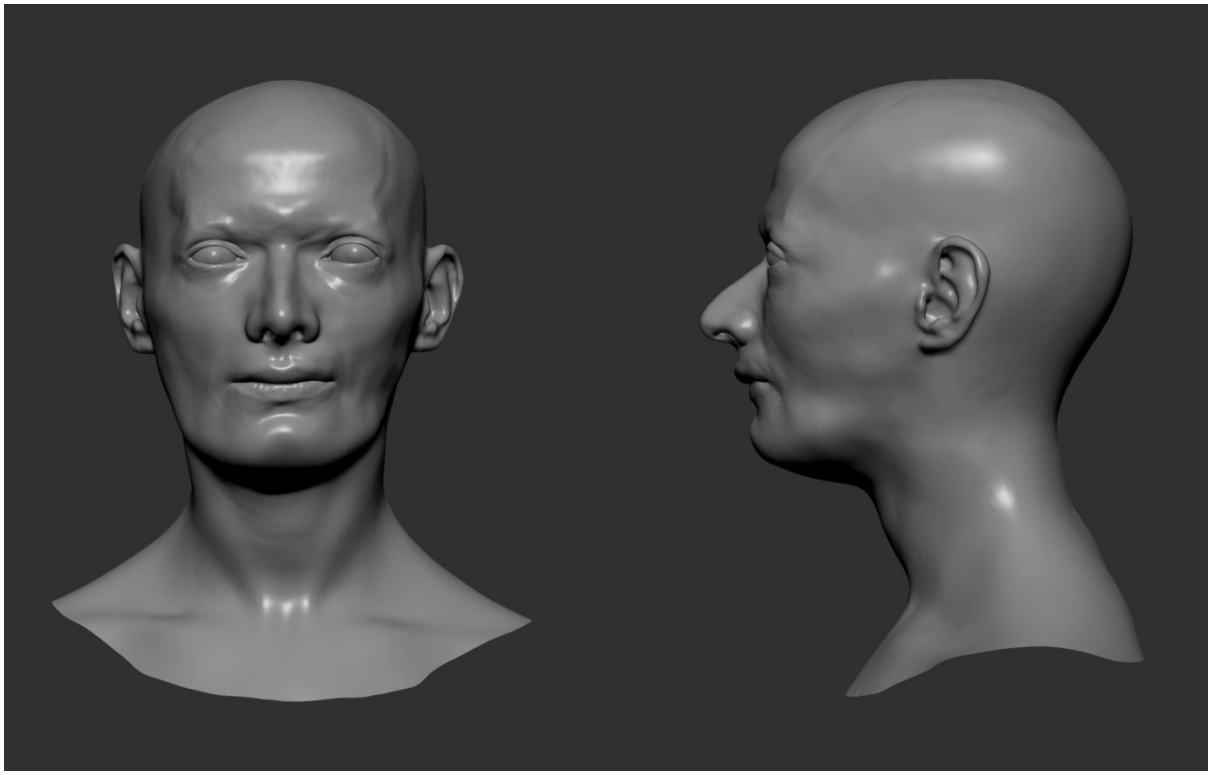

Figure 5.54 - Facial representation of BAM-6.

6 Assessing facial morphology

~

The heritability of human facial shape has been a major focus of interest over the past decades. Some of the earlier anthropometric research on parent-offspring resemblance and twin similarity has confirmed that the variation in the morphology of the human face is under strong genetic control (Devor, 1987; Hauspie et al., 1985; Hunter et al., 1970; Kohn, 1991; Lobb, 1987; Lundström & McWilliam, 1988; Nakata et al., 1974; Susanne, 1977; Vandenberg & Strandskov, 1964). In more recent years, a combination of genome-wide association studies (GWAS), heritability analyses, and high-resolution three-dimensional images of the face have consistently mapped the spatial relationship between the face and specific genes. This research sets the background for our hypothesis: that geometric morphometrics may be used as a parallel tool to establish possible genetic relationships between subjects by analyzing the morphology of specific traits and the whole configuration of the face. This chapter lays out the methods and discusses the results of the statistical analyses performed on the Argaric faces.

6.1 Materials and methods

The three-dimensional models of the facial approximations were decimated within Zbrush® (Pixologic, LA, USA) using the Decimation Master plugin to decrease file size and optimize the collection of landmarks. The digital models were then exported in PLY file format and relabeled as a part of the protocol

for running the morphometric analyses. All digital files were grouped in a single sample, and a series of landmark coordinates were collected for further analysis.

Landmarks, traditionally classified as Type I, II and III by Bookstein (Bookstein, 1991; Rohlf & Bookstein, 1988), are defined as discrete anatomical loci identified in all individuals across the sample.[30] Figure 6.1 and Table 6.1 provide a list of the landmarks used for the analyses.

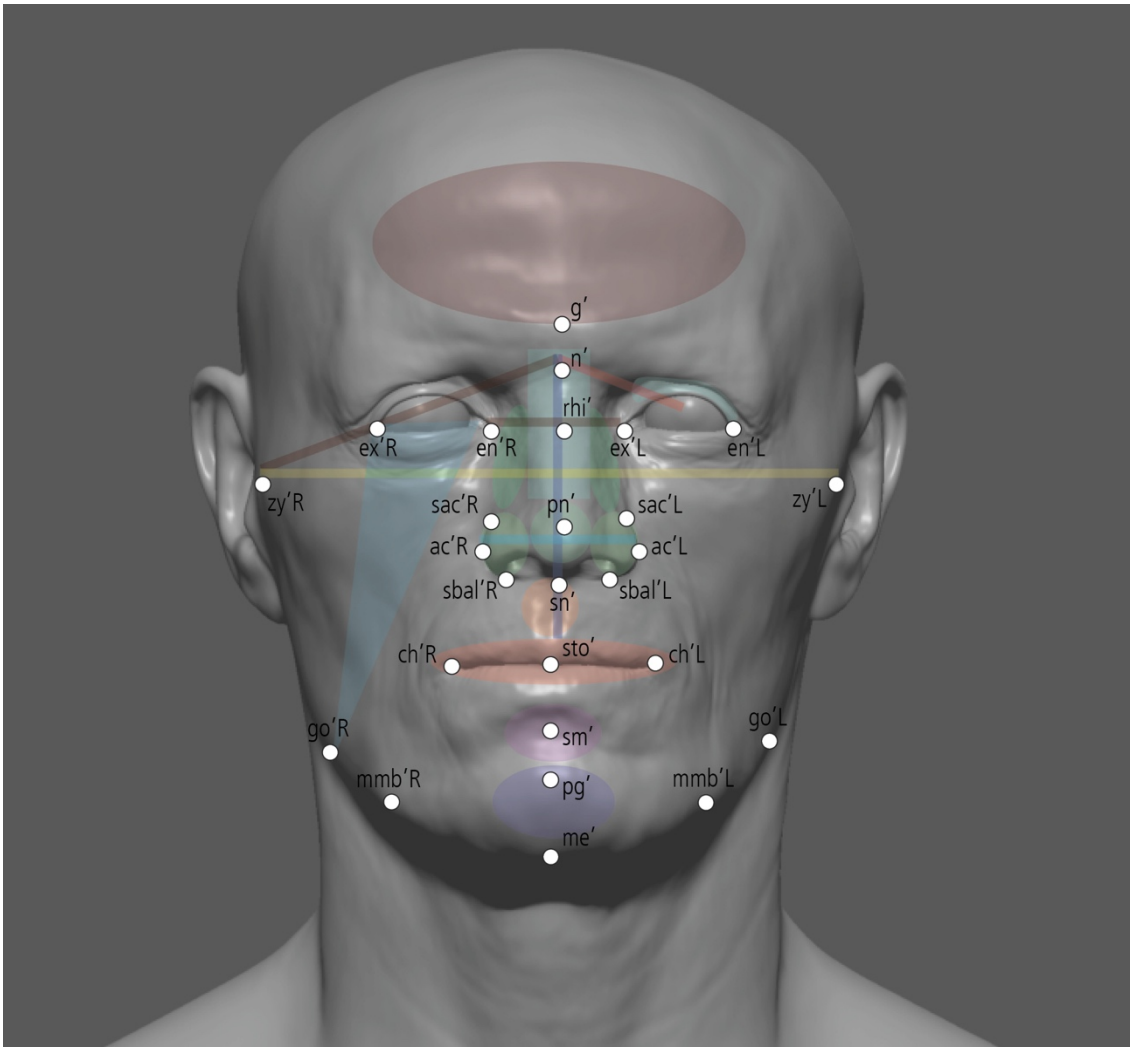

Figure 6.1 - Facial landmarks annotated on the face of the individual from AY5. The color-coded areas correspond with facial *loci* under genetic influence. Refer to Figure 6.2 for more details.

[30] The classification of landmarks into three different types relies on their potential to represent anatomical correspondence (Bookstein, 1991). Type I landmarks are located at the intersection of multiple sutures or tissues (e.g., bony nasion). Type II landmarks are placed on the maxima or minima of structures (e.g., the tip of the mastoid). Type III landmarks are located depending on the position of other landmarks, such as the farthest point from another point.

Table 6.1 - Facial landmarks used in this study.

#	Abr.	Landmark	Description	Side
1	g'	Glabella	Most anterior midline point on the forehead, in the region of the superciliary ridges.	Midline
2	n'	Nasion	Point directly anterior to the nasofrontal suture, in the midline, overlying *n*.	Midline
3	rhi'	Rhinion	Point overlying *rhi*, at the end of the internasal suture where the bone ends, and the cartilage begins.	Midline
4	pn'	Pronasale	The most anteriorly protruded point of the apex nasi. In the case of a bifid nose, the more protruding tip is chosen.	Midline
5	sn'	Subnasale	Median point at the junction between the lower border of the nasal septum and the philtrum area.	Midline
6	sto'	Stomion	Point of the labial fissure when the lips are closed naturally, with the teeth shut in the natural position.	Midline
7	sm'	Supramentale	Deepest point of the mentolabial sulcus.	Midline
8	pg'	Pogonion	Most anterior midpoint of the chin, located on the skin surface anterior to the identical bony landmark of the mandible.	Midline
9	me'	Menton	Most inferior median point of the chin.	Midline
10	en'L	Endocanthion	Most medial point of the palpebral fissure, at the inner commissure of the eye.	Left
11	en'R			Right
12	ex'L	Exocanthion	Most lateral point of the palpebral fissure, at the outer commissure of the eye.	Left
13	ex'R			Right
14	sac'L	Superior Alare Curvature	The most superior point on the alar curvature.	Left
15	sac'R			Right
16	ac'L	Alare	The most lateral point on the alar curvature.	Left
17	ac'R			Right
18	sbal'L	Subalare	The most inferior point on the alar curvature.	Left
19	sbal'R			Right
20	ch'L	Cheilion	Outer corners of the mouth where the outer edges of the upper and lower vermilions meet.	Left
21	ch'R			Right
22	mmb'L	Mid-mandibular border	Point directly overlying *mmb*.	Left
23	mmb'R			Right
24	go'L	Gonion	Most lateral point on the mandibular angle, adjacent to *go*, identified by palpation.	Left
25	go'R			Right

26	zyL	Zygion	Most lateral point overlying each zygomatic arch, identified as the point of maximum bizygomatic breadth of the face.	Left
27	zyR			Right

Landmark Editor (Wiley et al., 2005) was the main application used to manually place landmarks across the sample used in this project. It is important to mention beforehand that manual landmarking protocols have been criticized for being more error-prone and highly dependent not only on the type and image resolution of the data in the sample, but also on the level of expertise of the user collecting the landmarks (Tsagkrasoulis et al., 2017). To tackle these issues, a number of authors have proposed and advocated the use of semi-automated and automated algorithms to create a dense landmark set that captures morphological variation at a much finer level of granularity and removes human measurement errors.[31] In fact, a number of recent studies have addressed the sources of error in landmark collection. Shearer et al. (2017) , Daboul et al. (2018) and Robinson and Terhune (2017) have all concluded that while intra-observer error can be minimized with proper training and accumulated experience, the inter-observer error is usually much higher and much more concerning as it may be mistaken for real biological differences where none actually exist.

While an automated dense landmarking protocol might be a more suitable option to identify genetic craniofacial loci from face scans of "real" individuals (see, for instance, Claes et al., 2018; Huang et al., 2020), or address heritability patterns within a group that is known to share a genetic bond (like the study of Tsagkrasoulis et al., 2017), our sample comprises faces represented from the skull. This means that our study has different limitations and implications (see the previous discussion in Chapter 2 and section 6.3 in this chapter). First, it means that our aim is not to isolate and identify those specific aspects of face-shape variability between individuals that might be under genetic control, but rather assess if it is possible

[31] For reports on dense landmarking protocols see, for instance, the works of Cates et al. (2007); Claes et al. (2012); and Tsagkrasoulis et al. (2017) and refer to the original articles for detailed information on the annotation methods used in each protocol.

to infer genetic relatedness by comparing landmark configurations derived from facial approximations of anonymous subjects. For that reason, instead of distributing an array of landmarks across the totality of facial topography, the landmarks used in this study are selected and placed upon those areas of the face that have been reported as being under a strong genetic control (both by GWAS and heritability studies). Many of these areas overlap with specific points that can be predicted from a particular skull using facial approximation methods (Figure 6.2 and Table 6.2, and refer back to Figure 6.1).

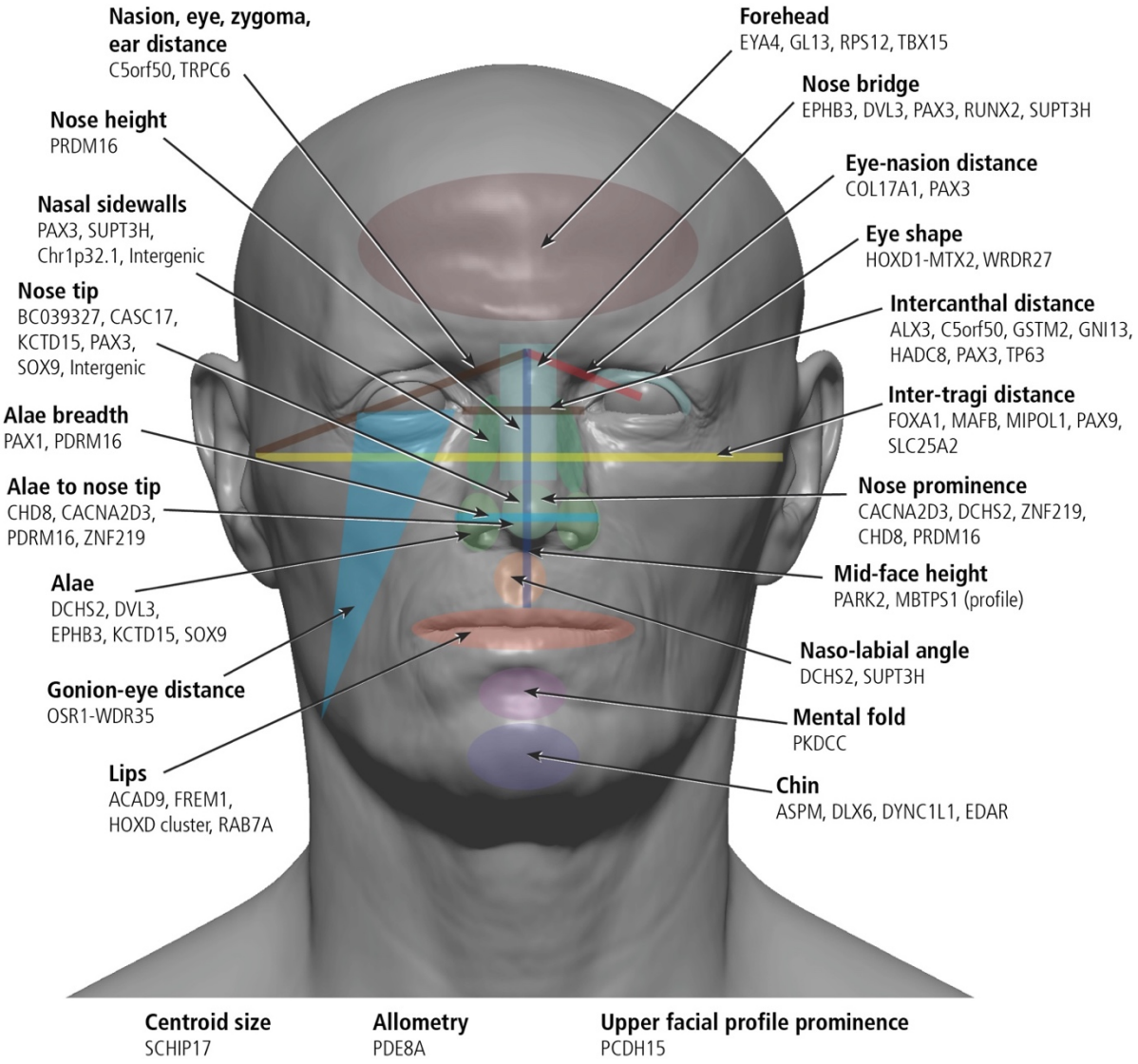

Figure 6.2 – Facial *loci* under genetic influence in normal populations.

Base reference is the face of the individual from Tomb AY5. After Richmond et al. (2018).

Table 6.2 - List of genes associated with facial loci that can be predicted using facial approximation methods.

Adapted from Richmond et al. (2018). Detailed information can be found in the original articles.

Facial feature	Phenotype	Genes	Reference

Face height	Mid-face height.	PARK2, MBTPS1	M. K. Lee et al. (2017); Crouch et al. (2018)
Face height/depth	Angle between the gonion and the eye.	OSR1-WDR35	Cha et al. (2018)
Face depth and width	Tragus to nasion. Intertragi distance.	TRPC6, PAX9, SLC25A2, MIPOL1, FOXA1, MAFB	Shaffer et al. (2016)
Upper facial profile prominence	Skeletal pattern/mandibular profile.	PCDH15	Crouch et al. (2018)
Forehead	Centralized prominence of the forehead with vertical depression above the orbits. Recessive central portion of forehead with prominence laterally.	TBX15, RPS12, EYA4	Claes et al. (2018)
Eye width	Distance between the eyeballs and nasion. Distance between the eyeballs. Intercanthi distance.	PAX3, TP63, PABP1-C1L2A, HADC8, GSTM2, GNAI3, ALX3	Liu et al. (2012); Shaffer et al. (2016)
Eye width and depth	Eye width and depth. Distance between eyeballs and nasion.	TMEM163, COL17A1	Liu et al. (2012); Crouch et al. (2018)
Eye shape	Curvature of eyelid.	HOXD1-MTX2	Cha et al. (2018)
Nasion prominence	Prominence and vertical position of nasion	PAX3	Paternoster et al. (2012)
Nasion, eyes and zygoma position	Nasion position relative to zygoma and eyeballs.	C5orf50	Liu et al. (2012)
Nose bridge	Increased prominence of the bridge of the nose. Shape of the tip. Nose bridge breadth.	Intergenic, EPHB3, DVL3, SUPT3H/RUNX2	Claes et al. (2018); Adhikari et al. (2016)
Nose height and prominence	Nose prominence, shape of the nose, height, columella inclination, nose tip inclination.	ZNF219, CHD8, SOX9, BC039327/CASC17, KCTD15, DCHS2, PRDM16	Shaffer et al. (2016); Cha et al. (2018); Claes et al. (2018); Adhikari et al. (2016)
Nose width	Nose width, alae width.	PRDM16, SOX9, DHX35, PAX1, PAX3, SUPT3H, GL13	Shaffer et al. (2016); Claes et al. (2018); Liu et al. (2012); Cha et al. (2018); Adhikari et al. (2016)
Upper lip	Central upper lip height.	FREM1	M. K. Lee et al. (2017)
Chin prominence	Chin shape and protrusion.	ASPM, DLX6, DYNC1L1, EDAR	Claes et al. (2018); Adhikari et al. (2016)
Allometry and centroid size	Scaling size and shape. Inner canthal shape, overall face shape and width. Centroid size. Face height and face width, but independent of centroid size.	PDE8A, SCHIP	Cole et al. (2017)

In this project, all 27 landmarks were annotated by the same user. To evaluate if the amount of intra-observer error present in landmark collection was somehow overwhelming the variation contained within the sample, the dataset was subjected to two precision tests before proceeding with the downstream analyses.

First, the landmark set was applied on ten replicates of the cranium and face of the male of AY90. The collected landmarks were then subjected to a generalized Procrustes analysis (GPA),[32] and the Procrustes distance between each replicate and the consensus landmark configuration was calculated. Then, ten different adult males from La Almoloya were landmarked using the same protocol. The landmark configurations were again subjected to a GPA, and Procrustes distances from each individual to the mean landmark configuration were calculated. The t-tests indicated that the mean Procrustes distance among replicates of the same specimen was significantly smaller than the distances between the ten different individuals of the same sex from the same population (Table 6.3).

Table 6.3 - Average pairwise Procrustes distances (d) for the full landmark configuration between ten trials on the same specimen (S), and between ten different individuals from the same population sample (X).

S	*d*	X	*d*
AY90_01	0.0154	**AY5**	0.0523
AY90_02	0.0163	**AY12**	0.0612
AY90_03	0.0192	**AY16**	0.0496
AY90_04	0.0139	**AY24M**	0.0540

[32] A generalized Procrustes analysis is a statistical method used to translate, scale and rotate the landmark configuration of each specimen around a common centroid through a least-squares algorithm that minimizes the distance between each shape and the origin (Gower, 1975; Zelditch et al., 2012). This process generates a new set of superimposed Cartesian coordinates which are then used to statistically compare shape configurations of different individuals. The shape differences between individuals is defined by their Procrustes distance, which is approximately the square root of the sum of squared distances between pairs of corresponding landmarks (Rohlf & Slice, 1990).

AY90_05	0.0169	**AY32**	0.0523
AY90_06	0.0129	**AY38M**	0.0638
AY90_07	0.0153	**AY67**	0.0567
AY90_08	0.0123	**AY68M**	0.0477
AY90_09	0.0183	**AY80M**	0.0683
AY90_10	0.0143	**AY82M**	0.0649
Average	**0.0155**		**0.0571**
	***p* = < 0.0001**		

The second precision test was performed to measure the variability at each individual landmark and assess which specific landmarks are most prone to user error. To do so, the Procrustes distances from each individual landmark to the mean landmark position were calculated for both the replicates and the different individuals. Table 6.4 compiles the consensus and the variance for the calculations of the distribution of Procrustes distances for each landmark in both samples. The t-tests performed in PAST v.05 (Hammer et al., 2001) indicated that the average Procrustes distances at each landmark were all significantly smaller for the replicates than for ten different individuals (Table 6.4 and Figure 6.3).

Table 6.4 - Average pairwise Procrustes distances and average variance for each landmark between ten trials on the same specimen (S), and between ten different individuals from the same population sample (X).

	Average distances		***Average variance***	
Landmark	***S***	**X**	**S**	**X**
Glabella	0.0017	0.0093	0.0000011	0.0000299
Nasion	0.0016	0.0098	0.0000005	0.0000269
Rhinion	0.0035	0.0077	0.0000039	0.0000163
Pronasale	0.0028	0.0131	0.0000012	0.0000246

Subnasale	0.0028	0.0089	0.0000001	0.0000137
Stomion	0.0020	0.0092	0.0000004	0.0000303
Supramentale	0.0010	0.0104	0.0000007	0.0000160
Pogonion	0.0017	0.0116	0.0000005	0.0000211
Menton	0.0017	0.0112	0.0000008	0.0000208
EndL	0.0022	0.0073	0.0000002	0.0000093
EndR	0.0024	0.0067	0.0000007	0.0000094
ExL	0.0016	0.0087	0.0000004	0.0000057
ExR	0.0019	0.0096	0.0000002	0.0000147
SupAlareL	0.0013	0.0086	0.0000031	0.0000062
SupAlareR	0.0011	0.0081	0.0000021	0.0000074
AlareL	0.0026	0.0069	0.0000015	0.0000036
AlareR	0.0025	0.0082	0.0000013	0.0000099
SubalareL	0.0024	0.0064	0.0000015	0.0000174
SubalareR	0.0015	0.0073	0.0000004	0.0000071
CheilionL	0.0018	0.0104	0.0000009	0.0000144
CheilionR	0.0019	0.0092	0.0000003	0.0000138
MmbL	0.0035	0.0101	0.0000043	0.0000057
MmbR	0.0025	0.0110	0.0000026	0.0000235
GonionL	0.0047	0.0143	0.0000045	0.0000160
GonionR	0.0018	0.0155	0.0000007	0.0000114
ZygionL	0.0056	0.0101	0.0000111	0.0000158
ZygionR	0.0046	0.0144	0.0000071	0.0000348
		***p* = < 0.0001**	***p* = < 0.0001**	

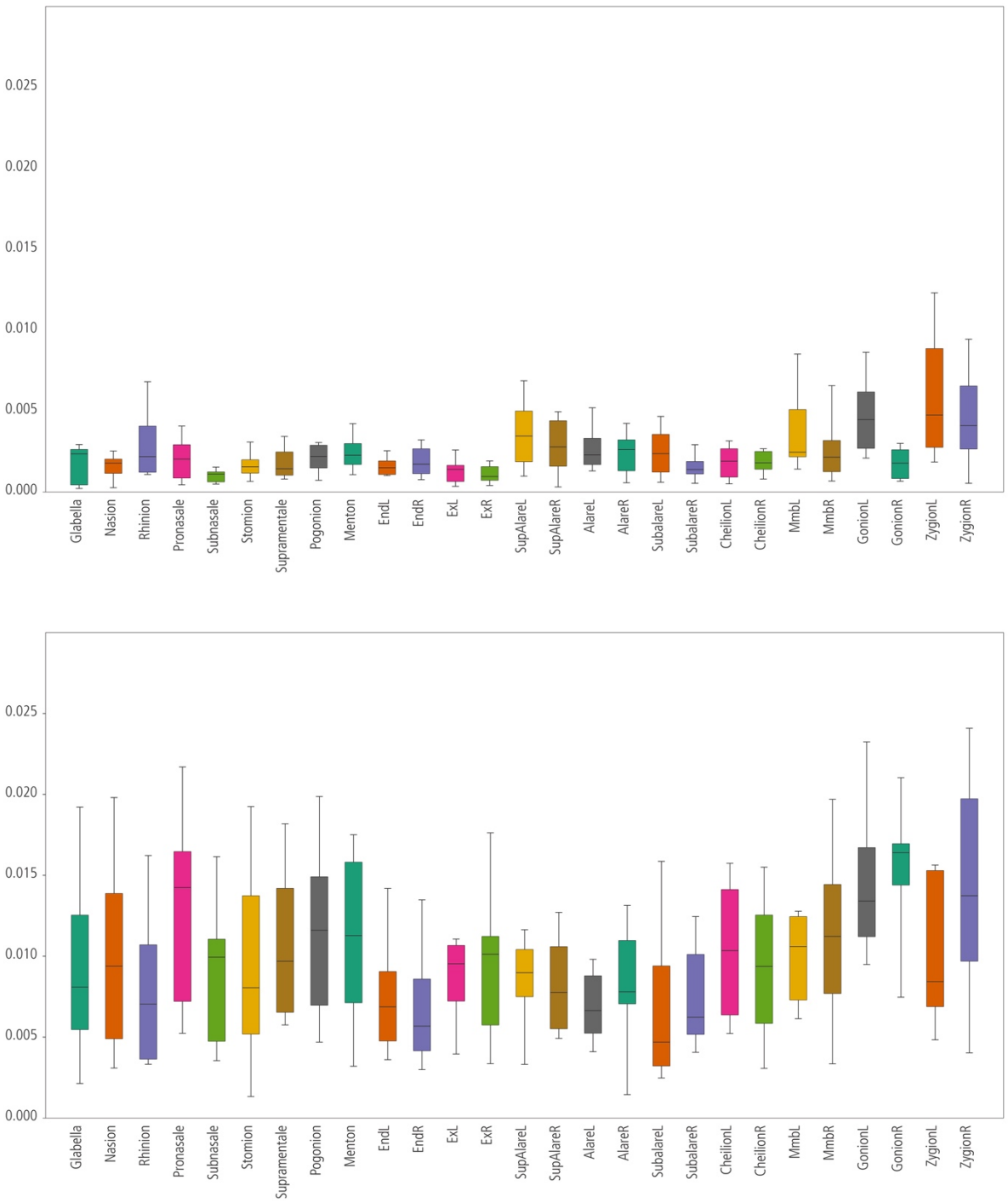

Figure 6.3 - Box plot comparison between the landmarks placed in the replicate series (top) and in different individuals (bottom).

All subsequent morphometric analyses were performed using a combination of MorphoJ (Klingenberg, 2011) and PAST v.4.05 (Hammer et al., 2001). The 3D Principal Component graphs were generated with plotly (Plotly Technologies Inc., 2015). Supplemental materials of the analyses can be found in Appendix C.

Finally, to aid in the visualization of the shape changes happening along the different PC axes, an average face was produced with one of the facial approximations extracted from the sample. Then, the average face was morphed in Landmark Editor (Wiley et al., 2005) to match the landmark coordinates that fall into specific areas of the PCA graphs.

6.2 Results

Figure 6.4 illustrates the entire sample (40 individuals) plotted into a three-dimensional Principal Components Analysis (PCA) (refer to Figure 6.5 for a scree plot of the analysis). The main shape variation driving Principal Component (PC) 1 is facial height. The positive end of PC 1 is grouping those individuals with "longer" faces. The individuals showing severe alveolar resorption affecting the prosthion, which causes a reduction in facial height and increases the projection of the chin, occupy the most negative values on PC 1. An analysis on a sub-sample without these individuals does not alter the attribution of variation in facial height to the first PC. Principal Component 2 is mostly driven by the width of the face and mandible, depth of the lower face and the shape of the nasal bones. At the negative end of PC 2, the mandibles are wider and shorter, leaving an impression of a face that is more "round" anteriorly and with a straighter nose. On PC 3, the main change in shape seems to be related with the nasal area: (1) the relative position of the pronasale to the subnasale, leading to a different angle of the columella; and depth of the nasal bridge, which in turn influences the projection of the nose, and the outer- and intercanthal spacing. The individuals in the negative values of PC 3 display noses that are more turned upwards and have wider nasal bridges. The cumulative variation of the three PC's in the graph accounts for 45.4 % of the whole shape captured by the landmark configuration. An examination of PC 4 (7.3 % of variance) and PC 5 (5.7 % of variance) shows that the first is related to facial asymmetry, prominence and height of the nose and angle of the forehead, while the second associates with the relative prominence of the maxilla in respect with the mandible. Figure 6.6 illustrates the main shape differences happening along the examined principal components.

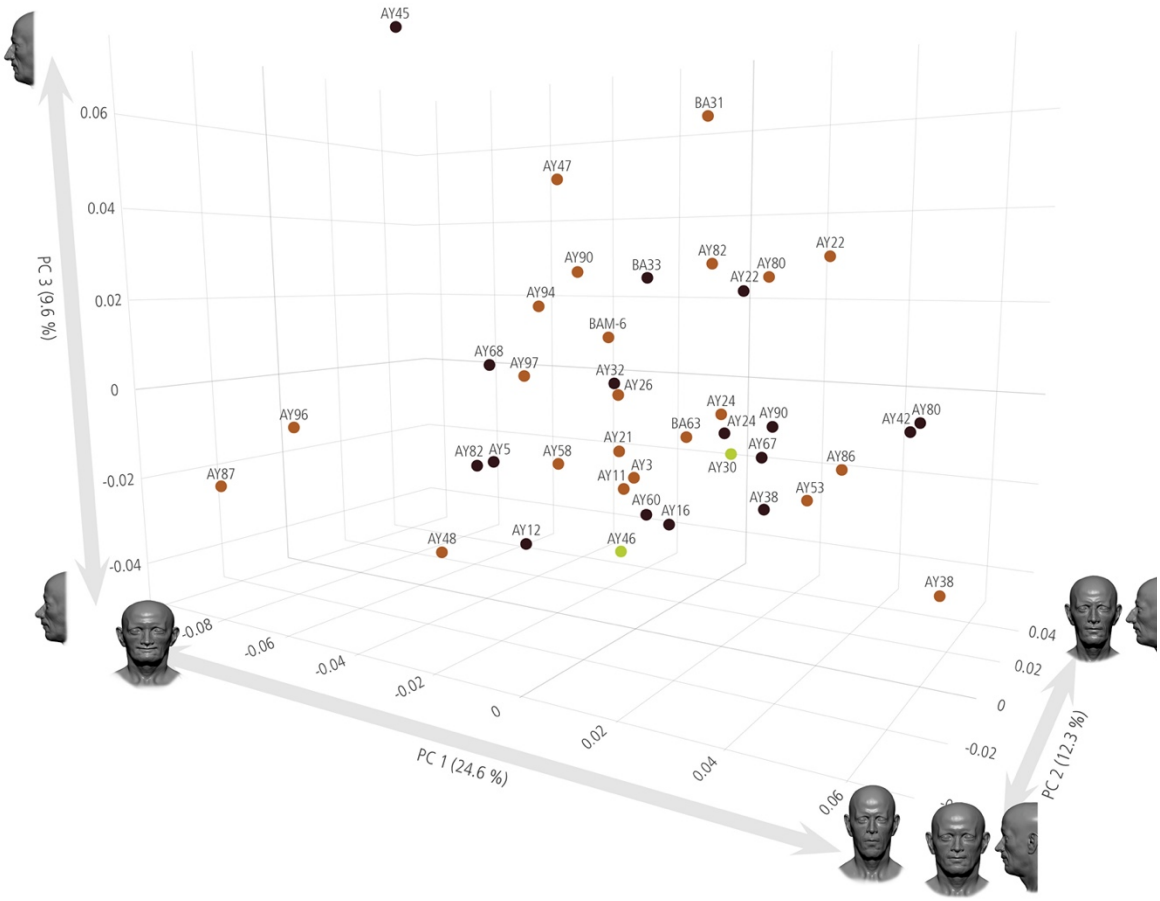

Figure 6.4 - Three-dimensional PCA of the Procrustes-aligned coordinates of the entire sample in Procrustes shape space. The faces illustrating the extremes of the axes are averages produced using the original variables.

A bigger version of this image can be visualized in Appendix C.

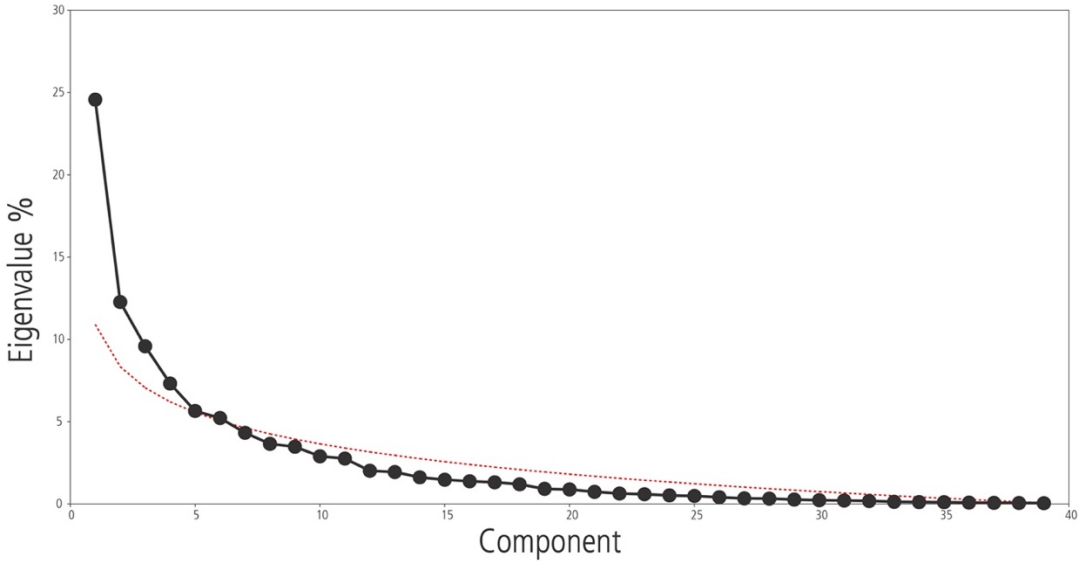

Figure 6.5 - Scree plot showing the variation on each Principal Component of the analysis of the entire sample.

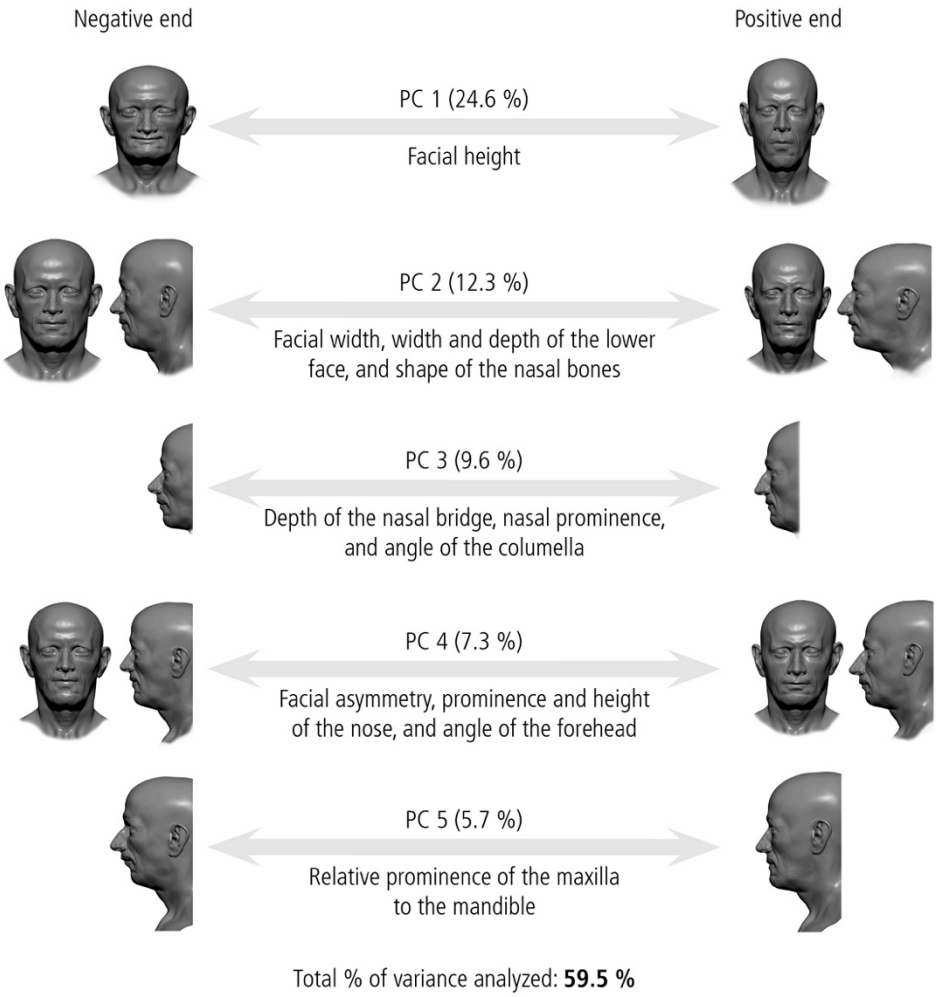

Figure 6.6 - Shape changes happening along the five PC axes analyzed for the entire sample.

A multivariate regression of facial height on log centroid size (henceforth referred to only as "size", for brevity) indicates that a significant percentage (31.5%, *p*-value: 0.0003) of the variation within this component of shape is influenced by size (used here as a proxy for growth) and sex (Figure 6.7), which is consistent with published anthropometric norms (Farkas, 1994). PC 3 is also driven by a well-known aspect of aging and sexual dimorphism, which is the development of the nose from childhood to adulthood and the shape and size of the nose,[33] respectively (Figure 6.8). In PC 3, 34.6 % of the shape variation is

[33] As mentioned previously in Chapter 3, children have a lower nasal bridge. The nose is shorter and rounder, with a concave profile, and a tip that turns upwards (Enlow & Hans, 1996). Several studies have determined that the nose

significantly correlated with size (*p*-value: <0.0001). Based on multivariate regressions of shape on size, we were also able to establish that the degree of shape changes along PC 2 (3.3 % of shape variation predicted by size, *p*-value: 0.2609), PC 4 (0.4 % of shape variation predicted by size, *p*-value: 0.4154) and PC 5 (1.2 % of shape variation predicted by size, *p*-value: 0.5011) are not significantly correlated with size.

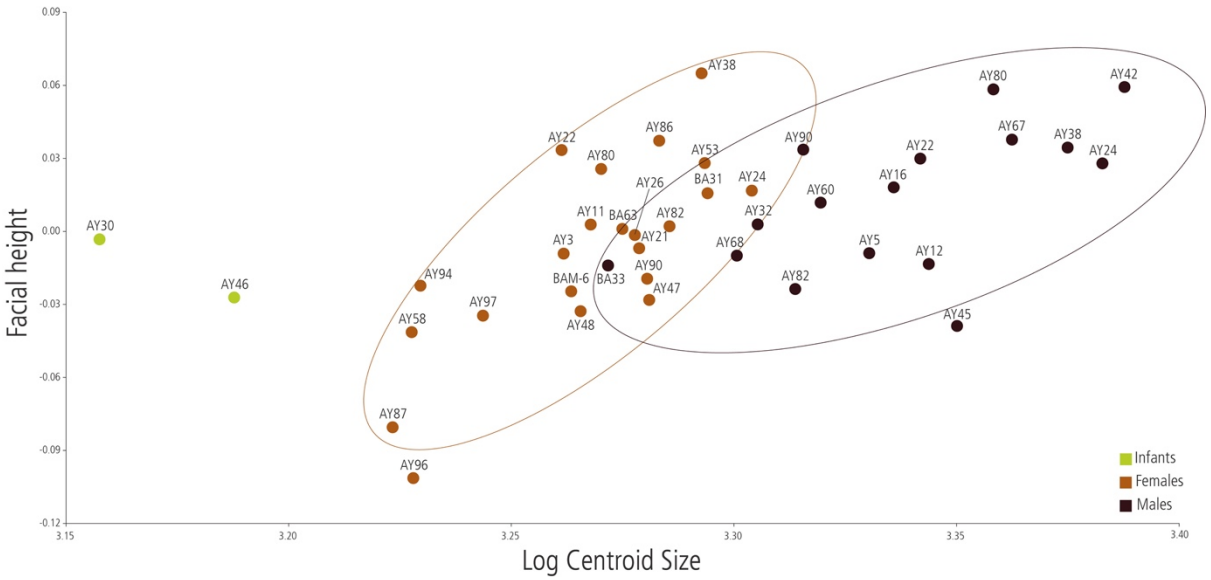

Figure 6.7 - Multivariate regression of facial height (PC 1) on size, considering the entire sample.

continues modifying even after reaching skeletal maturity, and that men have larger noses than women (see, for instance, Farkas, 1994; Holton et al., 2014; Sforza et al., 2011; Zankl et al., 2002).

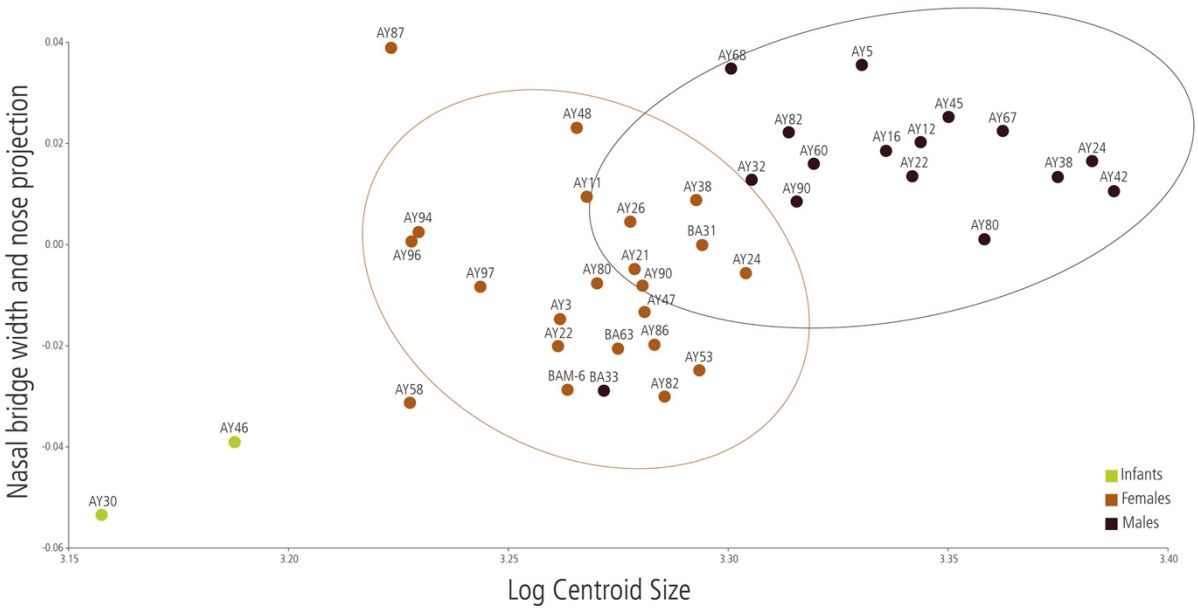

Figure 6.8 - Multivariate regression of nasal bridge width and depth (PC 3) on size, considering the entire sample.

The similarity matrices were generated in PAST v.4.05 (Hammer et al., 2001) using the Euclidean distance index and plotted into a two-dimensional PCA of the whole sample as minimum spanning trees (Figure 6.9). The minimum spanning trees connect pairs of the most similar individuals regarding the totality of the shape configuration (similarity indexes are gathered on Table 1, on Appendix C).

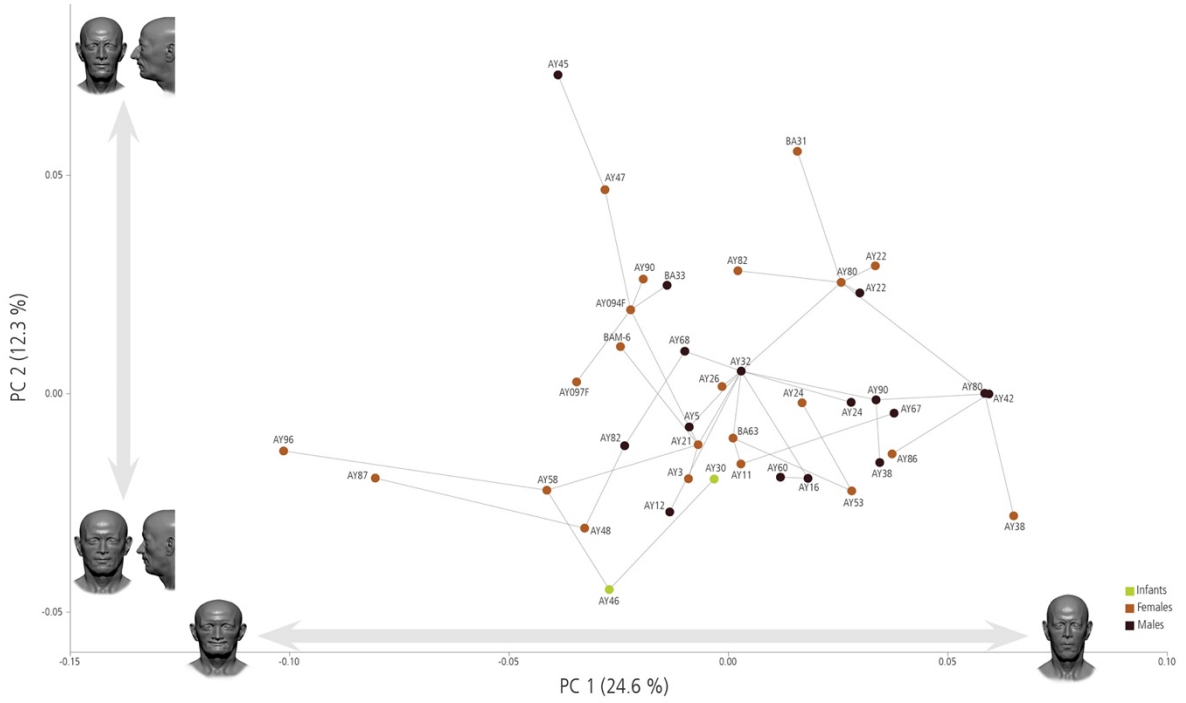

Figure 6.9 - Two-dimensional PCA of the entire sample illustrating the closest similarities between pairs of individuals. A larger version of this image can be visualized in Appendix C.

A phenetic tree was also generated in PAST v.4.05 (Hammer et al., 2001) as a first approach to observe which individuals cluster together (see Figure 3 in Appendix C). The chosen linkage was the neighbor-joining method (Saitou & Nei, 1987) based on Euclidean distances. The clustering pattern is merely exploratory at this stage and will require external validation but was examined in tandem with the Principal Component analyses.

6.3 Discussion

The proposition of inferring genetic relatedness from facial approximations is, at the very least, an ambitious and challenging task. As discussed in Chapter 2, facial approximations are not portraits but rather a depiction informed by the analysis of a particular skull and the application of published regression methods to estimate the placement and general morphology of facial features. It is expected that a variable amount of error permeates these estimates and, ultimately, it is necessary to acknowledge that these inaccuracies will likely interfere with the downstream morphometric analyses. Therefore, and considering the limitations related to method accuracy, testing the facial approximation protocol used on this project on a control group remains one of the main endeavors yet to be accomplished (see section 4.4 in Chapter 4). It is our hope that the pursuit of this goal in the near future will not only provide a reference value for the accuracy of the methods employed, but also inform on possible venues for the improvement of facial depictions from the skull.

There are sample limitations that have to be taken into account as well. The number of facial approximations derived from individuals from La Bastida is extremely small (it represents less than 2% of all the tombs identified and excavated to date), meaning that the probability of finding a close genetic relationship between them is very low. Still, it might be relevant to include them in inter-group comparisons with individuals from La Almoloya and other Argaric settlements, provided that the size of the sample can be increased in the future. Moreover, while the number of facial approximations of individuals from La Almoloya represents a substantial percentage of all burials excavated at the end of the fourth campaign (34.3 %), it is usually accepted that the total number of tombs underrepresents the actual number of people that inhabited the Argaric settlements. It appears that there were social mechanisms in place that dictated whom was to be buried *in situ* and whom was not (Lull et al., 2016a). The aDNA studies currently underway may provide better insight into this matter.

Our sample also contains individuals in different ontogenetic states. A multivariate regression of shape on size (which is here used as a proxy for ontogenetic change, due to the correlation between growth and age) shows that 11.9% of the variation contained in the entire sample relates to different age ranges and that it is a significant component of shape (p-value: <0.0001). Still, regarding the changes in shape

usually associated with aging[34], four female individuals (which account for 11% of the La Almoloya sample) show an important loss of alveolar bone in the maxilla that interferes with the original position of the prosthion. From a visual and practical point of view, this condition greatly diminishes the vertical height of the face and makes the chin appear more pronounced while also potentially introducing inaccuracies in the estimation of the nasal profile (Rynn et al., 2010). Hence, it is not surprising that these individuals are grouped at the negative end of PC 1 and cluster together on the phenetic tree (see Figure 6.9 and Figure 3 in Appendix C).

Finally, the limitations regarding the state of preservation of the remains used to perform facial approximations introduce a taphonomical bias that also needs to be acknowledged. The taphonomical bias not only has the potential of deforming the original materials, thus affecting the outcome of the visual representation, but also of randomly reducing the sample size available. Limited samples sizes are a recurrent issue in archaeological and paleontological analyses, and it has been demonstrated that some aspects, such as the definition of allometric trajectories, can be strongly affected by sampling error (Cardini & Elton, 2007). The same authors found that mean size, the standard deviation of size and variance of shape perform reasonably well even with smaller samples.

From the regression analyses on the different components of shape (Figure 6.7 and Figure 6.8), we can establish that the facial representations produced from the Argaric crania are consistent with published anthropometric norms and with known aspects of sexual dimorphism. Moreover, the position of BA33 in the same regression plots is also consistent with the osteoarchaeological reports that define the men from La Bastida as being more gracile than those from La Almoloya (C. Oliart, personal communication). Further inter-group comparisons with other settlements of the same chronological horizon and modern populations may prove useful in providing a more thorough definition of the Argaric facial phenotype.

[34] Oral health issues can also be a result of a genetic predisposition to certain conditions (e.g., periodontitis) and other environmental causes such as poor dental hygiene.

Based on the general morphology of the face and specific facial traits, we hypothesize that the two males from tombs AY80 and AY42 and subjects AY38 (male) and AY30 might share a close genetic connection.

AY80 and AY42 cluster close together in the phenetic tree and share a very similar configuration regarding the morphological variation found in PC 1 and PC 2 (Figure 6.10 and Figure 6.11). As mentioned before, these two axes contain the shape variation related to facial height and width. According to the literature, it is still disputable which one of these dimensions is more heritable than the other, but both have been reported as being under genetic control (Cole et al., 2017; Tsagkrasoulis et al., 2017) (see also

Table 6.2 in this Chapter).

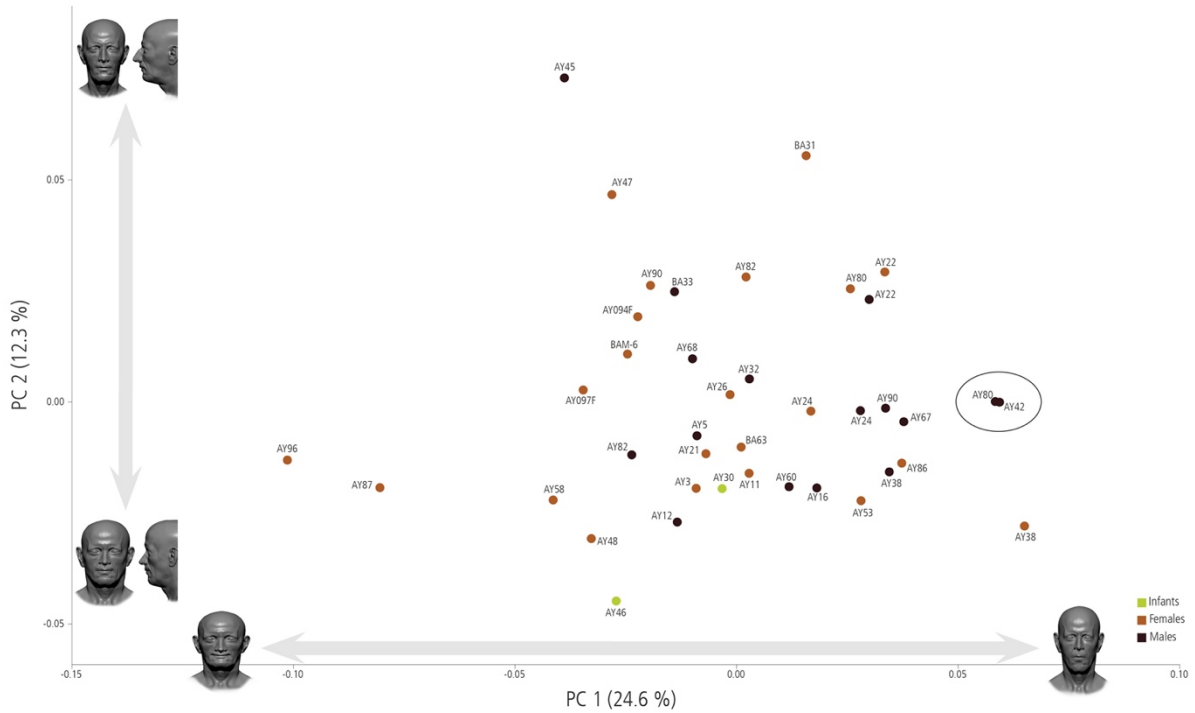

Figure 6.10 - Position of AY80 Male and AY42 Male in the two-dimensional plot of the entire sample.

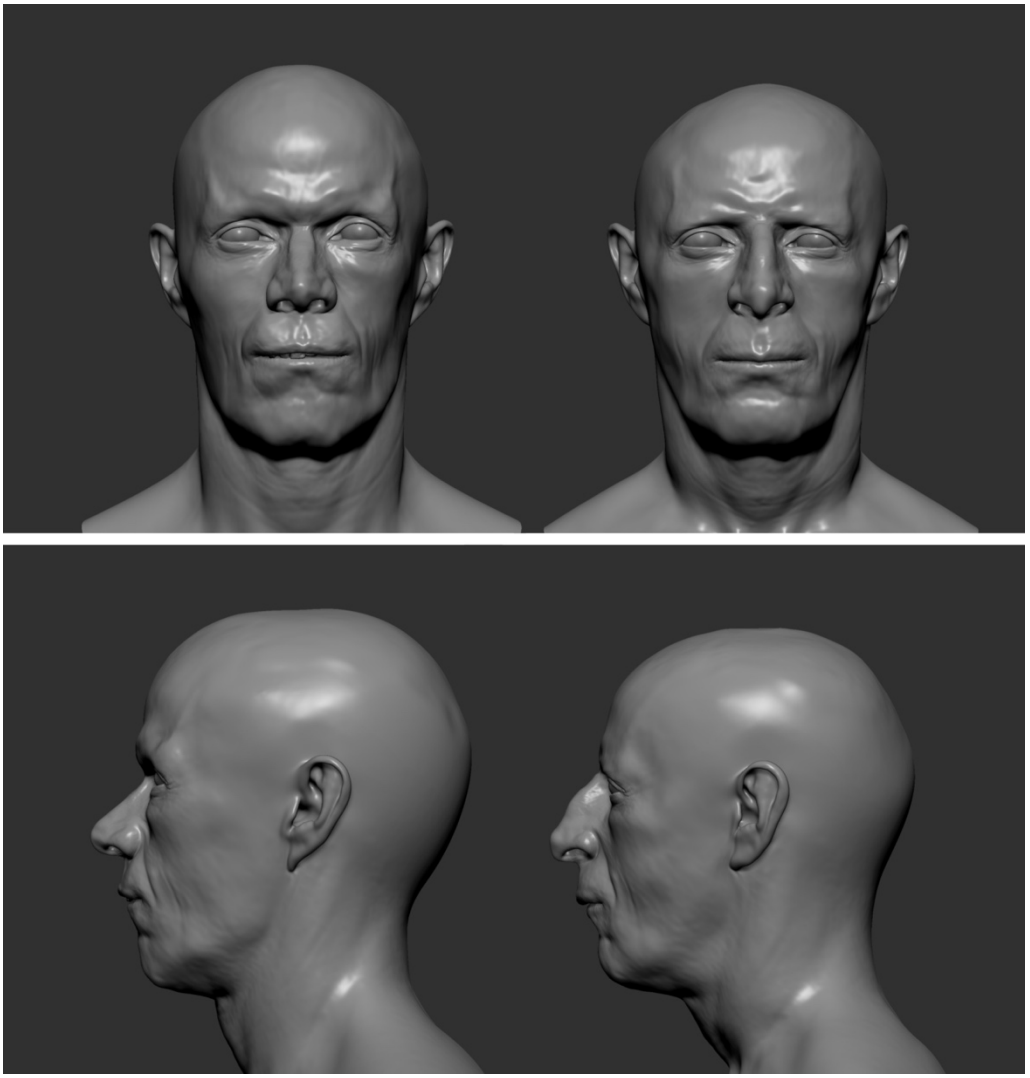

Figure 6.11 - Facial representations in front view and profile of individuals AY42 (left) and AY80 (right).

The male from tomb AY38 and the child from AY30 also stand out in our analyses of specific facial traits. Since it is widely accepted that retrognathic facial proportions (and other types of malocclusion) are controlled by models of polygenic inheritance (see, for instance, Cakan et al., 2012; Harris, 1975; Mossey, 1999a, 1999b; Proffit et al., 2006), we examined PC 2 and PC 5 together, which account for the shape variation concerning the depth of the lower face and the relative prominence of the maxilla in relation with mandible, respectively. Figure 6.12 shows that regarding this specific aspect of shape, the male from tomb AY38 and AY30 are closely related and separate from all the other individuals. Considering that

extreme facial phenotypes often have an underlying genetic outset (e.g., the prevalence of mandibular prognathism within the Habsburg family), we propose that these two individuals are closely genetically related (Figure 6.13).

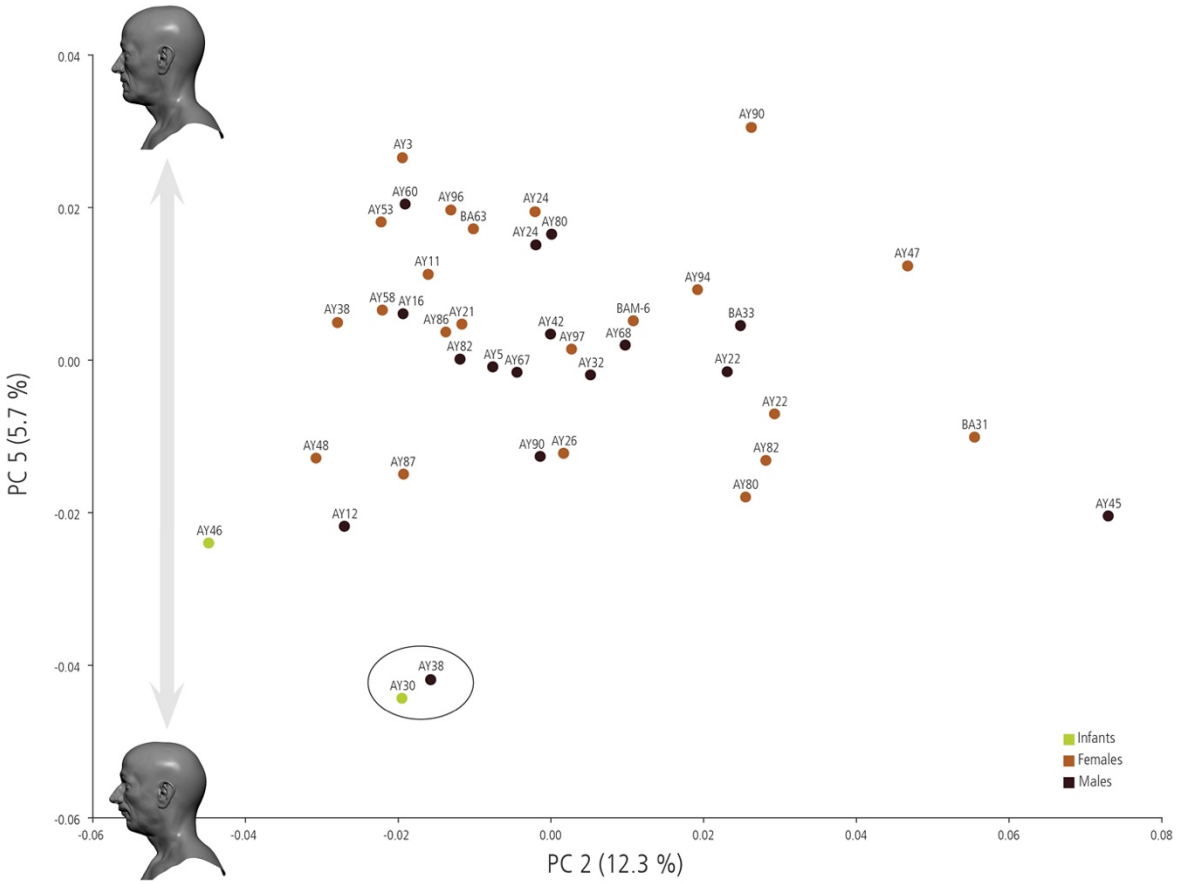

Figure 6.12 – Two-dimensional PCA of the entire sample displaying the variation on facial width and depth (PC 2) and relative position of the maxilla in relation to the mandible (PC 5). The position of individuals AY38 Male and AY30 is emphasized. A larger version of this image is given in Appendix C.

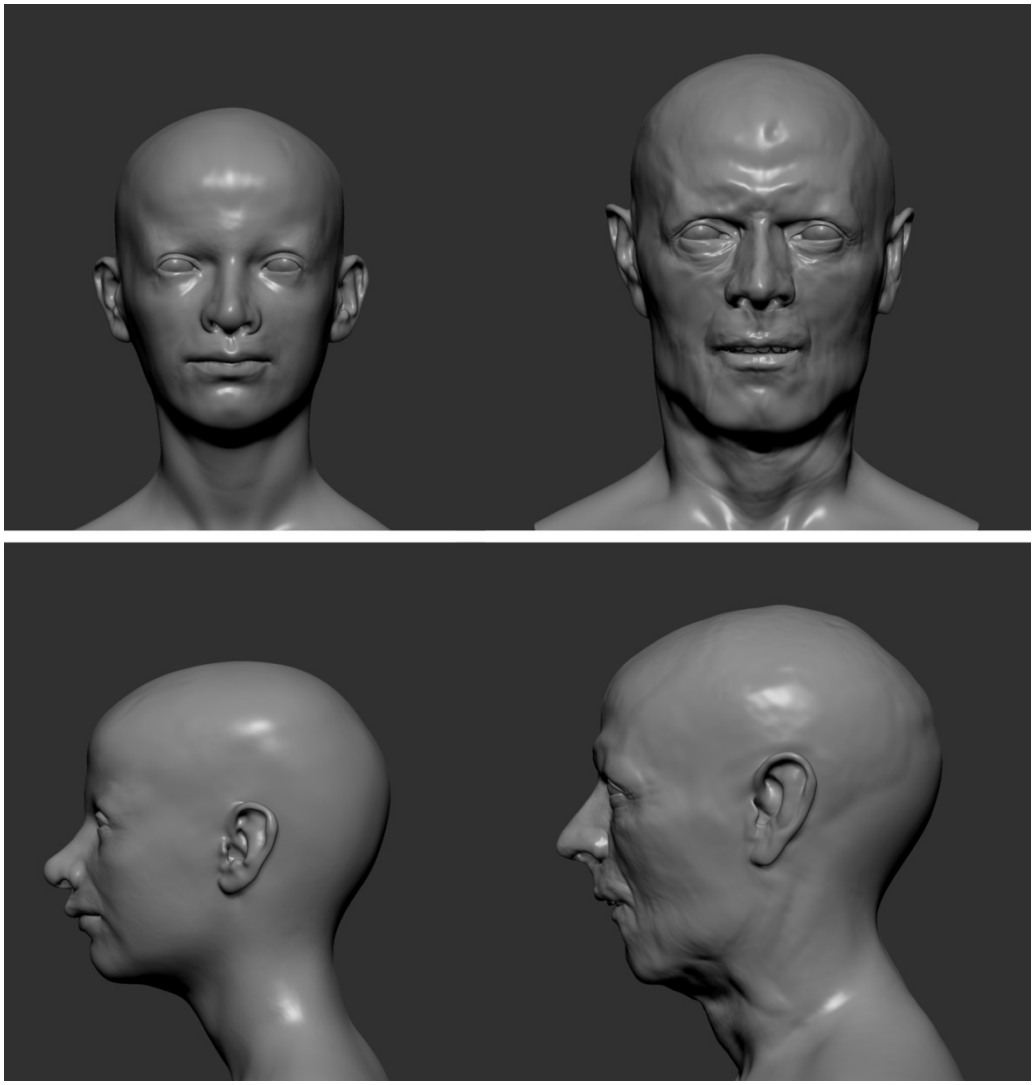

Figure 6.13 - Facial representations in front view and profile of individuals AY30 (left) and AY38 (right).

A visual inspection of the remaining facial approximations and their distributions in the graph (Figure 6.12) shows that many other individuals also present what seems to be a retrognathic profile. This phenotype is present both in individuals from both La Almoloya and La Bastida, albeit being less pronounced than in the subjects from AY38 and AY30. Whether this is a circumstance related to an underlying genetic condition (the predominant factor for the prevalence of retrognathism), or an

observation that might suggest a different etiology,[35] is a matter that requires caution. Further analyses on this aspect of shape would preferably include observations made with an outgroup of individuals bearing normal occlusion and diagnosed malocclusions to establish a wider range of possible variation that provides a broader context to our sample.

Despite the ongoing research on Bronze Age genetics and kinship that is being conducted by the team at the Universitat Autònoma de Barcelona and the Max Planck Institute, all the facial approximations were produced without previous knowledge of the existence (or absence) of any genetic relationship between the individuals included in the sample. Keeping this information shrouded from the practitioner was a deliberate strategy to avoid any bias that forced the facial depictions towards any suggested relatedness between individuals. The hypotheses presented here are based on a conservative analysis of morphological similarity derived from the selected configuration of landmarks and the sample. Thus, the next step in this investigation will be to contrast the morphometric analyses presented here against the aDNA results from the individuals of La Almoloya and La Bastida. It is expected that this will raise more research questions and motivate tests with different landmark configurations in individuals known to share a genetic bond and, finally, prompting further analyses of facial shape.

[35] There are several reports in the orthodontic literature that attribute Class II Division 1 malocclusion to non-nutritive sucking habits (e.g., "thumb sucking") that extend beyond the 18 months of age (see, for instance, Dimberg et al., 2010; Singh et al., 2008; Warren et al., 2005).

CONCLUSION

~

GENERAL CONSIDERATIONS

This dissertation project delineates a multidisciplinary approach to the Argaric society, integrated in the activities of the Research Group in Mediterranean Social Archaeoecology of the Universitat Autònoma de Barcelona (ASOME-UAB). This thesis presents 40 three-dimensional facial representations from the skull, incorporated into a study that investigates the place and potential of these representations in formulating archaeological hypotheses in kinship research. It compiles four faces from individuals from the Argaric settlements of La Bastida (Totana) and 36 from La Almoloya.

Faces are a multidimensional space. The depiction of a face based on the anthropological analysis of the skull is as controversial as it is fascinating. In short, a facial representation faces material, methodological, practical and perceptional challenges. While the fundamental goal of a facial representation in a forensic setting is to motivate recognition, this prospect becomes less plausible the older the skeletal remains are. More often than not, the faces represented from crania found in archaeological contexts are isolated events that cannot be cross-referenced with other images from the subjects they represent. The methods to predict features and estimate the depth of soft tissues still have limitations and create an average of the human anatomical variation, while some distinctive elements such as hair or eye color cannot be inferred from the skull at all. The result is ultimately determined by the quality of the bone reference available and permeated by the unsurpassable bias of representing a specific individual with generalized anthropometric values or an ancient population using modern standards. However, the quantitative assessments of accuracy made to this date hint at the potential of facial representations from the skull, establishing that approximately 70% of the face can be inferred with less than ± 2.5 mm deviation (W. J. Lee et al., 2015; W. J. Lee et al., 2012; Miranda et al., 2018; Short et al., 2014; Wilkinson et al., 2006a), and see Table 2.3 in Chapter 2.3).

On the other hand, our facial topography carries a portion of our genetic inheritance, evident in the notable resemblance between close relatives and the almost perfect similarity between identical twins. The dynamics between genomic and environmental influences on facial morphology have been addressed in a number of recent publications. How these two components intertwine is still a matter of debate, but researchers have so far identified more than 50 facial *loci* that associate with specific genes (refer to Richmond et al., 2018 for a review) and reported high genetic correlations for particular measurements (Cole et al., 2017; Tsagkrasoulis et al., 2017).

Our main research question derived from two premises. The first is the notion that it is possible to represent facial morphology from a bony reference to a certain level of precision and, the second, that a facial representation from the skull can be used to infer genetic relatedness between two individuals. These premises have been put to the test in two previous studies. As regards the first one, Richard Neave was asked to compare the facial morphology of two Egyptian brothers buried during the 12th Dynasty who seemed to be quite different (Prag & Neave, 1997; Wilkinson, 2004b). The genetic relatedness of Nekht-Ankh and Khnum-Nakht was suggested by the inscriptions on their coffins and was recently confirmed by aDNA sequencing (Drosou et al., 2018), but the morphology of their skulls and postcranium would imply otherwise. Musgrave et al. (1995) took a similar approach to faces from seven Late Bronze Age individuals from Grave Circle B in Mycenae and hypothesized that individuals G55 and G58 were related. The ancient mitochondrial DNA results confirm their hypothesis, showing that G55 and G58 are indeed brother and sister from the same mother (Bouwman et al., 2008).

ADDRESSING THE RESEARCH QUESTIONS

Our sample included 40 individuals from 30 different tombs excavated at La Almoloya and four tombs detected at La Bastida. To address whether there was a correlation between facial morphology represented from the skull and genetic information, I undertook a blind assessment using the faces generated from the Argaric skulls. These faces were modeled after a critical review of the methods to predict features from

bone and extensive cycles of revisions. Afterwards, I applied a three-dimensional geometric morphometrics approach to explore facial shape variation among the Argaric representations. The analyses were based on a sparse landmark-set of 27 points that were placed in areas that, reportedly, are under a strong genetic control. Many of these landmarks also overlap with points that can be placed through the application of facial approximation methods on a specific skull.

UNVEILING TWO POTENTIAL KINSHIP RELATIONS

Considering the three-dimensional geometric morphometric analysis of the 40 facial representations from the Argaric settlements of La Bastida (Totana) and La Almoloya, I present two hypotheses for possible close genetic relationships within the sample. The first involves the two men from AY42 and AY80. The second is between the man from AY38 and the oldest child from tomb AY30.

The first hypothesis relies on research on the heritability of facial dimensions and the overall shape of the face (Cole et al., 2017), and see Table 6.2 in Chapter 6). Both men from tombs AY80 and AY42 share a similar facial configuration in the combined components of facial height, width, and depth (nearly 37% of the total variance among the sample) (see Figure 6.10, in Chapter 6). Also, both stratigraphy and radiocarbon dating are in agreement with a close genetic relationship (unpublished data after C. Rihuete, personal communication).

The second hypothesis, which suggests a close genetic tie between the man from Tomb AY38 and the oldest child from AY30, finds support in the well-established genetic influence of extreme phenotypes (Harris, 1975; Mossey, 1999a, 1999b; Proffit et al., 2006), such the different types of malocclusion. Together with the relative projection of the maxilla, morphometric analysis of facial width and depth demonstrates that both individuals display a retrognathic mandible and differ from the rest of the sample in that aspect of shape (see Figure 6.12, in Chapter 6). As in the previous case, both stratigraphy and radiocarbon dating are in agreement with a close genetic relationship (unpublished data after C. Rihuete, personal communication).

The genomic study, which will enable an external validation of these hypotheses, is currently in preparation (Villalba-Mouco et al., in prep) and will be used in the future to assess possible correlations between the facial morphology and the amount of shared DNA between subjects.

TOWARDS AN ARGARIC FACIAL PHENOTYPE: A PRELIMINARY ACCOUNT

Our results also revealed some unexpected finds that might be worth exploring in the future. The analyses show that a retrognathic profile might be a common facial phenotype in the Argaric population, attested in individuals from both La Almoloya and La Bastida (Figure 6.12). More analyses combining the excavated skeletal remains, the facial representations and data from modern populations are necessary to further investigate the hypothetical prevalence of retrognathism among Argaric populations, along with its possible etiology.

The multivariate regressions of shape on size determines that the faces predicted from the Argaric crania follow well-established patterns of growth and sexual dimorphism (see Figure 6.7 and Figure 6.8, in Chapter 6). Furthermore, the location of BA33 in the regression plots finds an echo in the osteoarchaeological reports that characterize the men from La Bastida as being more gracile than those from La Almoloya (C. Oliart, personal communication). More studies, including additional individuals from La Bastida and other settlements, are needed to create a more detailed account of what the Argaric facial phenotype would be.

ENVISIONING THE FUTURE

Here, I argue that facial representations from the skull should be regarded as a valuable tool to formulate hypotheses, especially when other resources (e.g., DNA) are not available. Despite the potential that facial

representation encloses, I must stress again that heritability patterns are still somewhat elusive, due to the combination of genetic and environmental factors. It remains possible that the heritability of facial attributes may be population-specific as well as driven by different underlying genetic variants (Cole et al., 2017). Also, facial similarity cannot be instantly assumed as synonymous with genetic relatedness, nor dissimilarity taken as an indicator of its inexistence. For that reason, hypotheses of relatedness derived from facial representations from the skull should be carefully addressed and integrated into a multidisciplinary archaeological approach. Future explorations of this dataset should also include other covariables whose investigation is still ongoing, such the precise chronological sub-phase of El Argar these individuals lived in (as temporal proximity is essential to establish lines of descent) and their allocation to one of the five social categories defined for El Argar (Lull & Estévez, 1986).

Facial representations from the skull produced in the framework of an archaeological project are usually at the very end of the production line, being frequently requested to dress museum walls, to inform and attract the public's attention into a specific research or historical period. I stated before that looking at a sitting model for hours makes one wonder how much life is behind all that stillness. Putting a face on someone is also a step towards humanizing them, and that was the very first string that pulled me into studying archaeology. These remains are much more than generic bones or labels for numbered tombs inside an archaeological complex. They are people with a common history and personal stories. They probably shared laughs with their peers. They buried their dead with reverence and ritual. They spoke in a language we would not understand today. Their ways were probably nothing like ours, and yet, physically, we are quite alike.

At the genesis of my path, I wondered if an image, produced within a scientific framework and following validated guidelines, would somehow enclose something *more*. Should the hypotheses presented here be validated by the genomic studies underway (Villalba-Mouco et al., in prep), this research will contribute to cement the role of facial depictions as valuable assets to construct an archaeological discourse.

BIBLIOGRAPHIC REFERENCES

Adams, E., & Stephan, C. N. (2005). The effect of maceration and hydration on cranial dimensions: a study of Oryctologus cuniculus. *Anthropological Review, 68*, 65-75.

Adhikari, K., Fontanil, T., Cal, S., Mendoza-Revilla, J., Fuentes-Guajardo, M., Chacón-Duque, J.-C., . . . Acuña-Alonzo, V. (2016). A genome-wide association scan in admixed Latin Americans identifies loci influencing facial and scalp hair features. *Nature Communications, 7*(1), 1-12.

Albrecht, G. H. (1976). *A multivariate analysis of the craniofacial morphology of the Sulawesi macaques (Primates: Cercopithecidae).* (PhD dissertation). University of Chicago

Albrecht, G. H. (1978). The craniofacial morphology of the Sulawesi macaques. *Contributions to primatology, 13*, 1-151.

Albrecht, G. H. (1983). Humidity as a source of measurement error in osteometrics. *Am J Phys Anthropol, 60*(4), 517-521. doi:10.1002/ajpa.1330600414

Alexander, M., & Laubach, L. L. (1968). Anthropometry of the human ear. (A photogrammetric study of USAF flight personnel). AMRL-TR-67-203. *Amrl tr*, 1-28.

Almeida, N. H. d., Michel-Crosato, E., Paiva, L. A. S. d., & Biazevic, M. G. H. (2013). Facial soft tissue thickness in the Brazilian population: New reference data and anatomical landmarks. *Forensic science international, 231*(1-3), 404. e401-404. e407.

Álvarez, G., & Ceballos, F. C. (2015). Royal Inbreeding and the Extinction of Lineages of the Habsburg Dynasty. *Human Heredity, 80*(2), 62-68.

Álvarez, G., Ceballos, F. C., & Quinteiro, C. (2009). The Role of Inbreeding in the Extinction of a European Royal Dynasty. *PLOS ONE, 4*(4), e5174.

Anastassov, G. E., & van Damme, P. A. (1996). Evaluation of the anatomical position of the lateral canthal ligament: clinical implications and guidelines. *Journal of Craniofacial Surgery, 7*(6), 429-436.

Anderson, K. J., Henneberg, M., & Norris, R. M. (2008). Anatomy of the nasal profile. *Journal of anatomy, 213*(2), 210-216.

Angel, J. L. (1978). *Restoration of head and face for identification.* Paper presented at the The 30th Annual Meeting of the American Academy of Forensic Sciences, St. Louis, MO.

Ansón, M., Hernández Fernández, M., & Saura Ramos, P. A. (2015). *Paleoart: Term and Conditions (A survey among paleontologists).* Paper presented at the Current Trends in Paleontology and Evolution: XIII Encuentro en Jóvenes Investigadores en Paleontología (XIII EJIP), Madrid, Spain.

Arriaza, B. (1994). Tipología de las momias Chinchorro y evolución de las prácticas de momificación. *Revista Chungara, 26*(1), 11-24.

Asai, Y., Yoshimura, M., Nago, N., & Yamada, T. (1996). Why do old men have big ears? Correlation of ear length with age in Japan. *BMJ, 312*(7030), 582-582.

Ashley-Montagu, M. (1939). Location of porion in the living. *American Journal of Physical Anthropology, 25*(2), 281-295.

Aufderheide, A. C. (2009). *Overmodeled Skulls*. Florida: Heide Press, L. L. C.

Augusteyn, R. C., Nankivil, D., Mohamed, A., Maceo, B., Pierre, F., & Parel, J.-M. (2012). Human ocular biometry. *Experimental eye research, 102*, 70-75.

Aung, S. C., Foo, C. L., & Lee, S. T. (2000). Three dimensional laser scan assessment of the Oriental nose with a new classification of Oriental nasal types. *British Journal of Plastic Surgery, 53*(2), 109-116.

Balueva, T., & Lebedinskaya, G. (1991). Anthropological reconstruction. *Moscow: Russian Academy of Sciences.*

Balueva, T., Veselovskaya, E., & Kobyliansky, E. (2009). Cranio-facial reconstruction by applying the ultrasound method in live human populations. *International Journal of Anthropology, 24*(2), 87-111.

Balueva, T., Veselovskaya, E., Lebedinskaya, G., & Pestrjakov, A. (1988). Anthropological Types of the Ancient Population at the Territory of USSR, Zubov AA. In: Nauka, Moscow (In Russian).

Bartosiewicz, L. (2008). Taphonomy and palaeopathology in archaeozoology. *Geobios, 41*(1), 69-77.

Beatty, K. E. (2015). *Skin and bone: the face in the archaeological imagination.* (PhD). University College Cork, Cork, Ireland.

Benazzi, S., Bertelli, P., Lippi, B., Bedini, E., Caudana, R., Gruppioni, G., & Mallegni, F. (2010). Virtual anthropology and forensic arts: the facial reconstruction of Ferrante Gonzaga. *Journal of Archaeological Science, 37*(7), 1572-1578.

Benazzi, S., Bookstein, F. L., Strait, D. S., & Weber, G. W. (2011). A new OH5 reconstruction with an assessment of its uncertainty. *Journal of Human Evolution, 61*(1), 75-88.

Benazzi, S., Fantini, M., De Crescenzio, F., Mallegni, G., Mallegni, F., Persiani, F., & Gruppioni, G. (2009). The face of the poet Dante Alighieri reconstructed by virtual modelling and forensic anthropology techniques. *Journal of Archaeological Science, 36*(2), 278-283.

Benz, M. (2010). Beyond death: the construction of social identities at the transition from foraging to farming. In M. Benz (Ed.), *The Principle of Sharing: Segregation and Construction of Social Identities at the Transition from Foraging to Farming* (Vol. Studies in Early Near Eastern Production, Subsistence and Environment 14, pp. 249-276). Berlin: Ex oriente.

Bérard, P., Bradley, D., Nitti, M., Beeler, T., & Gross, M. (2014). High-Quality Capture of Eyes. *ACM Transactions on Graphics, 33*, 1-12.

Bhattacharya, S., Rai, A., & Shrivastava, P. (2006). Cleft data from surgical camps on rails: A doorstep health care delivery. *The Journal of Indian Prosthodontic Society, 6*(1), 38-42.

Bienert, H. D. (1991). Skull cult in the prehistoric Near East. *Journal of prehistoric religion, 5*, 9-23.

Birkner, F. (1907). Die Dicke der Gesichtsweichteile bei verschiedenem Alter, Geschlecht und Rasse. *Sitzungsber. Ges. f. Morph, u. Physiol. in München, 23*, 140-146.

Bocquentin, F., Kodas, E., & Ortiz, A. (2016). Headless but still eloquent! Acephalous skeletons as witnesses of Pre-Pottery Neolithic North- South Levant connections and disconnections. *Paléorient, 42.2*, 33-52.

Bodic, F., Hamel, L., Lerouxel, E., Baslé, M. F., & Chappard, D. (2005). Bone loss and teeth. *Joint Bone Spine, 72*(3), 215-221.

Bookstein, F. L. (1991). Morphometric tools for landmark data. Geometry and Biology. In: Cambridge University Press.

Bouwman, A. S., Brown, K. A., Prag, A. J. N. W., & Brown, T. A. (2008). Kinship between burials from Grave Circle B at Mycenae revealed by ancient DNA typing. *Journal of Archaeological Science, 35*(9), 2580-2584.

Boz, B., & Hager, L. (2013). Living above the Dead: Intramural Burial practices at Çatalhöyük. In I. Hodder (Ed.), *Humans and Landscapes of Çatalhöyük: Reports from the 2000–2008 Seasons* (pp. 413-440). London and Los Angeles: British Institute at Ankara and Cotsen Institute of Archaeology Press.

Bozkir, M. G., Karakaş, P., Yavuz, M., & Dere, F. (2006). Morphometry of the external ear in our adult population. *Aesthetic Plastic Surgery, 30*(1), 81-85.

British Museum, & Shore, A. (2017). Facing the past: the Jericho Skull. Retrieved from https://blog.britishmuseum.org/facing-the-past-the-jericho-skull/

Broadbent, T. R., & Mathews, V. L. (1957). Artistic relationships in surface anatomy of the face: application to reconstructive surgery. *Plastic and Reconstructive Surgery, 20*(1), 1-17.

Broca, P. (1874). De l'influence de l'humidité sur la capacité du crâne. *Bulletins et Memoires de la Societe d'anthropologie de Paris, 9*(1), 63-98.

Bron, A., Tripathi, R., & Tripathi, B. (1997). *Wolff's Anatomy of the Eye and Orbit, 8Ed*: Taylor & Francis.

Brucker, M. J., Patel, J., & Sullivan, P. K. (2003). A morphometric study of the external ear: age- and sex-related differences. *Plastic Reconstructive Surgery, 112*(2), 647-652; discussion 653-644.

Buchan, J., Pare, M., & Munhall, K. (2007). Spatial statistics of gaze fixations during dynamic face processing. *Social neuroscience, 2*, 1-13.

Buikstra, J. E., & Ubelaker, D. H. (1994). *Standards for Data Collection from Human Skeletal Remains: Proceedings of a Seminar at the Field Museum of Natural History, Organized by Jonathan Haas*: Arkansas Archeological Survey.

Bulut, O., Liu, C.-Y. J., Gurcan, S., & Hekimoglu, B. (2019). Prediction of nasal morphology in facial reconstruction: Validation and recalibration of the Rynn method. *Legal Medicine, 40*, 26-31.

Bulut, O., Sipahioglu, S., & Hekimoglu, B. (2014). Facial soft tissue thickness database for craniofacial reconstruction in the Turkish adult population. *Forensic science international, 242*, 44-61.

Buolamwini, J., & Gebru, T. (2018). *Gender Shades: Intersectional Accuracy Disparities in Commercial Gender Classification*. Paper presented at the Proceedings of the 1st Conference on Fairness, Accountability and Transparency, Proceedings of Machine Learning Research.

Burrows, A. M., & Cohn, J. F. (2009). Anatomy of Face. In S. Z. Li & A. Jain (Eds.), *Encyclopedia of Biometrics* (pp. 16-23). Boston, MA: Springer US.

Cakan, D. G., Ulkur, F., & Taner, T. U. (2012). The genetic basis of facial skeletal characteristics and its relation with orthodontics. *European journal of dentistry, 6*(3), 340-345.

Cardini, A., & Elton, S. (2007). Sample size and sampling error in geometric morphometric studies of size and shape. *Zoomorphology, 126*(2), 121-134.

Carey, J. C., Cohen Jr., M. M., Curry, C. J. R., Devriendt, K., Holmes, L. B., & Verloes, A. (2009). Elements of morphology: Standard terminology for the lips, mouth, and oral region. *American Journal of Medical Genetics Part A, 149A*(1), 77-92.

Cassill, K. (1980). Betty Pat Gatliff Sculpts Faces from Victims' Skulls—An Eerie Art That's Changing Criminal Science. *People Magazine, 14(3)*. Retrieved from https://people.com/archive/betty-pat-gatliff-sculpts-faces-from-victims-skulls-an-eerie-art-thats-changing-criminal-science-vol-14-no-3/

Castro, P., Chapman, R., Gili, S., Lull, V., Micó, R., Rihuete Herrada, C., . . . Sanahuja, M. (1999). *Proyecto Gatas 2. La dinámica arqueoecológica de la ocupación prehistórica*. Sevilla: Junta de Andalucía.

Cates, J., Fletcher, P. T., Styner, M., Shenton, M., & Whitaker, R. (2007). *Shape modeling and analysis with entropy-based particle systems*. Paper presented at the Biennial International Conference on Information Processing in Medical Imaging.

Cavanagh, D., & Steyn, M. (2011). Facial reconstruction: soft tissue thickness values for South African black females. *Forensic science international, 206*(1-3), 215. e211-215. e217.

Cha, S., Lim, J. E., Park, A. Y., Do, J.-H., Lee, S. W., Shin, C., . . . Kim, J.-S. (2018). Identification of five novel genetic loci related to facial morphology by genome-wide association studies. *BMC genomics, 19*(1), 1-17.

Chaitanya, L., Breslin, K., Zuñiga, S., Wirken, L., Pośpiech, E., Kukla-Bartoszek, M., . . . Walsh, S. (2018). The HIrisPlex-S system for eye, hair and skin colour prediction from DNA: Introduction and forensic developmental validation. *Forensic Science International: Genetics, 35*, 123-135.

Chu, G., Zhao, J.-m., Han, M.-q., Mou, Q.-n., Ji, L.-l., Zhou, H., . . . Guo, Y.-c. (2020). Three-dimensional prediction of nose morphology in Chinese young adults: a pilot study combining cone-beam computed tomography and 3dMD photogrammetry system. *International Journal of Legal Medicine, 134*(5), 1803-1816.

Chung, J.-H., Chen, H.-T., Hsu, W.-Y., Huang, G.-S., & Shaw, K.-P. (2015). A CT-scan database for the facial soft tissue thickness of Taiwan adults. *Forensic science international, 253*, 132. e131-132. e111.

Churchill, S. E., Shackelford, L. L., Georgi, J. N., & Black, M. T. (2004). Morphological variation and airflow dynamics in the human nose. *American Journal of Human Biology, 16*(6), 625-638.

Claes, P., Roosenboom, J., White, J. D., Swigut, T., Sero, D., Li, J., . . . Liebowitz, C. (2018). Genome-wide mapping of global-to-local genetic effects on human facial shape. *Nature genetics, 50*(3), 414-423.

Claes, P., Vandermeulen, D., De Greef, S., Willems, G., Clement, J. G., & Suetens, P. (2010). Computerized craniofacial reconstruction: Conceptual framework and review. *Forensic science international, 201*(1), 138-145.

Claes, P., Walters, M., & Clement, J. G. (2012). Improved facial outcome assessment using a 3D anthropometric mask. *International journal of oral and maxillofacial surgery, 41*(3), 324-330.

Clark, C. A. (2001). Evolution for John Doe: Pictures, and the Scopes Trial Debate. *Journal of American History, 87*, 1275-1301.

Clark, M. A., Worrell, M. B., & Pless, J. E. (1997). Postmortem changes in soft tissues. In W. D. Haglund & M. H. Sorg (Eds.), *Forensic taphonomy: the postmortem fate of human remains* (pp. 151-164). Boca Raton, London: CRC Press.

Clarke, T. H. (1986). *The Rhinoceros from Dürer to Stubbs, 1515-1799*: Sotheby's Publications.

Codinha, S. (2009). Facial soft tissue thicknesses for the Portuguese adult population. *Forensic science international, 184*(1-3), 80. e81-80. e87.

Cole, J. B., Manyama, M., Larson, J. R., Liberton, D. K., Ferrara, T. M., Riccardi, S. L., . . . Santorico, S. A. (2017). Human facial shape and size heritability and genetic correlations. *Genetics, 205*(2), 967-978.

Conway, J., Kosemen, C. M., & Naish, D. (2012). *All Yesterdays: Unique and Speculative Views of Dinosaurs and Other Prehistoric Animals*: Irregular Books.

Couly, G., Hureau, J., & Tessier, P. (1976). The anatomy of the external palpebral ligament in man. *Journal of Maxillofacial Surgery*.

Cox, C. E. (2017). Role of physical activity for weight loss and weight maintenance. *Diabetes Spectrum, 30*(3), 157-160.

Crouch, D. J., Winney, B., Koppen, W. P., Christmas, W. J., Hutnik, K., Day, T., . . . Nessa, A. (2018). Genetics of the human face: Identification of large-effect single gene variants. *Proceedings of the National Academy of Sciences, 115*(4), E676-E685.

Daboul, A., Ivanovska, T., Bülow, R., Biffar, R., & Cardini, A. (2018). Procrustes-based geometric morphometrics on MRI images: An example of inter-operator bias in 3D landmarks and its impact on big datasets. *PLOS ONE, 13*(5), e0197675.

Damas, S., Cordón, O., & Ibáñez, O. (2020). Relationships Between the Skull and the Face for Forensic Craniofacial Superimposition. In S. Damas, O. Cordón, & O. Ibáñez (Eds.), *Handbook on Craniofacial Superimposition: The MEPROCS Project* (pp. 11-50). Cham: Springer International Publishing.

Davies, A. (1932). A Re-Survey of the Morphology of the Nose in Relation to Climate. *The Journal of the Royal Anthropological Institute of Great Britain and Ireland, 62*, 337-359.

Davy-Jow, S. L., Decker, S. J., & Ford, J. M. (2012). A simple method of nose tip shape validation for facial approximation. *Forensic science international, 214*(1), 208.e201-208.e203.

De Greef, S., Claes, P., Vandermeulen, D., Mollemans, W., Suetens, P., & Willems, G. (2006). Large-scale in-vivo Caucasian facial soft tissue thickness database for craniofacial reconstruction. *Forensic science international, 159*, S126-S146.

De Greef, S., Vandermeulen, D., Claes, P., Suetens, P., & Willems, G. (2009). The influence of sex, age and body mass index on facial soft tissue depths. *Forensic science, medicine, and pathology, 5*(2), 60-65.

Devor, E. J. (1987). Transmission of human craniofacial dimensions. *Journal of Craniofacial Genetics and Developmental Biology, 7*(2), 95.

Diamond, R., & Carey, S. (1986). Why faces are and are not special: an effect of expertise. *Journal of Experimental Psychology. General, 115*(2), 107-117.

Dias, P. E. M., Miranda, G. E., Beaini, T. L., & Melani, R. F. H. (2016). Practical Application of Anatomy of the Oral Cavity in Forensic Facial Reconstruction. *PLOS ONE, 11*(9), e0162732.

Dimberg, L., Bondemark, L., Söderfeldt, B., & Lennartsson, B. (2010). Prevalence of malocclusion traits and sucking habits among 3-year-old children. *Swedish Dental Journal, 34*(1), 35-42.

Domaracki, M., & Stephan, C. N. (2006). Facial soft tissue thicknesses in Australian adult cadavers. *Journal of Forensic Sciences, 51*(1), 5-10.

Dorfling, H. F., Lockhat, Z., Pretorius, S., Steyn, M., & Oettlé, A. C. (2018). Facial approximations: Characteristics of the eye in a South African sample. *Forensic science international, 286*, 46-53.

Drake, R. L., Vogl, W., Mitchell, A. W. M., & Richardson, P. (2017). *Gray's Basic Anatomy*: Elsevier.

Drgáčová, A., Dupej, J., & Veleminska, J. (2016). Facial soft tissue thicknesses in the present Czech population. *Forensic science international, 260*, 106. e101-106. e107.

Drosou, K., Price, C., & Brown, T. A. (2018). The kinship of two 12th Dynasty mummies revealed by ancient DNA sequencing. *Journal of Archaeological Science: Reports, 17*, 793-797.

Duane, T. D., Jaeger, E. A., & Tasman, W. S. (1982). *Duane's foundations of clinical ophthalmology* (Vol. 2): Philadelphia: Harper & Row.

Duke-Elder, S. (1961). The anatomy of the visual system. *A System of Ophthalmology, 2*, 363-382.

Edmonds, M. R. (1999). *Ancestral Geographies of the Neolithic: Landscape, Monuments and Memory*. London: Routledge.

Efremov, I. A. (1940). Taphonomy: a new branch of paleontology: Pan-American Geologist, v. 74.

Eichorn, D. H., & Bayley, N. (1962). Growth in head circumference from birth through young adulthood. *Child Development, 33*(2), 257-271.

Enlow, D. H., & Hans, M. G. (1996). *Essentials of facial growth*. Philadelphia: Saunders.

Evagorou, M., Erduran, S., & Mäntylä, T. (2015). The role of visual representations in scientific practices: from conceptual understanding and knowledge generation to 'seeing' how science works. *International Journal of STEM Education, 2*(1), 11.

Faakuu, E., Abaidoo, C. S., Appiah, A. K., & Tetteh, J. (2020). Morphological study of the external ear among the Dagaabas in the Upper West region of Ghana. *Scientific African, 8*, e00408.

Farkas, L. G. (1994). *Anthropometry of the head and face*. New York: Raven Press.

Farkas, L. G., Hreczko, T. A., Kolar, J. C., & Munro, I. R. (1985). Vertical and horizontal proportions of the face in young adult North American Caucasians: revision of neoclassical canons. *Plastic Reconstructive Surgery, 75*(3), 328-338.

Farkas, L. G., Ross, R. B., Posnick, J. C., & Indech, G. D. (1989). Orbital measurements in 63 hyperteloric patients: Differences between the anthropometric and cephalometric findings. *Journal of Cranio-Maxillofacial Surgery, 17*(6), 249-254.

Fayz, F., & Eslami, A. (1988). Determination of occlusal vertical dimension: A literature review. *The Journal of Prosthetic Dentistry, 59*(3), 321-323.

Fedosyutkin, B. A., & Nainys, J. V. (1993). The relationship of skull morphology to facial features. In M. Y. İşcan & R. P. Helmer (Eds.), *Forensic Analysis of the Skull: Craniofacial Analysis, Reconstruction, and Identification* (Vol. 199). New York: Wiley-Liss.

Ferrario, V. F., Sforza, C., Ciusa, V., Serrao, G., & Tartaglia, G. M. (1999). Morphometry of the normal human ear: a cross-sectional study from adolescence to mid-adulthood. *Journal of Craniofacial Genetics and Developmental Biology, 19*(4), 226-233.

Ferrario, V. F., Sforza, C., Schmitz, J. H., Ciusa, V., & Colombo, A. (2000a). Normal growth and development of the lips: a 3-dimensional study from 6 years to adulthood using a geometric model. *Journal of anatomy, 196 (Pt 3)*(Pt 3), 415-423.

Ferrario, V. F., Sforza, C., & Serrao, G. (2000b). A Three-Dimensional Quantitative Analysis of Lips in Normal Young Adults. *The Cleft Palate-Craniofacial Journal, 37*(1), 48-54.

Flower, H. I. (1996). *Ancestor Masks and Aristocratic Power in Roman Culture*: Clarendon Press.

Franciscus, R. G., & Long, J. C. (1991). Variation in human nasal height and breadth. *American Journal of Physical Anthropology, 85*(4), 419-427.

Fries, F. N., Youssef, P., Irwin, P. A., Tubbs, R. I., Loukas, M., & Tubbs, R. S. (2016). Comparing the left and right Whitnall's tubercles and their relation to the frontozygomatic suture: Application to symmetry following lateral orbital surgery. *Orbit, 35*(6), 305-308.

Fuentes, O. (2013). The depiction of the individual in prehistory: human representations in Magdalenian societies. *Antiquity, 87*(338), 985-1000.

Fuessinger, M. A., Schwarz, S., Neubauer, J., Cornelius, C.-P., Gass, M., Poxleitner, P., . . . Schlager, S. (2019). Virtual reconstruction of bilateral midfacial defects by using statistical shape modeling. *Journal of Cranio-Maxillofacial Surgery, 47*(7), 1054-1059.

Garlie, T. N., & Saunders, S. R. (1999). Midline facial tissue thicknesses of subadults from a longitudinal radiographic study. *Journal of Forensic Sciences, 44*(1), 61-67.

Gatliff, B. P. (1984). Facial sculpture on the skull for identification. *The American Journal of Forensic Medicine and Pathology, 5*(4), 327-332.

Gatliff, B. P., & Snow, C. C. (1979). From skull to visage. *The Journal of Biocommunication, 6*(2), 27-30.

George, R. M. (1987). The lateral craniographic method of facial reconstruction. *Journal of Forensic Sciences, 32*(5), 1305-1330.

George, R. M. (1993). Anatomical and artistic guidelines for forensic facial reconstruction. In M. Y. İşcan & R. P. Helmer (Eds.), *Forensic Analysis of the Skull: Craniofacial Analysis, Reconstruction, and Identification* (Vol. 199, pp. 215-227). New York: Wiley-Liss.

Gerasimov, M. M. (1955). *Vosstanovlenie lica po cerepu*. Moskva: Izdat: Akademii Nauk SSSR.

Gerasimov, M. M. (1971). *The Face Finder*. London: Hutchinson.

Ghosh, D., Amenta, N., & Kazhdan, M. (2010). Closed-form Blending of Local Symmetries. *Computer Graphics Forum, 29*(5), 1681-1688.

Giuffra, V., Panetta, D., Salvadori, P. A., & Fornaciari, G. (2014). A historical case of amelogenesis imperfecta: Giovanna of Austria, Grand Duchess of Tuscany (1547-1578). *European Journal of Oral Sciences, 122*(1), 1-6.

Glanville, E. V. (1969). Nasal shape, prognathism and adaptation in man. *American Journal of Physical Anthropology, 30*(1), 29-37.

Glob, P. V. (1969). *The Bog People: Iron-Age Man Preserved (translated from the Danish by R. Bruce-Mitford)*. New York: Cornell University Press.

Gold, J. M., Mundy, P. J., & Tjan, B. S. (2012). The perception of a face is no more than the sum of its parts. *Psychological science, 23*(4), 427-434.

Gonçalves, R. d. C., Raveli, D. B., & Pinto, A. d. S. (2011). Effects of age and gender on upper airway, lower airway and upper lip growth. *Brazilian Oral Research, 25*, 241-247.

Gower, J. C. (1975). Generalized procrustes analysis. *Psychometrika, 40*(1), 33-51.

Gray, L. (1965). The Deviated Nasal Septum—1—Ætiology. *The Journal of Laryngology & Otology, 79*(7), 567-575.

Grine, F. E., Gunz, P., Betti-Nash, L., Neubauer, S., & Morris, A. G. (2010). Reconstruction of the late Pleistocene human skull from Hofmeyr, South Africa. *J Hum Evol, 59*(1), 1-15.

Gunz, P., Mitteroecker, P., Neubauer, S., Weber, G. W., & Bookstein, F. L. (2009). Principles for the virtual reconstruction of hominin crania. *Journal of Human Evolution, 57*(1), 48-62.

Guo, J., Tan, J., Yang, Y., Zhou, H., Hu, S., Hashan, A., . . . Tang, K. (2014). Variation and signatures of selection on the human face. *Journal of Human Evolution, 75*, 143-152.

Gupta, A., Mithun, N. C., Rudolph, C., & Roy-Chowdhury, A. K. (2018, 23-27 July 2018). *Deep Learning Based Identity Verification in Renaissance Portraits.* Paper presented at the 2018 IEEE International Conference on Multimedia and Expo (ICME).

Guyomarc'h, P. (2011). *Reconstitution faciale par imagerie 3d: variabilité morphométrique et mise en oeuvre informatique.* (PhD). Bordeaux 1,

Guyomarc'h, P., Coqueugniot, H., Dutailly, B., & Couture-Veschambre, C. (2010). Anatomical placement of the human eyeball in the orbit – new metric data and guidelines proposal for facial identification. *The 79th annual meeting of the American Association of Physical Anthropologists, 141*.

Guyomarc'h, P., Dutailly, B., Charton, J., Santos, F., Desbarats, P., & Coqueugniot, H. (2014). Anthropological Facial Approximation in Three Dimensions (AFA3D): Computer-Assisted Estimation of the Facial Morphology Using Geometric Morphometrics. *Journal of Forensic Sciences, 59*.

Guyomarc'h, P., Dutailly, B., Couture, C., & Coqueugniot, H. (2012). Anatomical placement of the human eyeball in the orbit - validation using CT scans of living adults and prediction for facial approximation. *Journal of Forensic Sciences, 57*(5), 1271-1275.

Guyomarc'h, P., Veleminsky, P., Jaroslav, B., Lynnerup, N., Horák, M., Kučera, J., . . . Vellev, J. (2018). Facial approximation of Tycho Brahe's partial skull based on estimated data with TIVMI-AFA3D. *Forensic science international, 292*, 131-137.

Guyomarc'h, P., & Stephan, C. N. (2012). The validity of ear prediction guidelines used in facial approximation. *Journal of Forensic Sciences, 57*(6), 1427-1441.

Hadi, H., & Wilkinson, C. (2016). Estimation and reconstruction of facial creases based on skull crease morphology. *Australian Journal of Forensic Sciences, 50*(1), 42-56.

Haglund, W. D. (1998). Forensic 'art' in human identification. In J. G. Clement & D. L. Ranson (Eds.), *Craniofacial Identification in Forensic Medicine* (pp. 235-243). London: Arnold.

Haglund, W. D., & Reay, D. T. (1991). Use of facial approximation techniques in identification of Green River serial murder victims. *American Journal of Forensic Medicine and Pathology, 12*(2), 132-142.

Hammer, O., Harper, D., & Ryan, P. (2001). PAST: Paleontological Statistics Software Package for Education and Data Analysis. *Palaeontologia Electronica, 4*, 1-9.

Hancock, P. J. B., Bruce, V., & Burton, A. M. (2000). Recognition of unfamiliar faces. *Trends in Cognitive Sciences, 4*(9), 330-337.

Hansen, J. (2008). Bach im Spiegel der Medizin / Bach through the mirror of medicine: Ausstellungskatalog / Exhibition Catalogue. In. Eisenach: Bachhaus Eisenach.

Haraway, D. J. (1989). *Primate Visions: Gender, Race, and Nature in the World of Modern Science*: Routledge.

Harris, J. E. (1975). Genetic factors in the growth of the head. Inheritance of the craniofacial complex and malocclusion.

Hauspie, R. C., Susanne, C., & Defrise-Gussenhoven, E. (1985). Testing for the presence of genetic variance in factors of face measurements of Belgian twins. *Annals of Human Biology, 12*(5), 429-440.

Hayes, S. (2014). Facial approximation of 'Angel': Case specific methodological review. *Forensic science international, 237*, e30-e41.

Hayes, S. (2015). Faces in the museum: revising the methods of facial reconstructions. *Museum Management and Curatorship, 31*(3), 218-245.

Hayes, S. (2016). A geometric morphometric evaluation of the Belanglo 'Angel' facial approximation. *Forensic science international, 268*, e1-e12.

Hayes, S., & Milne, N. (2011). What's wrong with this picture? an experiment in quantifying accuracy in 2D portrait drawing. *Visual Communication, 10*(2), 149-174.

Hayes, S., Shoocongdej, R., Pureepatpong, N., Sangvichien, S., & Chintakanon, K. (2017). A Late Pleistocene woman from Tham Lod, Thailand: The influence of today on a face from the past. *Antiquity, 91*, 289-303.

He, Z. J., Jian, X. C., Wu, X. S., Gao, X., Zhou, S. H., & Zhong, X. H. (2009). Anthropometric measurement and analysis of the external nasal soft tissue in 119 young Han Chinese adults. *Journal of Craniofacial Surgery, 20*(5), 1347-1351.

Heathcote, J. A. (1995). Why do old men have big ears? *BMJ, 311*(7021), 1668.

Helmer, R. P., Rohricht, S., Petersen, D., & Mohr, F. (1993). Assessment of the reliability of facial reconstruction. In M. Y. İşcan & R. P. Helmer (Eds.), *Forensic Analysis of the Skull: Craniofacial Analysis, Reconstruction, and Identification* (Vol. 199). New York: Wiley-Liss.

Hershkovitz, I., & Yakar, R. (1988). Nahal Hemar Cave: The Modelled Skulls. *Atiqot, 18*, 59-63.

His, W. (1895). Anatomische Forschungen über Johann Sebastian Bach's Gebeine und Antlitz nebst Bemerkungen über dessen Bilder. *Abhandlungen der mathematisch-physikalischen Klasse der Königlichen Sachsischen Gesellschaft der Wissenschaften, 22*, 379-420.

Hoffman, B. E., McConathy, D. A., Coward, M., & Saddler, L. (1991). Relationship Between the Piriform Aperture and Interalar Nasal Widths in Adult Males. *Journal of Forensic Sciences, 36*(4), 1152-1161.

Holton, N. E., Yokley, T. R., Froehle, A. W., & Southard, T. E. (2014). Ontogenetic scaling of the human nose in a longitudinal sample: Implications for genus Homo facial evolution. *American Journal of Physical Anthropology, 153*(1), 52-60.

Houlton, T. M., Jooste, N., Uys, A., & Steyn, M. (2020). Lip height estimation in a southern African sample. *South African Dental Journal, 75*, 415-424.

Howells, W. W. (1973). *Cranial Variation in Man: A Study by Multivariate Analysis of Patterns of Difference Among Recent Human Populations*: Peabody Museum of Archaeology and Ethnology, Harvard University.

Huang, Y., Li, D., Qiao, L., Liu, Y., Peng, Q., Wu, S., . . . Grünewald, S. (2020). A genome-wide association study of facial morphology identifies novel genetic loci in Han Chinese. *Journal of Genetics and Genomics*.

Hubbe, M., Hanihara, T., & Harvati, K. (2009). Climate signatures in the morphological differentiation of worldwide modern human populations. *Anatomical Record (Hoboken), 292*(11), 1720-1733.

Huggins, C. (1937). The composition of bone and the function of the bone cell. *Physiological Reviews, 17*(1), 119-143.

Hunter, W. S., Balbach, D. R., & Lamphiear, D. E. (1970). The heritability of attained growth in the human face. *American Journal of Orthodontics, 58*.

Hwang, H. S., Park, M. K., Lee, W. J., Cho, J. H., Kim, B. K., & Wilkinson, C. (2012). Facial soft tissue thickness database for craniofacial reconstruction in Korean adults. *Journal of Forensic Sciences, 57*(6), 1442-1447.

İşcan, M. Y., & Steyn, M. (2013). *The human skeleton in forensic medicine* (3 ed.): Charles C Thomas Publisher, Limited.

Iskra, A., & Gabrijelčič, H. (2016). Eye-tracking analysis of face observing and face recognition. *Journal of Graphic Engineering and Design, 7*, 5-11.

Jimenez, G. A., Subías, S. M., & Romero, M. S. (2014). *The Archaeology of Bronze Age Iberia: Argaric Societies*: Taylor & Francis.

Jordanov, J. A. (2003). *Head reconstruction by the skull*. Sofia, Bulgaria: Marin Drinov Academic Publishing House.

Karl, R. (2015). Visualising the unknown knowns in archaeology: why prehistory must not always look the same. In K. J. Leskovar (Ed.), *Interpretierte Eisenzeiten. Fallstudien, Methoden, Theorie. Tagungsbeiträge der 6. Linzer Gespräche zur interpretativen Eisenzeitarchäologie* (Vol. 6, pp. 141-152). Linz.

Kenyon, K. M. (1956). Jericho and its Setting in Near Eastern History. *Antiquity, 30*(120), 184-197.

Kenyon, K. M. (1957). *Digging Up Jericho*. London: Ernest Benn Lmt.

Kim, K. D., Ruprecht, A., Wang, G., Lee, J. B., Dawson, D. V., & Vannier, M. W. (2005). Accuracy of facial soft tissue thickness measurements in personal computer-based multiplanar reconstructed computed tomographic images. *Forensic science international, 155*(1), 28-34.

Kim, S., Lee, W. J., Cho, J., Wilkinson, C., Choi, C., & Lee, S. (2020). An investigation of environmental factors influencing quantitative accuracy and recognition rate of craniofacial reconstructions. *Journal of Environmental Biology, 41*(3), 539-548.

Kim, S. R., Lee, K. M., Cho, J. H., & Hwang, H. S. (2016). Three-dimensional prediction of the human eyeball and canthi for craniofacial reconstruction using cone-beam computed tomography. *Forensic science international, 261*, 164.e161-164.e168.

King, T. E., Fortes, G. G., Balaresque, P., Thomas, M. G., Balding, D., Delser, P. M., . . . Schürer, K. (2014). Identification of the remains of King Richard III. *Nature Communications, 5*(1), 5631.

Klingenberg, C. P. (2011). MorphoJ: an integrated software package for geometric morphometrics. *Molecular ecology resources, 11*(2), 353-357.

Knipper, C., Rihuete Herrada, C., Voltas, J., Held, P., Lull, V., Micó, R., . . . Alt, K. W. (2020). Reconstructing Bronze Age diets and farming strategies at the early Bronze Age sites of La Bastida and Gatas (southeast Iberia) using stable isotope analysis. *PLOS ONE, 15*(3), e0229398.

Kohn, L. A. P. (1991). The role of genetics in craniofacial morphology and growth. *Annual Review of Anthropology, 20*(1), 261-278.

Kollman, J., & Bückly, W. (1898). Die Persistenz der Rassen und die Reconstruction der Physiognomie prahistorischer Schädel. *Archiv für Anthropologie, 25*, 329-359.

Kraus, D., Formoly, E., Iblher, N., Stark, G. B., & Penna, V. (2019). A morphometric study of age- and sex-dependent changes in eyebrow height and shape☆. *Journal of Plastic, Reconstructive & Aesthetic Surgery, 72*(6), 1012-1019.

Krogman, W. M. (1946). *The Reconstruction of the Living Head from the Skull*: FBI Law Enforcement Bulletin.

Krogman, W. M. (1962). *Human Skeleton in Forensic Medicine*: Thomas.

Krogman, W. M., & İşcan, M. Y. (1986). *The human skeleton in forensic medicine*. Springfield: Charles C. Thomas, Publisher.

Kuhn, T. S. (1996). *The Structure of Scientific Revolutions*. Chicago and London: The University of Chicago Press.

Kujit, I. (2000). Keeping the peace: Ritual, skull caching, and community integration in the Levantine Neolithic. In I. Kujit (Ed.), *Life in Neolithic Farming Communities: Social Organization, Identity, and Differentiation*. New York: Kluwer Academic / Plenum Publishers.

Kujit, I. (2001). Place, death and the transmission of social memory in early agricultural communities of the Near Eastern Pre-Pottery Neolithic. *Archaeological Papers of the American Anthropological Association, 10*, 80-99.

Kujit, I. (2008). The regeneration of life: Neolithic structures of symbolic remembering and forgetting. *Current Anthropology, 49*(2), 171-197.

Kumar, A., Kanojia, R. K., & Saili, A. (2014). Skin dimples. *International Journal of Dermatology, 53*(7), 789-797.

Lacruz, R. S., Stringer, C. B., Kimbel, W. H., Wood, B., Harvati, K., O'Higgins, P., . . . Arsuaga, J.-L. (2019). The evolutionary history of the human face. *Nature Ecology & Evolution, 3*(5), 726-736.

Larrabee, W. F., Makielski, K. H., & Henderson, J. L. (2004). *Surgical Anatomy of the Face*: Lippincott Williams & Wilkins.

Latta, G. H. (1988). The midline and its relation to anatomic landmarks in the edentulous patient. *The Journal of Prosthetic Dentistry, 59*(6), 681-683.

Lebedinskaya, G. (1998). Rekonstrukcia lica po cerepu (metodiceskoje rukovodstvo). *Moskva: Staryj sad.*

Lee, K. M., Lee, W. J., Cho, J. H., & Hwang, H. S. (2014). Three-dimensional prediction of the nose for facial reconstruction using cone-beam computed tomography. *Forensic science international, 236*, 194.e191-195.

Lee, M. K., Shaffer, J. R., Leslie, E. J., Orlova, E., Carlson, J. C., Feingold, E., . . . Weinberg, S. M. (2017). Genome-wide association study of facial morphology reveals novel associations with FREM1 and PARK2. *PLOS ONE, 12*(4), e0176566.

Lee, U. Y., Kim, H., Song, J.-K., Kim, D.-H., Ahn, K.-J., & Kim, Y.-S. (2020). Assessment of nasal profiles for forensic facial approximation in a modern Korean population of known age and sex. *Legal Medicine, 42*, 101646.

Lee, W. J., & Wilkinson, C. (2016). The unfamiliar face effect on forensic craniofacial reconstruction and recognition. *Forensic science international, 269*, 21-30.

Lee, W. J., Wilkinson, C., Hwang, H.-S., & Lee, S.-M. (2015). Correlation Between Average Tissue Depth Data and Quantitative Accuracy of Forensic Craniofacial Reconstructions Measured by Geometric Surface Comparison Method. *Journal of Forensic Sciences, 60*.

Lee, W. J., Wilkinson, C., & Hwang, H. S. (2012). An accuracy assessment of forensic computerized facial reconstruction employing cone-beam computed tomography from live subjects. *Journal of Forensic Sciences, 57*(2), 318-327.

Lefohn, A., Budge, B., Shirley, P., Caruso, R., & Reinhard, E. (2003). An Ocularist's Approach to Human Iris Synthesis. *Computer Graphics and Applications, IEEE, 23*, 70-75.

Lessard, M.-L., & Daniel, R. K. (1985). Surgical anatomy of septorhinoplasty. *Archives of Otolaryngology, 111*(1), 25-29.

Lindsten, R. (2002). The effect of maceration on the dental arches and the transverse cranial dimensions: a study on the pig. *The European Journal of Orthodontics, 24*(6), 667-676.

Lippi, D., Pierleoni, F., & Franchi, L. (2011). Retrognathic maxilla in "Habsburg jaw": Skeletofacial analysis of Joanna of Austria (1547–1578). *The Angle Orthodontist, 82*(3), 387-395.

Liu, F., Van Der Lijn, F., Schurmann, C., Zhu, G., Chakravarty, M. M., Hysi, P. G., . . . Ikram, M. A. (2012). A genome-wide association study identifies five loci influencing facial morphology in Europeans. *PLoS Genet, 8*(9), e1002932.

Liu, F., Visser, M., Duffy, D. L., Hysi, P. G., Jacobs, L. C., Lao, O., . . . Wollstein, A. (2015). Genetics of skin color variation in Europeans: genome-wide association studies with functional follow-up. *Human genetics, 134*(8), 823-835.

Lobb, W. K. (1987). Craniofacial morphology and occlusal variation in monozygous and dizygous twins. *The Angle Orthodontist, 57*.

Lull, V. (1979). *La cultura de El Argar: ecología, asentamientos, economía y sociedad.* (PhD thesis). Universidad de Barcelona,

Lull, V. (1983). *La "cultura" de El Argar (un modelo para el estudio de las formaciones económico-sociales prehistóricas).* Madrid: Akal.

Lull, V. (1988). Hacia una teoría de la representación en arqueología. *Revista de Occidente, 81*, 62-76.

Lull, V. (2017). ¿De qué se ocupa la arqueología? *Marq, arqueología y museos*(8), 9-22.

Lull, V., & Estévez, J. (1986). Propuesta metodológica para el estudio de las necrópolis argáricas. In *Homenaje a Luis Siret (1934-1984)*. Sevilla: Consejería de Cultura de la Junta de Andalucía.

Lull, V., Micó, R., Rihuete Herrada, C., & Risch, R. (2005). Property Relations in the Bronze Age of South-western Europe: an Archaeological Analysis of Infant Burials from El Argar (Almeria, Spain). *Proceedings of the Prehistoric Society, 71*, 247-268.

Lull, V., Micó, R., Rihuete Herrada, C., & Risch, R. (2009). El yacimiento arqueológico de La Bastida (Totana): pasado y presente de las investigaciones. *Cuadernos de la Santa, 11*, 205-217.

Lull, V., Micó, R., Rihuete Herrada, C., & Risch, R. (2011a). El Argar and the beginning of class society in the western Mediterranean. In S. Hansen & J. Müller (Eds.), *Sozialarchäologische Perspektiven: gesellschaftlicher Wandel 5000-1500 v. Chr. zwischen Atlantik und Kaukasus (Archäologie in Eurasien 24, Deutsches Archäologisches Institut, Eurasien Abteilung)*. Mainz: Philipp von Zabern.

Lull, V., Micó, R., Rihuete Herrada, C., & Risch, R. (2011b). "Proyecto La Bastida": economía, urbanismo y territorio de una capital argárica. *Verdolay. Revista del Museo Arqueológico de Murcia, 13*(3), 57-70.

Lull, V., Micó, R., Rihuete Herrada, C., & Risch, R. (2013a). Funerary practices and kinship in an Early Bronze Age society: a Bayesian approach applied to the radiocarbon dating of Argaric double tombs. *Journal of Archaeological Science, 40*(12), 4626-4634.

Lull, V., Micó, R., Rihuete Herrada, C., & Risch, R. (2013b). *Political collapse and social change at the end of El Argar.* Paper presented at the 1600 – Kultureller Umbruch im Schatten des Thera-Ausbruchs? 4. Mitteldeutscher Archäologentag vom 14. bis 16. Oktober 2011 in Halle (Saale) / 1600 – Cultural

change in the shadow of the Thera-Eruption?, 4th Archaeological Conference of Central Germany October 14–16, 2011 in Halle (Saale), Halle (Saale).

Lull, V., Micó, R., Rihuete Herrada, C., & Risch, R. (2014a). The La Bastida fortification: new light and new questions on Early Bronze Age societies in the western Mediterranean. *Antiquity, 88*(340), 395.

Lull, V., Micó, R., Rihuete Herrada, C., & Risch, R. (2016a). Argaric Sociology: Sex and Death. *Complutum, 27*(1), 31-62.

Lull, V., Micó, R., Rihuete Herrada, C., Risch, R., Celdrán Beltrán, E., Fregeiro, M. I., . . . Velasco Felipe, C. (2016b). La Almoloya (Pliego-Mula, Murcia): palacios y élites gobernantes en la Edad del Bronce. In J. A. Zapata Parra (Ed.), *El legado de Mula en la Historia* (pp. 39-59): Ayuntamiento de Mula, Integral. Sociedad para el Desarrollo Rural.

Lull, V., Micó, R., Rihuete Herrada, C., Risch, R., Celdrán Beltrán, E., Fregeiro Morador, M. I., . . . Velasco Felipe, C. (2013c). *Memória actuación arqueológica La Almoloya de Pliego, Murcia (Report)*. Universidad Autónoma de Barcelona.

Lull, V., Micó, R., Rihuete Herrada, C., Risch, R., Celdrán Beltrán, E., Fregeiro Morador, M. I., . . . Velasco Felipe, C. (2014b). *Memória actuación arqueológica La Almoloya de Pliego, Murcia (Report)*. Universidad Autónoma de Barcelona.

Lull, V., Micó, R., Rihuete Herrada, C., Risch, R., Celdrán Beltrán, E., Fregeiro Morador, M. I., . . . Velasco Felipe, C. (2015a). *La Almoloya (Pliego, Murcia). Ruta Argárica. Guías Arqueológicas. nº2*.

Lull, V., Micó, R., Rihuete Herrada, C., Risch, R., Celdrán Beltrán, E., Fregeiro Morador, M. I., . . . Velasco Felipe, C. (2015b). *Memória actuación arqueológica La Almoloya de Pliego, Murcia (Report)*. Universidad Autónoma de Barcelona.

Lull, V., Micó, R., Rihuete Herrada, C., Risch, R., Celdrán Beltrán, E., Fregeiro Morador, M. I., . . . Velasco Felipe, C. (2016c). *Memória actuación arqueológica La Almoloya de Pliego, Murcia (Report)*. Universidad Autónoma de Barcelona.

Lundström, A., & McWilliam, J. (1988). Comparison of some cephalometric distances and corresponding facial proportions with regard to heritability. *The European Journal of Orthodontics, 10*(1), 27-29.

Lyman, R. L. (2010). What taphonomy is, what it isn't, and why taphonomists should care about the difference. *Journal of Taphonomy, 8*(1), 1-16.

Macho, G. A. (1986). An appraisal of plastic reconstruction of the external nose. *Journal of Forensic Sciences, 31*(4), 1391-1403.

Macho, G. A. (1989). Descriptive morphological features of the nose—an assessment of their importance for plastic reconstruction. *Journal of Forensic Sciences, 34*(4), 902-911.

Mahoney, G., & Wilkinson, C. (2012). Computer-generated facial depiction. In C. Wilkinson & C. Rynn (Eds.), *Craniofacial Identification* (pp. 222-237). Cambridge: Cambridge University Press.

Mala, P. Z. (2013). Pronasale Position: An Appraisal of Two Recently Proposed Methods for Predicting Nasal Projection in Facial Reconstruction. *Journal of Forensic Sciences, 58*(4), 957-963.

Mala, P. Z., & Veleminska, J. (2016). Vertical Lip Position and Thickness in Facial Reconstruction: A Validation of Commonly Used Methods for Predicting the Position and Size of Lips. *Journal of Forensic Sciences, 61*(4), 1046-1054.

Mala, P. Z., & Veleminska, J. (2018). Eyeball Position in Facial Approximation: Accuracy of Methods for Predicting Globe Positioning in Lateral View. *Journal of Forensic Sciences, 63*(1), 221-226.

Maltais Lapointe, G., Lynnerup, N., & Hoppa, R. D. (2016). Validation of the New Interpretation of Gerasimov's Nasal Projection Method for Forensic Facial Approximation Using CT Data. *Journal of Forensic Sciences, 61*(S1), S193-S200.

Mangino, M. (2014). Genomics of ageing in twins. *Proceedings of the Nutrition Society, 73*(4), 526-531.

Manhein, M. H., Listi, G. A., Barsley, R. E., Musselman, R., Barrow, N. E., & Ubelaker, D. H. (2000). In vivo facial tissue depth measurements for children and adults. *Journal of Forensic Sciences, 45*(1), 48-60.

Marano, L. A., & Fridman, C. (2019). DNA phenotyping: current application in forensic science. *Research and Reports in Forensic Medical Science*(9), 1-8.

McGregor, J. H. (1926). Restoring Neanderthal Man. *Natural History, 26*, 288-293.

Meijerman, L., van der Lugt, C., & Maat, G. J. (2007). Cross-sectional anthropometric study of the external ear. *Journal of Forensic Sciences, 52*(2), 286-293.

Merkel, F. (1900). Reconstruction der büste eines Bewohners des Leinegaues. *Archiv für Anthropologie, 26*, 449-457.

Miranda, G. E., Wilkinson, C., Roughley, M., Beaini, T. L., & Melani, R. F. H. (2018). Assessment of accuracy and recognition of three-dimensional computerized forensic craniofacial reconstruction. *PLOS ONE, 13*(5), e0196770.

Modabber, A., Galster, H., Peters, F., Möhlhenrich, S. C., Kniha, K., Knobe, M., . . . Ghassemi, A. (2018). Three-Dimensional Analysis of the Ear Morphology. *Aesthetic Plastic Surgery, 42*(3), 766-773.

Molina, F., Rodríguez-Ariza, M. O., Jiménez, S., & Botella, M. (2003). La sepultura 121 del yacimiento argárico de el Castellón Alto (Galera, Granada). *Trabajos de prehistoria, 60*(1), 153-158.

Moore, D. S., McCabe, G. P., & Craig, B. A. (2014). *Introduction to the Practice of Statistics* (8th ed.). New York: W. H. Freeman and Company.

Moser, S. (1992). The visual language of archaeology: a case study of the Neanderthals. *Antiquity, 66*(253), 831-844.

Moses, Y., Adini, Y., & Ullman, S. (1994). *Face recognition: The problem of compensating for changes in illumination direction.* Paper presented at the European Conference on Computer Vision, Berlin, Heidelberg.

Mossey, P. A. (1999a). The heritability of malocclusion: Part 1. Genetics, principles and terminology. *British Journal of Orthodontics, 26*(2), 103-113.

Mossey, P. A. (1999b). The heritability of malocclusion: Part 2. The influence of genetics in malocclusion. *British Journal of Orthodontics, 26*(3), 195-203.

Musgrave, J., Neave, R., & Prag, A. (1995). Seven faces from Grave Circle B at Mycenae. *The Annual of the British School at Athens, 90*.

Nakata, M., Yu, P.-L., Davis, B., & Nance, W. E. (1974). Genetic determinants of cranio-facial morphology: a twin study. *Annals of human genetics, 37*(4), 431-443.

Nanda, R. S., & Ghosh, J. (1995). Facial soft tissue harmony and growthin orthodontic treatment. *Seminars in Orthodontics, 1*(2), 67-81.

Nawrocki, S. P. (2016). Forensic taphonomy. In S. Blau & D. H. Ubelaker (Eds.), *Handbook of Forensic Anthropology and Archaeology* (2nd ed.). New York: Routledge.

Neave, R. (1998). Age changes in the face in adulthood. In J. G. Clement & D. L. Ranson (Eds.), *Craniofacial Identification in Forensic Medicine*. Sydney: Arnold Publications.

Nellhaus, G. (1968). Head circumference from birth to eighteen years. Practical composite international and interracial graphs. *Pediatrics, 41*(1), 106-114.

Neubauer, S., Gunz, P., Mitteroecker, P., & Weber, G. (2004). Three-dimensional digital imaging of the partial Australopithecus africanus endocranium MLD 37/38. *Canadian Association of Radiologists journal = Journal l'Association canadienne des radiologistes, 55*, 271-278.

Ngeow, W. C., & Aljunid, S. T. (2009). Craniofacial anthropometric norms of Malays. *Singapore Medical Journal, 50*(5), 525-528.

Oliart, C. (2021). *Aproximación osteoarqueológica a las condiciones de vida de una comunidad argárica. Análisis de las colecciones esqueléticas de La Bastida (Totana, Murcia)*. (PhD Dissertation). Universitat Autònoma de Barcelona,

Oyen, O. J., Rice, R. W., & Samuel Cannon, M. (1979). Browridge structure and function in extant primates and Neanderthals. *American Journal of Physical Anthropology, 51*(1), 83-95.

Ozdemir, S. T., Sigirli, D., Ercan, I., & Cankur, N. S. (2009). Photographic facial soft tissue analysis of healthy Turkish young adults: anthropometric measurements. *Aesthetic Plastic Surgery, 33*(2), 175-184.

Paternoster, L., Zhurov, A. I., Toma, A. M., Kemp, J. P., Pourcain, B. S., Timpson, N. J., . . . Smith, G. D. (2012). Genome-wide association study of three-dimensional facial morphology identifies a variant in PAX3 associated with nasion position. *The American Journal of Human Genetics, 90*(3), 478-485.

Pazos, J., Suazo, I., Cantin, M., & Matamala, D. (2008). Sexual Dimorphism in the Nose Morphotype in Adult Chilean. *International Journal of Morphology, 26*, 537-542.

Peacock, Z. S., Klein, K. P., Mulliken, J. B., & Kaban, L. B. (2014). The Habsburg Jaw-re-examined. *American Journal of Medical Genetics. Part A, 164a*(9), 2263-2269.

Pessa, J. E., Zadoo, V. P., Adrian, E. K. J., Yuan, C. H., Aydelotte, J., & Garza, J. R. (1998a). Variability of the Midfacial Muscles: Analysis of 50 Hemifacial Cadaver Dissections. *Plastic and Reconstructive Surgery, 102*(6), 1888-1893.

Pessa, J. E., Zadoo, V. P., Garza, P. A., Adrian Jr., E. K., Dewitt, A. I., & Garza, J. R. (1998b). Double or bifid zygomaticus major muscle: Anatomy, incidence, and clinical correlation. *Clinical Anatomy, 11*(5), 310-313.

Pevsner, J. (2019). Leonardo da Vinci's studies of the brain. *The Lancet, 393*(10179), 1465-1472.

Phillips, V., & Smuts, N. (1996). Facial reconstruction: utilization of computerized tomography to measure facial tissue thickness in a mixed racial population. *Forensic science international, 83*(1), 51-59.

Plotly Technologies Inc. (2015). Collaborative data science. Montréal, QC. Retrieved from https://plot.ly

Pluym, J. V., Shan, W., Taher, Z., Beaulieu, C., Plewes, C., Peterson, A., . . . Bamforth, J. (2007). Use of magnetic resonance imaging to measure facial soft tissue depth. *The Cleft Palate-Craniofacial Journal, 44*(1), 52-57.

Podro, M. (1998). *Depiction*. New Have & London: Yale University Press.

Pokines, J., & Symes, S. A. (2013). *Manual of Forensic Taphonomy*. Boca Raton: CRC Press.

Ponce De León, M. S., & Zollikofer, C. P. E. (1999). New evidence from Le Moustier 1: Computer-assisted reconstruction and morphometry of the skull. *The Anatomical Record, 254*(4), 474-489.

Prag, J., & Neave, R. (1997). *Making Faces: Using Forensic and Archaeological Evidence*: Texas A & M University Press.

Prahl-Andersen, B., Ligthelm-Bakker, A. S., Wattel, E., & Nanda, R. (1995). Adolescent growth changes in soft tissue profile. *American Journal of Orthodontics and Dentofacial Orthopedics, 107*(5), 476-483.

Proffit, W. R., Fields Jr, H. W., & Sarver, D. M. (2006). *Contemporary orthodontics*: Elsevier Health Sciences.

Prokopec, M., & Ubelaker, D. H. (2002). Reconstructing the shape of the nose according to the skull. *Forensic Science Communications, 4*(1).

Purkait, R., & Singh, P. (2007). Anthropometry of the normal human auricle: a study of adult Indian men. *Aesthetic Plastic Surgery, 31*(4), 372-379.

Quibell, J. E. (1909). *Excavations at Saqqara, 1907-1908*: Le Caire, Imprimerie de l'Institut Français d'Archéologie Orientale.

Ramanathan, N., Chellappa, R., & Chowdhury, A. K. R. (2004, 24-27 Oct. 2004). *Facial similarity across age, disguise, illumination and pose.* Paper presented at the 2004 International Conference on Image Processing, 2004. ICIP '04.

Renwick, N. (2012). Ear lobe morphology and its relationship to the mastoid process. *Centre for Anatomy and Human Identification, University of Dundee, Dundee. AXIS: The Online Journal of CAHId, 12*.

Rhine, J. S., & Moore, C. E. (1984). *Tables of facial tissue thickness of American Caucasoids in forensic anthropology.*: Maxwell Museum Technical series.

Richards, A. R. (2003). Argument and Authority in the Visual Representations of Science. *Technical Communication Quarterly, 12*(2), 183-206.

Richmond, S., Howe, L. J., Lewis, S., Stergiakouli, E., & Zhurov, A. (2018). Facial Genetics: A Brief Overview. *Frontiers in Genetics, 9*(462).

Ridel, A. F., Demeter, F., Liebenberg, J., L'Abbé, E. N., Vandermeulen, D., & Oettlé, A. C. (2018). Skeletal dimensions as predictors for the shape of the nose in a South African sample: A cone-beam computed tomography (CBCT) study. *Forensic science international, 289*, 18-26.

Ridley, G. (2005). *Clara's Grand Tour: Travels with a Rhinoceros in Eighteenth-century Europe*: Grove Press.

Robinson, C., & Terhune, C. E. (2017). Error in geometric morphometric data collection: Combining data from multiple sources. *Am J Phys Anthropol, 164*(1), 62-75.

Rohlf, F. J., & Bookstein, F. L. (1988). *Proceedings of the Michigan Morphometrics Workshop*.

Rohlf, F. J., & Slice, D. (1990). Extensions of the Procrustes Method for the Optimal Superimposition of Landmarks. *Systematic Zoology, 39*(1), 40-59.

Rose, B., & Lovink, M. (2014). Recreating Roman wax masks. *Expedition Magazine, 56*(3), 34-37.

Rosenstein, T., Talebzadeh, N., & Pogrel, M. A. (2000). Anatomy of the lateral canthal tendon. *Oral Surgery, Oral Medicine, Oral Pathology, Oral Radiology, and Endodontology, 89*(1), 24-28.

Roughley, M. A., & Wilkinson, C. M. (2019). The Affordances of 3D and 4D Digital Technologies for Computerized Facial Depiction. In P. M. Rea (Ed.), *Biomedical Visualisation* (Vol. 2, pp. 87-101). Cham: Springer International Publishing.

Rubens, B. C., & West, R. A. (1989). Ptosis of the chin and lip incompetence: Consequences of lost mentalis muscle support. *Journal of Oral and Maxillofacial Surgery, 47*(4), 359-366.

Ruhland, K., Andrist, S., Badler, J., Peters, C., Badler, N., Gleicher, M., . . . McDonnell, R. (2014). *Look me in the eyes: A survey of eye and gaze animation for virtual agents and artificial systems*. Paper presented at the Eurographics 2014, Strasbourg, France.

Russell, M. D., Brown, T., Garn, S. M., Giris, F., Turkel, S., İşcan, M. Y., . . . Živanović, S. (1985). The Supraorbital Torus: "A Most Remarkable Peculiarity" [and Comments and Replies]. *Current Anthropology, 26*(3), 337-360.

Rynn, C., Balueva, T., & Veselovskaya, E. (2012). Relationships between the skull and face. In C. Wilkinson & C. Rynn (Eds.), *Craniofacial Identification* (pp. 193-202). Cambridge: Cambridge University Press.

Rynn, C., & Wilkinson, C. (2006). Appraisal of traditional and recently proposed relationships between the hard and soft dimensions of the nose in profile. *American Journal of Physical Anthropology, 130*(3), 364-373.

Rynn, C., Wilkinson, C., & Peters, H. (2010). Prediction of nasal morphology from the skull. *Forensic science, medicine, and pathology, 6*, 20-34.

Sahni, D., Jit, I., Gupta, M., Singh, P., Suri, S., & Sanjeev, K. (2002). Preliminary study on facial soft tissue thickness by magnetic resonance imaging in Northwest Indians. *Forensic Science Communications, 4*(1).

Saitou, N., & Nei, M. (1987). The neighbor-joining method: a new method for reconstructing phylogenetic trees. *Molecular Biology and Evolution, 4*(4), 406-425.

Salvi, S. M., Akhtar, S., & Currie, Z. (2006). Ageing changes in the eye. *Postgraduate medical journal, 82*(971), 581-587.

San Juan, R. M. (2018). Chapter 4 - Gaetano Zumbo's anatomical wax model: From skull to cranium. In C. Ambrosio & W. MacLehose (Eds.), *Progress in Brain Research* (Vol. 243, pp. 75-105): Elsevier.

Sanders, K. (2009). *Bodies in the Bog and the Archaeological Imagination*. Chicago and London: The University of Chicago Press.

Sanín Matías, M., & Serrulla Rech, F. (2017). Informe antropológico forense: aproximación facial: proceso de aproximación facial forense. *Cadernos do Laboratorio Xeolóxico de Laxe: Revista de xeoloxía galega e do hercínico peninsular, 39*, 73-88.

Sarilita, E., Rynn, C., Mossey, P. A., Black, S., & Oscandar, F. (2018). Nose profile morphology and accuracy study of nose profile estimation method in Scottish subadult and Indonesian adult populations. *International Journal of Legal Medicine, 132*(3), 923-931.

Schlager, S. (2013). *Soft-tissue reconstruction of the human nose: population differences and sexual dimorphism.* (PhD). Albert-Ludwigs-Universität Freiburg,

Schlager, S. (2017). Chapter 9 - Morpho and Rvcg – Shape Analysis in R: R-Packages for Geometric Morphometrics, Shape Analysis and Surface Manipulations. In G. Zheng, S. Li, & G. Székely (Eds.), *Statistical Shape and Deformation Analysis* (pp. 217-256): Academic Press.

Schlager, S., Profico, A., Di Vincenzo, F., & Manzi, G. (2018). Retrodeformation of fossil specimens based on 3D bilateral semi-landmarks: Implementation in the R package "Morpho". *PLOS ONE, 13*(3).

Schlager, S., & Rüdell, A. (2015). Analysis of the human osseous nasal shape—population differences and sexual dimorphism. *American Journal of Physical Anthropology, 157*(4), 571-581.

Schlager, S., & Wittwer-Backofen, U. (2013). Images in Paleoanthropology: Facing Our Ancestors. In W. Henke & I. Tattersall (Eds.), *Handbook of Paleoanthropology* (pp. 1-23). Berlin, Heidelberg: Springer Berlin Heidelberg.

Schmandt-Besserat, D. (2013). The Plastered Skulls. In D. Schmandt-Besserat (Ed.), *Symbols at 'Ain Ghazal ('Ain Ghazal Excavation Reports Vol. 3)*. Berlin: Ex-oriente.

Schmidlin, E. J., Steyn, M., Houlton, T. M. R., & Briers, N. (2018). Facial ageing in South African adult males. *Forensic science international, 289*, 277-286.

Schmidt, K., & Cohn, J. (2001). Human facial expressions as adaptations: Evolutionary questions in facial expression. *American Journal of Physical Anthropology, 116*, 3-24.

Schnalke, T. (1995). *Diseases in Wax: The History of the Medical Moulage*: Quintessence Publishing Company.

Schultz, A. H. (1918). Relation of the external nose to the bony nose and nasal cartilages in whites and negroes. *American Journal of Physical Anthropology, 1*(3), 329-338.

Schwartz, J. H., & Tattersall, I. (2000). The human chin revisited: what is it and who has it? *Journal of Human Evolution, 38*(3), 367-409.

Seltzer, A. P. (1944). The nasal septum: Plastic repair of the deviated septum associated with a deflected tip. *Archives of Otolaryngology, 40*(6), 433-444.

Semper-Hogg, W., Fuessinger, M. A., Schwarz, S., Ellis, E., Cornelius, C.-P., Probst, F., . . . Schlager, S. (2017). Virtual reconstruction of midface defects using statistical shape models. *Journal of Cranio-Maxillofacial Surgery, 45*(4), 461-466.

Senck, S., Coquerelle, M., Weber, G. W., & Benazzi, S. (2013). Virtual Reconstruction of Very Large Skull Defects Featuring Partly and Completely Missing Midsagittal Planes. *The Anatomical Record, 296*(5), 745-758.

Sequenzia, G., Allegra, D., Fatuzzo, G., Milotta, F. L. M., Stanco, F., & Oliveri, S. M. (2020). A method for similarity assessment between death masks and portraits through linear projection: The case of Vincenzo Bellini. *Digital Applications in Archaeology and Cultural Heritage, 17*, e00144.

Serrulla Rech, F., & Sanin Matias, M. (2017). Forensic anthropological report of elba. *Cadernos do Laboratorio Xeolóxico de Laxe: Revista de xeoloxía galega e do hercínico peninsular, 39*, 35-72.

Sforza, C., Grandi, G., Binelli, M., Dolci, C., De Menezes, M., & Ferrario, V. F. (2010). Age- and sex-related changes in three-dimensional lip morphology. *Forensic science international, 200*(1), 182.e181-182.e187.

Sforza, C., Grandi, G., Binelli, M., Tommasi, D. G., Rosati, R., & Ferrario, V. F. (2009a). Age- and sex-related changes in the normal human ear. *Forensic science international, 187*(1-3), 110.e111-117.

Sforza, C., Grandi, G., Catti, F., Tommasi, D., Ugolini, A., & Ferrario, V. (2009b). Age- and sex-related changes in the soft tissues of the orbital region. *Forensic science international, 185*, 115.e111-118.

Sforza, C., Grandi, G., De Menezes, M., Tartaglia, G. M., & Ferrario, V. F. (2011). Age- and sex-related changes in the normal human external nose. *Forensic Sci Int, 204*(1-3), 205.e201-209.

Shaffer, J. R., Orlova, E., Lee, M. K., Leslie, E. J., Raffensperger, Z. D., Heike, C. L., . . . Nidey, N. L. (2016). Genome-wide association study reveals multiple loci influencing normal human facial morphology. *PLOS Genetics, 12*(8), e1006149.

Shearer, B. M., Cooke, S. B., Halenar, L. B., Reber, S. L., Plummer, J. E., Delson, E., & Tallman, M. (2017). Evaluating causes of error in landmark-based data collection using scanners. *PLOS ONE, 12*(11), e0187452.

Short, L. J., Khambay, B., Ayoub, A., Erolin, C., Rynn, C., & Wilkinson, C. (2014). Validation of a computer modelled forensic facial reconstruction technique using CT data from live subjects: A pilot study. *Forensic science international, 237*, 147.e141-147.e148.

Sills, J. D. (1994). Computer photographic skull reconstruction (methods used in facial restoration). In L. G. Farkas (Ed.), *Anthropometry of the head and face*. New York: Raven Press.

Simmons-Ehrhardt, T. L., Monson, K. L., Flint, T., & Saunders, C. P. (2020). Quantitative accuracy and 3D biometric matching of 388 statistically estimated facial approximations of live subjects. *Forensic Imaging, 21*, 200377.

Singh, S. P., Utreja, A., & Chawla, H. S. (2008). Distribution of malocclusion types among thumb suckers seeking orthodontic treatment. *J Indian Soc Pedod Prev Dent, 26 Suppl 3*, S114-117.

Smith, K. (2018). Portraits, Likenesses, Composites? Facial Difference in Forensic Art. In P. Skinner & E. Cock (Eds.), *Approaching Facial Difference: Past and Present* (pp. 84-111). London: Bloomsbury Academic.

Smith, K., Roughley, M., Harris, S., Wilkinson, C., & Palmer, E. (2020). From Ta-Kesh to Ta-Kush: The affordances of digital, haptic visualisation for heritage accessibility. *Digital Applications in Archaeology and Cultural Heritage, 19*, e00159.

Snell, R. S., & Lemp, M. A. (2013). *Clinical Anatomy of the Eye*. Somerset: Wiley.

Snow, C. C., Gatliff, B. P., & McWilliams, K. R. (1970). Reconstruction of facial features from the skull: An evaluation of its usefulness in forensic anthropology. *American Journal of Physical Anthropology, 33*(2), 221-227.

Song, W. C., Kim, S. H., Paik, D. J., Han, S. H., Hu, K. S., Kim, H. J., & Koh, K. S. (2007). Location of the infraorbital and mental foramen with reference to the soft-tissue landmarks. *Plastic Reconstructive Surgery, 120*(5), 1343-1347.

Sperber, G. H. (2017). Dental Wear: Attrition, Erosion, and Abrasion-A Palaeo-Odontological Approach. *Dentistry journal, 5*(2), 19.

Spindler, K. (1994). *The Man in the Ice: the discovery of a 5,000-year-old body reveals the secrets of the Stone Age*. New York: Harmony Books.

Srinivasan, R., Rudolph, C., & Roy-Chowdhury, A. K. (2015). Computerized Face Recognition in Renaissance Portrait Art: A quantitative measure for identifying uncertain subjects in ancient portraits. *IEEE Signal Processing Magazine, 32*(4), 85-94.

Stadtmüller, F. (1922). Zur Beurteilung der plastischen Rekonstruktions-methode der Physiognomie auf dem Schädel. *Zeitschrift für Morphologie und Anthropologie, 22*(3), 337-372.

Standring, S. (2016). *Gray's Anatomy: The Anatomical Basis of Clinical Practice* (41 ed.): Elsevier.

Steele, N. P., & Thomas, J. R. (2009). Surgical anatomy of the nose. In Springer (Ed.), *Rhinology and Facial Plastic Surgery*. Berlin Heidelberg.

Stephan, C. N. (2002a). Facial Approximation: Globe Projection Guideline Falsified by Exophthalmometry Literature. *Journal of Forensic Sciences, 47*, 730-735.

Stephan, C. N. (2002b). Position of superciliare in relation to the lateral iris: testing a suggested facial approximation guideline. *Forensic science international, 130*(1), 29-33.

Stephan, C. N. (2003a). Anthropological facial 'reconstruction--recognizing the fallacies, 'unembracing' the errors, and realizing method limits. *Science & Justice: Journal of the Forensic Science Society, 43*(4), 193-200.

Stephan, C. N. (2003b). Facial approximation: an evaluation of mouth-width determination. *American Journal of Physical Anthropology, 121*(1), 48-57.

Stephan, C. N. (2014). The Application of the Central Limit Theorem and the Law of Large Numbers to Facial Soft Tissue Depths: T-Table Robustness and Trends since 2008. *Journal of Forensic Sciences, 59*(2), 454-462.

Stephan, C. N. (2015a). Accuracies of facial soft tissue depth means for estimating ground truth skin surfaces in forensic craniofacial identification. *International Journal of Legal Medicine, 129*(4), 877-888.

Stephan, C. N. (2015b). Facial Approximation - From Facial Reconstruction Synonym to Face Prediction Paradigm. *Journal of Forensic Sciences, 60*(3), 566-571.

Stephan, C. N. (2017). 2018 tallied facial soft tissue thicknesses for adults and sub-adults. *Forensic science international, 280*, 113-123.

Stephan, C. N., & Davidson, P. L. (2008). The placement of the human eyeball and canthi in craniofacial identification. *Journal of Forensic Sciences, 53*(3), 612-619.

Stephan, C. N., & Henneberg, M. (2001). Building faces from dry skulls: are they recognized above chance rates? *Journal of Forensic Sciences, 46*(3), 432-440.

Stephan, C. N., & Henneberg, M. (2003). Predicting mouth width from inter-canine width - a 75% rule. *Journal of Forensic Sciences, 48*(4), 725-727.

Stephan, C. N., & Henneberg, M. (2006). Recognition by forensic facial approximation: Case specific examples and empirical tests. *Forensic science international, 156*, 182-191.

Stephan, C. N., Henneberg, M., & Sampson, W. (2003). Predicting nose projection and pronasale position in facial approximation: a test of published methods and proposal of new guidelines. *American Journal of Physical Anthropology, 122*(3), 240-250.

Stephan, C. N., Huang, A. J., & Davidson, P. L. (2009). Further evidence on the anatomical placement of the human eyeball for facial approximation and craniofacial superimposition. *Journal of Forensic Sciences, 54*(2), 267-269.

Stephan, C. N., Munn, L., & Caple, J. (2015). Facial soft tissue thicknesses: Noise, signal, and P. *Forensic science international, 257*, 114-122.

Stephan, C. N., & Murphy, S. J. (2008). Mouth width prediction in craniofacial identification: cadaver tests of four recent methods, including two techniques for edentulous skulls. *Journal of Forensic Odontostomatology, 27*(1), 2-7.

Stephan, C. N., & Simpson, E. K. (2008a). Facial soft tissue depths in craniofacial identification (part I): An analytical review of the published adult data. *Journal of Forensic Sciences, 53*(6), 1257-1272.

Stephan, C. N., & Simpson, E. K. (2008b). Facial soft tissue depths in craniofacial identification (part II): An analytical review of the published sub-adult data. *Journal of Forensic Sciences, 53*(6), 1273-1279.

Stephan, C. N., Simpson, E. K., & Byrd, J. E. (2013). Facial soft tissue depth statistics and enhanced point estimators for craniofacial identification: the debut of the shorth and the 75-shormax. *Journal of Forensic Sciences, 58*(6), 1439-1457.

Stewart, T. D. (1983). The points of attachment of the palpebral ligaments: their use in facial reconstructions on the skull. *Journal of Forensic Sciences, 28*(4), 858-863.

Stordeur, D., & Khawam, R. (2007). Les crânes surmodelés de Tell Aswad (PPNB, Syrie). Premier regard sur l'ensemble, premières réflexions. *Syria*, 5-32.

Straka, D., & Foster, J. (2018). Chapter 11 - Ptosis Repair and Blepharoplasty. In B. Azizzadeh, M. R. Murphy, C. M. Johnson, G. G. Massry, & R. Fitzgerald (Eds.), *Master Techniques in Facial Rejuvenation (Second Edition)* (pp. 120-130.e121): Elsevier.

Strapasson, R. A. P., Costa, C., & Melani, R. F. H. (2019a). Forensic Facial Approximation: Study of the Nose in Brazilian Subjects. *Journal of Forensic Sciences, 64*(6), 1640-1645.

Strapasson, R. A. P., Herrera, L. M., & Melani, R. F. H. (2017). Forensic Facial Reconstruction: Relationship Between the Alar Cartilage and Piriform Aperture. *Journal of Forensic Sciences, 62*(6), 1460-1465.

Strapasson, R. A. P., Stocco Baccarin, L., & Haltenhoff Melani, R. F. (2019b). Forensic Facial Reconstruction: A Systematic Review of Nasal Prediction Techniques. *Journal of Forensic Sciences, 64*(6), 1633-1639.

Strouhal, E. (1973). Five Plastered Skulls from Pre-Pottery Neolithic B Jericho : Anthropological Study. *Paléorient*, 231-247.

Sundelin, T., Lekander, M., Kecklund, G., Van Someren, E. J., Olsson, A., & Axelsson, J. (2013). Cues of fatigue: effects of sleep deprivation on facial appearance. *Sleep, 36*(9), 1355-1360.

Susanne, C. (1977). Heritability of anthropological characters. *Human biology*, 573-580.

Szécsényi-Nagy, A., Roth, C., Brandt, G., Rihuete Herrada, C., Tejedor-Rodríguez, C., Held, P., . . . Alt, K. W. (2017). The maternal genetic make-up of the Iberian Peninsula between the Neolithic and the Early Bronze Age. *Scientific Reports, 7*(1), 15644.

Tallman, M., Amenta, N., Delson, E., Frost, S. R., Ghosh, D., Klukkert, Z. S., . . . Sawyer, G. J. (2014). Evaluation of a New Method of Fossil Retrodeformation by Algorithmic Symmetrization: Crania

of Papionins (Primates, Cercopithecidae) as a Test Case. *PLOS ONE, 9*(7), e100833. doi:10.1371/journal.pone.0100833

Tandler, J. (1909). *Über den Schädel Haydns*: Selbstverl. der Anthropologischen Gesellschaft.

Taylor, K. T. (2001). *Forensic art and illustration*. Boca Raton, Florida: CRC Press.

Tedeschi-Oliveira, S. V., Beaini, T. L., & Melani, R. F. H. (2016). Forensic facial reconstruction: Nasal projection in Brazilian adults. *Forensic science international, 266*, 123-129.

Todd, T. W. (1923a). Cranial capacity and linear dimensions, in White and Negro. *American Journal of Physical Anthropology, 6*(2), 97-194.

Todd, T. W. (1923b). The effect of maceration and drying upon the linear dimensions of the green skull. *Journal of anatomy, 57*(4), 336.

Todd, T. W. (1925). The Nature of Mummification and Maceration Illustrated by the Male White Skull. *J Anat, 59*(Pt 2), 180-187.

Todd, T. W. (1926). The Nature of Mummification and Maceration: II. Female and Negro Skulls. *J Anat, 60*(Pt 3), 309-328.

Tolba, A., El-Baz, A., & El-Harby, A. (2006). Face recognition: A literature review. *International Journal of Signal Processing, 2*(2), 88-103.

Tsagkrasoulis, D., Hysi, P., Spector, T., & Montana, G. (2017). Heritability maps of human face morphology through large-scale automated three-dimensional phenotyping. *Scientific Reports, 7*, 45885.

Turner, W., Brown, R., Kelliher, T., Tu, P., Taister, M., & Miller, K. (2005). A novel method of automated skull registration for forensic facial approximation. *Forensic science international, 154*(2-3), 149-158.

Ullrich, H., & Stephan, C. N. (2011). On Gerasimov's Plastic Facial Reconstruction Technique: New Insights to Facilitate Repeatability*. *Journal of Forensic Sciences, 56*(2), 470-474.

Ullrich, H., & Stephan, C. N. (2016). Mikhail Mikhaylovich Gerasimov's authentic approach to plastic facial reconstruction. *Anthropologie, 54*, 97-107.

Utermohle, C. J., Zegura, S. L., & Heathcote, G. M. (1983). Multiple observers, humidity, and choice of precision statistics: factors influencing craniometric data quality. *American Journal of Physical Anthropology, 61*(1), 85-95.

Utsuno, H., Kageyama, T., Uchida, K., Deguchi, T., Miyazawa, H., & Inoue, K. (2008). Estimation of nasal tip position using lateral cephalometric X-ray images in Japanese male children: Applications in facial reconstruction. *Pediatric Dental Journal, 18*(1), 43-52.

Utsuno, H., Kageyama, T., Uchida, K., Kibayashi, K., Sakurada, K., & Uemura, K. (2016). Pilot study to establish a nasal tip prediction method from unknown human skeletal remains for facial reconstruction and skull photo superimposition as applied to a Japanese male populations. *Journal of Forensic and Legal Medicine, 38*, 75-80.

Van den Bosch, W. A., Leenders, I., & Mulder, P. (1999). Topographic anatomy of the eyelids, and the effects of sex and age. *The British Journal of Ophthalmology, 83*(3), 347-352.

Van der Heijden, P., Korsten-Meijer, A. G., Van der Laan, B. F., Wit, H. P., & Goorhuis-Brouwer, S. M. (2008). Nasal growth and maturation age in adolescents: a systematic review. *Archives of Otolaryngology - Head and Neck Surgery, 134*(12), 1288-1293.

Vandenberg, S. G., & Strandskov, H. H. (1964). A comparison of identical and fraternal twins on some anthropometric measures. *Human biology, 36*(1), 45-52.

Vanezis, M. (2008). *Forensic facial reconstruction using 3-D computer graphics: evaluation and improvement of its reliability in identification.* (Doctor of Phisolophy PhD). University of Glasgow, Glasgow.

Verzé, L. (2009). History of facial reconstruction. *Acta bio-medica: Atenei Parmensis, 80*, 5-12.

Vilas, R., Ceballos, F. C., Al-Soufi, L., González-García, R., Moreno, C., Moreno, M., . . . Álvarez, G. (2019). Is the "Habsburg jaw" related to inbreeding? *Annals of Human Biology, 46*(7-8), 553-561.

Villalba-Mouco, V., Oliart, C., Rihuete-Herrada, C., Childebayeva, A., Rohrlach, A., Micó, R., . . . al, e. (in prep). *Genomic transformation and social organization at the beginning of first state societies in Bronze Age southern Iberia.*

Virchow, H. (1912). Die anthropologische untersuchung der nase. *Zeitschrift für Ethnologie, 44*(H. 2), 289-337.

Von Eggeling, H. (1913). *Die Leistungsfähigkeit physiognomischer Rekonstruktionsversuche auf Grundlage des Schädels*: Archiv für Anthropologie, Völkerforschung und kolonialen Kulturwandel.

Walsh, S., Chaitanya, L., Breslin, K., Muralidharan, C., Bronikowska, A., Pospiech, E., . . . Kayser, M. (2017). Global skin colour prediction from DNA. *Hum Genet, 136*(7), 847-863.

Walsh, S., Chaitanya, L., Clarisse, L., Wirken, L., Draus-Barini, J., Kovatsi, L., . . . Kayser, M. (2014). Developmental validation of the HIrisPlex system: DNA-based eye and hair colour prediction for forensic and anthropological usage. *Forensic Science International: Genetics, 9*, 150-161.

Warren, J. J., Slayton, R. L., Bishara, S. E., Levy, S. M., Yonezu, T., & Kanellis, M. J. (2005). Effects of nonnutritive sucking habits on occlusal characteristics in the mixed dentition. *Pediatric Dentistry, 27*(6), 445-450.

Weale, R. A. (1982). *A biography of the eye: development, growth, age*: HK Lewis.

Weaver, D., & Bellinger, D. (1946). Bifid nose associated with midline cleft of the upper lip. *Archives of Otolaryngology, 44*(4), 480-482.

Weber, G. W. (2001). Virtual anthropology (VA): A call for Glasnost in paleoanthropology. *The Anatomical Record, 265*(4), 193-201.

Weber, G. W., & Bookstein, F. L. (2011). *Virtual anthropology: a guide to a new interdisciplinary field*. Wien, Austria: Springer-Verlag.

Weiner, J. S. (1954). Nose shape and climate. *American Journal of Physical Anthropology, 12*(4), 615-618.

Welcker, H. (1883). *Schiller's Schädel und Todtenmaske, nebst Mittheilungen über Schädel und Todtenmaske kant's*. Braunschweig: Viehweg F and Son.

White, R. (2006). The Women of Brassempouy: A Century of Research and Interpretation. *Journal of Archaeological Method and Theory, 13*, 250-303.

Whitnall, S. E. (1911). On a Tubercle on the Malar Bone, and on the Lateral Attachments of the Tarsal Plates. *Journal of Anatomy and Physiology, 45*(4), 426-432.

Whitnall, S. E. (1921). *The Anatomy of the Human Orbit and Accessory Organs of Vision*: Frowde and Hodder & Stoughton.

Whitnall, S. E. (1932). *The Anatomy of the Human Orbit and Accessory Organs of Vision*: Humphrey Milford, Oxford University Press.

Wilder, H. H. (1912). The Physiognomy of the Indians of Southern New England. *American Anthropologist, 14*(3), 415-436.

Wiley, D. F., Amenta, N., Alcantara, D. A., Ghosh, D., Kil, Y. J., Delson, E., . . . Hamann, B. (2005). *Evolutionary morphing*: IEEE.

Wilkinson, C. (2004a). Facial approximation: comments on Stephan (2003). *American Journal of Physical Anthropology, 125*(4), 329-330; discussion 330.

Wilkinson, C. (2004b). *Forensic facial reconstruction*. Cambridge: Cambridge University Press.

Wilkinson, C. (2010). Facial reconstruction – anatomical art or artistic anatomy? *Journal of anatomy, 216*(2), 235-250.

Wilkinson, C. (2015). A review of forensic art. *Research and Reports in Forensic Medical Science, 5*, 17-24.

Wilkinson, C., & Mautner, S. A. (2003). Measurement of eyeball protrusion and its application in facial reconstruction. *Journal of Forensic Sciences, 48*(1), 12-16.

Wilkinson, C., Motwani, M., & Chiang, E. (2003). The relationship between the soft tissues and the skeletal detail of the mouth. *Journal of Forensic Sciences, 48*, 728-732.

Wilkinson, C., Rynn, C., Peters, H., Taister, M., Kau, C. H., & Richmond, S. (2006a). A blind accuracy assessment of computer-modeled forensic facial reconstruction using computed tomography data from live subjects. *Forensic science, medicine, and pathology, 2*(3), 179-187.

Wilkinson, C., Thompson, T., & Black, S. (2006b). Facial anthropology and reconstruction. In T. Thompson & S. Black (Eds.), *Forensic Human Identification* (pp. 231-256). Boca Raton: CRC Press.

Williams, P. G., Grafenauer, S. J., & O'Shea, J. E. (2008). Cereal grains, legumes, and weight management: a comprehensive review of the scientific evidence. *Nutrition Reviews, 66*(4), 171-182.

Winkler, F. (1938). *Die Zeichnungen Albrecht Dürers* (Vol. III). Berlin.

Witton, M., Naish, D., & Conway, J. (2014). State of the Palaeoart. *Palaeontologia Electronica, 17*(3), 5E: 10p.

Wolff, E. (1933). *The Anatomy of the Eye and Orbit: Including the Central Connections, Development, and Comparative Anatomy of the Visual Apparatus*: Lewis.

Wolff, E. (1976). *Anatomy of the eye and orbit*. London: H. K. Lewis & Co.

Yoshino, M., & Seta, S. (2000). Skull-photo superimposition. In J. A. Siegel, P. J. Saukko, & G. C. Knupfer (Eds.), *Encyclopedia of forensic sciences*. San Diego, CA: Academic Press.

Zaidi, A. A., Mattern, B. C., Claes, P., McEcoy, B., Hughes, C., & Shriver, M. D. (2017). Investigating the case of human nose shape and climate adaptation. *PLOS Genetics, 13*(3), e1006616.

Zankl, A., Eberle, L., Molinari, L., & Schinzel, A. (2002). Growth charts for nose length, nasal protrusion, and philtrum length from birth to 97 years. *American Journal of Medical Genetics, 111*(4), 388-391.

Zegers, R. H., Maas, M., Koopman, A. T., & Maat, G. J. (2009). Are the alleged remains of Johann Sebastian Bach authentic? *The Medical Journal of Australia, 190*(4), 213-216.

Zelditch, M. L., Swiderski, D. L., & Sheets, H. D. (2012). *Geometric Morphometrics for Biologists: A Primer*. London: Elsevier Science.

Zollikofer, C. P. E., & Ponce de León, M. P. (2005). *Virtual Reconstruction: A Primer in Computer-Assisted Paleontology and Biomedicine*: Wiley.